Ultra High Performance Concrete in Large Span Shell Structures

R.N. ter Maten

Ultra High Performance Concrete in Large Span Shell Structures

Delft University of Technology
Faculty of Civil Engineering and Geosciences
Structural and Building Engineering
Concrete Structures
Stevinweg 1, Delft, the Netherlands

Master thesis committee

Prof.dr.ir. J.C. Walraven	Concrete Structures
Ing. J. van der Windt	Zonneveld Ingenieurs B.V.
Ir. S. Pasterkamp	Structural and Building Engineering
Dr.ir. P.C.J. Hoogenboom	Structural Mechanics
Dr.ir. S. Grünewald	Concrete Structures / Hurks Beton

Graduation coordinator

Ir. K.C. Terwel	Building Engineering

Preface

This document is the product of the graduation project 'Ultra High Performance Concrete in Large Span Shell Structures'. The graduation project is performed at the Building & Structural Engineering section at the Faculty of Civil Engineering and Geosciences at Delft University of Technology and in cooperation with Zonneveld Ingenieurs B.V. in Rotterdam.

The aspects which are combined within this research, being Ultra High Performance Concrete and large span shell structures, have appealing characteristics to me personally. Firstly, the potential for the use of Ultra High Performance Concrete is exciting and the material is likely to be more often used in the near future. Secondly, the structural behavior of thin shells goes hand in hand with material efficiency and the possibility for aesthetic appearances. This combination of engineering as well as architectural interest has always appealed to me since I was intrigued by the axial strength of empty Coke cans and the geometry of the Pantheon at young age.

I would like to thank my graduation committee, Prof.dr.ir. J.C. Walraven, Dr.ir. S. Grünewald, Dr.ir. P.C.J. Hoogenboom, Ir. S. Pasterkamp and Ing. J. van der Windt for their guidance and ideas during the project.

Rotterdam, October 2011

Richard Niels ter Maten

Summary

Part A. Ultra High Performance Concrete

Ultra High Performance Concrete (UHPC) is a contemporary concrete with a high compressive strength, extraordinary ductility and a far more durable character than conventional concrete. This high performance material offers a high potential for sustainable and economical applications with slim design in various fields of engineering which are capable of resisting heavier loads and span larger areas. For complete utilization of the advantages of the material distinctive knowledge is required for production, construction and design with UHPC.

The strength of UHPC, in comparison to conventional concrete, is not solely its compressive strength. Besides the compressive strength, also the tensile strength and the Young's modulus are distinguished characteristics. For the production of UHPC is highly demanding a requirement for successful production is a controlled precast environment and therefore the application of the material is most suitable for precast construction instead of in situ casting.

The excellent characteristics of UHPC are obtained by physical, chemical and adhesion optimization. This is mainly obtained by the absence of gravel within the mixture and the increase of the amount of cement. An important aspect of UHPC is the employment of fiber reinforcement which normally consists of high strength steel fibers. The failure of UHPC without fibers is of explosive nature, due to the effect of fibers the behavior becomes ductile. Further advantages of fiber reinforcement are the substantial contribution to crack width control and the resistance to concentrated forces. The combination between fiber reinforcement and passive or active reinforcement can be highly advantageous.

UHPC is distinctive from other materials for its outstanding qualities in terms of durability. The improved pore radius distribution and the corresponding low porosity improve the resistance to transport of harmful materials. It is stated that the durability characteristics cause the expected lifespan to be higher than 50 years, even 100 years.

Overall, the expectancy for economical savings of the project is not purely based on material savings but also involves fewer demands for the shell foundation, less necessary transport, less hoist handlings and an improved lifespan. Therefore the costs of the structure depend on multiple factors beside material investment costs.

Part B. Thin concrete shells

Shell structures present immense structural and architectural potential. Generally speaking, shells are spatially curved surface structures which support external applied loads. The exceptional behavior of shell structures can be referred to as 'form resistant structures'. This implies a surface structure whose strength is derived from its shape, and which resists load by developing stresses in its own plane.
Due to the initial curvature and low thickness to radius ratio a thin shell has a much smaller flexural rigidity than extensional rigidity. When subjected to an applied load it mainly produces in-plane actions, called membrane forces.

A consequence of the relatively small thickness is that shell design is mostly governed by requirements involving buckling capacity. A shell can however fail due to material nonlinearity, such as cracking and crushing, or by a combination of both geometry- and material non-linearity. So, besides being a 'from resistant structure' shell structures are also 'imperfection-sensitive structures'.

A shell will have a pure membrane behavior provided certain boundary requirements, loading conditions and geometrical configurations are satisfied. In practice, shell structures are regularly provided with an edge ring. The actual support displacement conditions impose constrains to such free boundary displacements and hence disturb the pure membrane field. In regions where the membrane theory does not hold, also entitled disturbed zones, bending field components are produced to compensate the inadequacies of the membrane field.

Sandwich and rib-stiffened shells are called composite shells which principles can be applied to improve the inertia and use of the cross-section. The disadvantages of sandwich panels, mainly being more complex production and temperature differences over the cross-section, lead to the preference not to apply this principle. Rib-stiffening is applied since it can severely increase the critical load of the whole shell structure in an economical, material efficient, manner.

Part C. Computational modeling

The finite element method (FEM) is a numerical analysis technique for obtaining approximate solutions to boundary value problems for engineering problems by solving partial differential equations. The analysis is particularly suited for solving partial differential equations on complex geometries and can be largely automated. This will save time and energy and is especially suitable for cases in which the design is likely to be adapted. Together with its diversity and flexibility as an analysis tool, it is well suited to efficient computer implementation within the engineering industry.

Since the development of the method and computers nowadays the application of several FEM-software packages is used on wide-scale. The analytical method can be integrated within the software. Therefore the input of elements and mesh generation is severely simplified. Beside the simple application sufficient knowledge on the background of the applied software is often useful in practice. In this research Scia Engineer is applied, which is an example of a wide-scale used commercial software package.

Part D. Analysis & design

The application of the principle of precast elements is based on the production demands for UHPC and the possibility for a significant overall increased economic value of construction. Successful construction of a prefabricated shell structure depends upon the design of the moulds and procedures developed to, repeatedly, use them. The production of thin elements, especially when connection provisions are to be applied, requires the moulds to be manufactured with precise tolerances. The experience from the reference projects is used which make use of moulds of plate steel, which had high accurate precision of ±0.3mm in the project of Pont du Diable, as opposed to a typical production tolerance of ±3mm. To improve the financial feasibility it is proposed to make use of a master mould which can be adapted for the production of various elements.

The geometry of the elements is influenced by the demands of hauling and transport. Together with the fact that the application of ribs and stiffeners is positive, relatively thicker element edges are applied which will ultimately form the ribs and stiffeners of the shell. The effect of curved element, as opposed to flat elements, is found to be highly positive for the bearing capacity of the shell and is therefore applied, which leads to only slightly curved precast elements. Furthermore the element edges have been influenced by principles from tunnel engineering. The edges make use of a dowel and socket system on behalf of element placement as well as load introduction. Also the elements are provided with neoprene gaskets which ensure watertight connection and serve as placement assistance.

Both the production method as the transport possibilities have their influence on the maximum size of the elements. This influences the number of elements, necessary handlings on site, the weight of the elements and its corresponding demands on crane capacity, the minimum amount of connections and the construction time.
Based on the principle of prefabrication and an estimated maximum size of the elements an element division of the total surface is applied. The element configuration is proposed to be done by a geometrical straightforward composition, called the 'ribbed dome', which makes use of more or less rectangular elements which mutually differ only slightly. This is considered to be advantageous in consideration of element size, production, storage, transport and handling. With this configuration, which is not entirely compatible for flat elements, the edges of the curved elements will form ribs and stiffeners.

For the elements to become an integral structure the joint construction is vital and is therefore subjected to high structural, physical and construction demands. Multiple connection methods are discussed and are found to be suitable connection methods for precast elements which are applicable for UHPC. The methods are compared with regard to load introduction, assembly method, suitability for UHPC, construction speed, durability and provisions to be taken. Two factors were decisive for the choice for local connections to be applied. Those are the fact that local force introduction is well feasible for UHPC and the fact that immediate connecting is favorable for a quick construction phase. Local connectors demand local connection facilities, which asks for provisions to be installed during the production of the elements. The provisions to be installed are designed based on common provision principles.

Calculations on design aspects

Multiple design aspects are optimized independently according to a principle known for research in economics named 'ceteris paribus'. This principle stands for the Latin phrase for 'all else being equal' or 'all other things held constant' and is often used for isolating descriptions or events from other potential environmental variables. After

the effects of the design aspects are known the results are combined for a final design of a spherical shell with a span of 150m and sagitta (height) of 37,5m.

It was confirmed that buckling under vertical loading is leading over compressive strength and that the effect of the various load cases does not have an influence on the final required concrete thickness other than buckling considerations. It is concluded that the prestressed edge ring has a significant effect on the ultimate buckling load. The fact that the buckling capacity of a fully hinged shell can be reached for an edge ring supported shell is positive and causes that this is aspired within the final design. It is seen that a rib stiffened shell has a major positive effect to the bearing capacity of the structure. Both the buckling load for constant vertical load and especially the safety against buckling for local effect are significantly increased. With an element maximum size of 8x4m² a shell thickness of 35mm with ribs and stiffeners of 180mm x 60mm was found to satisfy the structural demands. For an increase of the edge thickness it is concluded that the buckling resistance can be severely increased. Both an increase of edge thickness as well as a rib-stiffened shell show a shift of the buckling pattern to the top of the shell. Since rib-stiffening is applied within the elements in any case the increase of edge thickness is only applied if needed for edge disturbances.

The calculations for connection requirements is executed for the final design where the design aspects are combined. It is determined that the connection can be executed by local connectors which do not require a large cross-section and can be made by standard bolts. Since tensile force introduction can be complex the element is enforced with standard reinforcement bars per rib and stiffener. The elements are connected by a standard, fast and non-labor-intensive method of bolt- and rebar-anchors with a maximum diameter for the 8.8 bolt of 27mm and a reinforcement bar of 32mm.

To ensure that the structure shows sufficient structural coherence the design is tested for its bearing capacity and the effect to the force distribution in SLS for two load cases which involve openings in the shell surface. It is determined that the bearing capacity of the structures is hardly affected and the disturbed membrane behavior does not lead to difficulties. It is therefore concluded that the structure has sufficient structural coherence.

The dynamic behavior of the shell is tested by finding the eigenfrequencies of the structure. The value for the eigenfrequency of the structure of 6.8 Hz is not expected to cause possible dynamic magnifying effects for it is considered sufficient when the eigenfrequencies of the structure are larger than 5 Hz.
It is concluded that a concrete large span shell can be executed with internal insulation. With this, the UHPC can be exposed to the environment, meaning the durability aspects of UHPC are exploited and that roof covering is not to be replaced in the future. The thermal response mainly demonstrates in relatively small deformations, only at the edge of the shell small temperature stresses arise which do not lead to adjustments to the element dimensions.

It is noted that the buckling results of every design aspect calculation expose the occurrence of the phenomenon of compound buckling. Although it is found that the design adjustments have a severe effect on the buckling load itself, none of the adjustments affect the deviances between multiple adjacent critical loads, causing the geometry to be sensitive for imperfections.

Shell construction

The realization of shell structures can be challenging. The potential of the application ofUHPC and its material savings for the construction phase are investigated. The application of formwork is found to be inevitable but the lightweight construction by UHPC shows high potential for ease of construction and a short construction time.
In this study multiple construction possibilities are reflected by the relations to handling, erection, form control and temporary supports during construction. It was concluded that the idea to connect elements at ground level and subsequently place segments consisting of as many elements as possible per lift is most promising.

Because of the light-weight design a crane can lift and place numerous elements per handling. Within the design study the shell is divided in just 36 segments and can be constructed by one mobile crane. The segment itself is highly sensitive to deformations and is therefore proposed to be lifted by an assisting structure.

The right placement of the final segment is hard to be guaranteed. It is proposed to work with a final segment which is smaller than other segments. The available space can be determined in consolation with the building contractor and is to be filled with a field-cast joint fill solution of UHPC.

After the top segment is placed the installment of the prestress within the edge ring is to be applied. It is advised to remove the supports gradually per ring.

Conclusions and recommendations

In the design study it is demonstrated that the combination of UHPC and large span shell structures has a high potential. The most advantageous points for the design are the overall savings on material use and corresponding lower total weight of the shell which decreases the demands for the foundation and edge ring and fewer demands for transport. Also, it is proven that the shell can be built with making use of the durability aspects of UHPC which causes the expected lifespan to be higher than 50 years, even 100 years.

Together with these aspects it is believed that much profit with the application of UHPC for large span shell structures can be made within the construction phase. The described construction method makes use of the advantages of UHPC by making use of the ease of bolted connections which are fast to connect and make use of the force distribution ability of fiber reinforcement. Also, the light-weight structure can be handled and placed easily by a relatively few handlings.

Based on the results and conclusions of the research it can be concluded that the combination of UHPC and large span shell structures is a very promising concept. The most important recommendations are to perform further research and tests to the structural behavior of prefabricated concrete shell, especially to the effects of joint design, and that for the increase of the application of UHPC the design codes for UHPC are further developed.

Part E. Case study

The project named 'Fiere Terp' is a preliminary design for a shell structure and was the motive for the research within this thesis. The case study serves as a problem definition and guideline for the applied dimensions for a large span shell within the research. The design for Fiere Terp is improved wherein fundamental modifications were permitted. The original design for the project is based on the shape of a 'pompeblêd', meaning the leaf of a white water lily in the Frisian language. The design for Fiere Terp is discussed and improvements are proposed by deliberation of multiple variants and the preferences for the design based on the conclusions of earlier research.

From the reflections the most promising design variant is chosen as a recommended design. This judgment is based on both the positive structural behavior as well as the resemblance to the initial shape and favorable element production. Based on the results for a large span shell structure in earlier research it is declared that the design for this large span shell, with different geometry, is highly feasible as well.

Table of contents

Separate document:
Calculations

Calc.8.1.	Sagitta to span ratio
Calc.8.2.	Edge ring
Calc.8.3.	Rib stiffening
Calc.8.4.	Edge thickness
Calc.8.5.	Connection requirements
Calc.8.6	Dynamic response
Calc.8.7	Thermal response

1. Introduction

The aim of this graduation project is to analyze the possibilities for application of Ultra High Performance Concrete (UHPC) in combination with large span shell structures. The excellent material characteristics and the fact that shell structures may have aesthetic appearances can combine best of both engineering as well as architectural interest.

The thesis subject originates from the interest in the development of contemporarily concrete of Zonneveld Ingenieurs B.V. and a project involving a shell structure in preliminary design stage named 'Fiere Terp' which is described in part E of this report. The combination of these aspects has lead to the research aim to investigate the potential for UHPC in large span shell structures. The background of the subject and the research objectives of this Master's thesis are described in this chapter.

Ultra High Performance Concrete

Ultra High Performance Concrete (UHPC) is a concrete with a compressive strength of up to more than 200 MPa which, besides its superior compressive strength, encompasses extraordinary ductility and a far more durable character than conventional concrete.

Combined with further improved aspects concerning toughness, stiffness and thermal resistance, UHPC marks a leap in concrete technology. This high performance material offers a high potential for sustainable and economical applications with slim design in various fields of engineering.

The properties of UHPC are different to the properties of conventional concrete. For complete utilization of the advantages of the material distinctive knowledge is required with regard to production, construction and design with UHPC. The properties will be widely discussed in part A of the research.

Shell structures

A shell structure is defined as a structure with a thickness which is small compared to its span which usually has no interior columns or exterior buttresses. The most important feature of shells, which distinguishes shell structures from plated structures, is their initial curvature.

Due to this curvature, a shell is able to transfer an applied load by in-plane as well as out-of-plane actions. A thin shell subjected to an applied load mainly produces in-plane actions, which are called membrane forces. Thin shells are characterized by their three-dimensional load carrying behavior, which is determined by their geometry, by the manner in which they are supported and by the nature of the applied load.

The structural design of shell structures is multifaceted. A designer faces problems dealing with mechanical analysis, geometry and dimensions and shell construction. The aspects are described by the theory of thin shells and shell construction within this report.

Structural design

The combination of the material and mechanical aspects described above is investigated for its potential within structural design. For structural design the scientific knowledge related to structural mechanics and material science come together within a problem-solving progress which process is associated with reflection, creating solutions and alternatives, design considerations, execution aspects and improvement.

This report is a representation of the research and a process for a structural design for a large span shell structure in UHPC.

1.1. Aim of thesis

The research within this Master thesis concerns the possible collaboration between a promising contemporary material, Ultra High Performance Concrete, applied within the field of a structurally advantageous shape. The aim of the thesis is to investigate, analyze and report on the potential for the material in large span shell structures.

The thesis' outline consists of a combination of an analytical component and a structural design component. This subdivision arises from the analytical necessity along with required knowledge for shell design and the research for practical application of UHPC.

To get familiar with the contemporary material, the material characteristics and properties are discussed in part A of this report. Different aspects of the production and application are investigated and are checked by various reference projects.

The mechanical characteristics of thin shells are discussed in part B. The mechanical behavior, for which both the theoretical and practical knowledge are combined, leads to design considerations which are taken into account within further structural design.

The analysis comprehends the research on structural design as well as construction aspects. Before the design aspects optimized the calculation principles of the applied software are concisely described in part C, after which the acquired design principles are dealt with in part D, which represents the calculations and considerations for successful design and construction.

As mentioned, the thesis subject was inspired by a preliminary project at Zonneveld Ingenieurs named 'Fiere Terp', which design is elaborated in part E of this report. This project is in an early preliminary design stage and has lead to starting points for this research such as project location, objective span and shape. After the design principles are investigated in part D, the approach toward a structural design and its recommendations for this project are discussed in part E.

Altogether the results of the research lead to a definition of the use of UHPC in large span shell structures. The conclusions on the strengths, weaknesses and opportunities of the combination are given together with recommendations for further development.

1.2. Starting points and project scope

In this section the starting points and project scope are defined as:

- The research focuses on the construction material Ultra High Performance Concrete (UHPC) for its application within the design of large span shell structures. The used term 'large span shell structure' is specified as a shell with a diameter starting from 60m.

- The preliminary design for Fiere Terp acts as a design directive for the project location, general dimensions and type of shape. The preliminary design for Fiere Terp has a span of approximately 140m and a height (sagitta) of 35m. The design freedom for a final design is substantial, therefore modifications to the first design are not excluded.

- The research focuses on the aspects of structural design and analysis. The construction method is elaborated up to practical extend.

- The research focuses on shells with a positive Gaussian curvature (synclastic curvature). In the study design phase, spherical shells of revolution are researched to gain knowledge about the combination of UHPC and shell structures.

- The Eurocode, developed by the European Committee for Standardization, is used for loads and load factor determination. For the design and calculation in UHPC the French design recommendations for UHPC are applied.

- The thesis' outline consists of a combination of an analytical component and a structural design component. This subdivision arises from the analytical necessity along with required knowledge for shell design and the research for practical application of UHPC.

1.3. Prospects

The research described within this report focuses on the combination of UHPC and large span shell structures which is done in order to gain insight into the material characteristics, the practical applicability of the material within shells and the dimensions and geometrical properties of large shells.

The advantages of the application of concrete in shell structures have been known to man for centuries. The dominant compressive stresses, the material processability and savings on material costs led to a successful combination.

The predominant compressive stress within properly shaped shell structures suspects a successful application of UHPC because of its high compressive strength. However, it is known that compressive strength is not expected to be leading within shell design. However, the high strength is still expected to be advantageous in compression as it excludes premature compressive crushing failure before the critical buckling load is reached.

As mentioned, within the design of shell structures, critical buckling and its considerations are known to be of main design importance. Beside the fact that compressive stresses are predominant also tensile stresses can occur within the cross-section of the shell. UHPC is expected to be advantageous, or at least give opportunities, for the design of thin shells because of the high modulus of elasticity and the high tensile strength.

These characteristics are combined with superior durability characteristics and the fact that fiber reinforcement is advantageous for among other things crack width control, stress distribution and that passive reinforcement, and its required cover, has less necessity. Altogether the combination of UHPC in shell design is expected to lead to slim structural dimensions with an inherent total weight reduction. These aspects are appealing to be optimized since slim design results in fewer costs in material costs, transport and possible savings in construction. The opportunity to utilize the superior durability characteristics has the potential for cost savings in the life span of the structure. Therefore this research focuses on the exploitation of all excellent material characteristics and opportunities.

Part A
Ultra High Performance Concrete

Table of contents Part A

2. Material aspects

2.1. Introduction on UHPC

In this part the construction material Ultra High Performance Concrete (UHPC) is presented. A representation of the history of concrete as building material and the development of the material UHPC are described. The material components and characteristics are enumerated. The durability properties are described and subsequently an overview of the design recommendations is given. The chapter contains a description of the affordability of UHPC and is concluded by an evaluation on the literature on UHPC.

The term 'Ultra High Performance Concrete' refers to fiber reinforced materials with a cement matrix and a characteristic compressive strength in excess of 150 MPa, attaining up to 250 MPa. The addition of fibers is made in order to achieve ductile behavior under tension and, if possible, to dispense with the need for passive or active reinforcement.

The high performance material offers a variety of interesting applications as it allows the construction of sustainable and economic buildings with an extraordinary slim design. The combination between its high strength and superior ductility causes the expectancy that UHPC is the ultimate building material e.g. for bridge decks, storage halls, thin-wall shell structures and highly loaded columns.

2.1.1. History and development

Since ancient time, mankind has been developing in the search for, and application of, construction materials with better performance so we can build taller, longer and better structures. The Romans were skilful builders who have left their mark in a substantial part of the world. The concrete at that time was a mixture of lime, sand, stone and water.

The first applications of unreinforced concrete were solid structures which were merely subjected to compressive forces. The composition of the concrete was heterogeneous and had a relatively low compressive strength in the range of 10 MPa. The compressive strength of the ancient cement, in combination with brick and stone, allowed the Romans to build large arches and great domes.

An example is the Pantheon in Rome, built around 125 AD, with a dome that spans 43.3 meters constructed by stones and Roman concrete, which was the largest dome in the world for almost 1900 years. In the 19th century Portland cement was officially introduced by Josepf Aspdin in 1824 and reinforced concrete was first patented by W.B. Wilkinson in 1854. Accordingly, the history of reinforced concrete is only about 150 years.

Methods to enhance the characteristics of concrete traditionally are based on the principles of improving the particle density and lowering the water/cement-factor which in practice has a minimum proportion of 0.4, for lower values cause a severe loss of processability. The technology of ultra high performance concretes is based on both principles above.

Fundamental investigations on 'reactive powder concretes' were developed in the 1980s and 1990s in France and Canada. The maximum grain size of these fine-grained concretes is smaller than 1 mm. The principles for these high performance concretes are optimized grain packings of the fine reactive and the non-reactive components as well as the harmonized hydraulic and puzzolanic processes. In the 1990s, the technology of ultra high performance concretes was expanded to coarser grain sizes (up to 5mm). In principle, all ultra high performance concretes contain a high content of fine powder <250 μm and fitting coarse grains. The crucial optimizations are taking place in the fine grain size area only.

There are two main reasons urging the use of such type of concretes today:
- The need for structures which are capable of resisting heavier loads and with larger spans due to the 'endless' increasing congestion of the populated metropolitan regions.
- Green concrete demands; smaller cross section of concrete elements which require less concrete volume along with increased durability, which yields improvements in the sustainability of the structures.

Today, we are basically utilizing concrete, steel and timber in practically all constructions. Composites and fiber reinforced polymers are rather new introductions; they have yet to establish their field of applications. Similarly, UHPC can be considered a new material which is often said to not really be concrete anymore. It is stated that its application should not follow the path of regular concrete. It is anticipated that, with time, new structural concepts will be developed that can better utilize the superb properties of UHPC.

Beside its improved strength properties the outstanding resistance against all kinds of corrosion is an additional milestone on the way towards no-maintenance constructions. UHPC has distinctive properties that are remarkably different to the properties of normal and high performance concrete. For complete utilization of the superior properties of UHPC, sufficient knowledge is required for production, construction and design.
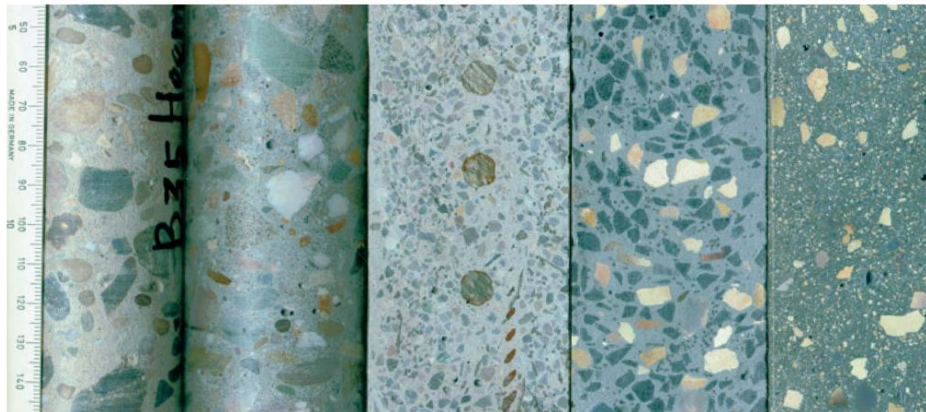

Fig.A1.   B 35, B 85, B 130/150, B 200 (Densit) & B 200 (BSI).   [31]

2.1.2. Principles of UHPC

The principle concept of UHPC relies on a couple of basic principles; they are the improvement of homogeneity, packing density, microstructure and ductility. The improvement of the first three aspects can be seen in figure A1 for conventional concrete towards UHPC. The principle aspects are fulfilled by the use of fine materials with various diameters, possible heat treatment and the use of fibers. The main positive characteristics of UHPC are described below:

Strength
> Higher strength offers savings in material use. The weight, or the structural dead load, is a major loading in the design of structures. With strength close to 200 MPa, the UHPC is almost like steel except its tensile capacity is comparatively low.
> Regarding compression strength concrete can be divided in a conventional concrete (up to 65 MPa), high strength concrete (B65 to B105), high performance concrete (~B105 to B150) and ultra high strength concrete (~B150 and higher).

Durability
> With the design life of today's major bridges, usually being 100 to 150 years, we are in need of durable materials that will last a long time and are easy to maintain. UHPC does offer good potential with respect to possible no-maintenance structures. However, a certain amount of time will be needed to assure that the long term performance of the material is what the laboratory tests have shown. The performance is confirmed by the first structures built with UHPC of about five to ten years old.

2.2. Material components

2.2.1. Introduction

In table A1 the global characteristics of conventional concrete B45 (CC), high performance concrete B85 (HPC) and ultra high performance concrete B200 (UHPC) are given. The absence of gravel and the increase of cement demand towards higher strength concretes are remarkable. The sand fraction consists for the largest part of sand with a granule size up to 1 mm; the maximum granule diameter is 5 - 7 mm. There is a considerable quantity of fine filler necessary. The required quantity of water increases slightly, but because the quantities of cement and filler strongly increase, the water/cement ratio decreases. Consequently, a large quantity of super-plasticizers is needed for a processable mortar.

Component	Density per component per material (kg/m³)			
	B45	B85	B200	B800
Cement	360	475	1075	980
Silica Fume	-	25	165	225
Sand	790	785	1030	490
Gravel	1110	960	-	-
Steel Fibers (13mm)	-	-	235	-
Micro Fibers (3mm)	-	-	-	615
Quartz flour	-	-	-	380
Super plasticizers	0.5	4.6	39	18
Water	145	150	200	185
Total density	2400	2400	2750	2895
Water / binder ratio	0.4	0.3	0.16	0.14

Tab. A1.   Global composition of concrete mortar   [31]

The fine components play an important role in high performance concretes. In particular, the fine powder - water matrix is responsible for the performance of the concrete system, both in the fresh concrete and in the hardened concrete. Ultra high performance concretes have a dense microstructure which can be optimized at very low water content. The following fundamental effects are responsible for this:

- High packing density particularly in the fine grain size area   (physical optimization)
- Hydraulic and pozzolanic reactions in the powder area   (chemical optimization)
- Improvement of the interfacial transition zone between cement stone matrix and aggregates
  (adhesion optimization)

A dense, non-porous solid structure attains a high performance very rapidly due to the short diffusion paths at hydration, pozzolanic reactions and other physical-chemical reactions.

2.2.2. Cement

High performance concrete mixtures usually are mixtures existing of ordinary Portland cement. In literature, another type of cements, such as Pretoria Portland Cement, are only scarcely mentioned.

2.2.3. Water/binder-ratio

Mixtures for UHPC are generally made with a very low water-cement ratio (w/c), even below 0.2, which is significantly lower than the assumed practical minimum value of 0.4. The lower the w/c-ratio; the lower the percentage of cement that can react with water. In spite of a low degree of hydration, very high strength values can be achieved. What counts is the intensity with which hydrating particles are glued together. The evolution of the strength can be correlated to the total contact area between solid particles. As the water to cement ratio is very low, UHPC often does not exhibit any drying (no weight loss can be measured) nor drying shrinkage.

2.2.4. Silica fume

Silica fume, of which the properties are shown in table A2, is the principal constituent of the new generation high and ultra-high performance concretes (HPC and UHPC) in combination with super-plasticizer. Due to its known superior properties, the micro filler effect and excellent pozzolanic properties, it is now possible to produce concretes with outstanding properties. The use of silica fume in concrete increases the calcium silicate hydrate (C-S-H) gel formation that is mainly responsible for the high strength, high durability of concrete structures and reduction of pore sizes.
Silica fume is an industrial by product from ferro-silicium alloys producing units, and hence its availability is limited. It also sometimes gives dark color to the concrete, which is due to the unburned coal contained in it, which can be an aesthetical problem. However, specially treated silica fumes are available, but they are expensive. Beside this, being an industrial by-product, homogeneity of the product can vary.

Decisive characteristic of the application silica fume are:
 – Dust free
 – Easy to handle
 – Ready to use
 – High quality particle size distributions

The influence of Silica Fume (SF) on UHPC is noticeable in multiple aspects:

Compressive strength
 – The use of SF is necessary for the production of HPC. The cube compressive strength studies indicate that the optimum percentages of CSF are 7.5% and 5% for OPC and PPC concrete.
 – The compressive strength of SF concrete increases with increase in age of curing.
 – The use of SF in concrete improves the early strength for OPC concrete.

Split tensile strength
 – The rate of increase of split tensile strength with compressive strength is less.
 – The ratio of tensile strength to compressive strength decreases with increase in compressive strength.
 – The tensile strength does not increase significantly with increase SF content

Durability-acid resistance test
 – The durability of silica fume concrete are more resistance to H_2SO_4 and HCl where a significant damage is observed in plain concrete mix, the addition of silica fume has shown a significant improvement.

Chemical properties	Percentage (%)
SiO_2	90-96
Al_2O_3	0.5-0.8
MgO	0.5-1.5
Fe_2O_3	0.2-0.8
CaO	0.1-0.5
Na_2O	0.2-0.7
K_2O	0.4-1
C	0.5-1.4
S	0.1-0.4
Loss on ignition (LOI)	0.7-2.5

Physical properties	
Specific gravity	2.2
Surface area	20,000 m^2/Kg
Size	0.1 micron
Bulk density	576 Kg/ m^3

Tab. A2.   Properties of Condensed Silica Fume [5]

2.2.5. Fibers

To achieve ductile post failure behavior in compression and to increase tensile strength and ductility of UHPC, often fibers, normally high strength steel fibers, are added. Thus very high flexural strengths can be achieved, particularly for thin structural members. In contrast to this, UHPC without fibers behaves brittle, if no additional measure such as confinement is chosen.

Under addition of fibers the load-displacement behavior and consequently the ductility and fracture toughness can be improved. This can be traced back to the fact that the fibers are able to transfer emerging loads by bridging the cracks. Here the fibers make an impact not until the appearance of cracks. That means after reaching the maximum load the descending arm of the load-displacement curve doesn't drop down at once. Depending on the kind of fiber, fiber length especially, and the fiber content, slow and even reduction of loads appear, coming along with increasing deformations.

UHPC with fibers shows, depending on the type and quantity of fibers contained in the mix, ductile behavior under compression as well as in tension. Since the pre-peak behavior does not show significant differences, the elastic properties of UHPC with and without fibers can be described in common whereas the influence of fibers has to be described separately.
A consequence of the dense material is the improvement of the contact zones between the cement matrix and the aggregates as well as the fiber reinforcement which allows a short length of fibers.

In general the influence of fibers on the compression strength is low. Due to 2.5 vol.-percent of fibers, an increase of the compressive strength of about 15 % has been noted. For UHPC, the geometry of test specimens seems to have less influence on the compressive strength. However, contradictory results from different sources exist with respect to this question.

For UHPC a pronounced descending branch can be developed by the effect of the fibers. The slope of the descending branch depends on:
- Fiber content
- Fiber geometry (length, diameter)
- Fiber length in relation to maximum aggregate size
- Fiber stiffness (in case of fiber cocktails)
- Fiber orientation

Within the fiber geometry a mixture, or cocktail, of fiber lengths is preferred. The role of the different fiber lengths is explained in figure A2.
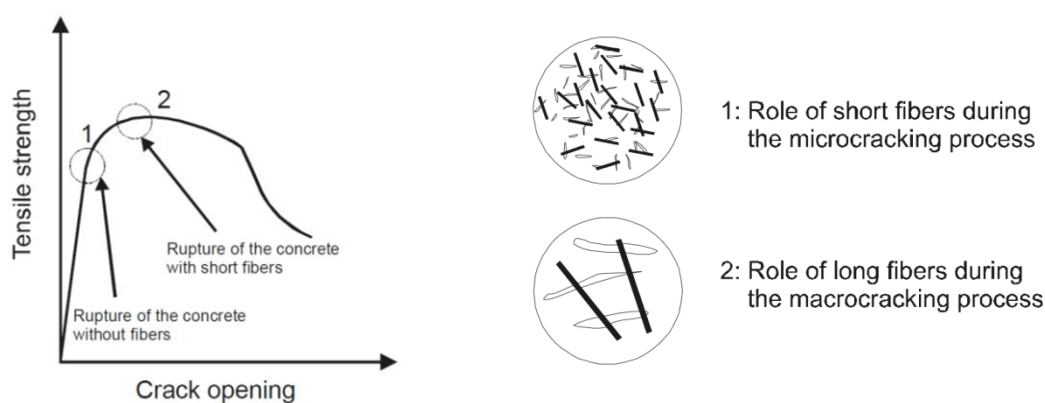

Fig. A2.   The role of fibers in different stages of tensile cracking   [15]

Different types of purposeful fiber types can be chosen for the UHPC mixture. Thus, the steel fibers, polypropylene fibers and glass fibers will be used in respect of the following effects:

• Steel Fibers:
- Increase of fracture energy, subsequent improvement of ductility
- Increase of strength (compressive strength, tensile strength)
- Reduction of tendency for cracking

• Polypropylene Fibers (PP fibers):
- Decrease of microscopic crack growth with high loading
- Gain in fire resistance
    Note: Eurocode EN-1992-1-2:200411 specifies the addition of PP fibers into HSC to prevent explosive spalling.
- Decrease of early shrinkage

• Glass Fiber:
- Reduction of internal stresses within young concrete

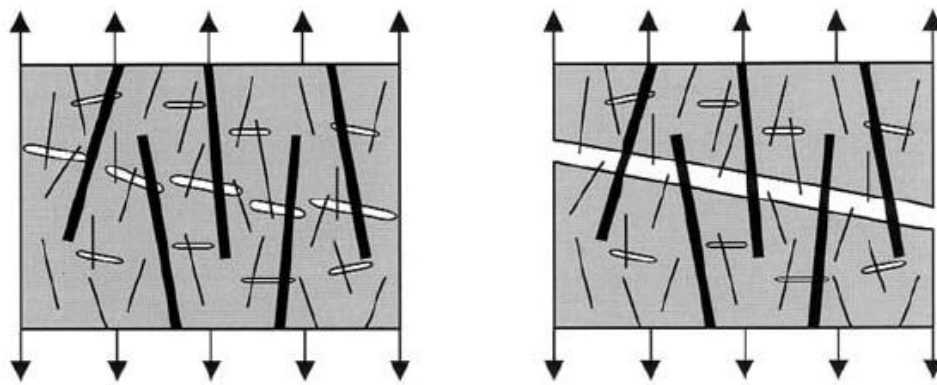

Fig. A3.   Left: Activating of short fibers by micro cracking
            Right: Activating of long fibers by macro cracking   [35]

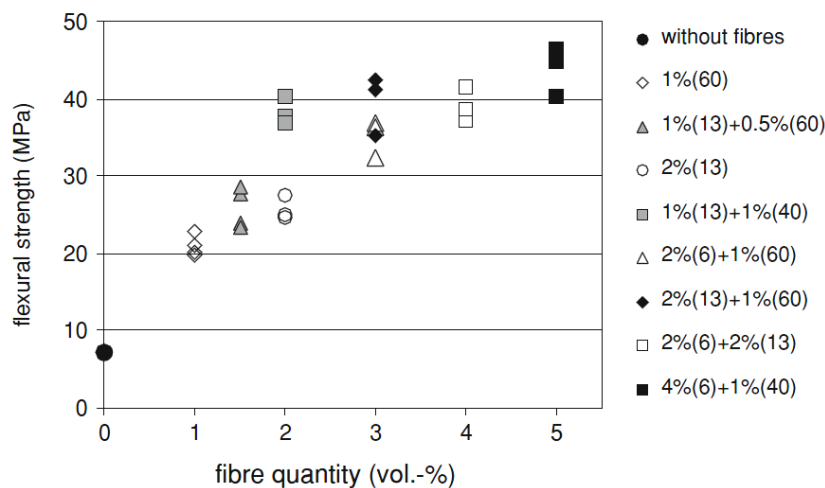Fig. A4.   Flexural strength of hybrid FRC   [35]

The fiber orientation is of high importance. The most ideal situation is when the fibers are randomly distributed in all directions. However, the direction of the fibers is of high causality with the casting method.

The influence of the fiber orientation has been studied by Bernier und Behloul, of which the results can be seen in figure A5.
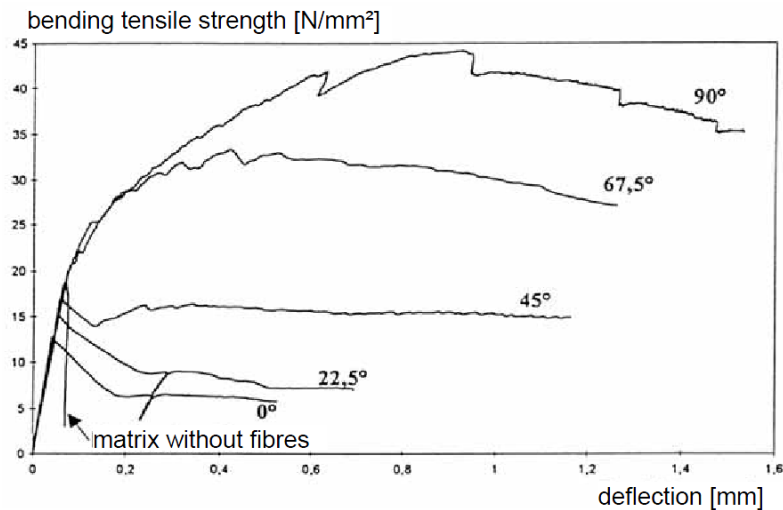

Fig. A5.   Influence of fiber orientation   [12]

Tests at TU Delft show that especially the flow direction during the casting process affects the fiber orientation and thus the tensile strength and ductility properties. It is recommended to cast slender specimens in a horizontal position to utilize the material's potential up to the fullest.

With the start of the development and application of fiber reinforced concrete the addition of fibers was not optimized. The effect of the fibers to the mechanical performance of the material were found to be diverse. A disadvantage of the adding of fibers was found to be that the processability showed a severe decrease for a required fiber content. Later, the effect of the dimensions of the fiber and its correlation to the aggregate material was discovered to be interactive. Figure A6 shows that the smaller the diameter of the aggregate material; the better the fiber distribution.
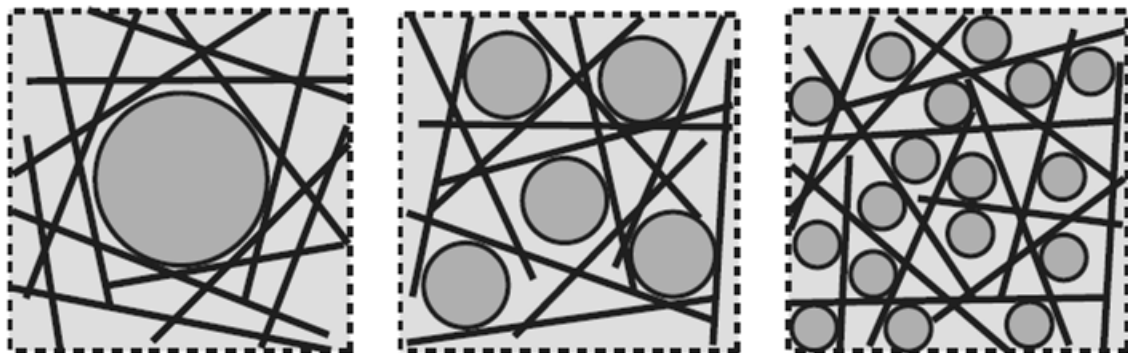

Fig. A6.   Influence of aggregate diameter to fiber distribution   [36]

Due to the fibers and their contribution to the behavior in tension UHPC shows a different tensile behavior than ordinary concrete. This has an important influence on the design of structures in UHPC. It can be concluded that:

- Major tension stresses should be taken by reinforcement bars or pre-stressed steel to guarantee a reliable and efficient tension bearing.
- The strain hardening effect caused by the fibers leads to a well distributed multi cracking. This eliminates the need of minimal reinforcement for crack distribution.
- The bond between reinforcement and the fiber reinforced cement matrix is higher than the bond strength of conventional concrete, tests show strengths which are about 10 times. This leads to a theoretical short development length, which could make connection of precast elements very easy.
- Shear reinforcement and reinforcement for the punching zones are not needed for minor shear stresses due to the high tensile strength respectively the high shear strength.

For applied fibers often the aspect ratio (l/d) is mentioned. The fiber length is usually between 9-17 mm and diameter can vary between 0,16 – 2 mm. The maximum volume percentage found to be up to 4.0%.
One example found in [35] is replicated here:

1,6 vol. % fibers. Length 13mm, diameter 0.16mm
1,6% = 0,016m^3 steel in 1 m^3 UHPC
1 fiber: $0,25*\pi*0,16^2 *13 = 0,26mm^3$
$0,016 / 0,26*10^{-9} = 61,5*10^6$ fibers per m^3
61,5 fibers per cm^3

This number of fibers per cm^3 is remarkable considering the individual fiber length of 13mm.

From this point on the term Ultra High Performance Fiber Reinforced Concrete will be abbreviated to UHPC. Both 'UHPC' as 'UHPFRC' are considered to be correct terms since the content of fiber reinforcement is inevitable for the structural application of the material, and therefore, the term 'UHPC' is considered to be common.

2.2.6. Combination of reinforcement and fibers

To resist tensile loads beyond the tensile strength of fiber reinforced UHPC in tensile members, fibers can be combined with conventional bar reinforcement or prestressing steel. Thereby, the structural and deformation behavior in serviceability as well as in ultimate limit state is affected significantly.

Differences in the load bearing and the deformation behavior compared to conventional reinforced concrete and prestressed concrete result from the interaction of continuous reinforcement elements and discontinuously distributed short fibers. In particular stiffness and cracking, but also bearing capacity and ductility, are significantly affected by the reinforcement configuration.

Tests at the University of Kassel show that results for a UHPC obtained for a fiber content of only 0.9 vol.-%, combined with reinforcement bars from 8 to 10mm, confirm that the fiber concrete itself does not need to show strain hardening behavior to achieve progressive crack formation with very small crack spacings and crack widths, which enables very durable structures. Since the costs of the fibers mainly determine the costs of UHPC, this finding is of high economical importance.

The application of the combination of reinforcement bars and fibers is deliberated further in this research.

2.2.7. Super-plasticizers

Super-plasticizers are chemical admixtures which can be added to concrete mixtures to improve workability. Unless the mix is 'starved' of water, the strength of concrete is inversely proportional to the amount of water added or water-cement (w/c) ratio. In order to produce stronger concrete, less water is added (without 'starving' the mix), which makes the concrete mixture very unworkable and difficult to mix, necessitating the use of plasticizers, water reducers, superplasticizers or dispersants.

Super plasticizers are also often used when pozzolanic ash is added to concrete to improve strength. This method of mix proportioning is especially popular when producing high-strength concrete and fiber reinforced concrete.

Adding 1-2% super plasticizer per unit weight of cement is usually sufficient. However, most commercially available super plasticizers come dissolved in water, so the extra water added has to be accounted for in mix proportioning. Adding an excessive amount of super plasticizer will result in excessive segregation of concrete and is not advisable. Some studies also show that too much super plasticizer will result in a retarding effect.

2.2.8. Heat treatment

Various types of UHPC undergo heat treatment (HT) which consists in raising the temperature of components to a relatively high level, with temperatures between 60 and 90°C for 48 to 72 hours, starting a few hours after the concrete has set. This kind of treatment must be carried out only after the concrete has set in order to avoid any risk of Delayed Ettringite Formation (DEF), a form of internal sulfate attack believed to be caused by improper heat curing. Heat treatment therefore requires good knowledge of the setting time.

The main effects of heat treatment are as follows:
-    The concrete strengthens faster (compressive and tensile strengths)
-    Delayed shrinkage and creep effects reduce substantially once the heat treatment is finished
-    Durability characteristics are considerably improved

2.2.9. Types of UHPC

Examples of UHPC currently marketed are the following:

- Different kinds of Ductal® concrete, including RPC (Reactive Powder Concrete), resulting from joint research by Bouygues, Lafarge and Rhodia, and marketed by Lafarge and Bouygues,

- Ceracem® concrete, which technology has evolved from BSI "Béton Spécial Industriel" (special industrial concrete), developed by Eiffage in association with Sika.

- BCV® being developed by cement manufacturer Vicat and Vinci group. Rather few available data is on hand in literature.

- ®Cemtec multiscale, developed by P. Rossi at LCPC, with first available results around 2002 and site application in 2004. It represents one available solution of UHPC with multi-scale (hybrid) fiber reinforcement (with about 10 % total fiber content – about 3 % for the longest fibers).

All of these materials have been used at least once in a real-size project, for either a new bridge or a repair operation. Other similar materials are also under development in France, especially at CERIB and EDF. Historically CRC (compact reinforced cement) developed by Bache in Denmark has a lot of properties close to those of UHPC.

Considering UHPC (presently available), the sources of difference can be listed as follows:
- The choice of fibers percentage and type, which is mainly governed by the required post-cracking ductility, and also interacts with size of the elements;
- Possible heat treatment, which is especially applied for Ductal®. Hydration is thus boosted during a 48 hours heat treatment (90°C) 2 days after setting, which further strongly reduces creep and shrinkage deformations. This treatment is of specific interest for pre-fabricated segments assembled by post-tensioning;
- Possible addition of organic fibers, in general polypropylene fibers at about 1 to 2% in mass of the cement content, in order to improve fire resistance of the elements by prevention of palling. This addition has generally little influence on the rest of the mixture proportions;
- Maximum aggregate size : while some Ductal® materials only contain cement or very fine sand (< 2 mm), Ceracem® includes up to 7 mm-sized ultra-hard natural aggregate (but at a rather low content as compared to micro-concrete). These aggregate have a beneficial effect with respect to shear transfer, but they imply using longer fibers;
- Cement type, chemical nature of fine additives and type of silica fume: these choices have generally been optimized in the "premix" industrially available UHPC, however there are still a lot of possible variations depending on possible requirements of chemical durability, economical and local feasibility, etc.;
- Super plasticizer type, which induces some differences in the rheological behavior of UHPC at the fresh state. While vibration is generally avoided, due to the risks on the fiber repartition, some UHPC types are definitely self-compacting with a low viscosity, some of them may require adapted casting in order to eliminate bubbles and prevent thixotropic hardening.

More information on Ductal® and Ceracem® is represented below.

Ductal®

A technological breakthrough took place in the 90's with the development of Reactive Powder Concrete (RPC), offering compressive strength exceeding 200 MPa and flexural strength over 40 MPa, showing some ductility. Based on the RPC initial research, the Ductal® technology was then developed. Comprehensive physical analysis and experimental results have confirmed the ability to achieve and combine several properties, usually considered as contradictory. As a result of the ductility and very high compressive strength of such material, it is today possible to avoid passive reinforcements in structural elements. The Ductal® technology has been introduced as a first reference, in several countries, both in structural and architectural segments of construction and currently developing through innovative applications in large projects at various stages of development. It has local adapted variations under license in Korea, Japan, USA, Canada and Australia where bridge projects have been built.

Ductal® refers to a simple concept, minimizing number of defects such as micro-cracks and pore spaces, which allows in achieving a greater percentage of the potential ultimate load carrying capacity defined by its components

and provide enhanced durability properties. To apply that concept, a concrete was proportioned with particle sizes down to less than 0.1 mm to obtain a very dense mixture which minimized void spaces in the concrete.

A Ductal® research program was conducted based on the following principles:

- Enhancement of homogeneity by elimination of coarse aggregates,
- Enhancement of density by optimization of the granular mixture,
- Enhancement of the microstructure by post-set heat-treatment,
- Enhancement of ductility by incorporating adequate size fibers,
- Maintaining mixing and casting procedures as close as possible to existing practice.

Ceracem®

SIKA has developed a range of products called CERACEM, in the frame of a partnership with the EIFFAGE Company in Paris, France. CERACEM has the advantage of being both self-compacting and ultra high-performance material. As it is self-compacting and as it does not need any further heat treatment, it bears several advantages on the job site, like faster setting and hardening, less noise and harmless to the workers due to the use of vibrators. With this type of concrete, it is possible to reduce or eliminate passive reinforcement and the thickness of the concrete elements can be reduced, which results in material and cost savings.

CERACEM is the result of an optimization of the nature and the composition of different raw materials. It is composed of a premix, a new super plasticizer, fibers and water. The fibers can be either metallic or synthetic. A new type of Polycarboxylate-ether (PCE) of super plasticizer was found to combine strong water reduction with reduced set retardation and modifying the rheology of the paste in a way, that the fresh concrete becomes self-compacting.

2.3. General material characteristics

The term 'Ultra-High-Performance-Concrete' is an all-embracing expression for multiple compositions of mixtures leading to a satisfying 'new material' with high performance demands. Because of this multiple compositions it is in this chapter, which discusses de material characteristics, therefore not possible to discuss several compositions. The characteristics of UHPC are therefore discussed in general.

2.3.1. Compressive behavior

The typical compressive strength of UHPC is in the range of 150 to 220 MPa. Until about 70 to 80 % of the compressive strength, UHPC shows a linear elastic behavior (Figure A7). According to experimental evidence as obtained until now, this holds true for UHPC regardless of the maximum aggregate size. The failure of UHPC without fibers is of explosive nature. No descending branch in the stress-strain-diagram does exist.
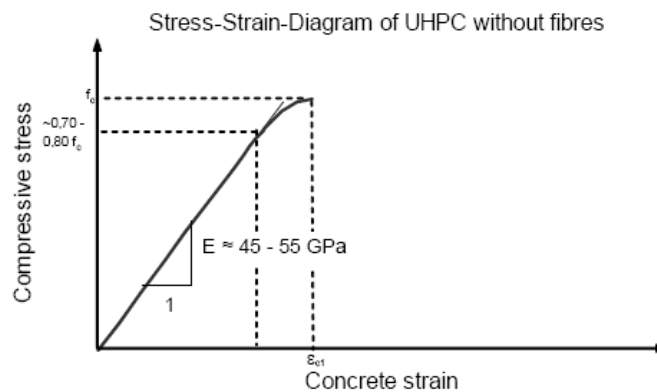

Fig. A7. Compressive stress-strain-diagram of UHPC without fibers [10]
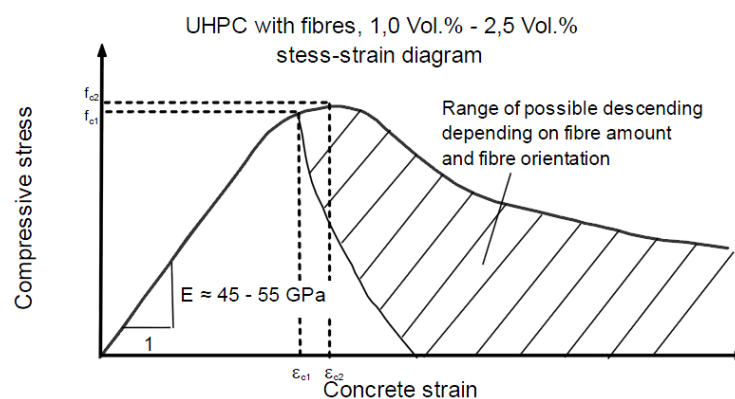

Fig. A8. Compressive stress-strain-diagram of UHPFRC [10]

2.3.2. Tensile behavior

The tensile behavior of UHPC is characterized by:
  – An elastic stage limited by the tensile strength of the cement matrix
  – A post-cracking stage characterized by the tensile strength of the composite material after the matrix has cracked
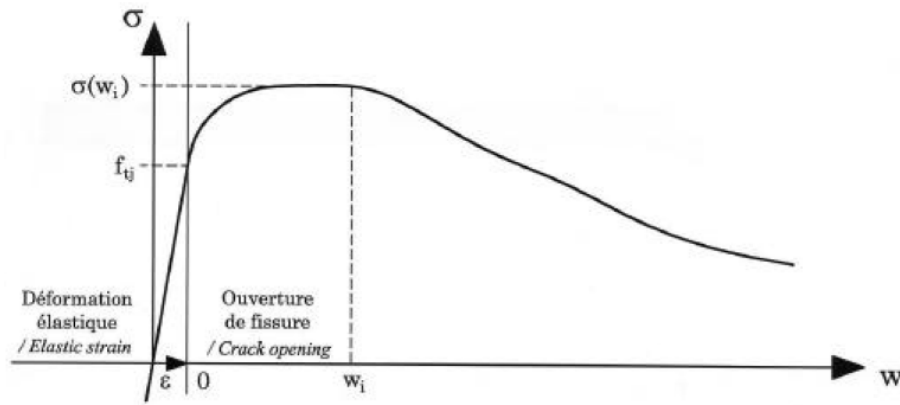
Fig. A9. Example of tensile constitutive law of a UHPC   [1]

The tensile strength can be determined experimentally using prismatic or cylindrical specimens. It may be advantageous to use probes sawn out of plates. In principle, it is possible to use specimens with or without notches. Direct tension tests on UHPC without fibers have delivered tensile strength values between 7 and 10 MPa. According to results obtained at the Universities of Kassel and Leipzig, there are only small differences between UHPC with fine or coarse aggregates. The failure is rather brittle, hence without a significant descending branch. Depending on the amount, type and orientation of fibers, the tensile strength of UHPC can be increased beyond the matrix strength. Values in the range between 7 and 15 MPa have been recorded. Due to the effect of fibers, the behavior becomes ductile. After onset of cracking, the material may be characterized by the stress-crack-opening-diagram. The typical behavior is depicted in Figure A10. It should be noted, that the slope of the descending branch can be very different, depending on the fiber orientation and the content and type of fibers.
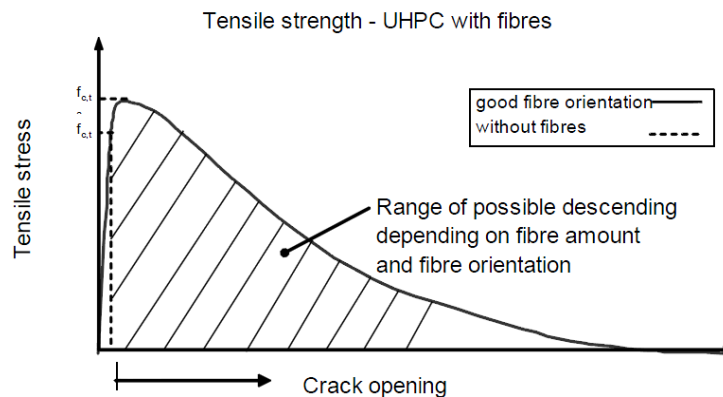

Fig. A10. Typical stress-crack-opening-curve for UHPC   [10]

2.3.3. Modulus of elasticity

Due to the dense structure, the elastic modulus of UHPC is higher than for normal- and high strength concrete when using identical aggregate types. Experimental results with different kinds of UHPC known to date demonstrate that:

- There is no usable simple formula to determine a satisfying estimation
- A homogenization model theory can be used, giving good results
- Otherwise, tests should be run to directly measure the modulus of elasticity

If nothing is known at the preliminary project design stage, a guideline value of 55 GPa can be considered. At more detailed design stages, the modulus taken into account must be the result of a test.

2.3.4. Creep

An essential precondition for a reliable design of UHPC constructions is a substantiated knowledge about the time-dependent stress-strain behavior of this material.

Creep of UHPC is generally less than for concrete with lower strength. Heat treatment in addition significantly reduces creep. If nothing is known at the preliminary design stages, guideline long-term creep coefficients, Φ, of 0.8 can be considered if there is no heat treatment, and 0.2 with heat treatment.

2.3.6. Shrinkage

Main parameters affecting shrinkage are the water/binder-ratio and the, compared to normal strength concrete, considerably higher cement content which increases the total shrinkage deformation.

UHPC shrinkage is mainly autogenous. When it has been heat treated, UHPC has no further shrinkage. If nothing is known at the preliminary design stages, a guideline value of 550 μm/m can be considered.

The autogenous shrinkage is the macroscopic volume reduction of unloaded cementations materials when cement hydrates after initial setting. It is the combination of chemical shrinkage and volumetric contraction caused by self-desiccation (dehydration) under sealed isothermal conditions. The high autogenous shrinkage of UHPC and its quick development indicate a high risk of micro cracking at early ages, if a construction element made of UHPC is restrained. From this point of view, the restrained UHPC without coarse aggregate is more sensitive to cracking than UHPC containing coarse aggregate.

The development of drying shrinkage of UHPC is similar as of HPC. Due to the high density of the matrix structure, however, the amount of drying shrinkage is reduced in comparison to HPC. For heat treated UHPC, drying shrinkage can practically be neglected after the end of the heat treatment.

2.3.7. Thermal expansion

As for NSC, the coefficient of thermal expansion is age-related. For UHPC with fine aggregates, 10.4-11.8 μm/mK have been recorded in French recommendations as general value. This value is in the same range as for NSC of about 11,0 μm/mK. For very young UHPC, less than 3 days, further research is necessary.

2.3.8. Fire resistance

Like all concretes, UHPC:
-    Is non-combustible
-    Makes no contribution to the development of a fire
-    Has low thermal conductivity, at about 1.6 W/m/K.

Again, like all concretes, the mechanical performance of UHPC (modulus of elasticity and strength) changes during fire. In application of the French DTU code of practice for building works it is possible to avoid systematic testing and to perform safety checks by means of a number of conventional calculations which take account, among other things, of an safe conventional drop in mechanical performance, the drop being defined by a curve giving the residual strength versus the maximum temperature attained.

Due to the extremely high density of UHPC, high water pressure can arise when UHPC is exhibited to fire. This can lead to deterioration and spalling of the concrete structure. The problem can be overcome by the use of fibers, e.g. polypropylene fibers. One effect of the fibers is that they create capillary pores due to melting and burning. Furthermore, around the fibers transition zones to the cement matrix are formed. By this, the existing transition zones between aggregates and matrix are interlinked so that the steam pressure is reduced. By the use of polypropylene fibers explosive spalling can be limited and the spalling depths can be reduced.

The Eurocode (EN-1992-1-2. 6.2) describes methods to increase the fire resistance for High Strength Concrete. Beside the possibility to add polypropylene fibers and protection layers the use of a reinforcement mat, with a cover of 15mm and a minimum nominal diameter of 2mm, is given as a positive measure.

2.3.9. Fatigue

Normally, fatigue is hardly of interest for conventional, rather massive concrete structures. But since UHPC provides the possibility to design more slender fatigue can become decisive. Fatigue can occur for instance due to traffic loads (bridges) or wind loads (off-shore wind turbines).

Only a few studies exist on the fatigue behavior of ultra high performance fiber reinforced concretes (UHPC). This is due to the fact that these materials have only been developed recently and research in that field is still in progress.

At TU Delft a research project was carried out in which the behavior of different types of HPFRC under fatigue loading was investigated. The results are that an approximate value of 65% of the average static failure load corresponds within 10^7 cycles.

Also fatigue loading test under compression at the University of Kassel for UHPC have shown a rather good-natured behavior. Thus, it can be said, that in contrast to other high strength materials, the high strength of UHPC with fibers does not lead to disadvantages with regard to fatigue.

Considering these test results economic design of UHPC structures under cyclic loading is feasible.

2.4. Durability

UHPC is very different to the materials which are usually encountered in civil engineering. Apart from being far stronger than conventional concrete, it has outstanding qualities in terms of durability. The durability of concrete is determined to a great extent by its porosity and the related pore radius distribution. These two characteristics have very small values in UHPC compared to concrete with conventional strength classes. The transport of water and solutions, transporting harmful materials as chlorides, is occurred by capillary pores. As the value of capillary pores decreases the resistance to transport of harmful materials improves. What is more, the first structures built with UHPC about five to ten years old, confirm good durability and natural-ageing results.

This performance means UHPC can have interesting applications, such as for structures in highly aggressive environments, waste storage or structures for the nuclear industry and makes it possible to envisage structural components with very long lifetimes without maintenance or repair. In addition, the properties of UHPC mean thin structural elements can be made: the gain in durability compensates the reduction in thickness. What is more, these results make it possible to consider a decrease in concrete cover because of the enhanced durability.

The following table gives the principal results obtained for UHPCs compared to the values corresponding to traditional concrete and to HPC. The mutual value for first three durability aspects distinct, the amount of portlandite content is an undesirable phase in concrete because it precipitates reactions near aggregates. The result is a porous aggregate interface that increases concrete permeability and reduces compressive strength. Portlandite is also subject to acid attack and carbonation.

	OC	HPC	VHPC	UHPC
Water porosity [%]	14-20	10-13	6-9	1.5 - 5
Oxygen permeability [m²]	10^{-16}	10^{-17}	10^{-18}	$<10^{-19}$
Chloride-ion diffusion factor [m²/s]	$2. 10^{-11}$	$2. 10^{-12}$	10^{-13}	2.10^{-14}
Portlandite content [kg/m³]	76	86	66	0

Tab. A3. Durability indicators for concrete [1]

2.5. Design recommendations

Up till now, there are no internationally accepted design recommendations for the application of UHPC. Partially this is due to insufficient information with regard to the properties of the material. An example of this is the durability of high performance concrete. It is mentioned that designing thin-walled structural elements applying reinforced or prestressed HPFRC allows slender and large span structures. If standard recommendations for conventional concrete would be applied for such structures large covers would be applied and the advantage of using HPFRC would be significantly reduced.

In comparison with existing codes for structural concrete new design aspects have to be added. Light, large span, elegant and material saving structures in HPFRC are for instance only possible if reliable rules for control of fatigue loading are available. Other aspects of significance in design are crack width control and the possible use of steel fibers as shear reinforcement.

There are design guidelines that provide the necessary information to fully design and calculate in UHPC. These are:

French	SETRA-AFGC	Recommandations provisoires,	2002
German	DAfStB	Sachstandbericht UHPC	2003
Japanese	JSCE	Recommendations UHSFRC	2008
Australia	Univ. NSW	Design Guide RPS	

As the German recommendations for UHPC are more of an addition to the French recommendations than a separate new set of design guidelines, this research will use the French recommendations for UHPC. Since the French Recommendations are used, there is no need to apply the Japanese recommendations as well. This was recommended by thesis committee.

2.5.1. French recommendations

The first French recommendations for Ultra-High Performance Fiber Reinforced Concretes (UHPC) were published in 2002, in bilingual English-French version. These recommendations integrate feedback from experience with the first industrial applications and experimental structures described below, as well as more than 10 years of laboratory research.
They are intended to constitute a reference document serving as a basis for use of this new material in civil engineering applications. These recommendations are divided in three parts:

- A first part devoted to characterization of UHPC, giving specifications on the mechanical performance to be obtained and recommendations for characterizing UHPC. This part also deals with checks of finished products and of the concrete as it is produced.
- A second part deals with the design and analysis of UHPC structures, the particularity of which is to integrate the participation of fibers and the existence of non-prestressed and/or non-reinforced elements.
- A third part deals with the durability of UHPC.

An interesting part of the French Recommendation is part 1.4.6. considering shells:

Shells are not considered to be a separate kind of structural element:
- Thick shells are designed in the same way as beams; the test specimens are prisms
- Thin shells are designed in the same way as thin slabs

The distinction between the thickness of thick and thin is made in which the barrier lies at three times the length of the individual fibers. The other distinction is made with the proportion of the span of the slab to the fiber length.

2.5.2. German recommendations

In Germany a work group of the German Commission on Reinforced Concrete (Deutsche Ausschuss für Stahlbeton, DAfStb) has presented a state of the art report on UHPC.

The design application is generally based on the author's elaborations. The aim of these suggestions is to combine the design with the standards DIN 1045 (German code) and the Eurocode respectively. A reinforced UHPC could then be designed based on these applications.

2.5.3. Japanese recommendations

The Concrete Committee of Japan Society of Civil Engineers has published the research report as 'Recommendations for Design and Construction of Ultra High Strength Fiber Reinforced Concrete Structures, - Draft'. The recommendations prescribe a procedure for examining safety and serviceability performance, which differs from conventional reinforced concrete, in consideration of the resistance to tensile stress of UHPC (named UFC in these recommendations) without applying any reinforcing bars. The recommendations determined that the standard lifespan is 100 years under normal environmental conditions and that examinations of many items regarding durability are not necessary.

2.5.4. Australian recommendations

With the support of VSL (Australia), the University of New South Wales, Australia, published a "Design Guide for RPC (Reactive Powder Concrete) Prestressed Concrete Beams" consistent with the design philosophy of the Australian Code AS3600-1994. This document provides design examples and material design guidance for compressive, Flexural shear, and torsion strength, as well as recommended flexural crack control limits, deflection control, fire performance, fatigue, prestress losses, and guidance on anchorage zones. Not much information about these recommendations is found, it is only once named in a reference article.

2.6. Material affordability

The costs of a shell structure, which is the result of the thesis, are not within the project scope. However, for UHPC to be used in practice, the material costs are of decisive importance. UHPC is mentioned to have a 'high' cubic price. The total costs are for approximately two thirds part governed by the addition of steel fibers, which leads to believe that a combination with reinforcement bars can be more economic.

A cubic price of 445 euro/m³, which counted for a prestressed sheet pile [18] with a compressive strength of 120MPa, can be seen as a lower limit. The target price for Ductal, as discussed in paragraph 2.2.9., is about 1600 euro/m³. This value includes company assistance, the premix and the development costs. Since many factors are of influence on the eventual total costs the ultimate value is relative. Since independent production of UHPC has an economical advantage over commercial premixes the value of 1600 euro/m³ is seen as upper limit. Independent production would imply separate parties which deliver the material components. For this, an overall an indication of a cubic price of 700 euro/m³ can be applied.

These values can, although relatively inaccurate, be compared to a price for conventional concrete of approximately 120 euro/ m³. It can be concluded that UHPC is significantly more expensive than conventional concrete, therefore the multiple other advantages of UHPC should be exploited. Beside the savings on material costs the total cost consideration of application of UHPC should also involve maintenance costs, more economical transport and lighter construction equipment.

Because UHPC is still a 'new material' the common acceptation and application of the material looks like a 'chicken and egg' question. A potentially good but expensive material may become affordable when its application is more widespread due to mass production, while its application can only get widespread if its cost is sufficiently low. A mass production of today's UHPC is still considered to be not very economical. The cost is rather high because if we use UHPC to replace regular concrete, such high strength may not offer sufficient advantage in most types of today's structures or structure sections such as walls and floors. The possible application of UHPC within the field of more special structure like shell structures can be of higher potential.

Within a shell structure mostly compression stresses will occur. Because of this reason and the high contribution of fibers to the total costs the idea emerges to locally reduce the amount of fibers, especially when combined with passive reinforcement. The fibers provide, along with tensile capacity, a substantial contribution to brittle behavior, crack width control and the resistance to concentrated forces. It is concluded that a minimum of fiber amount is required.

Overall the expectancy for economical savings of the project is mostly based on material savings of the shell, less demands for the shell foundation, less necessary transport and less hoist handlings. Therefore the costs of the structure depend on multiple factors beside material costs and is high interwoven with the construction method.

2.7. Considerations for shell design

2.7.1. General remarks

The study on UHPC confirms the high expectations which apply for this material. In the introduction of this chapter the expectancy for UHPC to be an ultimate material for bridge decks, storage halls, thin-wall shell structures and highly loaded columns was mentioned. The principles and characteristics of the material described in this chapter confirm this prospect.

Where high compressive strength, high durability properties and ductility are combined, for only a slight increase of cubic weight compared to conventional concrete, one might ask what the disadvantage of this material is. Till thus far, the high demands on mixing, the affordability and unknowns in behavior of a UHPC-shell in case of fire together with general inexperience with the application of the material are the most important disadvantages found. For these aspects the 'chicken and the egg'-dilemma is in effect. In the future the further use of UHPC in practice will have to cause a more regular application and there more development of knowledge and possible increase of affordability.

The UHPC casting and compacting compared with normal concrete is very distinctive, especially regarding the complex processing, due to its ductile consistency. The manufacture of UHPC of constant quality and on an industrial scale requires state-of-the-art, technically sound machinery and equipment and almost ideal circumstances, not likely to happen often in practice. Therefore the application of UHPC is most suitable for precast instead of in situ casting.

Fibers contribute significantly to the material toughness and the ability to withstand splitting forces. Additionally, fibers provide a multiplication of resistance to concentrated loads by a factor 2 to 4. Moreover, the contribution to crack width control and distributed multi cracking, as described above, cannot be neglected. It is concluded that beside that fact that the mechanical behavior of shell structures is generally based on compressive behavior and the significant contribution of fibers to the material costs, and therefore a possible cost-cutting on fibers, a minimum volume percentage of fibers remains essential.

The possible combination of fiber and conventional bar reinforcement has interesting effects on the structural and deformation behavior in serviceability as well as in ultimate limit state. Stiffness and cracking, but also bearing capacity and ductility, are significantly affected by the reinforcement configuration. However, within shell design mostly compressive stresses are expected and traditional reinforcement requires more production work and a concrete cover. Because of the traditional reinforcement bars require concrete cover; the potential of thin elements may be counteracted. The possibilities of merely applying generally fiber reinforced elements is therefore preferred and investigated.

2.7.2. Reference projects

The application of UHPC in realized projects is described and evaluated in Appendix 3 in which it is pleasant to see that, with the expectancies of the material itself, the successful application of UHPC in practice is promising. The conclusions from the evaluation are presented here since they are design aspects for further research.

All reference projects make use of precast elements, often with additional heat-treatment. There is no reference to a consideration for possible in-situ casting, except for the Field Cast UHPC Joints described in article 3.11. The main reasons mentioned for the choice of precasting are the advantages considering heat treatment, shrinkage and creep. Also possible tight tolerances and superior finishing for precast solutions are presented; the steel moulds of the LRT station and the Pont de Diable footbridge are examples which present a production with an accurate precision of ±0.3mm. Cast in-situ applications require further development work.

The utilization of all positive characteristics of UHPC is mentioned to be of vital importance. It is stated that the durability causes the expected lifespan to be higher than 50 years, even 100 years.

All projects show the successful application of UHPC in practice and the possibility for UHPC to be designed in very thin elements starting from 20mm, which is seen in the LRT station project.

Multiple types of connections such as prestressing, fiber joints and glued connections, for precast elements show to be having high potential and are proven to be feasible in combination with UHPC.

Part B
Thin Concrete Shells

Table of contents Part B

3. Structural concept

3.1. Introduction to thin concrete shells

This chapter the main characteristics of thin concrete shells are presented. After an introduction to concrete thin shells the theory of shells is elaborated for spherical shells. The aspects on structural failure of shells are described followed by a number of design considerations for further design. Within this chapter a number of terms to describe the geometry of shells are used. The clarification of these terms, dimensions and their relations is found in appendix 4.

Generally speaking, shells are spatially curved surface structures which support external applied loads. The American Concrete Institute defines a thin shell as a: 'Three-dimensional spatial structure made up of one or more curved slabs or folded plates whose thicknesses are small compared to their other dimensions. Thin shells are characterized by their three-dimensional load carrying behavior, which is determined by the geometry of their forms, by the manner in which they are supported, and by the nature of the applied load.'
The exceptional behavior of shell structures can be referred to as 'form resistant structures'. This implies a surface structure whose strength is derived from its shape, and which resists load by developing stresses in its own plane.

Shells are found in a variety of natural structures such as eggs, plants, leaves and skeletal bones. The opportunities and advantages of shell structures have also been recognized by man since ancient time. Shell domes of masonry and stone are still found in existence in parts of the world.

Shell structures present immense structural and architectural potential in various fields of civil, mechanical, architectural, aeronautical and marine engineering. Concrete shell roofs are just an example of the variety of the field of shell structures. In recent times, with the development of various high strength, fiber reinforced and laminated composite materials, the domain of potential, application and range of structural efficiency of shell forms is has even more increased.

3.1.1. Research shell geometry

This research focuses on large span shell structures and is influenced by the design geometry of a reference project named Fiere Terp of which the characteristics are described in part E. The type of shell geometry where this research focuses on comprehends the type of shell geometry based on this design, implying that the research focuses on shell surfaces with positive Gaussian curvature, which principle is described below.

Also, in the study design phase, spherical shells of revolution are researched to gain knowledge about the combination of UHPC and shell structures.

Shells of revolution

A shell of revolution is a shell whose geometric form is defined by a middle surface that is formed by the revolution of a meridional generator line around a single axis through 2π radians. The shell can be of any length.
In case of cylindrical and conical surfaces, the meridional curve consists of a line segment. In case of a spherical cap, of which examples are given below, the meridional curve is a segment of a circle.
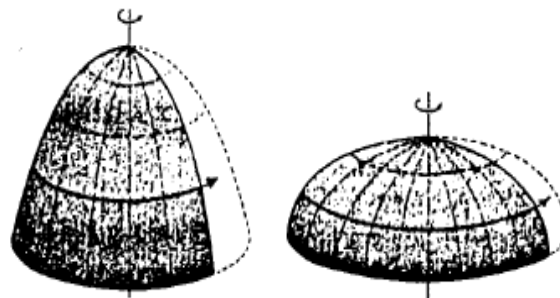

Fig.B1.   Examples of surfaces of revolution   [42]

Gaussian curvature

In geometry, Gaussian curvature is a term which for a given point on a surface is the product of the principal curvatures, κ_1 and κ_2, of the point. Hereby the Gaussian curvature is defined as $K = \kappa_1 \cdot \kappa_2$. The local surface shape and the sign of the Gaussian curvature have the following relations:

K > 0.   Synclastic surfaces. The normal curvatures have the same sign in all directions, the tangent plane touches the surface at one point. Examples are spheres and elliptic paraboloids.
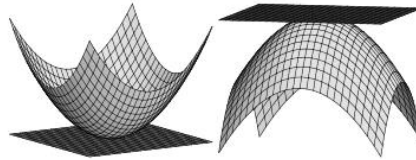
Fig.B2.   Positive Gaussian curvature K > 0   [50]

K < 0.   Anticlastic surfaces. The principle curvatures are of opposite sign. The surface is locally saddle-shaped.

Fig.B3.   Negative Gaussian curvature K < 0   [50]

K = 0.   Cylindrical surface. At least one principal curvature is zero. At such a point the surface is nether convex/concave nor saddle-shaped, as seen at the bottom middle and right images of Fig. 2.
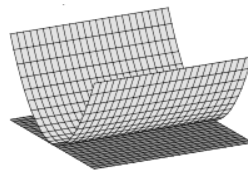
Fig.B4.   Zero Gaussian curvature K = 0   [50]

3.2. Theory of shells

Shells structures with a small thickness in comparison to their radii of curvature of the shell mid-surface are considered as thin shell structures. A thin shell, due to this small thickness-to-radius ratio, has a much smaller flexural rigidity than extensional rigidity. As a result, when subjected to an applied load, it mainly produces in-plane actions, which are called membrane forces. So, due to the initial curvature of shells it is caused that these three-dimensional spatial structures are able to transfer applied loads by in-plane as well as out-of-plane actions.

In this chapter the mechanical behavior of shell structures, with the focus on shells of revolution is described. The knowledge of the mechanical behavior and the underlying theory of the structure is essential. The types of analysis described in this chapter are the membrane- and the bending theory of shells, the theories consider a shell geometry considered as being perfect.

The in-plane membrane forces described above are actually resultants of the normal stresses and the in-plane shear stresses that are uniformly distributed across the thickness. The corresponding theory, the *membrane theory,* of this membrane behavior is described in this chapter followed by the description of the *bending* behavior which applies for regions where the membrane theory will not hold.

In this chapter the theoretical elastic mechanical behavior of thin shell structures and the design outcome of the theories are described. Physical non-linear performance and geometric non-linear performance are not considered and the resistance to shear in the direction normal to the surface is not taken into account for the description of the membrane - and bending behavior. The purpose of this chapter is to gain insight in spherical shell behavior for further design.

Since this report focuses on spherical shells the geometry and therefore mechanical behavior of a hemisphere is chosen as a starting point to gain insight in the theory and behavior of spherical shells. A hemisphere, which naming originates from 'hēmisphairion' meaning 'half of a sphere', is an example of a shell of revolution. This chapter deals with the membrane behavior and bending behavior of a hemisphere under axisymmetric loading.

The approach described in this chapter is based on 'Theory of shells' by Blauwendraad and Hoefakker. The theory described in this chapter and the results of Finite Element analysis are mutually checked in appendix 5.

Consistent with other theories in continuum mechanics, the theory of shells is based on three sets of equations being the kinematic equations, the constitutive equations and the equilibrium equations. Both the analysis for the membrane theory and bending theory are evaluated in the order of the force method. Which implies; first the equilibrium relations, than the constitutive relations and finally the kinematic relations. Vectors are used to describe these relations. The relations between the three sets of equations is schematized in figure B5.
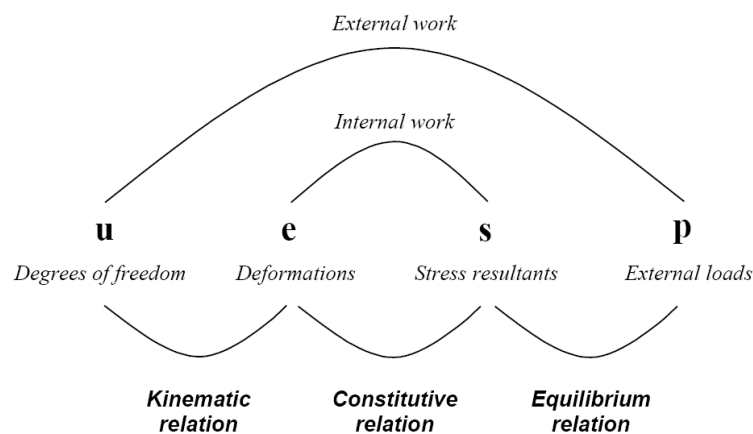

Fig.B5.   Scheme of relations within structural mechanics   [40]

3.2.1. Membrane theory for spherical shells

The membrane theory assumes that in a thin shell only in-plane membrane forces are present which produce a pure membrane stress field and bending stress actions are assumed not to be developed. To be able to use the theory in hand calculation, the relations are simplified by ignoring shear deformation and restricting them to small deformations and slender cross-sections. It is, thus, impossible for this theory to analyze large deformation (nonlinear-) problems. In addition it is assumed that the shell is homogeneous and isotropic.

To complete the description for the mathematical relations, the boundary conditions of the particular problem are ought to be introduced. These boundary conditions, as well as loading conditions, which are required to satisfy the equilibrium and/or displacement requirements for the membrane theory are presented below:

(a)
Membrane compatible

(b)
Membrane incompatible

(c)
Localised edge effects
(Deformation constraint)

(d)
Concentrated load

(e)
Change in the geometry
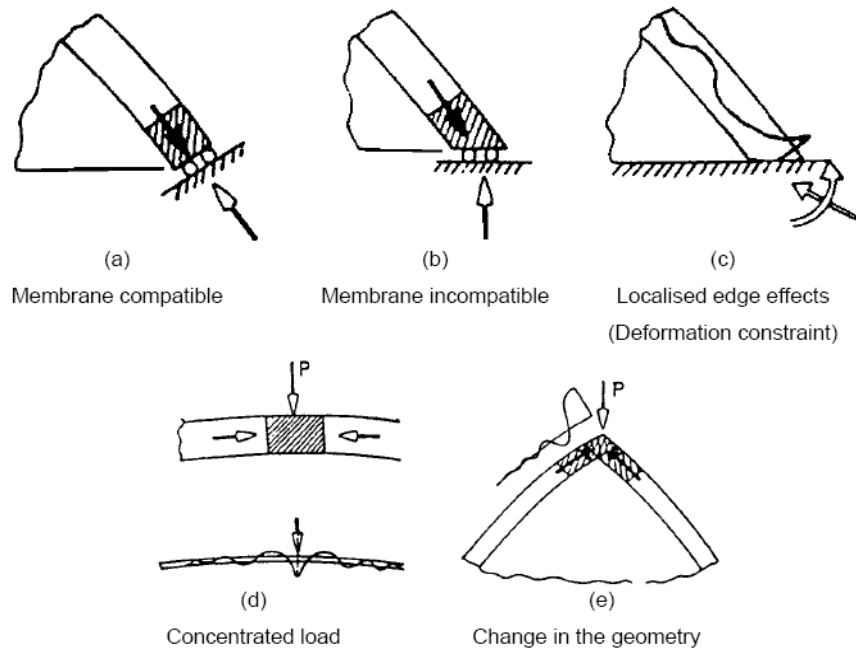
Fig.B6.   Membrane compatible and membrane incompatible boundary conditions in a shell [42]

Figure (B6.b) and (B6.c) are examples of boundary conditions and deformation constraints that are incompatible with the requirements of a pure membrane field, as well as concentrated loads (B6.d) and a geometrical change in smooth surface (B6.e).

Since revolutionary surfaces are generated by a meridian and an axis of revolution an arbitrary point of the middle surface of a shell can be described by an angular distance θ of its plane from that of the datum meridian, the angle ϕ describes the angle between the axis of revolution and the normal of the shell surface. Figure B7 shows these angles.
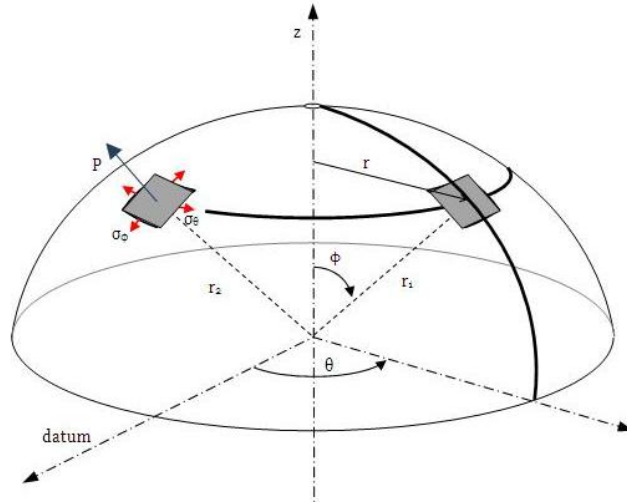
Fig.B7.   Parameters in shell geometry   [RtM]

Because the spherical surface the coordinate system (ϕ,θ,z) is employed instead of a conventional Cartesian coordinate system (x,y,z). The following vectors are ultimately used:

Degrees of freedom $\mathbf{u} = [u_\phi \quad u_z]^T$

Deformations $\mathbf{e} = [\varepsilon_{\phi\phi} \quad \varepsilon_{\theta\theta}]^T$

Stress resultants $\mathbf{s} = [n_{\phi\phi} \quad n_{\theta\theta}]^T$

External loads $\mathbf{p} = [p_\phi \quad p_z]^T$

Equilibrium equation

The membrane theory is based on the assumption that bending stress resultants can be neglected and that the transverse shearing stress resultants are correspondingly equal to zero. Only the in-plane stress resultants are dealt with and the longitudinal shearing stress resultant $n_{\phi\theta}$ is equal to zero because of symmetry considerations. For the membrane theory the *stress resultant vector* $\mathbf{s}$ is thus defined by:

$\mathbf{s} = [n_{\phi\phi} \quad n_{\theta\theta}]^T$

For a small element also two force equilibrium conditions between the stress resultants and the load components can be set up. The positive action of the load components, acting on the middle surface of the shell element, is taken according to the positive directions of the three axes as shown in figure B7 and so the *load component vector* $\mathbf{p}$ is defined by:

$\mathbf{p} = [p_\phi \quad p_z]^T$
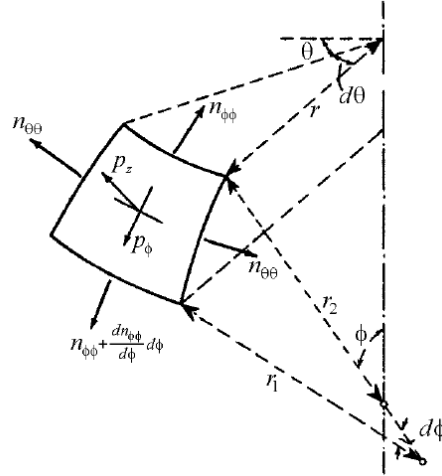
Fig.B8.   Load components and stress resultants on an infinitesimal element   [40]

For axisymmetric loaded shells of revolution the derivations of the membrane equations leads to:

The summation of forces parallel to the tangent at the meridian:

$$\frac{\partial(n_{\phi\phi}r)}{\partial\phi} - n_{\theta\theta}r_1\cos\phi + p_\phi rr_1 = 0$$

The summation of the forces perpendicular to the middle surface:

$$-n_{\phi\phi}r - n_{\theta\theta}r_1\sin\phi + p_z rr_1 = 0$$

These equations can be rewritten and presented as:

$$\begin{bmatrix} -\dfrac{1}{r_1}\dfrac{d}{d\phi} & \dfrac{1}{r_3} \\[2ex] \dfrac{1}{r_1} & \dfrac{1}{r_2} \end{bmatrix} \begin{bmatrix} n_{\phi\phi}r \\[1ex] n_{\theta\theta}r \end{bmatrix} = \begin{bmatrix} p_\phi r \\[1ex] p_z r \end{bmatrix} \qquad \text{In symbols:} \qquad \mathbf{B^T(s\it{r})} = \mathbf{p}\it{r}$$

Constitutive equation

The membrane assumption poses that a thin shell produces a pure membrane stress field and that bending stress actions are not developed. The stresses are thus uniformly distributed. The *stress vector* **s** is known as:

Stress resultants $\mathbf{s} = [n_{\phi\phi} \quad n_{\theta\theta}]^T$

For the constitutive relations the shell is assumed to behave according to Hooke's law. The stresses and strains are uniformly distributed over the thickness due to the assumption that the shell is in pure membrane behavior with no bending actions. The deformation of the middle surface is described by the normal strains $\varepsilon_{\phi\phi}$ and $\varepsilon_{\theta\theta}$. The stress-strain relation for the linear elastic shell is described by:

Deformations $\mathbf{e} = [\varepsilon_{\phi\phi} \quad \varepsilon_{\theta\theta}]^T$

The constitutive equation, also known from theory of plates, is written as:

$$\begin{bmatrix} n_{\phi\phi} \\ n_{\theta\theta} \end{bmatrix} = \frac{Et}{1-v^2} \begin{bmatrix} 1 & v \\ v & 1 \end{bmatrix} \begin{bmatrix} \varepsilon_{\phi\phi} \\ \varepsilon_{\theta\theta} \end{bmatrix} \qquad \text{In symbols:} \qquad \mathbf{s} = \mathbf{D}\,\mathbf{e}$$

The stress resultants can be determined from the strains by multiplication with the shell thickness t.

<u>Kinematic equation</u>

The deformation due to the transverse shearing stress resultants is neglected and therefore the deformation is only related to the translations of the middle surface. Furthermore, because of the membrane assumption, the influence of the rotations is neglected. Consistent with the two load terms in the load component vector **p**, the *displacement vector* **u** is defined by two displacements:

$$\mathbf{u} = [u_\phi \quad u_z]^T$$

The displacement u_ϕ is the displacement along the meridian and the displacement u_z is the displacement normal to the shell.

The meridional strain $\varepsilon_{\phi\phi}$ and the circumferential strain $\varepsilon_{\theta\theta}$ of the middle surface are respectively defined as the elongation of an infinitesimal element divided by the original length of that infinitesimal element:

$$\varepsilon_{\phi\phi} = \frac{\Delta ds_\phi}{ds_\phi} \qquad\qquad \varepsilon_{\theta\theta} = \frac{\Delta ds_\theta}{ds_\theta}$$

To derive the displacements conveniently their radii of curvature are introduced. The distance of an arbitrary point on the surface to the axis of rotation is r and r1 is its radius of curvature. The second radius of curvature is the length r2 that is measured on a normal of the meridian between its intersection with the axis of rotation and the middle surface. For hemispheres it holds that r1 = r2 = a.

Another radius of curvature r_3 is applied to investigate the equilibrium and the deformation of the shell. In the ϕr-plane, r_3 is measured on a tangent to the surface between its intersection with the axis of rotation and the middle surface. These radii and positive directions of the displacements are illustrated in figure B9.
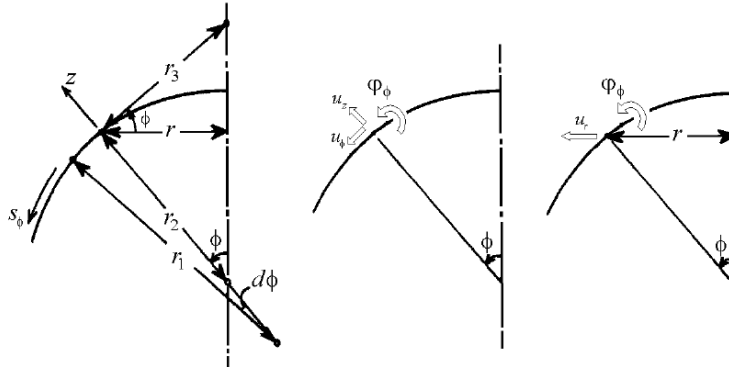

Fig.B9.   Geometry of the meridian and positive directions of the displacements   [40]

From the derivation of the meridional - and circumferential strain and the introduction of the three radii of curvature it is found that:

$$\varepsilon_{\phi\phi} = \frac{1}{r_1}\left(\frac{du_\phi}{d\phi} + u_z\right)$$
$$\varepsilon_{\theta\theta} = \frac{1}{r_2}\left(u_\phi \cot\phi + u_z\right)$$

The circumferential strain $\varepsilon_{\theta\theta}$ is rewritten to express the radial displacement in the θr-plane.

$$\varepsilon_{\theta\theta} = \frac{u_\phi}{r_3} + \frac{u_z}{r_2} = \frac{1}{r}(u_\phi \cos\phi + u_z \sin\phi)$$

The kinematic equation can now be written as:

$$\begin{bmatrix} \varepsilon_{\phi\phi} \\ \varepsilon_{\theta\theta} \end{bmatrix} = \begin{bmatrix} \dfrac{1}{r_1}\dfrac{d}{d\phi} & \dfrac{1}{r_1} \\ \dfrac{1}{r_3} & \dfrac{1}{r_2} \end{bmatrix}\begin{bmatrix} u_\phi \\ u_z \end{bmatrix} = \begin{bmatrix} \dfrac{1}{r_1}\dfrac{d}{d\phi} & \dfrac{1}{r_1} \\ \dfrac{1}{r}\cos\phi & \dfrac{1}{r}\sin\phi \end{bmatrix}\begin{bmatrix} u_\phi \\ u_z \end{bmatrix}$$

In symbols: **e = Bu**

Concluding remarks on membrane theory

Equilibrium:
$$\begin{bmatrix} -\dfrac{1}{r_1}\dfrac{d}{d\phi} & \dfrac{1}{r_3} \\ \dfrac{1}{r_1} & \dfrac{1}{r_2} \end{bmatrix}\begin{bmatrix} n_{\phi\phi}r \\ n_{\theta\theta}r \end{bmatrix} = \begin{bmatrix} p_\phi r \\ p_z r \end{bmatrix}$$

In symbols: **B$^{\text{T}}$(sr) = pr**

Constitutive:
$$\begin{bmatrix} n_{\phi\phi} \\ n_{\theta\theta} \end{bmatrix} = \dfrac{Et}{1-v^2}\begin{bmatrix} 1 & v \\ v & 1 \end{bmatrix}\begin{bmatrix} \varepsilon_{\phi\phi} \\ \varepsilon_{\theta\theta} \end{bmatrix}$$

In symbols: **s = D e**

Kinematic:
$$\begin{bmatrix} \varepsilon_{\phi\phi} \\ \varepsilon_{\theta\theta} \end{bmatrix} = \begin{bmatrix} \dfrac{1}{r_1}\dfrac{d}{d\phi} & \dfrac{1}{r_1} \\ \dfrac{1}{r}\cos\phi & \dfrac{1}{r}\sin\phi \end{bmatrix}\begin{bmatrix} u_\phi \\ u_z \end{bmatrix}$$

In symbols: **e = Bu**

In general, the formula describing the external work in figure B5 becomes: **pr= B$^{\text{T}}$ (sr)D B u**

With the formulas obtained from the equilibrium equations it becomes possible to derive the stress distribution in a spherical shell loaded by its own weight. The membrane solution describing the in-plane stresses becomes:

$$n_{\phi\phi} = \frac{1}{r\sin\phi}F(\phi)$$

$$n_{\theta\theta} = p_z r_2 - \frac{1}{\sin^2\phi}\frac{F(\phi)}{r_1}$$

With:

$$F(\phi) = \int f(\phi)d\phi = \int (p_z\cos\phi - p_\phi\sin\phi)rr_1 d\phi$$

For a spherical shell submitted to its dead weight p, a high contribution to the final total load, the membrane behavior of the shell leads to a meridional stress resultant $n_{\phi\phi}$ and a circumferential stress resultant $n_{\theta\theta}$. It is noted that the solution is only applicable for the area close to the support when the support conditions are compatible when they allow deformation in circumferential direction.

For a spherical shell it holds that:

$$r = a\sin\phi$$
$$r_1 = r_2 = a$$
$$p_\phi = p\sin\phi$$
$$p_z = -p\cos\phi$$

The membrane stress resultants are given by:

$$n_{\phi\phi} = -pa\frac{(1-\cos\phi)}{\sin^2\phi} = -pa\frac{1}{1+\cos\phi}$$ and $$n_{\theta\theta} = pa\left(\frac{1}{1+\cos\phi} - \cos\phi\right)$$
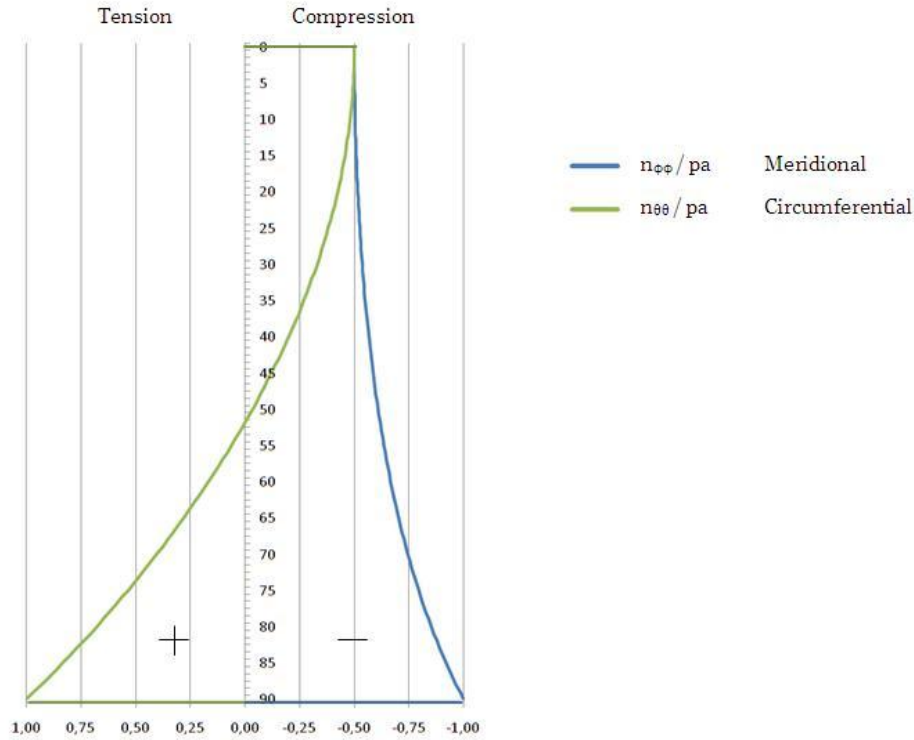
Fig.B10. Distribution of meridional and circumferential stress

The interesting results from the formulas above are illustrated by plotting the formulas $\dfrac{1}{1+\cos\phi}$ for the meridional stress and $\left(\dfrac{1}{1+\cos\phi}-\cos\phi\right)$ for the circumferential stress from the top (ϕ=0) to the base of a hemisphere (ϕ = π/2).

The equations for the membrane stresses give useful results for the design of spherical shells and are shown in figure B11. It is noticed that the stress along the meridian $n_{\phi\phi}$ is always compressive and increases when the angle ϕ increases from the top to the bottom of the shell. This is positive for concrete shells since the material is highly advantageous in compression.
In the perpendicular direction, the circumferential stress $n_{\theta\theta}$ is compressive and has the same value as the meridian stress at the top of the sphere. The circumferential stress $n_{\theta\theta}$ however, decreases along the sphere and for a certain angle will turn into a tensile stress.

This is angle is determined for $\left(\dfrac{1}{1+\cos\phi}-\cos\phi\right)=0$ which leads to ϕ=51,8°.

It is interesting to know that ancient engineers were well aware of this structural behavior of domes. When building domes with masonry or comparable materials which are relatively weak in tension but strong in compression, they would confine their dome to the compression zone or, for higher domes, would reinforce them in the tensile region with for instance wooden ties along the parallel.
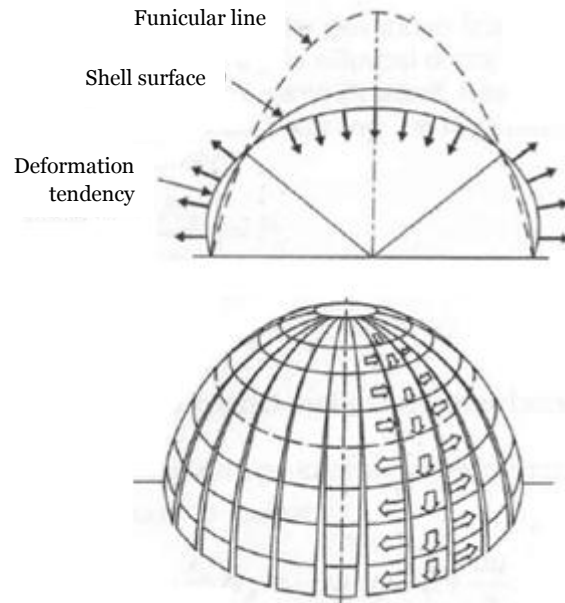
Fig.B11.   Line of thrust of the load (Funicular line) in relation to the Shell surface and the corrective hoop-forces [50]

In practice, shell structures will likely be subjected to non-axisymmetric loading such as wind forces or possible temperature gradients. The mathematical analyses of these phenomena are not within the extent of this research. However, the method for the analysis is also based on the same relations as described above.

3.2.2. Bending theory for spherical shells

In the previous chapter it is mentioned which conditions are demanded for the membrane theory to be valid. In regions where the membrane theory does not hold, also entitled disturbed zones, bending field components are produced to compensate the inadequacies of the membrane field. The corresponding analysis to these phenomena describes the bending theory of thin elastic shells. This theory is (briefly) described in this chapter for spherical shells under axisymmetric loading. The chapter is concluded by the concept of the influence length, which is of interest for practical shell design.

As can be seen in the boundary conditions, which mainly are associated to boundary conditions, the disturbances of the membrane field are often restricted to *edge disturbances* and the bending field component has a local range of influence. As a result, the undisturbed and major part of the shell behaves like a true membrane provided that the loads are distributed. This is a unique property caused by the initial curvature of the spatial structure.

Additionally, the subsequent four assumptions are stated which are obliged to obtain a bending theory for a thin elastic shell, often referred to as the classic shell theory:

I.   All points lying on a normal of the middle surface before deformation remain on that normal, which remains a normal of the deformed middle surface.
II.   For all kinematic relations it is assumed that the distance z of a point from the middle surface remains unaltered by the deformation.
III.   The stress component σ_{zz} normal to the middle surface is considered to be very small in comparison to the other stress components and is therefore neglected.
IV.   All displacements are so small that they are negligible in comparison to the radii of curvature of the middle surface. Consequently, their higher powers can be neglected and the first derivatives of the lateral displacement u_z, the slopes, are negligible compared to unity.

Assumption I. is known as the Bernoulli hypothesis, well-known from classical beam theory, which implies that the deformations due to the transverse shearing stress resultants are neglected.
Assumptions II. & III. regard that what happens in the direction normal to the middle surface of the shell, stress or strain, are of no significance to the solution. This turns out to be agreeable if the shell is thin.

Assumption IV. is required for a linear equation. The result of this assumption is that for deformed elements and non-deformed elements the equilibrium equations are identical. Hereby geometric non-linear behavior cannot be analyzed.

Similar to the method for finding the membrane equations the approach for finding the bending behavior is based on the relations found in figure B5. The investigation of the deformation of the shell of revolution is limited to the displacement u_x along the meridian and the displacement u_z normal to the middle surface. The following vectors now apply:

Degrees of freedom $\qquad$ $\mathbf{u} = [u_x \quad u_z]^T$

Deformations $\qquad$ $\mathbf{e} = [\varepsilon_{xx} \quad \varepsilon_{yy} \quad \kappa_{xx} \quad \kappa_{yy}]^T$

Stress resultants $\qquad$ $\mathbf{s} = [n_{xx} \quad n_{yy} \quad m_{xx} \quad m_{yy}]^T$

External loads $\qquad$ $\mathbf{p} = [p_x \quad p_z]^T$
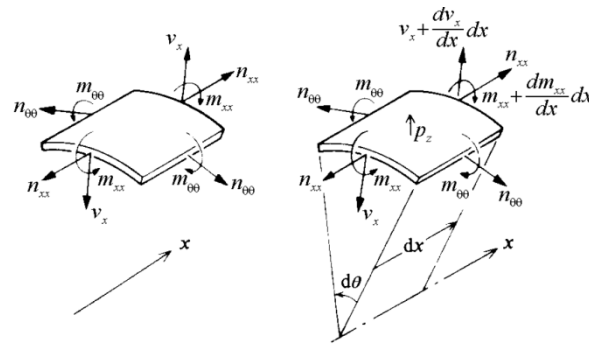
Fig.B12. Stress resultants on an axisymmetrically loaded shell element $\qquad$ [40]

<u>Equilibrium equation</u>

The load component p_y is zero and the equilibrium of forces in the same direction needs not to be investigated because the stress resultant n_{yy} is constant in the circumferential direction. The non-trivial equilibrium equations consider the equilibrium of forces for the meridional direction and for the direction normal to the middle surface. For a shell of revolution under axisymmetric loading and without transverse shearing stress resultant v_y equal the equilibrium equations read:

$$\frac{dn_{xx}}{dx} + p_x = 0$$

$$\frac{dv_x}{dx} + k_x n_{xx} + k_y n_{yy} + p_z = 0$$

Corresponding to known theory of bending action of a flat plate, the equilibrium of moments with respect to the y -direction yields for the transverse shearing stress resultant:

$$\frac{dm_{xx}}{dx} - v_x = 0$$

Neglecting the transverse shearing stress resultant v_x, the resulting two equilibrium equations between the stress resultant vector $\mathbf{s}$ and the load component vector $\mathbf{p}$ become:

$$\begin{bmatrix} -\dfrac{d}{dx} & 0 & 0 & 0 \\ -k_x & -k_y & -\dfrac{d^2}{dx^2} & 0 \end{bmatrix} \begin{bmatrix} n_{xx} \\ n_{yy} \\ m_{xx} \\ m_{yy} \end{bmatrix} = \begin{bmatrix} p_x \\ p_z \end{bmatrix} \qquad \text{In symbols:} \qquad \mathbf{B}^T \mathbf{s} = \mathbf{p}$$

Constitutive equation

The constitutive relation for the combined stretching and bending behavior of a thin shell is thus described by the membrane behavior of the shell in combination with the bending behavior of a flat plate.
The *extensional rigidity* D_m (membrane behavior) and the *flexural rigidity* D_b (bending behavior) are respectively defined by:

$$D_m = \frac{Et}{(1-v^2)}$$

$$D_b = \frac{Et^3}{12(1-v^2)}$$

The relation between the strain vector **e** and the stress resultant vector **s** becomes:

$$\begin{bmatrix} n_{xx} \\ n_{yy} \\ m_{xx} \\ m_{yy} \end{bmatrix} = \begin{bmatrix} D_m & vD_m & 0 & 0 \\ vD_m & D_m & 0 & 0 \\ 0 & 0 & D_b & vD_b \\ 0 & 0 & vD_b & D_b \end{bmatrix} \begin{bmatrix} \varepsilon_{xx} \\ \varepsilon_{yy} \\ \kappa_{xx} \\ \kappa_{yy} \end{bmatrix}$$
    In symbols: **s = D e**

Kinematic equation

For the membrane strains the relation of the membrane behavior is used. It is rewritten for the axisymmetric behavior eliminating γ_{xy} and u_y.

$$\begin{bmatrix} \varepsilon_{xx} \\ \varepsilon_{yy} \end{bmatrix} = \begin{bmatrix} \frac{d}{dx} & -k_x \\ 0 & -k_y \end{bmatrix} \begin{bmatrix} u_x \\ u_z \end{bmatrix}$$

The deformation vector contains the changes of curvature κ_{xx} and κ_{yy}, they are derived from the rotations φ_x and φ_y.

$$\varphi_x = -\frac{du_z}{dx}$$

$$\kappa_{xx} = \frac{d\varphi_x}{dx} = -\frac{d^2 u_z}{dx^2}$$

And:

$$\varphi_y = 0$$

$$\kappa_{xx} = 0$$

Consequently, the kinematic relation reads:

$$\begin{bmatrix} \varepsilon_{xx} \\ \varepsilon_{yy} \\ \kappa_{xx} \\ \kappa_{yy} \end{bmatrix} = \begin{bmatrix} \frac{d}{dx} & -k_x \\ 0 & -k_y \\ 0 & -\frac{d^2}{dx^2} \\ 0 & 0 \end{bmatrix} \begin{bmatrix} u_x \\ u_z \end{bmatrix}$$
    In symbols: **e = Bu**

Concluding remarks on membrane theory

Equilibrium: $$\begin{bmatrix} -\frac{d}{dx} & 0 & 0 & 0 \\ -k_x & -k_y & -\frac{d^2}{dx^2} & 0 \end{bmatrix} \begin{bmatrix} n_{xx} \\ n_{yy} \\ m_{xx} \\ m_{yy} \end{bmatrix} = \begin{bmatrix} p_x \\ p_z \end{bmatrix}$$
    In symbols: **B^T s = p**

Constitutive:

$$\begin{bmatrix} n_{xx} \\ n_{yy} \\ m_{xx} \\ m_{yy} \end{bmatrix} = \begin{bmatrix} D_m & vD_m & 0 & 0 \\ vD_m & D_m & 0 & 0 \\ 0 & 0 & D_b & vD_b \\ 0 & 0 & vD_b & D_b \end{bmatrix} \begin{bmatrix} \varepsilon_{xx} \\ \varepsilon_{yy} \\ \kappa_{xx} \\ \kappa_{yy} \end{bmatrix}$$

In symbols: $\mathbf{s = D\ e}$

Kinematic:

$$\begin{bmatrix} \varepsilon_{xx} \\ \varepsilon_{yy} \\ \kappa_{xx} \\ \kappa_{yy} \end{bmatrix} = \begin{bmatrix} \dfrac{d}{dx} & -k_x \\ 0 & -k_y \\ 0 & -\dfrac{d^2}{dx^2} \\ 0 & 0 \end{bmatrix} \begin{bmatrix} u_x \\ u_z \end{bmatrix}$$

In symbols: $\mathbf{e = Bu}$

In general, the formula describing the external work in figure B5. becomes: $\mathbf{p = B^T D B u}$

<u>Influence length</u>

The influence length is introduced to determine over what area the edge disturbances occur. The analysis for this parameter contains severe mathematical work. This can be summarized by formulating the differential equation for the axisymmetric problem. Here, the equilibrium equation is used which leads to a single forth order differential equation which is represented below:

$$D_b \frac{d^4 u_z}{dx^4} + D_m(1-v^2)k_y^{\ 2} u_z = p_z - (k_x + vk_y)\int p_x dx$$

One of the interesting conclusions of the analysis is that the inhomogeneous solution to this differential equation describing the bending behavior of a circular cylindrical shell is identical to the membrane solution.
For the behavior under axisymmetric loading the homogeneous solution is therefore adapted as the edge disturbance, representing the bending action of the shell and the influence of the edge disturbance is found to be local. With this theory the bending behavior of thin shells of revolution can also be analyzed.

For membrane-compatible load types, like axisymmetric- and lateral load types, the inhomogeneous solution to the bending theory can be used as the membrane solution. If the membrane displacements at the boundaries are not consistent with the actual boundary conditions due to edge disturbances, the homogeneous solution to the bending equations can be used as a discontinuity to the membrane behavior. It turns out that that, for the axisymmetric case, the influence of this edge disturbance is local and that the influence length is often much smaller than the length of the structure.

Setting the load terms at the right-hand side of the formula equal are set to zero and the parameter µ is introduced:

$$\mu^4 = \frac{D_m(1-v^2)k_y^{\ 2}}{4D_b} = \frac{D_m}{D_b}\frac{(1-v^2)\left(\dfrac{1}{r_y}\right)^2}{4D_b} = \frac{3(1-v^2)}{(r_y t)^2}$$

$$\frac{d^4 u_z}{dx^4} + 4\mu^4 u_z = 0$$

The general solution of this reduced differential equation can be written as:

$$u_x(x) = e^{-\mu x}\left[C_1 \cos \mu x + C_2 \sin \mu x\right] + e^{\mu x}\left[C_3 \cos \mu x + C_4 \sin \mu x\right]$$

In this expression the first term is an oscillating function that decreases exponentially with increasing x. The other term increases exponentially with increasing x. Both separate terms of the general solution are presented below with all constants chosen equal to 1.
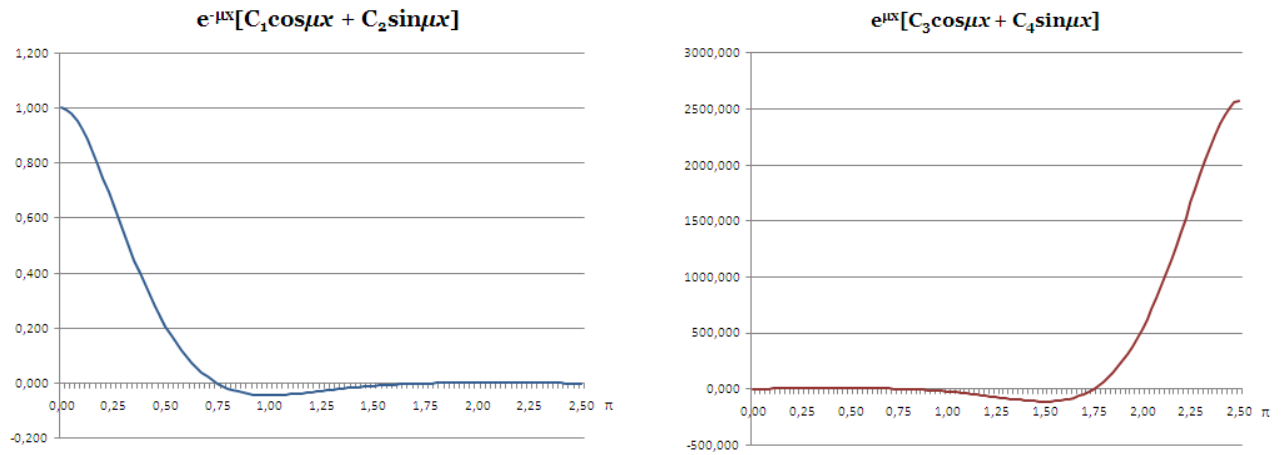
Fig.B13.   Influence lengths of a dome

After elaboration the factors C_3 and C_4, and therefore the exponential increasing second term, are not found to have a significant contribution to the final solution. Therefore, the solution to the differential equation perpendicular to the edge can be rewritten and frequently appears in literature as:

$$f = f_{max}e^{-\mu x}\cos \mu x \qquad\text{or}\qquad f = f_{max}C_5 e^{-\mu x}\sin \mu x = f_{max}\sqrt{2}e^{\frac{1}{4}\pi}e^{-\mu x}\sin \mu x$$

Where f can represent displacements, moments, shear- or membrane forces i.e. situations which produce out-of-plane actions.
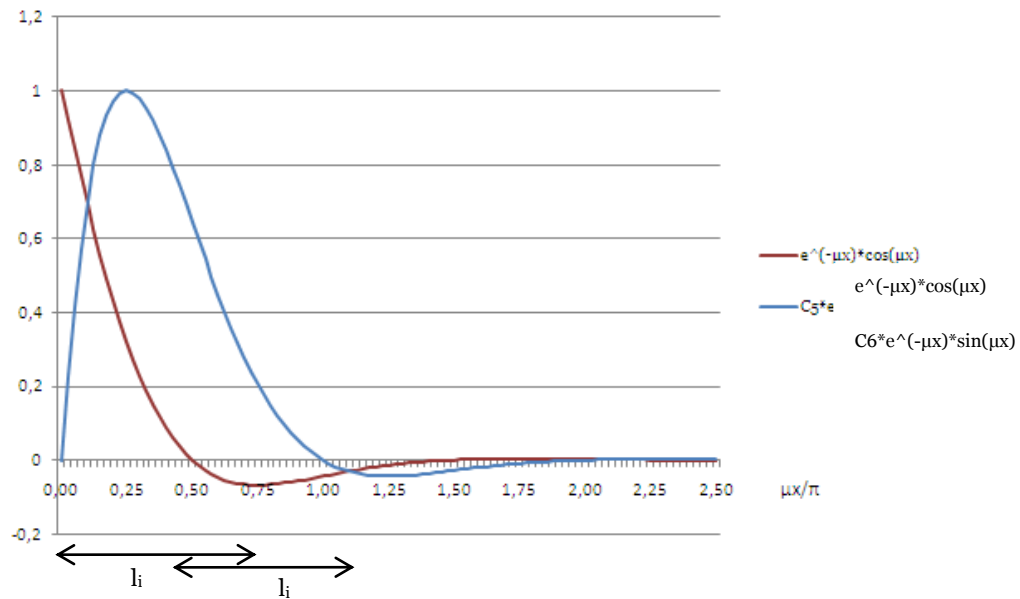
Fig.B14.   Influence lengths of a dome

From the graph above, where the relative values of the formulas for out-of-plane actions are shown, it can be seen that for a distance $\mu x > \pi$ the value of f has decreased over 95% of the original value. This corresponds with the theory that the edge disturbance is not negligible for a length that is about equal to half of the natural wavelength of 2π. The influence length l_i is therefore defined as:

$$l_i = \frac{\pi}{\mu} \qquad\text{so}\qquad l_i = \frac{\pi\sqrt{Rt}}{\sqrt[4]{3(1-\upsilon^2)}}$$

This leads to:

$$l_i \approx \pi . \frac{\sqrt{Rt}}{\sqrt[4]{3}} \approx 2,4\sqrt{Rt}$$

Figure B15. shows the influence length on a spherical shell. The concept 'influence length' can now be used to check the locations of the bending moments in results of the FEM-model calculations. An additional practicality of the concept is the possible use for a choice of the finite element mesh. It is found that the at least 6 elements in the length l_i are needed to provide sufficient accuracy.
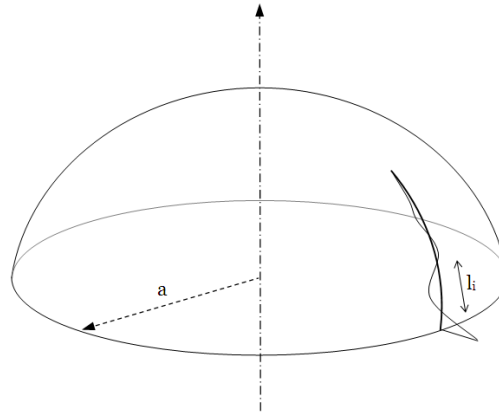

Fig.B15.   Influence lengths of a dome

3.3. Structural failure

It is cited before that the structural efficiency of shell structures is caused by three-dimensional in-plane resistance to external forces and little to no bending behavior. A consequence of the positive effect caused by the possible relatively small thickness is that the shell design strength is mostly governed by their buckling capacity.
A shell can however, fail due to material nonlinearity, such as cracking and crushing, or by a combination of both geometry- and material non-linearity. So, besides being a 'from resistant structure' shell structures are also imperfection-sensitive structures.

Buckling is a mathematical instability which may occur for structures that are generally subjected to loads which cause in-plane compressive forces. The buckling failure mode is characterized by visibly large transverse deflection in one of the possible instability modes. Buckling instability can be characterized as a premature failure mechanism caused by eccentricity of compression forces, initiated by deformations or initial geometric imperfections. For this research it is interesting to note that shell structures, typically subjected to compressive forces, may fail due to insufficient stability rather than high compressive strength exceeding the material strength.

In fact, dimensioning of shell thicknesses is usually based on buckling considerations rather than material strength. It is therefore that for the high performance concrete, applied in this research, it holds that the performance aspects beside the material strength caused expectancy for fertile use of UHPC within large span shell structures.

Theoretically, buckling is caused by a bifurcation in the solution to the equations of static equilibrium. This mode of failure is also described as failure due to elastic instability. In practice, buckling is characterized by a sudden failure of a structural member subjected to compressive stress where the actual compressive stress at the point of failure is less than the ultimate compressive stresses that the material is capable to resist.

Buckling of a structural component may affect the strength or stiffness of an entire structure resulting in significant and rather unpredictable deformations which may even trigger unexpected global failure of the structure. Therefore, it is important to be able to predict the buckling capacity of structures in order to avoid premature failure.

Also for this chapter it holds that the approach is based on 'Theory of shells' by Blauwendraad and Hoefakker.

3.3.1. Buckling

<u>Linear critical loading</u>

Buckling is a phenomenon mathematically challenging problem, especially since for curved surfaces more mathematical complexities arise. The structural behavior of shells including large displacements is described by an eight order differential equation.

$$\frac{Et^3}{12\left(1-v^2\right)}\nabla^2\nabla^2\nabla^2\nabla^2 u_z + Et\Gamma^2 u_z = \nabla^2\nabla^2\left(p_z - n_{xx}u_{z,xx} - 2n_{xy}u_{z,xy} - n_{yy}u_{z,yy}\right)$$

Where u_z is the displacement perpendicular to the shell surface, p_z is the loading perpendicular to the surface. ∇^2 and Γ^2 are the operators:

$$\nabla^2 = \frac{\delta^2(.)}{\delta x^2} + \frac{\delta^2(.)}{\delta y^2}$$

$$\Gamma = k_x \frac{\delta^2(.)}{\delta y^2} - 2k_{xy}\frac{\delta^2(.)}{\delta x\delta y} + k_y\frac{\delta^2(.)}{\delta x^2}$$

Provided that $p_x = p_y = 0$ and k_x, k_y , k_{xy} are constant.

The x and y direction often are not linear but are plotted on the surface of the shell. The differential equation can be solved analytically for elementary shell shapes, like spherical shells, and elementary loading, like uniform pressure. The classical buckling load for a perfect elastic sphere under uniform pressure p_{cr}^{lin} is derived as:

Critical loading:

$$p_{cr}^{lin}[N/m^2] = \frac{-2}{\sqrt{3(1-v^2)}}\frac{Et^2}{R^2} \approx -1,16\frac{Et^2}{R^2}$$

(Formula 3.3.1.1.)

Critical membrane force:

$$n_{cr}^{lin}[N/m] = \frac{-1}{\sqrt{3(1-v^2)}}\frac{Et^2}{R} \approx -0,58\frac{Et^2}{R}$$

(Formula 3.3.1.2.)

These formulas are suitable for hand calculations. With this formula it is found that although a hemispherical dome with an opening angle of ϕ=90° differs geometrically from that of an 'incomplete' spherical shell with the same radius, the critical local buckling pressure of both shells is nonetheless of the same order of magnitude. There are however some differences in the buckling behavior of hemispherical domes and spherical shells.

Also, when the span becomes very large, global buckling may take place. This is illustrated by a circular tube cylinder. Global buckling behavior is not predicted correctly by the equation above since this is derived for small deformations.
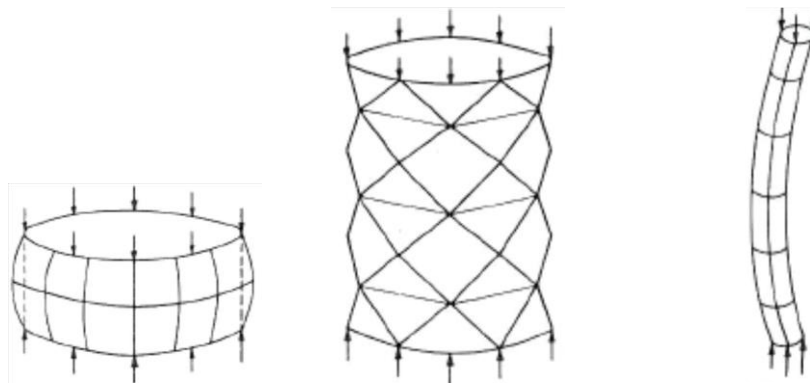
Fig.B16.   Buckling in very short cylinder, moderately long cylinder and long cylinder [42]

Compound buckling

The fact that in these equations the buckling mode or shape is not part of the equation indicates that the particular buckling mode is not defined. For shells it applies that several buckling modes are associated with the same linear critical load, this confirms that spherical shells as well as other types of shells exhibit compound buckling behavior, sometimes referred to as multi-mode buckling. In general, thinner shells experience compound buckling up to a higher degree than thicker shells.

Compound buckling is a phenomenon which refers to buckling modes associated with the same critical load, causing the structure to be highly sensitive to imperfections because of the interaction of buckling modes, which result in a strong softening response after the bifurcation point.

Unlike buckling in columns and plates, shells experience a sudden decrease in load carrying capacity after the bifurcation point. This bifurcation point marks a point of equilibrium which may occur at a certain stage of loading. In this point there are two possible stages of equilibrium. After the bifurcation point the primary path becomes unstable after buckling. The structure could diverge to a new stable path, the secondary path, of deformation. The loading condition corresponding to the bifurcation point is normally called the critical load.
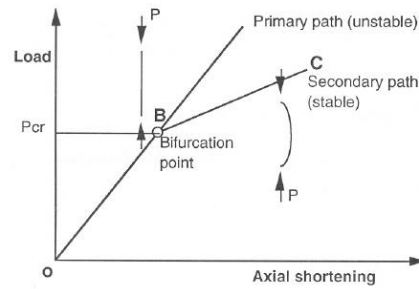
Fig.B17.   Theoretical relations & bifurcation buckling of an axially compressed column   [42]

Within the linear range the buckling modes of a shell are independent and uncorrelated. In the post-buckling regime the modes start to interact, causing the load carrying capacity to fall down. In general, thinner shells experience this compound buckling up to a higher degree than thicker shells.

Buckling of domes

In hemispherical domes instability could inflict the whole shell or may snap-through confined to a limited region. The occurrence of these types of buckling depends mainly on thickness and shell radius. For spherical shells, the loss of stability can appear by symmetrical of unsymmetrical deformations. Both modes can extend to the whole shell surface. The post-critical behavior of spherical shells differs from that of complete domes. A spherical shell can pass to a post-buckling equilibrium position produced by deformations much larger than those of the corresponding dome.
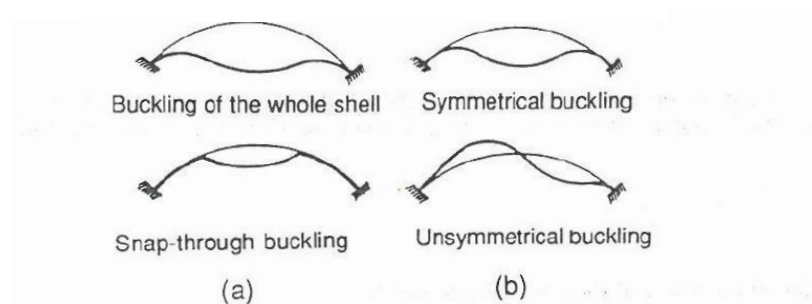
Fig.B18.   Symmetrical and non-symmetrical buckling modus of domes   [42]

Non-linearity

In practice it was found that shells are very sensitive to initial geometric imperfections. This causes the bifurcation point never to be reached. Differences between experiments and theory are beside geometric imperfections also caused by material nonlinearities such as cracking and crushing.
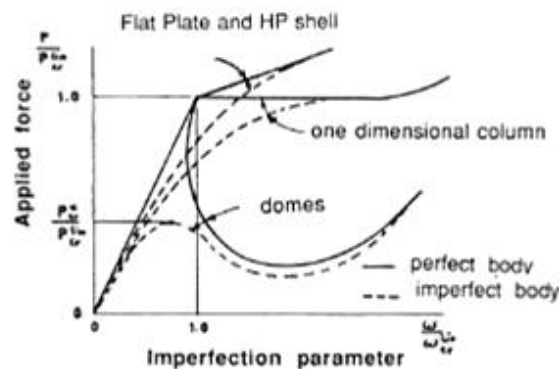
Fig.B19.   Schematic representation of buckling behavior of various structural elements   [47]

In [43] research on these nonlinearities is presented. The factor 1.16, found in formula 2.3.1.1. has been highly discussed over the years. In 1939 the lowest point of the post-critical load-displacement curve was described by Von Karman and Tsien with the constant 0,365. Over the years more and more additions to the research for the 'true value' were done resulting in a value as low as 0,126 found by Dostanova and Raizer in 1973.

The insecurities about the nonlinearities and buckling behavior were solved by using high safety factors for shell design. Further design considerations resulting from theory and experiments are discussed in the next chapter.
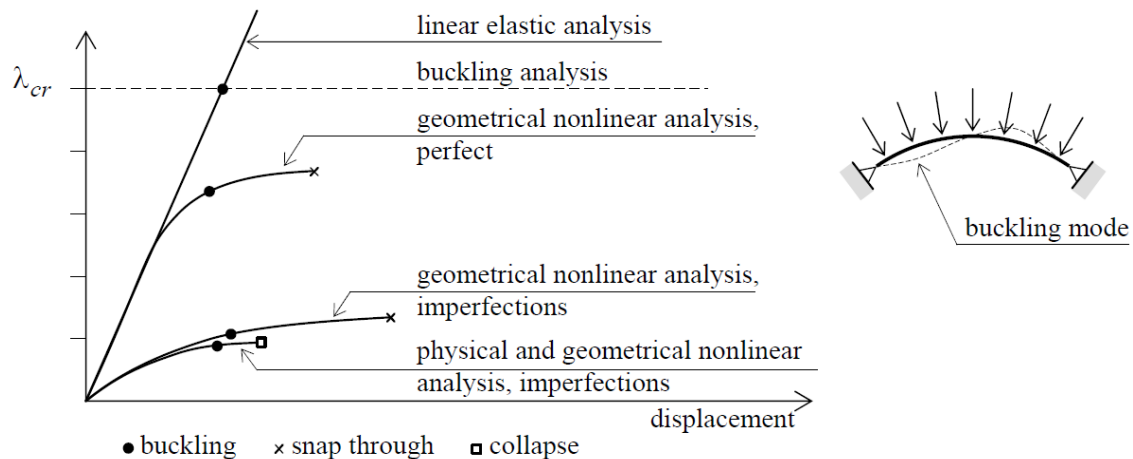
Fig.B20. Shell finite element analysis of a shallow dome   [47]

3.3.2. Failure aspects

The formulas described in paragraph 3.1.1. are derived for perfect elastic shells. It is acknowledged that buckling is highly dependent on small deviations from the perfect shell. These deviations cannot be neglected for they appear in multiple contents like initial differences in the geometry, residual stress, temperature stress, inhomogeneities, creep, shrinkage, eccentricities of loading and first order deformations. The practical buckling capacities of the shell structures are therefore significantly lower than the theoretical buckling values. Results from experiments show, due to these numerous imperfection components, a large dispersion.
Aspects of importance for further design, resulting from the failure aspects, are described in chapter 3.4.1.

Koiter's laws

Warner T. Koiter was an influential mechanical engineer and the Professor of Applied Mechanics at Delft University of Technology in the Netherlands from 1949 to 1979 and is primarily known for his asymptotic theory of initial post-buckling stability. It explains the considerable difference that was found between critical loads and experimental maximum loads, which puzzled scientists for decades.

Koiter's laws clarify that initial geometrical imperfections in the shell cause the theoretical critical load never to be reached and lead to limit point buckling at a considerably lower load. The size of the imperfections determines the limit load at which the shell fails. In case of plastic buckling, the fall-back is further intensified by material nonlinearity.
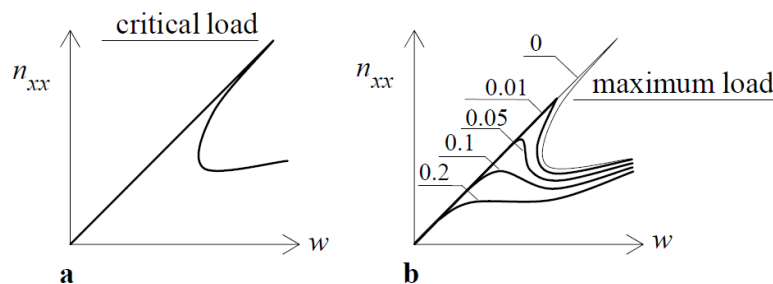

Fig.B21. Buckling of cylinders for different geometric imperfection amplitudes   [41]

According to Koiter, the equilibrium of a perfect system can be described by:

$$\frac{\lambda}{\lambda_{cr}} = 1 - c_1 w - c_2 w^2$$

Where λ is the load factor, λ_{cr} is the critical load factor, w is the amplitude of the deflection, c_1 and c_2 are constants characterizing the given structure. There are three types of post critical behavior displayed in figure B22. Type I behavior occurs when $c1 = 0$ and $c2 < 0$. The structure is not sensitive to imperfections.

Type II behavior occurs when $c1 = 0$ and $c2 > 0$. The structure is sensitive to imperfections. The coefficient ρ is introduced which depends on the imperfection shape. Also, imperfection amplitude parameter w_0 is introduced, which completes the $\frac{2}{3}$ power law. The maximum load factor is equal to:

$$\frac{\lambda}{\lambda_{cr}} = 1 - 3 \left(w_0 \frac{1}{2} \rho \sqrt{c_2} \right)^{\frac{2}{3}}$$

Type III behavior occurs when $c1 > 0$. The structure is very sensitive to imperfections and can be described by the $\frac{1}{2}$ power law. The maximum load factor is then equal to:

$$\frac{\lambda}{\lambda_{cr}} = 1 - 2 \left(w_0 \frac{1}{2} \rho \sqrt{c_2} \right)^{\frac{1}{2}}$$
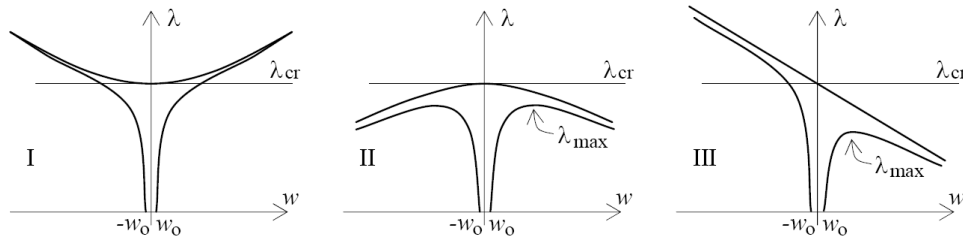
Fig.B22. Basic types of post buckling behavior   [41]

In-extensional deformation

It is explicated that shells obtain their strength from in-plane action and resistance with mostly in-plane action and little bending moments. In case of in-extensional deformation however the strains of the middle surface are equal to zero and resistance is small caused by mostly bending action. A thin walled structure, which is much stiffer in-plane than perpendicular to its plane, a shell can easily deform to such deformations because they do differ the strain energy. Hence, when the deformation is in-extensional the Gaussian curvature does not change.

This interesting feature of shell structures explains that shells can be referred to as form resistant structures. Whereas beams resist to lateral load by deflection, extension and intern bending moment the structural principle of shells is produced by the fact that a shell is only a shell when it stays in its original shape when subjected to loading. If not, in-extensional deformation occurs.
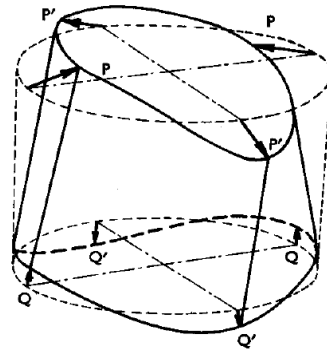
Fig.B23. In-extensional deformation of a circular cylindrical shell   [40]

Yoshimura pattern

In the previous paragraphs some remarkable aspects of shell structures are discussed. The mainly important aspects for further research and design have been highlighted. Another notable aspect of shell buckling is the contingency for shell to buckle into a diamond shape, called a Yoshimura pattern.

In paragraph 3.3 the buckling mode was found to be of no significance to the solution of formula (2.3.1.1). From experiments it appears that the buckled shape which belongs to the equation is either a local ring buckling mode or a local square (chess-board) buckling mode. Whether a shell buckles in ring mode or square mode depends on the shell thickness and its radius.

When loading and buckling progresses it may occur that the ring buckling mode will convert into the square pattern. The material of the shell starts to deform plastically and the pattern becomes diamond-shaped. This shape is called a Yoshimura Pattern, which is basically an in-extensional deformation. In practice, large extensions are needed before the Yoshimura pattern is achieved.
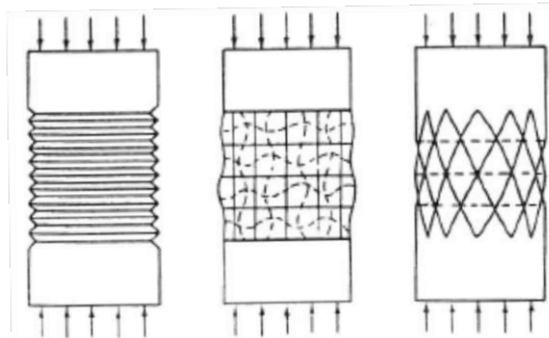
Fig.B24. Buckling modes of an axially compressed cylinder [42]

Fig.B25. Experiment on an aluminum hyperboloid toothbrush holder (Yoshimura pattern) [RtM]

3.4. Design considerations

Now the theory for shells is described it is time to transfer the theoretical knowledge to their consequences within structural design. Overall, the requirements on the main bearing structure can be specified as follows:

A.   Requirements on safety against failure
B.   Requirements on serviceability in normal use
C.   Requirements on durability

The requirements on the safety against failure imply the unfavorable combinations of factors affecting the resistance of the structure, the possibility of accidental loads and gross errors. Factors affecting the resistance are load combinations, material strength, structural dimensions, imperfections and minor damages. Accidental loads are loads with a single occurrence with a significant magnitude. Gross errors can be caused by insufficient design work, material production and construction errors.

The requirements within normal apply, in most cases, to deformations and vibrations. Large deformations highly interlink with inconveniences for they can lead to damaging of building components, discomfort to the people within the building or can even disturb of impair the functions within the building.

The durability requirements concern the material within normal use and circumstances. The life span of the material is influenced by the characteristics of abrasion and penetration of external substances. The requirements are highly associated with the serviceability aspects.

To maximize the fulfillments of the requirements on safety the shell structure shall be designed, fabricated and constructed in a way that the probability of failure becomes significantly low. This implies adequate design and sufficiently large factors of safety, optimal prevention of accidental loads and adequate engineering. This last aspect involves proper calculation and schematizing, minimizing the possibility of construction errors. Both aspects demand appropriate knowledge of people involved and a well organized construction process.

The fulfillments of the requirements of serviceability also imply prevention. Within the engineering phase the effects of ultimate displacements and deflections are to be limited on global and local level. The preventing concerns also concern the durability aspects. As mentioned in part A, the combination of fine powders and chemical reactivity, and therefore low porosity, provide the superior durability characteristics of UHPC.

The stability failure aspects of shells, as described in chapter 3.3, lead to the fact that dimensioning of shell thicknesses is usually based on buckling considerations rather than material strength. Along with many others, the failure requirements may to some extent be varied with respect to the balance between quality level and costs.

Spherical shell structures are, due to the leading buckling considerations, frequently accompanied by strengthening members such as stiffeners, edge and/or ridge beams and end diaphragms. To expand the moment of inertia of the shell ribs and stiffeners and/or sandwich panels can be applied.

In case of sandwich and rib-stiffened shells we speak of composite shells. Both types of shells, standard or composite, have in common that they may fail not only by overall but also by local buckling. The critical load intensities of these two kinds of buckling generally differ from each other and therefore do not interact. If, however, the proportions of a composite shell cause overall and local buckling to occur at about the same load the critical load may considerably reduce, a phenomena known as compound buckling.

3.4.2. Span to sagitta ratio

It is concluded that the effect of curvature is positive concerning overall buckling stability. The curvature of the shell depends on the ratio between the span and the sagitta. A larger curvature of the general surface, meaning small shell radii, leads to higher opening angles at the edges of the shell. This may cause the existence of tension forces in the base of the shell. In case these forces exceed the capacity of UHPC it can be withstand by additional, passive, reinforcement.

For the circumferential stress in a spherical shell a relation was found in paragraph 3.1.4. with the conclusion that the circumferential stress changes sign, from compression to tension, for the aperture angle of $\phi = 51,8°$.

This angle serves as a design guideline which is of interest for the ratio between the sagitta (height) and the span of the spherical shell.
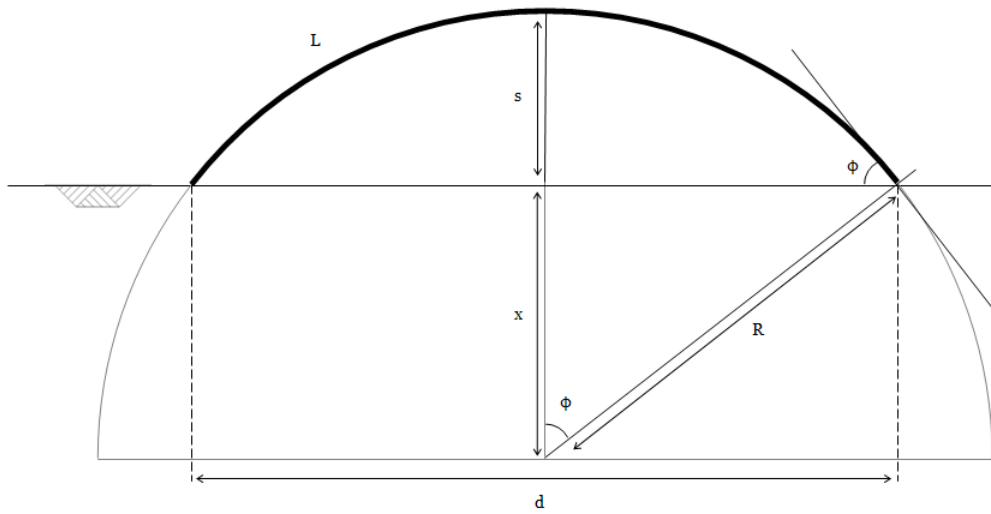

Fig.B26. Proportions in shell design

With the parameters in figure B26 it shows that:

$$\sin \Phi = \frac{d}{2R}$$

$$\tan \Phi = \frac{d}{2x}$$

$$s = R - x = \frac{d}{2\sin \Phi} - \frac{d}{2\tan \Phi}$$

$$\max. \frac{s}{d} = \frac{1}{2\sin \Phi} - \frac{1}{2\tan \Phi} = \frac{1}{2\sin(51,8)} - \frac{1}{2\tan(51,8)} = \frac{1}{4,12}$$

With this value known it can be used as a maximum design guideline for the rise-to-span-ratio gained from theoretical dead load analysis. Domes executed in practice usually have ratios between 1/6 (ϕ=36,9°) and 1/10 (ϕ=22,6°), of which the last are considered to be flat shells. In [45] Scordelis describes usual sagitta to span ratios of 1/4.82 to 1/7.46.

The effect of the ratio of sagitta to span is investigated in chapter 8.1. The maximum value as found above serves as guideline and is tested for a spherical shell subjected to loading as found in the next chapter.

3.4.3. Edge ring

A shell will have a pure membrane behavior provided certain boundary requirements, loading conditions and geometrical configurations are satisfied. In order for membrane theory to be totally applicable, the forces and the displacements at the shell boundaries must be force-compatible and deformation-compatible with the true membrane behavior of the shell. Alongside with these aspects, the exceptional behavior of shell structures was referred to as from resistant structures.

The most prominent conditions consider concentrated forces and deformation constrains. The membrane behavior displacement requirements are illustrated in figure B6. In these cases, pure membrane action requires that the domes subjected to applied loading or temperature variations have free boundary displacements. In practice, the actual support displacement conditions impose constrains to such free boundary displacements and hence disturb the pure membrane field.

In shell structures, based on the form resistance aspect and buckling considerations, domes are regularly provided with an edge supporting ring. To stiffen a shell the designer may apply a stiffening ring at the foundation or an intersection of the shell with other structural elements. The overall membrane behavior of domes with or without rings is represented in figure B27 where the domes have distributed supports and are subjected to axisymmetric vertical loading.

The Eurocode [1993-1-6] describes an 'base ring' as a structural member that passes around the circumference of the shell of revolution at the base and provides a means of attachment of the shell to a foundation or other structural member. It is needed to ensure that the assumed boundary conditions are achieved in practice.
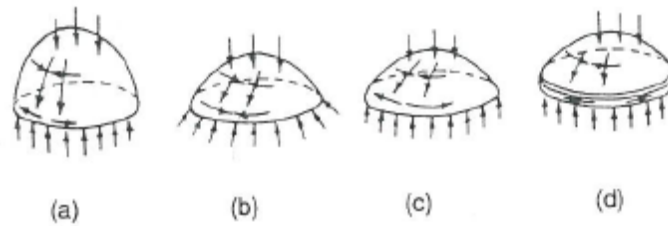

Fig.B.27. Membrane behavior of axisymmetrial loaded domes.   [42]
(a) A 'high rise' dome with vertical support
(b) A low rise dome with hinged support
(c) A low rise dome with vertical support
(d) A low rise dome with vertical support and edge ring

In figure B.27a the hemispherical shell without edge ring shows compressive stress in meridional direction. The hoop forces changes sign, as explained in part B. The hoop tension is taken by the shell itself.

Figure B.27b shows a spherical cap with a membrane field, meridional and hoop direction, which is totally compressive. At the edges of this shell, the inclined meridional force is carried through the support, which is hinged. The equilibrium requirements of membrane behavior are satisfied for membrane behavior.

Figure B.27c shows that, for having only vertical support and where the radial deformation of the edge of the spherical cap is not prevented, a severe disturbance of the membrane state develops. A state of stress develops within a narrow band adjacent to the edge which will displace outwards. At the edge a considerable tensile stress develops in circumferential direction and bending stresses in meridional direction. This implies yield stress or snap through to be reached for lower values than predicted.

The spherical cap of figure B.27d has a supporting ring at the edge beside its vertical support. Here, the horizontal thrust is totally carried by the ring. It is here explained that domes are usually accompanied with edge rings which are designed so that sufficient stability, stiffness and bearing capacity of the entire structure are achieved.
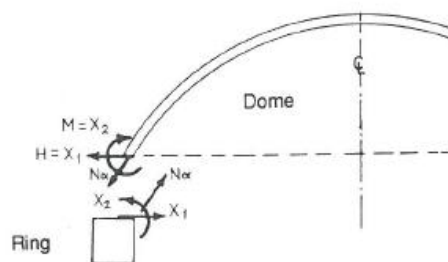

Fig.B.28. Interaction between an axisymmetric shell and its edge ring [42]

3.4.4. Rib-stiffened shell

Rib-stiffening can severely increase the critical load of the whole shell structure in an economical, material efficient, manner. It holds that the distance between the ribs needs to be smaller than the buckling length of the unstiffened skin itself. If not, the shell is insufficiently stiffened and will buckle at the same stress as the unbuckled state. The structure is this case will be less economical than when the material of the ribs was used to increase the shell thickness.

Thus, for common engineering structures, the distances between the ribs have to be chosen inferior to the buckling lengths of the unstiffened shell. Since the buckling length increases during buckling process choosing a rib distance smaller than the linear theoretical buckling length benefits to the safety of the design. As a simple rule

to find a directive for the necessitated stiffness of the ribs it can be stipulated that the ribs are capable of carrying all the load acting on the skin and on the ribs, assuming infinitely elastic behavior.

Ribs and stiffeners can be introduced to resist large concentrated loads on a thin wall shell. Both strengtheners contribute in distributing the load over a larger part of the shell surface. In comparison, a point load on an unstiffened shell results primarily in a rapidly growing, nonlinear radial deformation which can become of an order of several times the shell thickness. A local yield failure as well as buckling may take place, especially for very shallow shells. While large concentrated loads are not expected on the spherical shell it is blatant that the application of stiffeners significantly contributes to the shell rigidity.

The Eurocode [Design of steel structures: Strength and Stability of Shell Structures 1993-1-6] describes a rib as a local member that provides a primary load carrying path for bending down the meridian of the shell, representing a generator of the shell of revolution. It is used to transfer or distribute transverse loads by bending. The same article describes a ring stiffener as a local stiffening member that passes around the circumference of the shell of revolution at a given point on the meridian. It is normally assumed to have no stiffness for deformations out of its own plane , being meridional displacements of the shell, but is stiff for deformations in the plane of the ring. It is provided to increase the stability or to introduce local loads acting in the plane of the ring.

3.4.5. Edge thickness

In multiple aspects of shell behavior it is concluded that a relative increase of the shell thickness at its edges can severely enhance the structural behavior and bearing capacity. Compatibility requirements, such as local increase of moments, occur at the supports together with the largest meridional stress and displacements. Also, buckling is likely to occur at the shell edges. The opportunity for more effective material use close to the supports again recognized.

The distribution of material along the meridional axis is optimized in the design calculations of chapter 8.4. As an early estimate the formula for the influence length and its development along the axis can be used for the length where the increase of shell thickness is most effective.

3.4.6. Sandwich shell construction

Thin UHPC-structures under compression are in danger of stability failure far below the admissible concrete compression stress. Sandwich-elements are one possibility to improve the inertia and use of the material. Sandwich construction, like the name implies, usually consists of two faces which are kept separate by a middle core. The faces, which in this design consist of UHPC, usually carry the in-plane primary loads while the core resists the transverse shear. The two faces regularly are composed of the same material and have the same thickness, which places the neutral axis at the mid-plane of the cross section. By enlarging the structural height of the element the moment of inertia is magnified significantly. It is noted that the faces obviously have to be fastened to the core in such a way to assure structural rigidity within the element.

Solid cross section
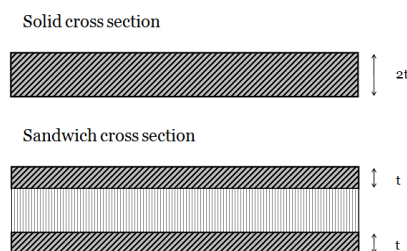
2t

Sandwich cross section

t

t

Fig.B.29. Cross-section of solid- and sandwich construction

The core is commonly multi-used by application of heat insulating material. Polyurethane and polystyrene heat insulation, shaped at the surface, are especially suited for the core layer which also strengthens the top layers against local buckling.

Beside the advantages given above sandwich panels entail disadvantages considering the production, differences in temperature strains in the top and bottom layer, probable condensation at the bottom layer and complicated

force introduction and distribution. Sandwich-elements are however a possibility to improve the use of the bearing material. Therefore this principle is taken into consideration within further design.

3.4.7. Imperfections and non-linearity

As mentioned, the practical buckling capacities of shell structures are significantly lower than the theoretical critical buckling values. This is caused by extreme softening of a shell after buckling. As shown in figure B21 a small imperfection causes a large reduction of the maximum load. Furthermore, thin shells have been shown to be among the so-called imperfection-sensitive structures. This means that buckling is highly dependent on imperfections in shell geometry and loading.

Imperfections include dents, residual stresses, temperature stresses, inhomogeneities, creep, shrinkage, eccentricity of loading and first order deformations. Because of this imperfection sensitivity and buckling considerations, dimensioning of shell thickness is usually not based on material strength criteria. Hence, the hypothesis of this research which considers the possible advantages of UHPC being the increased tensile strength and modulus of elasticity.

The negative effects on the structure bearing capacity should be minimized as far as possible. This approach for this starts within the design phase, where it is acknowledged that problems considering the material, connections and construction should be excluded up to maximum extend and are therefore interwoven with the design, production and construction phase.

Knock-down factor

The knock-down factor is a factor which indicates the difference between the linear critical buckling load and the actual critical buckling load. The factor takes into account imperfections and geometrical and physical nonlinearities which influence to the failure mode of spherical shells where buckling, cracking and crushing highly interact and which is known as compound buckling. It is, because of these multiple phenomena, therefore coherent that the factor is experimentally determined. If little about these phenomena for a project is known the factor $C = \frac{1}{6}$ can be used.

In shell design often the following procedure is used. First the critical loading is computed by using formulas or a finite element program. Than this loading is reduced by a factor that accounts for imperfection sensitivity. The result needs to be larger, in absolute value, than the design loading determined by regulation.
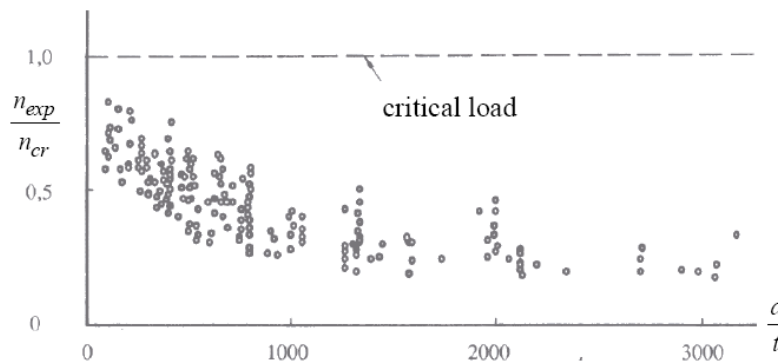

Fig.B30. Experimental maximum loads of 172 axially loaded cylinders   [41]

As seen in the scattered results of figure B30, the value for the knock down factor is determined empiric. This is explained by the fact that cracking, crushing and buckling strongly interact with shell failure. The extend of these aspects are influenced by type of loading, shell thickness and proportions, material properties and geometrical imperfections. Therefore, it is impossible to formulate a general expression for the knock-down factor with sufficient accuracy. Because of this, the value of $C = \frac{1}{6}$ is applied within the design calculations of this research.

3.4.8. Optimal geometry

The design of shell structures depends heavily in the relationship between structural behavior and geometry. For this, the optimization of geometrical features has been researched over the decades. Multiple types of geometrical

optimization, such as form finding by hanging models and curved edges and minimizing strain energy are known. Two aspects of finding possible geometry optimization are highlighted since they might be of influence to the geometry of this research.

Fully stressed dome

As described for the catenary line, the effects for dead load on a shell is of major importance. Where the catenary line merely describes the geometrical mid-surface of the shell it is acknowledged that enlarging the shell thickness close to the edges will have a positive effect on the stresses.

The principle for finding the 'optimal geometry' for a shell is based a shell which has optimal material use and is subjected to an equal compression stress everywhere in the structure subjected to vertical load. This principle is known as the fully stressed dome. Figure B31 shows that a subdivision of the geometry, the rectangle, is as well a possible geometry for a fully stressed dome.
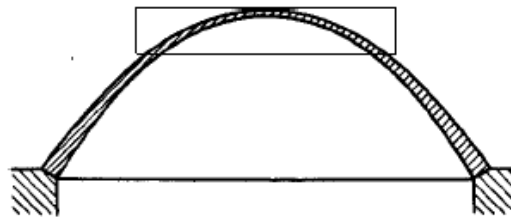
Fig.B31.   Cross-section of a fully stressed dome [48]

Based on the results of [39] it is remarked that the geometrical description, for spans from 10 to 200m, is given by the formula:

$$y \cong \gamma \cdot x^2 \cdot \frac{\rho \cdot g}{f}$$

with γ =0,25, 'ρ' is the material density, 'g' the gravitational constant and 'f' the reduced compression strength.

The increase of thickness from the top to the supports is then given as the linear proportion of the increase of stress. Within the research of [39] the use of C28/35 was used. The result gave the aspect ratios between the sagitta and the span of a fully stressed dome and had a maximum span to sagitta ratio of 9 for a span of 200m with an increase of thickness has maximum of 25%.

When for these results the characteristics of UHPC are filled in, the sagitta of is found to be much smaller than for C26/35. This holds since the compression strength of UHPC is much larger for only a slight increase of density compared to the conventional concrete. This results in sagittae which are approximately 7 times lower, resulting in an negligible overall curvature. This of course, is highly disadvantageous for buckling the bearing capacity and the aesthetical demands of a shell structure.

It is therefore that the fully stressed dome is acknowledge as an scientific interesting principle, but has no further impact on the further research of this report on the application of UHPC in shells.

Catenary

In figure B10 the membrane force distribution in a hemisphere is shown. The top half of the figure shows the principle of the funicular line. The principle and its possible design consequences are discussed.

For shell- as well as arch analysis and design, the dead load is an important component. It is therefore that the pressure line caused by the dead load is analyzed, causing it to highly influence the optimal geometry. The dead weight of an arch can easily be analyzed with and inversed experiment which are known by hanging models.

These experiments make use of the fact that objects, for instant chains, subjected to their own dead weight will describe their ideal curve with merely tension in its material, preventing internal moment to occur. This curve is referred to as the catenary of the object. If inverted, the geometry describes the geometry which ideally results in merely compressive normal forces in the middle surface of an arch of shell to arise if subjected to its dead load.
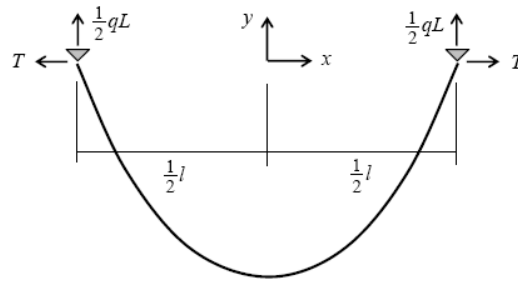
Fig.B32. Catenary   [41]

The equation of a catenary curve is simply described by a hyperbolic cosine:

$$y = a \cosh\left(\frac{x}{a}\right)$$

This mathematical function of a catenary differs severely from a circle, which is illustrated below. Here a hemisphere is described by $y^2 + x^2 = 75^2$ [0 ≤ y ≤ 50] and the catenary by $y = 46.4 \cosh\left(\dfrac{x}{46.4}\right)$. The catenary is determined with a maximum equal to 50.
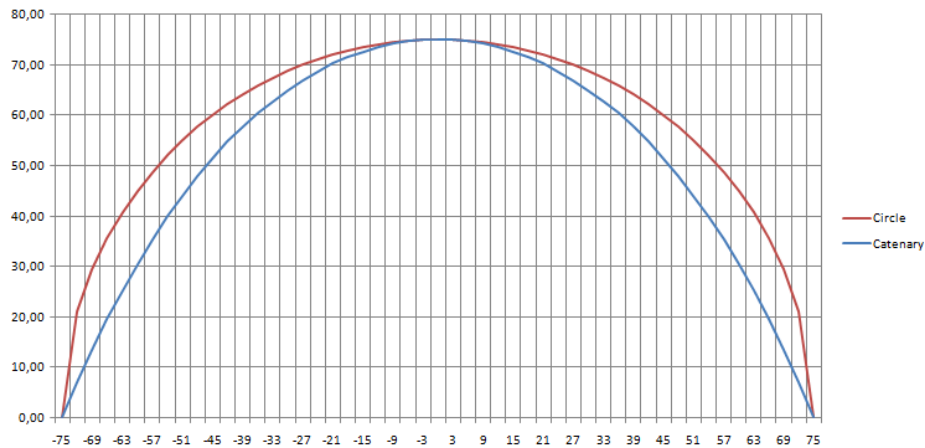

Fig.B33. Catenary and circular line   (d/s = 2)

The geometries of the catenary and circular line show a significant difference to each other. For shell, and arches, with lower sagitta to span ratios the deviance is significantly lower than for the hemispherical example above . Below a sagitta to span ratio of 1 over 4 is shown, the average difference between the lines is 5,6%.
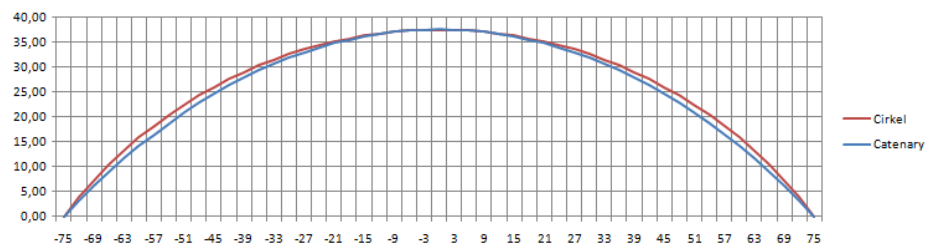
Fig.B34. Catenary and circular line   (d/s = 4)

Because the fact that the deviance for small ratios is small it is questioned whether the geometry of a catenary is effective for the shell design within this research. A shell geometry based on a part of a circle as meridional generator line has the advantage that the amount of curvature along the span is equal. This is seen as an advantage over the catenary, since an equal amount of curvature is advantageous for reusability of formwork.

Part C
Computational Modeling

4. Finite Element Method

4.1. Introduction to FEM

The finite element method (FEM) is a numerical analysis technique for obtaining approximate solutions to boundary value problems for engineering problems by solving partial differential equations. The analysis is particularly suited for solving partial differential equations on complex geometries and can be largely automated. Together with its diversity and flexibility as an analysis tool, it is well suited to efficient computer implementation within the engineering industry. This chapter gives a brief description, disregarding mathematical descriptions, of the fundamentals of the method and a description of the application of the method in this research.

For complex geometries and possible complex load cases it is not hard to imagine that if an approach where governing equations, known from mechanical theory, are combined with their boundary conditions will not lead to simple analytical solutions. The application of the finite element method leads to systems of equations, and therefore matrices, which can be solved using a computer. This will save time and energy and is especially suitable for cases in which the design is likely to be adapted.

4.1.1. Fundamentals of FEM

While modeling a real life problem in mechanics an element of any dimension basically possess an infinitesimal number of parametrical values for multiple characteristics on each generic point in the body. Hence, a schematization is desirable which diminishes the problem to an infinite number of unknowns.

By dividing the model into elements and by expressing the unknown field variable in terms of approximating functions within each element the finite element procedure reduces the problem to one of a finite number of unknowns. The approximating functions, or interpolation functions, are defined in terms of the values of the field variables at specified nodes. The nodes typically lay on the element boundaries where elements are connected. Together with possible interior nodes these nodes together with the interpolation functions define the mechanic behavior of the element. Evidently, the nature of the solution and the accuracy depend not only on the size and number of the nodes and elements used and on the interpolation functions selected.
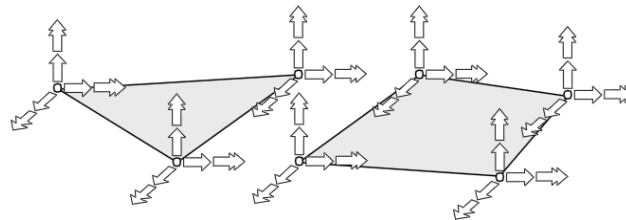

Fig.C1.   Examples of flat elements and their degrees of freedom [41]

A crucial step is to divide the particular geometry into elements. Within a model a variety of shapes may be employed. The elements are combined with nodes, by which the interpolation function will describe the mechanical behavior of the element in between the nodes. For these interpolation function often polynomials are selected since their differentiation is straight-forward. Once the finite element model has been established the matrix equations, based on the same relations as seen in figure B5., expressing the properties of the individual elements are set.

The basis for the assembly procedure holds that in a node, where elements are interconnected, the value of the field variable is the same for each element sharing that node. By this the overall model is assembled as a network of elements. The matrix equations of the elements itself can hereby be combined with the equations for the entire model.

The system equations of the model are ready for solution if the boundary conditions of the problem are formulated. The boundary condition describe the nodal its degree of freedom concerning displacements and rotations. Essential boundary conditions are support- and symmetry conditions. These conditions restrain the modeled structure against rigid body motions by modeling for instance a foundation and appear in many practical problems.

Now a set of equations for the entire model is described the FEM-model involves a set of equations which together with the boundary conditions can be used to obtain the unknown nodal values of the problem.

4.2. Commercial software

The history of finite element analysis is congruent with the development of computer technology. The first development of the essentials of the method is often ascribed to R. Hrennikoff and R. Courant in the 1940's.

As throughout the following decennia the possibilities, and thereby the popularity of the finite element method, began to grow more mathematicians, engineers and physicist became involved. It was within the late 1960's that the mathematical literature on the finite element method grew considerably.

The first notion of commercial is found within this period, of which an example is found where mesh generators where non-available, causing users to manually imply element by element and node by node. In the decennium after, the application was restricted to industries where mainframe computer where applicable.

Since the development of the method, computers and software nowadays the application of several FEM-software packages is used on wide-scale. The analytical method can be integrated within the software. Therefore the input of elements and mesh generation is severely simplified. Still, users are ought to be careful with the application of the method, the input and results of the calculations need to be checked. Beside the simple application, with input of structural elements like columns, slabs etc., sufficient knowledge on the background of the applied software is often useful in practice.

4.2.1. Scia Engineer

Scia Engineer is an example of a wide-scale used commercial software package. This software is primarily designed to serve civil engineers but is nevertheless also used in other engineering fields. A graphical system is used for the input of geometry and can be used to present calculation results. The software offers the opportunity for calculations for 1-dimensional problems to 4-dimensional problems which contain analysis of distribution of internal forces over time.

Within this research the choice to apply Scia Engineer is based on multiple aspects. The convenient interface and straight-forward utilization of the program causes that the program suits with a design research where multiple models and parameters are compared. The experience of other engineers engineering firms confirms this statement. Furthermore the availability of program causes students to make use of practically all possibilities of the program.

4.3. Calculation aspects

4.3.1. Mesh

In general it holds that the smaller the elements, the more accurate the results of calculations will be. Experience with the application of FEM-software and iterative comparison between results will lead to satisfying results. A procedure to check whether the calculation are sufficiently accurate is to execute a calculation with a defined mesh and to compare the results with a calculation for a mesh with half the size. If the results do not differ significantly the initial mesh was sufficient. Otherwise, the procedure should be iteratively used.

For FEM-analysis a guideline describes that the size of two-dimensional element is ought to be chosen about 1 to 2 times the thickness of the plates of slabs in the project, in which the 'size' describes the average edge length. For this research-project however, since it is a large-scale project which focuses on the overall behavior of the structure, the mesh size is determined to give satisfying results for a mesh size of 2.0m. This is validated with a comparison between the theory as found in part B and the FEM of Scia Engineer as described above in appendix 5.

4.3.2. Shell buckling and dynamics

One of the most important aspects on shell design is the resistance of the structure against buckling. With Scia Engineer stability calculations can be made to determine the global buckling modes of a structure under given loading. The software gives the opportunity to determine multiple buckling modes, for which the structure will fail for the lowest value. Within this research the calculations are made for four buckling modes to observe the difference between them. As was explicated in Part B, section 2.3.1, the fact that multiple buckling modes are close to each other it is expected that the shell is sensitive to compound buckling.

The calculation results give a ratio between the buckling load and the applied load. In addition the ratio between the buckling load and the applied load is given. Within this research several design considerations are deliberated and compared on buckling behavior. For this it is chosen to load the structure with a unit load of 1.0 kN/m² by which the above-mentioned ratio λ gives the structure its ultimate buckling load. Obviously the buckling load, which results from a linear buckling analysis, shall be multiplied by the knockdown factor.

Calculations on dynamic response of the structure can, as well as for buckling calculations, be executed to determined multiple modes, in this case being eigenfrequencies. The dynamic calculation is carried out on defined dynamic load cases.

4.3.3. Types of analysis

FEM-software packages can generally execute many types of structural analysis. It is important to know which type of analysis, preferably being an uncomplicated analysis, will provide sufficient results. As a guideline a list of types of calculation an analysis to be used is given in [41]:

– Stresses in the ultimate limit state   linear analysis
– Stresses due to support settlements   linear analysis
– Displacements in the serviceability limit state   linear analysis, second order analysis
– Buckling critical load factors   buckling analysis
– Concrete crack widths (SLS)   hand calculation or physical nonlinear analysis
– Load factor at collapse   geometrical and physical nonlinear analysis incl. creep & imperfections

If the structure is well designed and performs properly the displacements and deformations will be small and nonlinear effects are negligible. If not, indications of large stresses can be used to design a better shape and optimize dimensions. If the displacements within the serviceability limit state are small, which is likely for properly designed shell structures, second order analysis is not required.

Part D
Analysis & Design; Shell of revolution

Table of contents Part D

5. Loading

Before the beginning of the analysis and design of the structure the loads and load-factors are obtained from the Eurocode and described in this chapter.

5.1. Applied codes

The Eurocodes are developed by the European Committee for Standardization. These building codes are used for loads and load factor determination on the structure. The structure is considered to be built in the north of the Netherlands, based on the preliminary design for Fiere Terp which is described in part E. The following codes are applied:

EN 1990:   Basis of structural design
EN 1991:   Eurocode 1; Actions on structures

        Part 1-1: General actions - Densities, self-weight, imposed loads for buildings
        Part 1-3: General actions - Snow loads
        Part 1-4: General actions - Wind actions

EN 1992:   Eurocode 2; Design of concrete structures

For this research the concrete shell structure is subjected to permanent and variable loads. Lateral wind loads are taken into account as static variable load case. The dynamic effects are later examined within the calculation of chapter 8. Accidental loads, caused by for instance explosions of collisions, are initially neglected since they are considered to be of no significance to the research. The design will be checked for structural coherence by investigating the response to openings in the structure.

5.2. Permanent load

Permanent loads, labeled by Eurocode 1990 as G, are caused by the dead weight of the shell, finishing and installations. Within this set of loads the dead weight is dominant. It was found that UHPC has a specific weight of about $25 - 28$ kN/m^3. Ductal with metallic fibers and heat treatment has a specific weight of 25 kN/m^3 [74].

Dead Load: 25 kN/m^3

This weight, multiplied with the shell thickness, gives a surface load. This load is dependent on a possible varying shell thickness over the meridian and the angle ϕ in relation to the vertical axis. The magnitude of the deadweight is automatically generated by Scia Engineer.

This permanent load is completed with a assumption for the roof finishing with a design value of 0,25 kN/m^2.

5.3. Live load

Permanent loads, labeled by Eurocode 1990 as Q, are divided in wind loads, snow loads and roof maintenance load. The design values are found in Eurocode 1991. For both snow and wind loading minimum and maximum values are presented since the values depend on the design dimensions.

5.3.1. Wind load

Wind loads are represented by a simplified collection of pressures or forces of which the effects are comparable to the extreme effect of turbulent wind. The characteristic values are based on a yearly change of exceeding of 0.002, which corresponds to a return period of 50 years.

The determination of the wind load depends on several aspects. The basic wind velocity depends on the wind climate and is found in the national annex. The mean wind velocity and the peak velocity pressure take the height of the structure into account. In the method described below the wind pressures are found also taking into account the size and shape of the structure.

The basic wind velocity v_b is based on its fundamental value $v_{b,0}$ which is the characteristic value for the 10 minute mean wind velocity, independent of the wind direction and time of the year, on 10m above ground surface in an open area.

$$v_b = c_{dir} \cdot c_{season} \cdot v_{b,0}$$

Both the wind direction factor c_{dir} and the season factor c_{season} have a recommended value of 1,0. The fundamental value of basic wind velocity according to article 4.2 in the national annex for wind region II is 27,0 m/s.

The peak velocity pressure can be determined by a formula with the turbulence intensity and the mean wind velocity, which are both found after filling in several factors. A less labor intensive is found in article 4.5. The formula for the peak velocity pressure is simplified:

$$q_p(z) = (1 + 7 \cdot I_v(z)) \cdot \frac{1}{2} \cdot \rho \cdot v_m^2(z) = c_e(z) \cdot \frac{1}{2} \cdot \rho \cdot v_b^2$$

Where ρ represents the air density of 1,25 kg/m³. The value for the exposure factor $c_e(z)$ can be easily found in the figure below, which is valid for flat terrain where the orography factor, taking into account elevated terrain, and the turbulence factor are equal to one.

Since the structure for Fiere Terp is planned in an open area without obstacles terrain category I is chosen. The maximum optimal height is expected not to exceed 50m. This is lightly based on a design maximum shell span of 200m and a minimal span/ sagitta of 4.2. These values may change during the research.
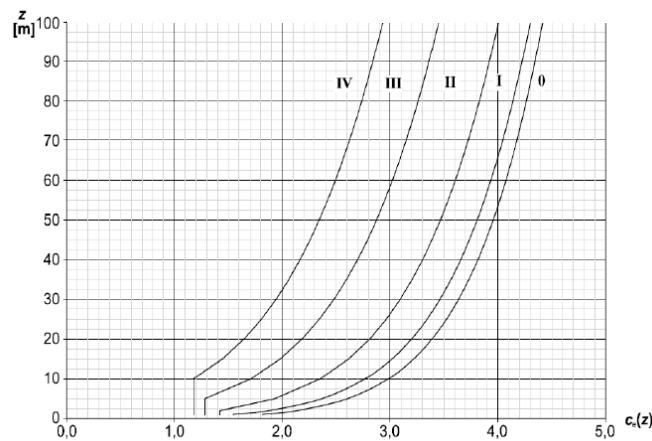

Fig.D1.   Exposure factor $c_e(z)$ for $c_0=1,0$ and $k_1=1,0$ [3]

The value for the exposure factor is approximately equal to 3.8. The peak velocity pressure becomes:

$$q_p(z) = c_e(z) \cdot \frac{1}{2} \cdot \rho \cdot v_b^2 = 3.8 \cdot \frac{1}{2} \cdot 1,25 \cdot 27^2 = 1731.4 kg/ms^2 = 1.73 kN/m^2$$

This surface load is multiplied with pressure (or suction) coefficients depending on the geometry of the structure. The wind external wind pressure on exterior w_e is determined with expression:

$$w_e = q_p(z_e) \cdot c_{pe}$$

The coefficients are ought to describe the aerodynamic effects of the structure. Depending on the geometry the following coefficients are taken into effect by the Eurocode:
- Internal & external pressure for buildings
- Nett pressure
- Friction
- Force

Other effects than external pressure do not apply or are not within the scope of this research.

For curved roofs and domes article 7.2.8. applies. Here the global external pressure coefficient is determined using figure D2.
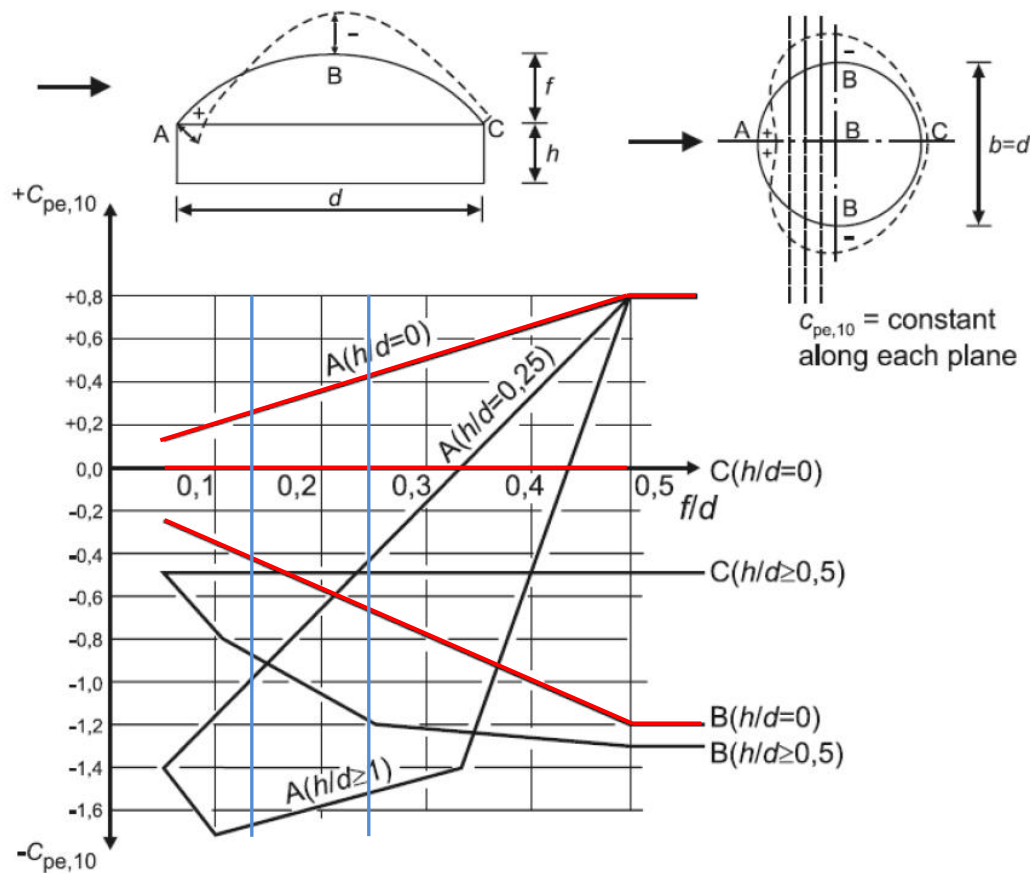

Fig.D2.   Recommended values for external wind pressure coefficients for spheres [3]

The sagitta/span-ratio is this research is expected be limited to 0.125 to 0.25. The values for $C_{pe,10}$ are multiplied with the peak velocity pressure. The peak velocity factor was determined for a sagitta of 50m, this results in external pressure coefficients and loads.

Zone	$c_{pe,10}$ Min	Max	w_e (kN/m²) Min	Max
A	+0,26	+0,43	+0,45	+0,78
B	-0,41	-0,68	-0,71	-1,18
C	0,0	0,0	0,0	0,0

Tab.D1.   Wind factors and loads

The transition zones between A,B & C can be determined by interpolation. In this analysis however, the zones are schematized by linear distributed zones. Derived from figure D3. the altering location between pressure and suction between zone A and B is found. The ultimate angle is found by the proportion between Φ_1 and Φ_2, see the figure below.
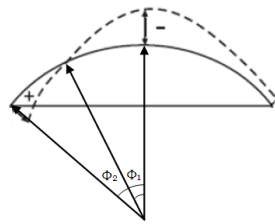

Fig.D3.   External wind pressure distribution for spherical roofs [3]

With this figure 7.12 from article 7.2.8. it is found that $\Phi_1 \approx 0,5 * \Phi_2$. Because of the proportion between these angles, which is verified by Eurocode figure 7.11 for cylindrical roofs, the schematization is made to locate the altering location between pressure and suction at a quarter of the arch length.

For schematization the external wind pressure distribution, as shown in the figure above, is based on the region distribution for cylindrical roofs.
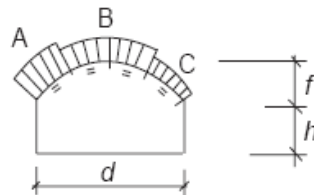

Fig.D4.   External wind pressure distribution for cylindrical roofs [3]

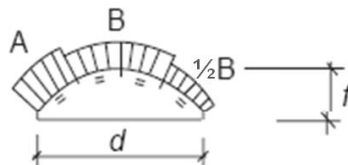By this, the wind load in this research is schematized as:

Fig.D5.   Schematized external wind pressure distribution for cylindrical roofs

The transition from region A to region B as seen from above is determined by figure D6, which is bases on the figure on the top right of figure D2. Here the top view shows an angle α of approximately 32 degrees. The angle β, which defines the angle between regions B and C, is approximately 45 degrees. Hereby, the wind loads are known.
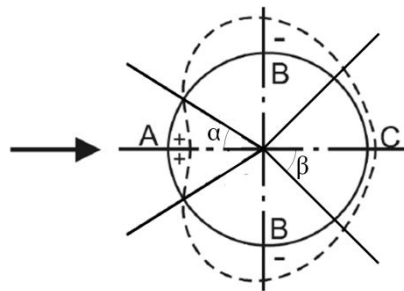

Fig.D6.   Schematized external wind pressure distribution for spheres (Fig.D2)

5.3.2. Snow load

Snow loads act mainly vertically on the shell surface and are projected on a horizontal line. The Eurocode does not consider spherical roofs. The load distribution is based on the standard for cylindrical roofs and is schematized in figure D7. The design and calculation considers that snow loads can occur in different patterns on a roof, which is influenced by a number of factors. Within this research the load distribution is made according to article 5.2 by:

a)   Evenly distributed snow load
b)   Redistributed snow load after rearranging (by e.g. wind)

The snow load on roofs is defined as:

$$s = \mu_i . C_e . C_t . s_k$$

The warmth coefficient factor C_t takes possible melting due to heat transition into account. This value is equal to 1,0 since the thermal transmission is lower than 1,0 W/m²K. The exposure factor C_e for open areas without obstacles is equal to 0,8. The characteristic value of snow load on ground level, according to article 4.1 in the national annex, is equal to 0,7 kN/m² for all of the Netherlands.
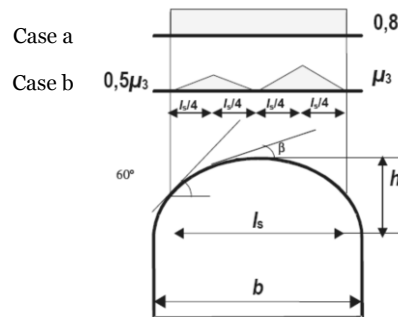

Fig.D7.   Snow load shape coefficients for cylindrical roofs   [3]

Since β is smaller than 60° the contribution of redistribution has of significant role. The proportion of h/b has an expected maximum of 0,25 and minimum of 0,10. Therefore, by article 5.3.5., the value of μ_3 has a minimum value of 1,2 and a maximum value equal to 2,0.

Since figure D7 considerate cylindrical roofs only, which have a geometrical difference to the revolutional surface, an assumption for spherical roofs is made. The maximum and minimum values for the distributed snow are based on a distribution according to a chessboard-pattern.
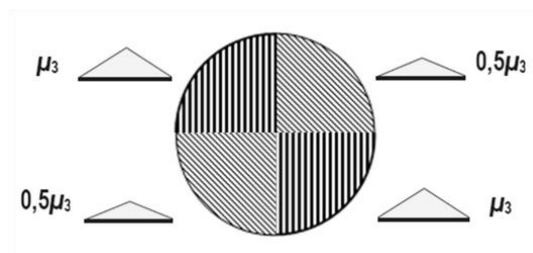

Fig.D8.   Snow load shape coefficients for cylindrical roofs (2)

The evenly distributed snow load, case a, to be applied is displayed in the table 2. For the value for μ_3 varies between 1.2 and 2.0 the minimum and maximum for the chessboard-pattern in figure D8 hold:

Case		Magnitude (kN/m²)
a	Evenly distributed	0,45
b	Left (min/max)	0,34 / 0,56
	Right (min/max)	0,67 / 1,12

Tab.D2.   Snow loads and cases

Similar to wind load the unevenly distributed snow load is schematized in multiple areas, for both fully loaded and half loaded regions, according to:
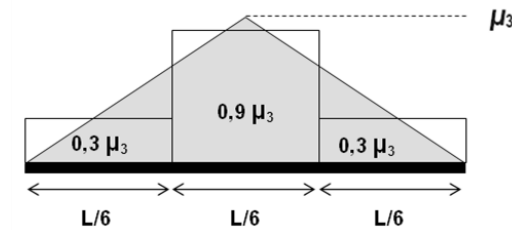

Fig.D9.   Snow load shape coefficients for cylindrical roofs (3)

5.3.3. Roof maintenance load

According to Eurocode 1991 1-1 art 6.3.4. roofs are dived three types. The roof of the shell structure is considered as roof type H, being only accessible for maintenance and repair operations. Irrespective to the recommended value of q_k = 0,4 kN/m², the larger value of 1,0 kN/m² found in the National Annex is chosen for roofs with small slopes up to 15°. The loaded area has a maximum of 10m², with a largest width of 5m. A point load Q_k = 1,0 kN is applied on an area of 0,1 m x 0,1 m.

5.4. Load combinations and factors

The defined load cases are combined in several load combinations. Loads of which the effects are not likely to act simultaneously because of physical or functional reasons should not be combined in a load combination. Therefore the load cases wind load, snow load and maintenance load are spit in separate load combinations but are, of course, all combined with the structure's dead weight.

Load factors are applied to the load cases per combination. This factorization follows from the requirements on the load carrying function of a structure. The requirements apply to both safety against serviceability in normal use and to failure. These two requirements can be quite different in nature and should thus be separated in the formulation of the two requirements. This can be achieved by performing the design analysis at two limit states with regard to the function of the structure:

- Ultimate limit state   (ULS);   the state where the structure is at the limit of failure
- Serviceability limit state (SLS);   the state where the structure is at the limit of not satisfying the requirements for normal use

The implication of the limit states are illustrated in figure D10, which illustratively shows the deflection versus load for a simply supported beam. The limit states are conceivable states of the structure. The requirements concerning safety against failure are, in principle, formulated such that the probability that any of the possible ULS shall be exceeded is satisfactorily low. The requirements with regard to serviceability in normal use are established in a corresponding way, such that the time during which exceeding occurs will be satisfactorily short.
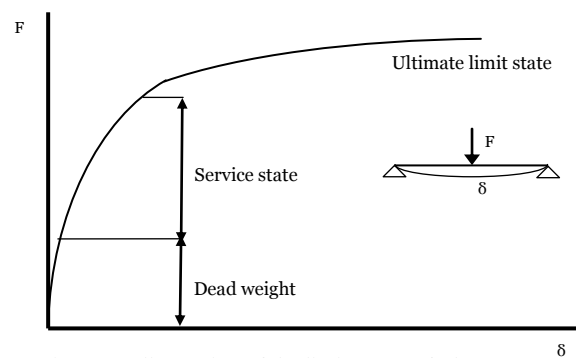

Fig.D10.   Illustration of the limit states of a beam

Combinations

LC1   Permanent load
LC2   Permanent load + Wind load
LC3   Permanent load + Snow load (evenly distributed)
LC4   Permanent load + Snow load (redistributed)

Load factors

Limit state		Load type	
		Permanent	Variable
ULS	Unfavorable	1,35	1,5
	Favorable	0,9	0
SLS	Unfavorable	1,0	1,0
	Favorable	1,0	1,0

Tab.D3.   Load factors in ULS and SLS

6. Prefabrication of elements

6.1. Introduction

Applying the principle of prefabrication within the construction of a shell surface implies a division of the total surface in multiple segments. The questions then arise what is the best achievable for the element production and how the connections of the elements will effectuate structural integrity. These two aspects are highly dependent and have a significant influence on the construction costs. Within a complex geometry small elements may imply a large repetition of unique elements, which on the other hand may lead to more connections and interrelated labor on site.

Precast concrete solutions have the advantage over in-situ casting that material and construction conditions can be under the best control. Consequently, the choice for precasting can provide superior finishes, small production deviances, the possibility of weight reduction by applying hollow elements and element forms which may be constructed for repeated use. On site, supplied elements contribute to the speed of construction due to the quicker assembly and the relative independence of weather conditions. On the whole, it is concluded that precast shell construction has a significant overall increased economic value.

Disadvantages of precasting are the need for cautious hauling and transport of the elements from the precasting plant. This leads, together with the erection, to possible damaging of the elements. Also, for the elements to become an integral structure the joint construction is vital. The possible advantage of replication of elements is opposed by the fact that a demanded repetition of elements results in the decrease of freedom of geometry and vice versa. In general, up to manageable size, it holds that the larger the elements, the smaller the handling cost per square meter of shell area. Concerning hauling and erection, it can be advantageous to cast the elements at the construction site rather than at a plant. One example is the Millau Tollgate described in appendix 3.5.

Typically, prefabricated concrete elements are flat, that is, without curvature. In addition, concrete reinforcement is often calculated using linear models for structural elements such as beams and columns. Furthermore the bending and assembling of reinforcement bars for curved shapes is considered difficult. With UHPC the application of fiber reinforcement offers the opportunity for elements without conventional reinforcement.

6.2. Casting of UHPC

It is concluded from the study on UHPC in part A that UHPC is most suitable to be applied in precast elements instead of being cast in-situ. The reason is found in the high demands for batching circumstances and after treatment. Crucial in producing UHPC is accurate control of ingredients and temperature. The control of the temperature is required since the amount of water or ice that is added is insufficient to affect a significant temperature raise. All ingredients have to be accurately weighed and a high shear mixer is required to disperse water onto the cement particles without heating the mix through kinetic energy generated by the mixing process.

The mixer demands a distinctive power consumption during the mixing of UHPC. The power consumption is initially low as the dry ingredients are blended, the increases is substantial when the water is added and dispersed. The power demand later drops as the superplasticizers take effect. Because the process of high speed mixing generates entrapped air into the mix that can lead to a weaker matrix and poor surface finish, it is necessary to slow the mixer at the end of the mix cycle to allow the entrapped air to escape.

It is recognized that the application of UHPC entails a challenge for both the personnel and the technical equipment involved. Batching and mixing of the components requires a demanding supervision. The UHPC casting and compacting compared with normal concrete is very distinctive, especially regarding the complex processing due to its ductile consistency.

During hardening of the concrete several factors such as autogenous shrinkage may cause difficulties within the formwork. The difficulties can for instance be settled by realizing a mould without restrained edges, guaranteeing no restrictions in deformations during hardening. Overall, the experience from practice shows that possible cracks occurring during casting remain small in proportion to attend fibers in the matrix.

6.2.1. UHPC mixture Ductal

In section 1.2.9. several types of UHPC mixtures are discussed. In this research the application of the UHPC type Ductal® is chosen. Several types of Ductal which are developed by Lafarge and Bouygues Travaux Publics. The variant Ductal BS1000 is applied for the structural elements. This type is accompanying for structural solutions for columns, long span roofs and floors, seismic elements, wall panels and modular precast systems. Ductal BS1000, like other UHPC-types, offers superior technical characteristics including ductility, strength and durability while providing highly moldable products, with a high quality surface aspect and a short bond development length. The high strength and ductility permit structures to be designed without passive - and shear reinforcement.

Other aspects of this type of Ductal, essential for design, are:

-   The Ductal mixture is accompanying to the decision for application of prefabricated elements since the requirement for a controlled precast environment to successful production.
-   Heat treatment of 90°C at 90% relative humidity for 48 hours is applied after final setting. The effects of this treatment are described in section 2.2.8.
-   The strength of Ductal allows for solutions to be designed with smaller elements, without the use of passive reinforcement.
-   For fire rated structures, the Ductal® AF formula is available and provides fire performance similar to normal concrete. This formulation uses metallic fibers to which organic fibers are added.

An important aspect of Ductal is that the material has been used in a number of applications worldwide such as the Sherbrooke Bridge, Clinker Silo Illinois and Seonyu Footbridge [Appendix 3]. The characteristics of this mixture, which are applied for further research and calculations, are represented below.

<u>Ductal characteristics</u>

Property	Value	Unit
Density	25	kN/m³
Compression (Mean)	180	MPa
Compression (Design)	150	MPa
Direct Tension (Mean)	10	MPa
Direct Tension (Design)	8	MPa
Young's Modulus	58	GPa
Flexural Strength	35	MPa

Fiber Length	14	mm
Fiber Diameter	0.2	mm
Fiber Content (approx.)	2	Vol. %

Poisson Ratio	0,2	
Shrinkage Factor	<10	µm/m
Creep Coefficient	0.3	
Thermal expansion coefficient	11,8	µm/m/^{o}C

Tab.D4.   Physical properties of Heat-Treated Ductal BS1000   [74]

6.3. Element geometry

The element geometry is highly dependent of the feasibility of production and of transportation possibilities. Both the production as the transport possibilities have their influence on the maximum size of the elements. This influences the number of elements and necessary handlings on site, the weight of the element and its corresponding demands on crane capacity, the minimum amount of connections and the construction time. In addition, the element geometry is of importance since the shape of applied elements influences the mould along with fabrication, possible different types of geometries, its reusability and the type of sharp or blunt angles of the element.

For these reasons it is advisable to search for the maximum element size with a simple geometrical shape, connection opportunities and possible protective measures which can be applied over a large portion of the shell area, for which the shell geometry is decisive.

When the rate of repetition of the elements is significant, so is the economical positive effects of prefabrication since the production mould can be highly effectively used, which is also positive in case of damaging of the elements. For this reason it is recognized that within a shell of revolution the curvature of the single elements is equal, causing the elements to be alike. This positive effect also counts for a shell which is based on a shell of revolution.

6.3.1. Cross section

Within paragraph 3.4 the advantages of composite structures are elaborated. It was concluded that two effective possibilities to expand the moment of inertia of the shell is to apply ribs and stiffeners and/or sandwich panels.

The disadvantages of the sandwich principle consider the production of the elements, differences in temperature strains in the top and bottom layer, expected condensation at the bottom layer and complicated force introduction and distribution. These disadvantages lead to the preference not to apply sandwich panels and to make use of a 'solid' cross section for the elements.

The possibility for rib-stiffening is tested for its potential to increase the critical load of the shell structure in this material efficient manner. It is noted that for the production of elements it is considered to be beneficial if one type of element can be applied. After the repetition of elements, as treated in section 5.6, it is beneficial to combine the application of ribs and stiffeners within the shell elements itself, instead of separate stiffeners and elements.

6.3.2. Edges

It is expected that the applied elements will have small dimensions the risks of damaging during handling, transport and placement of the elements. It is therefore concluded that, together with the fact that ribs and stiffeners can be positive for the bearing capacity of the shell, it is highly favorable to apply thicker element edges which will ultimately form the ribs and stiffeners of the shell. This will lead to the possibility that within the total shell only elements with local thickening will be applied, instead of separate elements, ribs and stiffeners.

The edges are chosen to be rectangular, implying the angle between the edges of the element in cross-section equal to 90 degrees, which was found to be one of the most suitable methods for the creation of a structurally solid connection within the research of [E. den Hartog, 2008]. Also, thicker edges improve the opportunity to provide a water tight connection.

6.3.1. Amount of curvature

The question arises in what order the exact consequence of curvature to a single element for a large span shell structure is. It is recognized that every arbitrary curved surface can be divided in a number of segments. To get an indication on dimensions which are required in an element a curved line is divided in straight segments. The relation between the amount of curvature and the number of flat elements which approximate the original shape is shown to be proportional. This is illustrated in figure D11 where the curve on the left, with high amount of curvature, requires more straight lines for a comparable approximation than the simpler curve on the right.
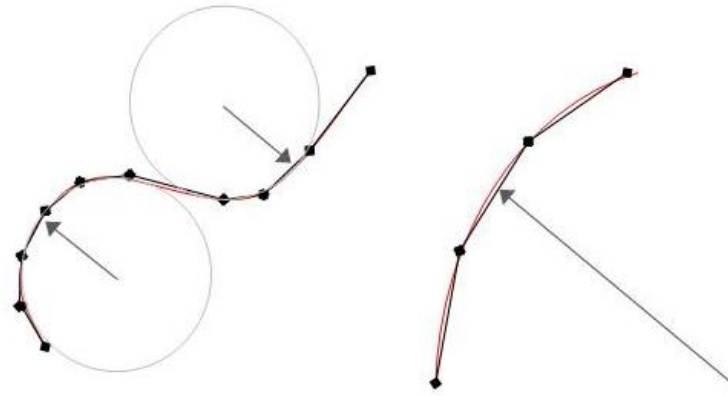
Fig.D11.   Curved lines approximated by multiple linear segments

For large spans which are divided by lengths accompanying to realistic prefabrication dimensions, the approximation of a curve by the straight segments gets close. This is clarified with an illustrative example for a small span and a high curvature.

For a shell which has a high curvature and is similar to Palazetto dello sport, which spans 60m and has a sagitta to span ratio of about 3, the corresponding radius is 32,5m and the opening angle is 67,38°. The arch-length is found to be 76,4m. All proportions used are clarified in appendix 4.

For practical reasons, the arch length is divided by a natural number which divides the shell length in a practical dimension. When divided in 16 segments a dimension of approximately 4,8m is found. Looking closer to a single element the following dimensions are found:
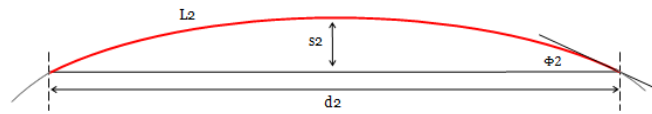

Fig.D12.   Section of element

The total shell length is:

$$L_1 = \frac{\phi_1 \pi R_1}{90} = \frac{67,38 \cdot \pi R}{90} = 76,44m$$

For the single shell element it holds that:

$$L_2 = \frac{L_1}{16} = \frac{76,44}{16} = 4,778m$$

$$R_1 = R_2 = R$$

$$d_2 = 2R\sin\left(\frac{90 L_2}{\pi R}\right) = 4,773m$$

$$s_2 = R - R\cos\left(\frac{90 L_2}{\pi R}\right) = 87,7mm$$

$$\frac{s_2}{d_2} = \frac{87,7}{4,773 \cdot 10^3} \approx \frac{1}{54}$$

As mentioned before, the curvature of the original shell surface of this example is large, leading to a maximum value for the proportion of sagitta to span of the single element. For a large span shell with a span of 150m and a span to sagitta ratio of 4 which is divided into 36 segments; the sagitta (s_2) is 31,1mm with a 'span' (d_2) of 4,83m. This gives a ratio of 1 over 155.

As a consequence the production of the curved elements the demands concerning the amount of curvature will not be very demanding for the majority of elements. In a spherical shell, which is implied in design calculations, all elements and their curvature are alike. For a more complex, but mostly spherical, shell, such as the Fiere Terp, other types and amounts of curvature occur. Still, large areas of the design correspond with the statement above and so the same observation holds for the single elements within the large spans.

It is shown that the dimensions of the total structure has a significant influence on the curvature and sagitta of the prefabricated elements. Physically, the consequence of the small initial curvature leads to a low initial variance in the dimension of the element and its formwork. This conclusion is important for the applicability of a casting method for the double curved elements.

6.3.2. Effect of element curvature

Despite the fact that the initial sagitta of the element itself is rather small it is questionable whether this curvature is obliged for a shell to behave mechanically up to its potential. The fact that the curvature of the elements is relatively small may lead to the idea of applying flat prefabricated elements, since the effect on the shell's aesthetics is almost negligible.

The effect of the application of curvature is examined for a number of thicknesses for a shell with a span of 150m and sagitta of (150 / 4 =) 37,5m. The entirely curved shell is compared to a shell divided into 216 flat elements. The results of the considerations are presented below.
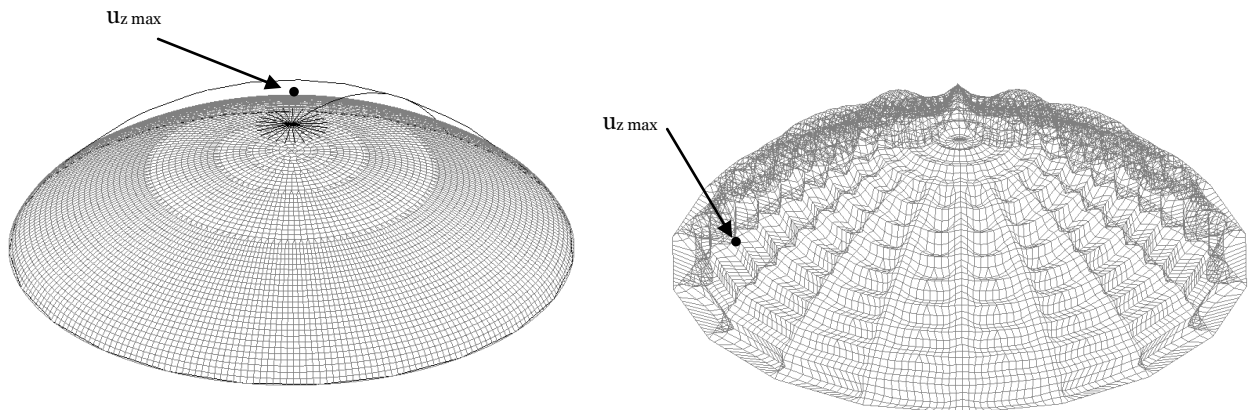

Fig.D13. Illustrative deflection-mode for curved shell (left) and shell with flat elements (right) under dead load
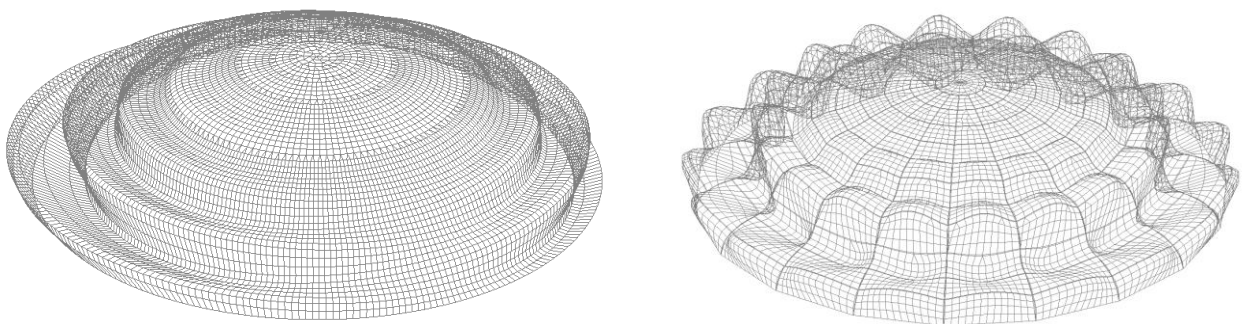

Fig.D14. Examples of typical buckling patterns for curved shell (left) and shell with flat elements (right) under vertical load

Thickness t [mm]	Max. deflection u_z [mm]		Buckling load [kN/m²]		Ratio
	Curved	Flat	Curved	Flat	(Curved / Flat)
50	3.5	13,5	17,7	2,3	7,7
75	3.1	8,2	43,5	7.0	6,2
100	3.0	6,2	74,6	15,2	4,9
200	3.0	3,7	284,9	98,0	2,9

Tab.D5. Results of calculations on the effect of curvature

It is concluded that the small curvature has a significant effect on the buckling load of the shell. The effect, expressed in the factor in the table, depends on the shell thickness; the thinner the shell element, the larger the effect of the curvature. This effect can be explained by the fact that flat elements initially deflect considerably more, with respect to their thickness, for thin elements when subjected to dead load, as can be seen in figure D13.

The values, as presented in table D5, apply for shells with perfect geometry. Although the theoretic values for the buckling load of a shell with flat elements is significantly less than for curved elements it is noted that the possible effects of imperfections is so far been neglected. When for curved elements a safety factor of 6 is taken into account, known as the knock-down factor, a more realistic value for the buckling load is found. The linear buckling value for perfect geometry for the flat element is to be divided by a smaller factor. for instance 2.

The ratio given in table D5 is determined by calculations for curved shell element and flat element with the same thickness. The comparison for a thin curved element and a slightly thicker flat element is of design interest. A comparable thickness is calculated and is illustrated broadly below.
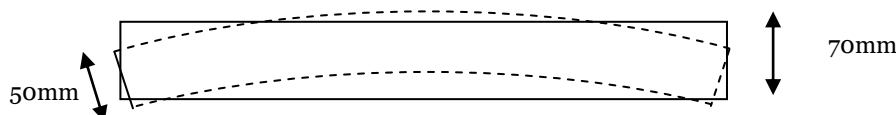

50mm

70mm

Fig.D15. Determination of comparable thicknesses; not to scale

The buckling load for the shell with curved elements (50mm) was found to be 17,7 kN/m². The shell with flat elements (70mm) is determined to be 5,9 kN/m². The ratio between these two values is (17,7/5,9) = 3, which is coincidentally equal to the ratio between the proposed safety values. It is thereby expected that the actual buckling loads for these configurations can be equal. The disadvantage of the application of the flat elements is that the material use, and therefore dead weight of the structure, is to be increased by approximately 40%, which conflicts with the objective to construct as slender as possible.

For flat elements the shell action within the middle surface of a perfect shell, as was considered in the theory described in part B, is disturbed. The flat configurations implies that the elements are angularly rotated to another, which leads to the fact that force distribution differs significantly when compared to curved elements. The use of flat elements implies, together with larger deflections, that the membrane forces will be carried by the edges of the elements. The disturbances cause (compatibility)moments within the shell connections. Therefore the application of flat elements leads to more demands for connections.

The conclusion for this comparison between flat and slightly curved elements is that the benefit of the application of curved elements is distinctive for thin elements. Given the little sagitta of the elements it is not expected that the application of curved elements is disadvantageous for production as well as for efficient transport. Since curved moulds may be more expensive to produce it is economically preferred to be able to repeat the elements as much as possible within the design. The aspects of transportation of the elements and the possible repetition of the moulds, which is highly interwoven with the element configuration, are treated in the next paragraphs.

6.3.3. Geometry tunnel lining elements

The utilization of prefabricated curved elements is frequently applied within concrete lining of shield tunnels. This field of engineering is of interest for this research since the tunnel shield is divided in prefabricated segments which satisfy high demands. The fact that the elements can be cast accurately and that the incorporation of

neoprene gaskets or similar materials, applied as compressible gaskets in the lining, can provide water-tightness causes that the principles for these tunnel elements can be applied for the large span shell.
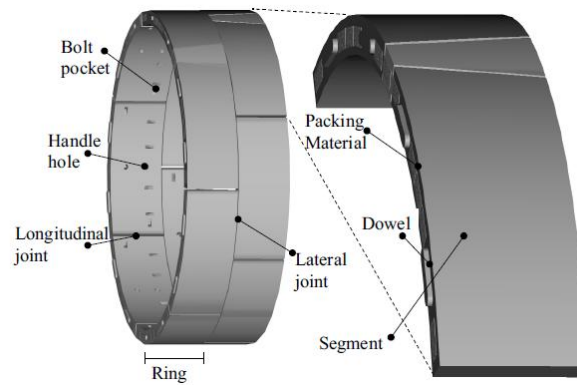

Fig.D16.   Tunnel lining definitions   [70]

Tunnel segments are often arranged as shown in figure 16. The joint are distinguished as lateral and longitudinal joints. At both types of joint the concrete elements are not equipped with straight edges which are applied alongside each other, this would be disadvantageous for both the placing of the elements as well as possible negative effects of production deviances. A production deviance can cause an unforeseen load introduction which is especially unfavorable at the corners of the elements. Therefore the element geometry make use of a reduced contact area, which makes sure that the location of the load introduction is excluded to be located at the corners and that the loads are spread over a larger area of the element(figure D17.a). Usually a dowel and socket system is applied in the joints (figure D17.b). This system additionally helps to centre the segments during the erection and limits deformation differences between adjoining rings. Dowel and socket systems can, opposite to figure D17, have a convex – concave joint configuration as shown in figure 18.
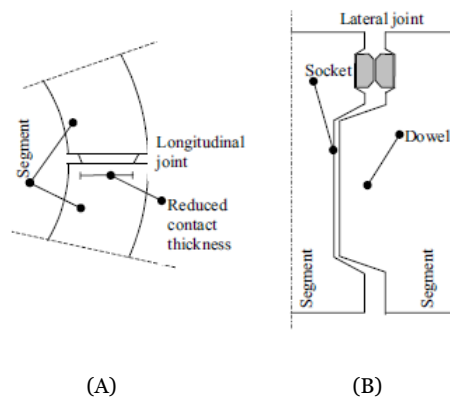

(A)   (B)

Fig.D17. Principles of (A) reduced contact area and (B) dowel & socket system   [70]

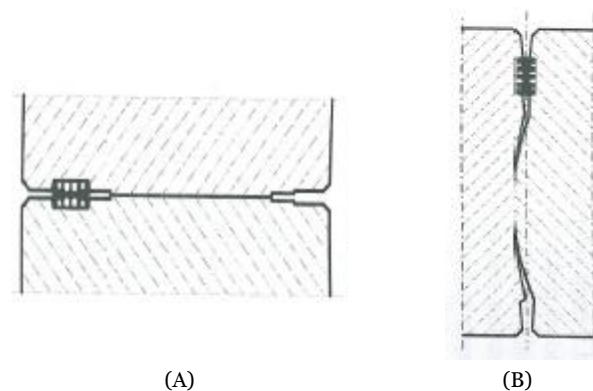(A)   (B)

Fig.D18.   Regular longitudinal (l) and lateral (r) joint shapes for concrete lining tunnels   [70; edited]

Rubber, mostly neoprene, gaskets are applied in the joints to assist to realize a water tight connection. The gaskets are glued at both edges. The axial compression forces compress the gaskets against each other when the rings are assembled. For an adequate sealing the gaskets need to be sufficiently compressed. During the placement of the elements there is contact between the gaskets of the new segments and the adjoining segments, which both causes protection for the elements as well as placement assistance. As a consequence the gaskets can slide over each other, protecting the elements from colliding.

Fig.D19. Close view of segment lining   [72]

Concrete tunnel lining elements are usually bolted together, this principle is elaborated in the next chapter. The location of the bolt pockets as well as the location of handle holes include a reduction of the concrete volume of the tunnel elements. Practice shows that cracking especially occurs at these areas. The introduction of the jack forces cause splitting forces in the concrete. The application of the three-dimensional orientation fiber reinforcement is expected to be advantageous for the load introduction. This aspect, together with the other considerations from tunnel lining practice, are used in the design for the elements in chapter 6.7.

6.4. Transport

6.4.1. Element size

Beside the fact that the fabrication method might limit the panel size it is remarked that transportation of fabricated elements is limiting the maximum dimensions. For this reason the maximum transport sizes by road within the Netherlands are searched for. These sizes are governing when precast elements are fabricated in a plant and have to be transported to the building site.

The fact that for large span shells a large amount of elements have little sagitta is advantageous for the efficiency of prefabricated elements by road. Especially when elements have the same dimensions, elements can be placed on transport with minimal efficiency loss when compared to flat elements.

The maximum dimension for road traffic are given by the 'Rijksdienst voor wegverkeer' (Government department for road traffic) in the Netherlands. The dimensions for traffic are limited by a total height of 4m, a width of 2.55m and a length of a flatbed trailer ('dieplader') with a maximum length of about 12.4 m. Within this research, assuming that the uncommon use of a site factory is not employed, a maximum precast element size of approximately 4 x 8 m² is used, for which it is noted that a larger element size can be possible. It is noted that one can occasionally deviate from these dimensions since elements can be for instance transported with a slight inclination, enlarging the maximum element width.

It is noted that the prefabrication of elements may also be advantageous while taking place at the building site where larger elements can be produced, which dimensions are then limited by for instance crane capacity. The reusability of the mould gets less important and the total shell will have a smaller magnitude of total edge length.

The Millau shell (appendix 3.5) construction shows the requisite for a site factory, which was established for the production of the approximately fifty large precast elements with dimensions equal to about 28 x 2 x 0.01 m³ which were casted vertically. The project demonstrates the prefabricating potential for large curved elements casted in a site factory.

Within this research the use of a site factory is not considered. The more unfavorable case where the elements are transported by road is concerned.

6.4.2. Transport considerations

Transport, handling and erection are critical operations and might be the determining factors of the design. During transport to the building site as well as storage and placing the elements the elements can be damaged. Since the elements within a UHPC-shell are likely to be very thin the edges of the elements can be easily damaged. However, UHPC has a uniform distribution of fibers the effects of unintentional loads is expected to be smaller than for conventional concrete.

Still, because of the thin elements it is remarked that an increase of thickness located at the edges of the elements might be of decisive for successful application of prefabricated elements.
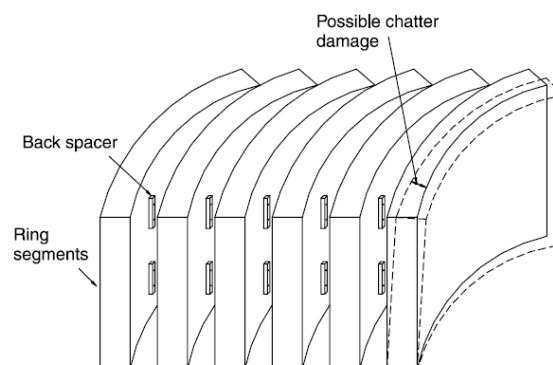

Fig.D20. Stacking concrete segments with back spacers to prevent chatter damage during transport   [69]

6.5. Formwork

Successful construction of a prefabricated shell structure depends upon design of the moulds and procedures developed to use them. Overall, the application of a formwork principle and its economical potential dependent highly of its reusability and size. The geometry of the shell is highly interlinked with the possible repetition of formwork. In general it holds that for a more complex the geometry, less repetition is achievable and vice versa.

The application of UHPC within prefabrication is different than other concretes, not only the because of the use of heat treatment, also traditional hand operation and finishing of UHPC is not possible because of the high viscosity and high fiber content of the plastic mix.

Mould construction and deflections are of high importance since they ultimately can lead to imperfections with mechanical effects. Attention to methods of release, orientation of the mould and product support are critical. In order to make demoulding possible without causing damage to the segments care must be taken on multiple aspects. It is common to ensure that the application of suitable lifting methods and lifting points can be employed. The mould design also has to accommodate significant initial autogenous shrinkage of the UHPC at a time when the material not has sufficient internal tensile capacity.

Research on other types of formwork, which are applicable for double-curved precast elements, have led to several types of methods such as milled-, flexible- and adjustable formwork. Though there has been many experiments on the fabrication of double curved elements a fabrication method which has been applied in practice and has proven its quality for large-scale production is not entirely developed. This research focuses on the combination of the large-scale use of UHPC and large span shell structures, therefore the feasibility of these prefabrication methods of curved elements is disapproved for this research.

The production of thin elements, especially when local connection provision are to be applied, requires the moulds to be manufactured with precise tolerances. This is illustrated by the fact that a typical production tolerance of ±3mm can increase the product thickness unneggligible for an element thickness of 60mm or smaller, which might cause an increase of the effect of imperfections. The experience from the reference projects of the Canadian LRT station (appendix 3.1) and the Pont du Diable footbridge (appendix 3.2) is used. Both projects made use of moulds of plate steel, which had high accurate precision of ±0.3mm in the project of Pont du Diable.

Fig.D21a. High precision steel mould for precast
element Pont du Diable [56]

Fig.D21b. High precision steel mould for precast
element LRT station [55]

The projects show that the successful application of the final product by making use of prefabricated UHPC elements was highly interlinked with the production of the mould. In general it holds that UHPC adopts the shape, and even texture, of the mould material. Within the project of the Canadian LRT station the application of an epoxy based liner on the contact service of the steel was used to smooth the surface of the steel, this was combined with a bees wax as dispersing agent. The base and side of the mould were first cleaned by compressed air and subsequently lubricated. The fact that UHPC adopts the shape of the mould can be applied highly beneficial for the creation of subtle edges and connection facilities. It is therefore chosen to make use of the same formwork production as the Canadian LRT station and the Pont du Diable footbridge, being moulds of plate steel. Thereby it is expected that, because of the small curvature and the consistency of UHPC during casting, that production by a single mould will satisfy the demands.

It is noted that the application of a steel mould can be expensive and can become financially feasible when they are used repeatedly. Therefore the successful application is highly dependent of the shell design and element configuration.

To improve the financial feasibility it is proposed to make use of a master mould which can be adapted for the production of various adjacent elements. The edges of the elements can be dimensioned in the same manner as the edges of the tunnel elements, with similar edges for all elements. Also, since adjacent elements can have the same amount of curvature, especially in a simple geometry, it might be advantageous to produce a base shape, illustrated by curved lines (1) and (2) below, which ensures multiple element types to be produced with exactly the same curvature. The combination of these two aspects support the idea of a master mould.
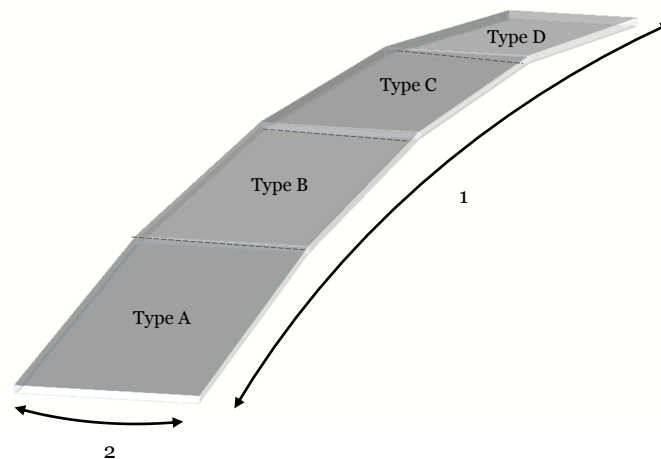

Fig.D22. Illustration of 4 different types of adjacent elements

A production tolerance of 0,3mm deviance, which goes with the steel mould production, is considered to be a very high precision. To possibly further improve the connections a casting method, named match-casting, is considered which is mostly used for concrete bridges. The purpose of the match-casting method to perfectly join and exclude any voids in between elements is very important for prestressed bridges, since if the contacting surfaces of the two segments are not perfectly matched, unforeseen stress concentrations may occur. Match casting for bridge construction starts with the production of the pier segment. When this segment has hardened sufficiently it will be used as the end socket for the first field segment. With this method the next segment will perfectly match with the pier segment.

Since a segmented shell structure exist of much more elements than bridges it is expected that the match-casting method is not as suitable to apply since the large number of elements in shell construction. Because within a three-dimensional shell structure all elements are to be connected to multiple other elements it is expected that the use of this method is too comprehensive to apply.

Practice with the production of the elements and testing their application will demonstrate whether production by steel moulds, as in the reference projects mentioned above, of the elements is sufficient. Since these reference projects show successful application, in particular in case of tightened elements as in Pont du Diable, of high precision steel moulds the application of this principle is assumed to be sufficient.

6.6. Element configuration

6.6.1. Possible configurations

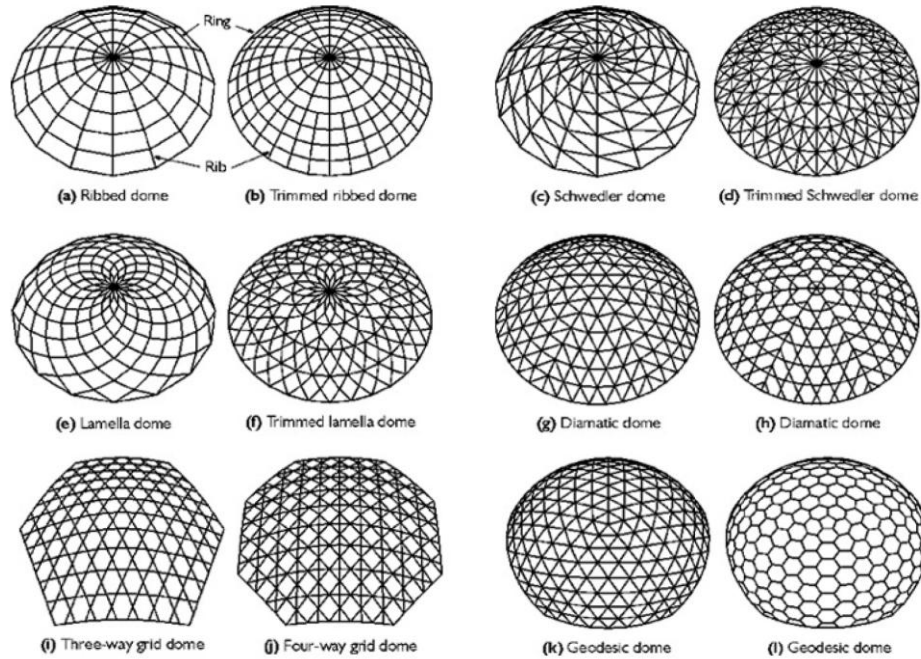A number of possible built-ups of elements for a spherical dome are shown in figure D23.

Fig.D23. Grid configurations for dome shapes [50]

In the collection of possible configurations the ribbed domes of (D23.a) and (D23.b) show the composition of trapezoid, but almost rectangular, elements which are repeatedly used along the circumferential axis. The geometrical straightforward composition of the ribbed dome is chosen for it is considered to be advantageous in consideration of element production, storage, transport and construction. To optimally make use of the maximum size of the prefabricated elements it is chosen to make use of a trimmed-ribbed dome configuration as in figure D23(b). With this configuration the edges of the elements form ribs and stiffeners, therefore it is deliberately chosen not to make use of a half-brick bond between the element rings.

The choice for the application of double curved elements in section 5.3.2. is also beneficial for the configuration of figure D23(b). Where the application of flat elements are a possibility within the ribbed dome configuration of figure D23(a), it is not for the trimmed rib dome, as illustrated below. This implies that the choice for flat elements and configuration (a) lead to a non-optimal use of element size and overall geometry.
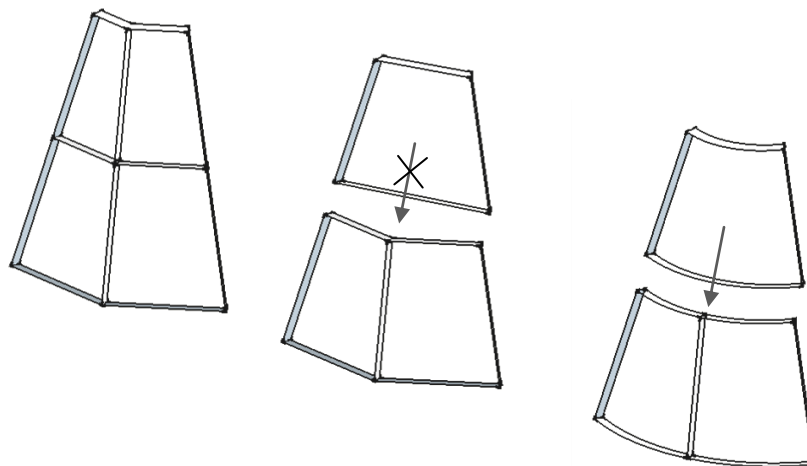

Fig.D24. Element positioning with and without curvature

The possibility of repetition of element types, which was explained to be if financial interest, is explicated in figures D23 above and in a project in figure D25. The arrangement of figure D25 shows a simple geometrical shape, being a spherical cap which spans 45m, divided in just six precast units. For a simple geometrical shape the advantages of repetition of the elements are multiple. The mould for the elements is used many times and therefore investment costs can be practically recovered because of their efficiency. Also, because of the constant amount of curvature within the shell the mould production has the opportunity to make use of the standard base shape. And, if an element is damaged the construction will not be delayed since every element can be replaced by the adjacent element in the same ring. To profit of the advantages of repeated elements, a more complex initial design may be adapted to be able to achieve a certain more simple division.
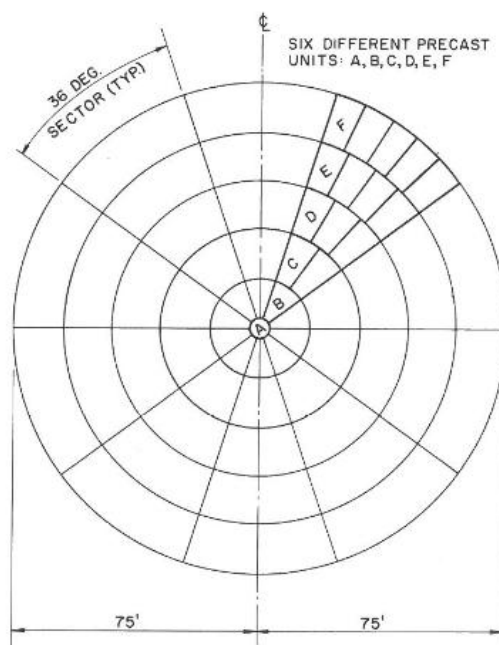

Fig.D25. Arrangement of precast panels for dome at Natick, USA   [46]

The difference between the configuration in figure D23(b) and figure D25 is the orientation of the elements. In figure D23(a) the elements are orientated horizontally along the circumferential direction, figure D25 shows the elements orientated in meridional, or vertical, direction. The second option has the advantage over the first for it demands less unique element types since the length from the base to the top of the shell is spanned by fewer elements. In addition, with the vertical orientation the elements itself are repeated more, making the production of the moulds even more beneficial.

6.6.2. Configuration proposal

Within section 6.4.1. it was determined that for further research an assumption is made to work with an approximate precast element size of 4 x 8 m², in which the length of 4m is based on the maximum height of transport on a flatbed trailer and can be slightly increased when elements are transported with an inclined position. The configuration is made on a shell of revolution with dimensions inspired by the Fiere Terp, the further calculations and considerations will be made for a shell with these dimensions. With the maximum dimensions and vertical orientation configuration known, a possible build-up of the elements over the total shell is described in this section. For this the proportions in shell design of appendix 4, proportions in shell design, are applied.

Diameter	d	150m
Sagitta	s	37.5m
Radius	R	93.75m
Arch length	L	~174m
Perimeter base	P	~470m
Shell Area	A	~22000m²

Tab.D6. Shell dimensions

The arch length (L) is divided by the proposed maximum length of the elements of 8m. When round off to a natural number the length is divided in 22 segments. The half of the arch length is divided by 11 and the corresponding angles (ϕ_n) are found by this division. The distance 'r' to the axis of revolution is found and leads to a corresponding circumferential perimeters which is to be divided in the most optimal mode by a maximum width. Also the composition of the trimmed rib ratio is to be applied to the elements, which holds that the ratio of the number of segments consists of natural numbers of for instance of 1:2:4:8 of 1:3:6:12. These ratios are applied, instead of for instance a half-brick-bond, since the application of ribs and stiffeners is expected to be more convenient for this build up as well as the connection of internal ribs. It now follows that:

Ring	ϕ_n	z (m)	r (m)	P (m)
1	53,1	0,0	75,0	471,2
2	48,3	6,1	70,0	439,8
3	43,5	11,8	64,5	405,3
4	38,6	17,0	58,5	367,8
5	33,8	21,6	52,2	327,8
6	29,0	25,8	45,4	285,4
7	24,2	29,3	38,4	241,0
8	19,3	32,2	31,0	194,9
9	14,5	34,5	23,5	147,4
10	9,7	36,2	15,7	98,8
11	4,8	37,2	7,9	49,6
12	0.0	37.5		

Tab.D7.   Shell parameters per ring

The tables below show the perimeter 'P' is divided by multiple angles, dividing the perimeter P into multiple segments. The obtained values are possible widths of the elements. The most applicable values are presented in black. Feasible element configurations, which correspond to the ratios given above, are shown in orange, green and blue.

Angle:	2	2,5	3	4	4,5	5	6	7,2	7,5	8
Ring Segments:	180	144	120	90	80	72	60	50	48	45
1	2,62	3,27	3,93	5,24	5,89	6,54	7,85	9,42	9,82	10,47
2	2,44	3,05	3,67	4,89	5,50	6,11	7,33	8,80	9,16	9,77
3	2,25	2,81	3,38	4,50	5,07	5,63	6,75	8,11	8,44	9,01
4	2,04	2,55	3,07	4,09	4,60	5,11	6,13	7,36	7,66	8,17
5	1,82	2,28	2,73	3,64	4,10	4,55	5,46	6,56	6,83	7,28
6	1,59	1,98	2,38	3,17	3,57	3,96	4,76	5,71	5,95	6,34
7	1,34	1,67	2,01	2,68	3,01	3,35	4,02	4,82	5,02	5,36
8	1,08	1,35	1,62	2,17	2,44	2,71	3,25	3,90	4,06	4,33
9	0,82	1,02	1,23	1,64	1,84	2,05	2,46	2,95	3,07	3,28
10	0,55	0,69	0,82	1,10	1,24	1,37	1,65	1,98	2,06	2,20
11	0,28	0,34	0,41	0,55	0,62	0,69	0,83	0,99	1,03	1,10

Angle:	9	10	12	15	18	20	24	30	36	40
Ring Segments:	40	36	30	24	20	18	15	12	10	9
7	6,02	6,69	8,03	10,04	12,05	13,39	16,07	20,08	24,10	26,78
8	4,87	5,41	6,50	8,12	9,74	10,83	12,99	16,24	19,49	21,65
9	3,68	4,09	4,91	6,14	7,37	8,19	9,83	12,28	14,74	16,38
10	2,47	2,75	3,29	4,12	4,94	5,49	6,59	8,24	9,88	10,98
11	1.24	1.38	1.65	2.07	2.48	2.76	3.31	4.13	4.96	5.51

Tab.D8.   Element widths and possible configurations

The orange configuration shown in table D8 causes the shell to be divided into 1050 elements, green into 954 and blue into 945. Since its favorable to divide the shell in the less elements as possible the orange configuration is declined. The other configurations are comparable in number of elements. It is chosen to work with the cofiguration presented in green since the edges of the elements are in this configuration closer to each other than for the blue configuration within the first four rings. This is favorable for multiple aspects within the design such as edge disturbances, as was explicated in part B. Also, the transition between the number of rings with a certain division to the next division is more gradually for the green configuration than for the blue division, which is expected to be favorable for the force distribution.

This configuration, known as a trimmed ribbed dome, leads to the following figure with 954 elements with an average surface of 23,5m².

Ring	# Elements	Element surface [m²]
1	144	25,0
2	144	23,1
3	144	21,2
4	144	19,1
5	72	33,6
6	72	28,9
7	72	23,9
8	72	18,8
9	36	27,0
10	36	16,3
11	9	21,8
Total	945	~22000

Tab. D9. Total build up of elements
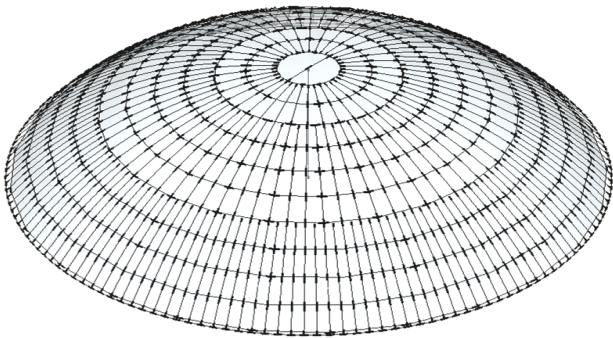
Fig. D26. Total build up of elements
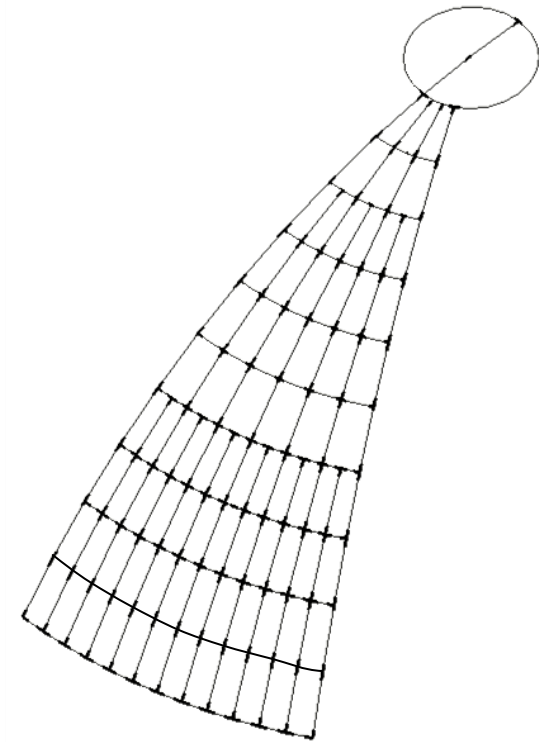
Fig. D27.   Section of element configuration

6.7. Element principle

The principles for the elements are represented below. It is noted that within this figure the curvature of the elements is barely visible.
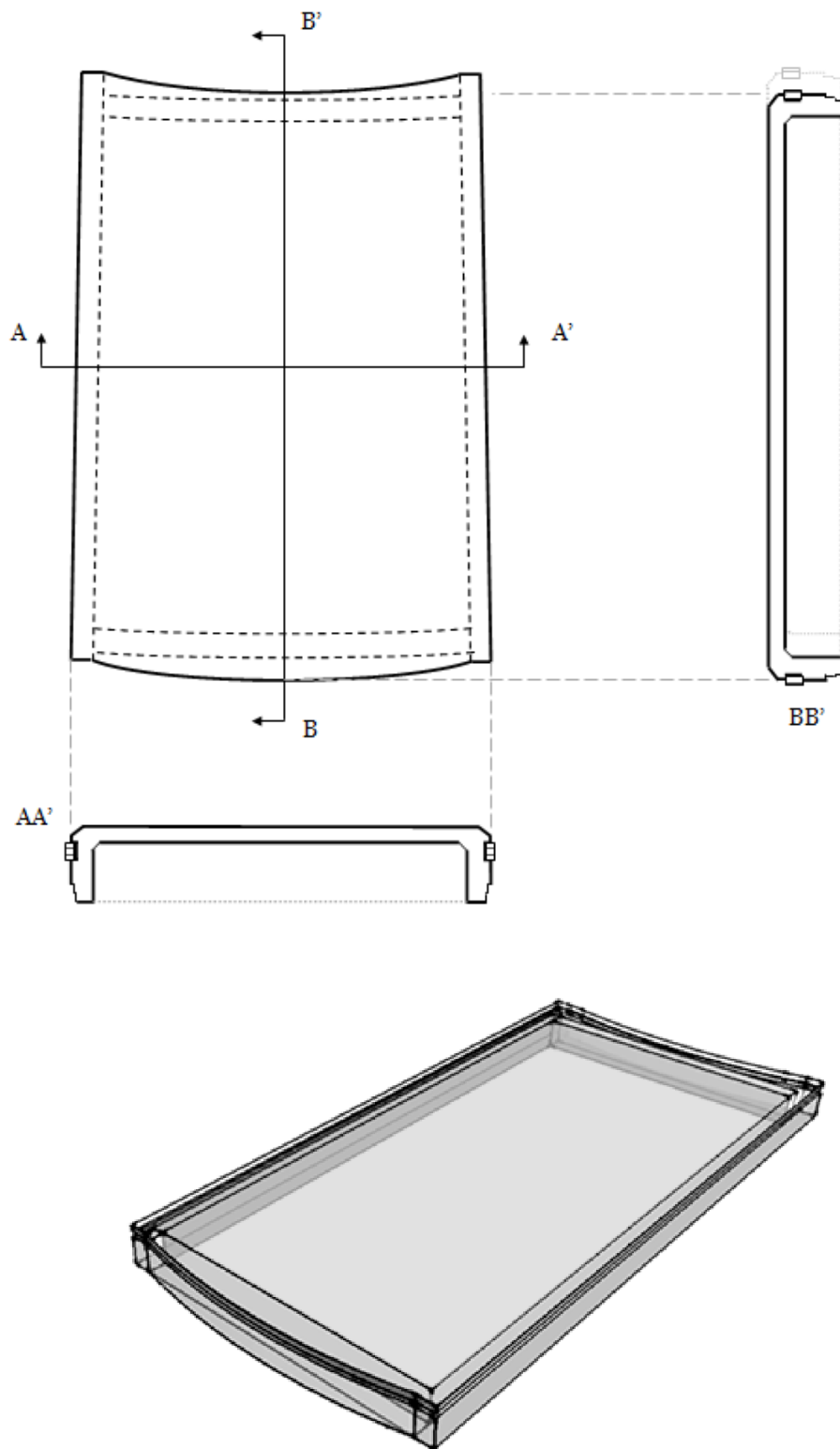
Fig. D28.   Principle of applied element   & isometric presentation

7. Connections

In precast shell structures, because of their three-dimensional mechanical behavior, the connection between the precast elements is of major structural importance for they ought to provide the overall structural integrity. Also the connection should provide fast and durable connections with sufficient strength to meet erection sequence, support requirements and to maintain compression of possible sealing gaskets. Connections of prefabricated elements are by definition labor intensive and its therefore advantageous to reduce the labor time to utilize the advantage of prefabrication. The possibilities for precasting elements and connections are described in this chapter. The described existing connection systems are deliberated and evaluated on multiple characteristics.

7.1. Requirements

In general it holds that the design of joints should provide for tight and durable connections with sufficient strength to meet multiple physical, structural and other requirements.

Structural requirements

Structural requirements can be different for different locations within the shell. In general connections can be subjected to:

- Normal forces
- Shear forces
- Bending moments

The theory of part B describes the membrane behavior of a thin shell. It is concluded that a curved shell will generally be subjected to normal forces. The analytical results for a shell subjected to dead load is given in figure B10. It was concluded that the distribution of the meridional stress for vertical load shows an overall compression which increases from top to bottom. The circumferential stress on the other hand shows a course from compression to possible tension. The calculations based on the load combinations considering wind and snow are elaborated within the calculations of chapter 8.

Physical requirements

The connections need to meet a set of physical requirements:

- Provisions (ducts, weld plates, etc.)
- Tolerances (size divergence/thermal expansion)
- Prevent water accumulation in connections
- Water tight (in case of internal insulation)

Further aspects

Other aspects which influence the degree of applicability of the connection system:

- Load introduction
- Assembly method
- Suitability for UHPC
- Construction speed
- Durability

7.2. Connection principles

To describe several types of possible precast connections a number of connection principles for standard flat elements are deliberated together with their applications within reference projects. As mentioned, the difference from the connection of standard flat elements to curved elements might complicate the applicability of certain types of connections. However, since the rate of curvature if low, the possible difficulties are restricted. The application of the connection types within realized reference projects with UHPC is mentioned for a number of connection types.

It is noted that the three-dimensional fiber orientation of UHPC can be an advantage considering local load introduction into the elements. Beside imposed local peak stresses other discrepancies and irregularities can occur in practice. The magnitude of the peak stresses and their locations are hard to predict since they depend on fabrication- and placement inaccuracies of the elements. In contrast to conventionally reinforced concrete the fibers are present in the entire concrete volume and are orientated in any direction. The orientation makes the fiber reinforcement highly efficient and capable to withstand local stresses, either intended or unintended.

7.2.1. Wet connection

For a wet connection the elements are placed at a specific distance. Conventional reinforcement can be placed within the seem as well as protruding out the prefabricated elements. The connection can be filled with a shrink-resistant mortar.

The advantages of this system are:
- Optimal possibilities with respect to tolerances
- Basic assembly handlings
- Equally introduced forces into the elements

The disadvantages of this system are:
- Placement of in-situ concrete is weather dependent
- The connection needs to harden before forces can be applied
- The joint often remains visible. Extra finishing might be required

Examples:
UHPC joints for precast decks (appendix 3.11)

7.2.2. Bolted connection

With bolted connections the elements are connected by bolts, this system requires provisions within the elements.
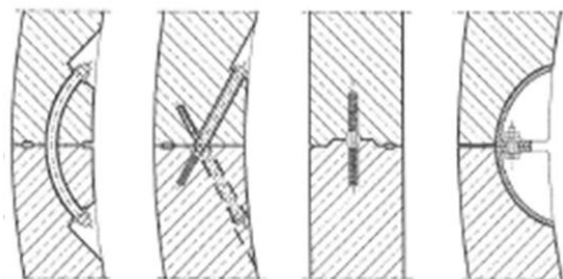

Fig.D29.   Bolt configurations for concrete lining tunnels   [70; edited]

The advantages of this system are:
- Simple and fast assembly handlings
- Good adjustment possibilities if right detailing of element connections
- Stays adjustable after assembling

The disadvantages of this system are:
- Often difficult to detail
- Costly connections if durable protection is needed
- Complex system if grid of the shell is an unstructured grid

Examples:
    LRT Station (appendix 3.1)
    Folly in UHPC (appendix 3.7)

7.2.3. Post-tensioning connection

Continuous post-tensioning connection

In a post-tensioning connections with continuous strands elements are provided with continuous ducts trough which tendons are placed over multiple elements. After the placement of the elements the continuous tendons are tensioned by for instance hydraulic jacks and then fixed.

The advantages of this system are:
    -    Strong connection
    -    Durable
The disadvantages of this system are:
    -    Thickness demands for connection to be applied
    -    Continuous ducts throughout element

        Examples:
        Gärtnerplatz - Bridge over River Fulda in Kassel (appendix 3.6)

Local post-tensioning connection

Local post-tensioning connection makes use of connection ducts which are, in contrast to continuous post-tensioning described above, not applied over the entire cross-section but merely on the parts close to the edges of the element. The idea to apply local post-tensioning is based on the Norm-teq Heli-system, as shown in figure D30, which is commercially applied to connect prefabricated, mostly cantilevering, elements to existing structures.

It is noted that figure D30 shows the principle is illustrative as well as the dimensions. It is noted that the dimensions of this connection method can be adapted so they can be applied within the project.
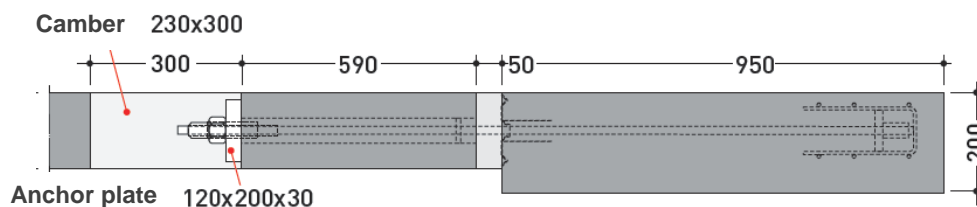
Fig.D30. Principle of Norm-teq Heli-system; vertical section of fixation of façade element   [79]

The advantages of this system are:
    -    Simple
    -    Quick assembly
The disadvantages of this system are:
    -    Thickness demands for connection to be applied

7.2.4. Welded connection

Precast elements can be welded together to form a permanent connection, steel provisions need to be inserted in the mould before casting.

The advantages of this system are:
    -    Optimal adjustment possibilities
    -    Strong connection
The disadvantages of this system are:
    -    The need for qualified welders
    -    Not adjustable after assembling
    -    Application of conservation and protecting coating on site

- Long construction process

7.2.5. Glued connection

In gluing technology the assembly parts are joined by the use of plastic or liquid adhesives that harden by chemical or physical processes. Glued connection are successfully applied within structures where they are under permanent compression. The response to tension, long-term behavior and behavior within fire are however questionable for successful application.

The advantages of this system are:
- Equally introduced forces

The disadvantages of this system are:
- Long term behavior unknown
- Slow construction

Examples:
Gärtnerplatz - Bridge over River Fulda in Kassel (appendix 3.6)

7.2.6. Fiber joint

Fiber joints make use of fibers, larger than the fibers in the UHPC, which work as an substitute for conventional concrete. The fibers of for instance 70mm length are inserted into a supporting ribbon that can serve as a formwork for the elements

The advantages of this system are:
- Equally introduced forces
- Easy assembly handlings

The disadvantages of this system are:
- The connection needs to harden before forces can be applied
- Durability aspects rather unknown
- Successful application in project unknown

7.3. Conclusions and selection

Most connection methods discussed are proven to be suitable connection methods for precast elements and are applicable for UHPC. The ease of construction of the connection type to be applied has great influence on the construction method, -time and quality of the structure. The accessibility together with placing tolerances and the economical features of the connection method are decisive. It is noted that it is a possibility to make use of, for instance, two connection principles, distinguishing the meridional and circumferential direction.

Local connectors and their local force introduction are well applicable for UHPC because of the toughness of the material and the fact that peak stresses can be distributed through the material as a result of the three-dimensional orientation of the fibers. Local connectors demand local connection facilities, which had its demands for the production phase.

Considering the construction method it is noted that the placing of the elements can give problems with respect to tolerances. Placing elements and connecting locally gives high demands on the placing technique. On the other hand, local connections can assure immediate linking of the elements. This immediate linking will result in a rapid construction phase, since elements which are linked obtain a immediate force distribution.

In general it holds that the more difficult the connection type is, the more professional skill is required on building site. For instance post-tensioning is known to require specific expertise and equipment for installation, these requirements make the connection type expensive. Furthermore, the analysis and control are complex for the correct post-tensioning forces. On the other hand, for UHPC the application of prestress could be exploited up to higher extend than for conventional concrete, this is noted for creep of UHPC and possible corroding of the strands is of less significance. Another example of a difficult connection type is a welded connection since the difficult assembling and the need for qualified welders.

As mentioned, it is considered to be possible to apply different types of connections within circumferential direction and meridional direction since the stress distribution in both directions is significantly different, which may result in different demands. The force distribution within shells subjected to dead load, as described within part B, showed that the compressive stress within the meridional direction for a shell exists of merely compressive force, which increases from top to bottom. This compressive force however may well be canceled by tension forces as a result of wind load when the shell is sufficiently thin.

Selection

It is concluded from early design calculation in paragraph 8.5 that the structural requirements show that the connections will be subjected to tension. Two factors influence the choice for the connections to be applied, that is the fact that local force introduction is well feasible for a fiber reinforced material like UHPC and the fact that immediate connecting is favorable for the construction phase. Therefore the choice is made to elaborate the principles of post-tensioning, either continuous over multiple elements or local between two elements, and more simple connecting bolts. Both principles can only be applied within a sufficiently thick concrete section. This coincides with the choice to apply thicker element edges as described in section 6.3.2. Within this thicker edges the connection can be applied.

Which of the chosen connection types will be applied within a design depends of both the magnitude of the tension forces within the edges as well as considerations of the construction phase. For instance the connecting of multiple elements by continuous tendons is more labor intensive than purely local connectors due to the implement of the ducts as well as installment at the anchors, this principle will for those reasons only be applied if necessary. The considerations concerning the demands are made in chapter 8 and 9. It is noted that multiple configurations of local post-tensioning, continuous post-tensioning and bolts are possible, of which a number are shown below. The principle details represent a presentation of corresponding possible and deliberated connections.
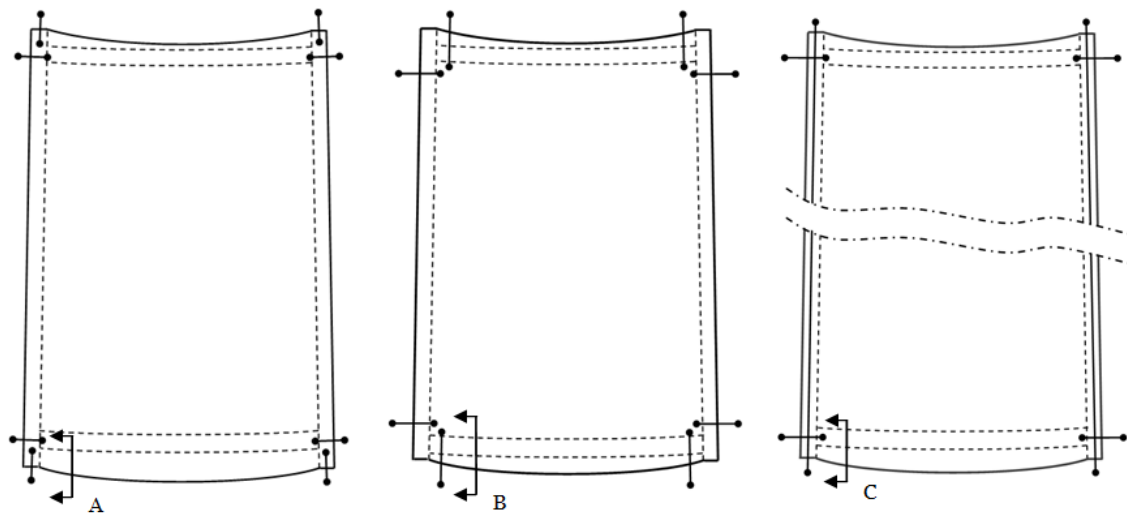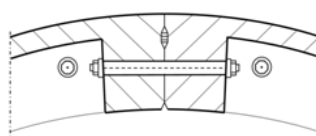
a). Element with merely local connections

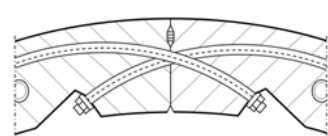b. Element with continuous tendons and local connections

Fig. D31a. Examples of connection configurations and locations
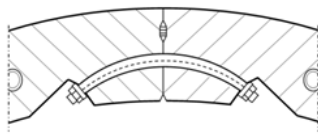
Principle A   Principle B   Principle C

Fig. D31b. Location possibilities of connections

8. Calculations on design aspects

In paragraph 3.4 several shell design aspects are explicated. In this chapter these aspects are deliberated concerning the sagitta to span ratio, rib stiffening, edge rings et cetera.

Structural design implies iterative analysis of these, and other, design aspects. Because the aspects may highly interfere an optimization of a structural model containing all aspects is likely to give an indistinct web of results when all parameters are subjected to adaptation for optimization. For instance the effect of the parameters of the edge ring is best researched when all other parameters are kept constant.

It is desired to find design directives based on optima for the several design aspects mentioned above. Also it is best to examine the multiple aspects to gain knowledge of the several aspects individually. It is for these reasons that the aspects are treated independently according to a principle known for research in economics named 'ceteris paribus'. This principle stands for the Latin phrase for 'all else being equal' or 'all other things held constant' and is often used for isolating descriptions or events from other potential environmental variables.

When implying this research approach the effects for design aspects are charted clearly. The results are interpreted and are leading as design directive and as recommendations when calculating a model concerning all design aspects. All the aspects are contemplated with values for a purely vertical load combination, being dead weight and a distributed snow load, and, if desired, a combination involving lateral load, involving dead weight and wind load.

Most aspects are contemplated for a shell with solid thickness. This choice is made because the behavior of a solid shell is well known and can therefore be well examined. Also, models can be simply checked and verified with theory and earlier found results. The thickness of the shell for some calculations is, in this stage of calculation, relatively irrelevant.

The aspect researches are made for shells with perfect geometry and with linear calculation consisting of the UHPC type Ductal with the help of Scia engineer. The finite element calculations are based on linear elastic theory, this implies that the materials are modeled as a continuous mass and elements are assumed to undergo infinitesimal strains and small deformations and an infinite elastic behavior of the relationship between stress and strain.

All aspects are limited and checked on their limitations. These limitations consistently involve the influence on the linear buckling failure and strength considerations. The shell geometries are tested on their linear buckling by loading in vertical direction.

<u>Design capacities</u>

The structural capacities of the UHPC Ductal® is calculated using the equations from the French recommendations [Bron].

Compressive capacity:

$$f_{cd} = \frac{0,85 f_{ck}}{\gamma_c} \qquad \text{with:}$$

f_{cd} =   Compressive strength
f_{ck} =   Mean compressive strength
γ_c =   Material factor (1,3 for fundamental combinations)

$$f_{cd} = \frac{0,85 f_{ck}}{\gamma_b} = \frac{0,85 \cdot 180}{1,3} \approx 117,7 N/mm^2$$

Tensile capacity:

$$f_{ctd} = \frac{0,7 f_{ctm}}{K \gamma_c}$$

f_{ctd} =   Direct tensile strength
f_{ctm} =   Mean tensile strength
K =   1,25   (for all loads other than local effects)
γ_c =   Material factor   (1,3 for fundamental combinations)

$$f_{ctd} = \frac{0,7 f_{ctm}}{K \gamma_c} = \frac{0,7 \cdot 10}{1,25 \cdot 1,3} \approx 4,3 N/mm^2$$

8.1. Sagitta to span ratio

- Calculation results in appendix Calculations 8.1 -

The proportions of the overall dimensions within shell design are described in appendix 4. Within this paragraph a consideration is made for the ratio of the span to the sagitta of the shell. For this calculations the shell is built up with a constant thickness. The design limitations will consider circumferential stress and buckling; which are presented in relation to the sagitta to span ratio. The supports are, in this phase, hinged over the entire perimeter of the edge.

It is noted that the ambition for Fiere Terp is to span approximately 150m. This dimension however, at this point is relatively irrelevant for it is the effect of the diameter to the sagitta ratio which is of design importance. The design geometry is limited by two aspects, being buckling load and internal stress. The relation between the buckling load and the sagitta to span ratio is considered first. The stress distribution is limited by the material capacity as determined above.

In order to determine whether the concrete thickness of a solid shell depends on buckling of compressive strength considerations can be predicted by formula 2.3.1.2. for the critical membrane force, while loaded perpendicular to the surface, and compressive strength.

$$n_{cr}^{lin}[N/m] = \frac{-1}{\sqrt{3(1-v^2)}} \frac{Et^2}{R} \approx -0,58 \frac{Et^2}{R}$$

The formula, or in fact the factor 0.58, is to be multiplied by the knock-down factor. In practice, the critical linear buckling load is found for a factor between 0.1 and 0.58. It is of interest to find the values for the radius to thickness ratio which are decisive for the failure mode. This is done by considering hypothetically that buckling and crushing take place at the same time. Only compressive stress, due to perpendicular load, is taken into account.

$$n_c[N/m] = -t \cdot \frac{f_{yd}}{1,5}$$

$$n_{cr}^{lin}[N/m] = -0,58 \frac{Et^2}{R} \qquad \text{and} \qquad n_{cr}^{lin}[N/m] = -0,1 \frac{Et^2}{R}$$

$$-t \cdot \frac{f_{yd}}{1,5} = -0,58 \frac{Et^2}{R} \qquad\qquad\qquad -t \cdot \frac{f_{yd}}{1,5} = -0,1 \frac{Et^2}{R}$$

$$\frac{R}{t} = 0.87 \frac{E}{f_{yd}} \qquad\qquad\qquad\qquad \frac{R}{t} = 0.15 \frac{E}{f_{yd}}$$

With the modus of elasticity and compressive strength of Ductal it is found that the limit values for R over t are:

$$\frac{R}{t} = 0.87 \frac{E}{f_{yd}} = 0.87 \frac{58000}{150} = 336.4 \qquad\qquad \frac{R}{t} = 0.15 \frac{E}{f_{yd}} = 0.15 \frac{58000}{150} = 58$$

It is concluded that a solid shell of Ductal will fail due to crushing if R/t < 58. The failure mode will be buckling for R/t > 336.4. In between the two values the failure mode can be either or in combination.

Since this result for the characteristics of Ductal is known it is again emphasized that buckling failure is of major importance for structural design considerations. That is, since the R/t-ratio of 336.4 is very likely to be exceeded for the final dimensions. It is noted that this consideration regards perpendicular compressive loading only, so the effects of other load types are not regarded yet.

Now, for these design calculations which consider multiple types of loading as described in chapter 5, the following parameters hold.

Parameters:

Parameters:		
Span:	d = 150m	
Thickness:	t = 100, 200, 300, 400	
Supports:	All hinged	
Loads:	According to Chapter 5 Load combinations and general vertical load	

Variables:		
Sagitta to Span - ratio:	1/2 to 1/10	
Design limitations:		
Buckling:	Linear elastic calculation	
Stress:	Design capacities UHPC	

Geometry parameters

The following parameters apply in this calculation. The wind factors apply for the research on required shell thickness.

d (m)	s (m)	d/s		R	ce(z)	qp		A	B		wA	wB	wC
150	75.00	2		75.00	4.1	1.87		0.80	-1.20		1.49	-2.24	-1.12
	50.00	3		81.25	3.8	1.73		0.55	-0.84		0.95	-1.45	-0.72
	37,50	4		93,75	3,6	1,64		0,43	-0,66		0,70	-1,08	-0,54
	25,00	6		125,00	3,3	1,50		0,30	-0,48		0,45	-0,72	-0,36
	18,75	8		159,38	3,1	1,41		0,24	-0,39		0,34	-0,56	-0,28
	15,00	10		195,00	3,0	1,37		0,20	-0,34		0,27	-0,46	-0,23

Tab.D9.   Parameters for sagitta span ratio calculations

8.1.1 Buckling

The effects of the variables for relation between the buckling load and the sagitta to span ratio can be predicted by a formula as derived in part B chapter 5.The linear buckling load for uniform pressure, perpendicular to the surface, was found to be:

$$p_{cr}^{lin}[N/m^2] = \frac{-2}{\sqrt{3(1-v^2)}} \frac{Et^2}{R^2} \approx -1,16 \frac{Et^2}{R^2}$$

In contrast to the uniform pressure perpendicular to the shell surface, which matches the formula for the linear buckling load, for this investigation a purely vertical load is applied to the structure, which corresponds to realistic loading which appears for dead load. The critical buckling load factor can be found as described in part C. To exclude any discrepancies considering load factorization a vertical load of 1,0 kN/m² is applied. The found buckling load can be multiplied with the knock down factor to find an estimation of the practical load capacity. The effects of the calculations are presented in the table below. It is noted that the perpendicular load is in the local coordinate system (LCS) and the vertical load in the global coordinate system (GCS).

It is expected, as described in the research hypothesis, that the high modulus of elasticity of UHPC has a significant effect on the buckling load. For design purposes and to visualize the difference of perpendicular and vertical buckling loads four shell thicknesses are tested for different sagittae.

The difference between the theoretical linear buckling load by perpendicular load, which is confirmed by FEM analysis in appendix 5, and by vertical load is given for solid shells. The effect of magnifying curvature, and therefore smaller radius, was concluded to be positive for buckling failure for perpendicular load and is given by the parabolic continuous line in the table below.

For vertical loading the buckling loads are determined by FEM-analysis. It is seen that for smaller sagitta the differences between the perpendicular load and vertical load gets relatively larger. This is easily explained as for a small span to sagitta ratio, of for instance 10, the direction of the loads only slightly differ geometrically whereas for shells with larger sagitta the load configuration differs significantly, leading to concentrated forces near the edges.
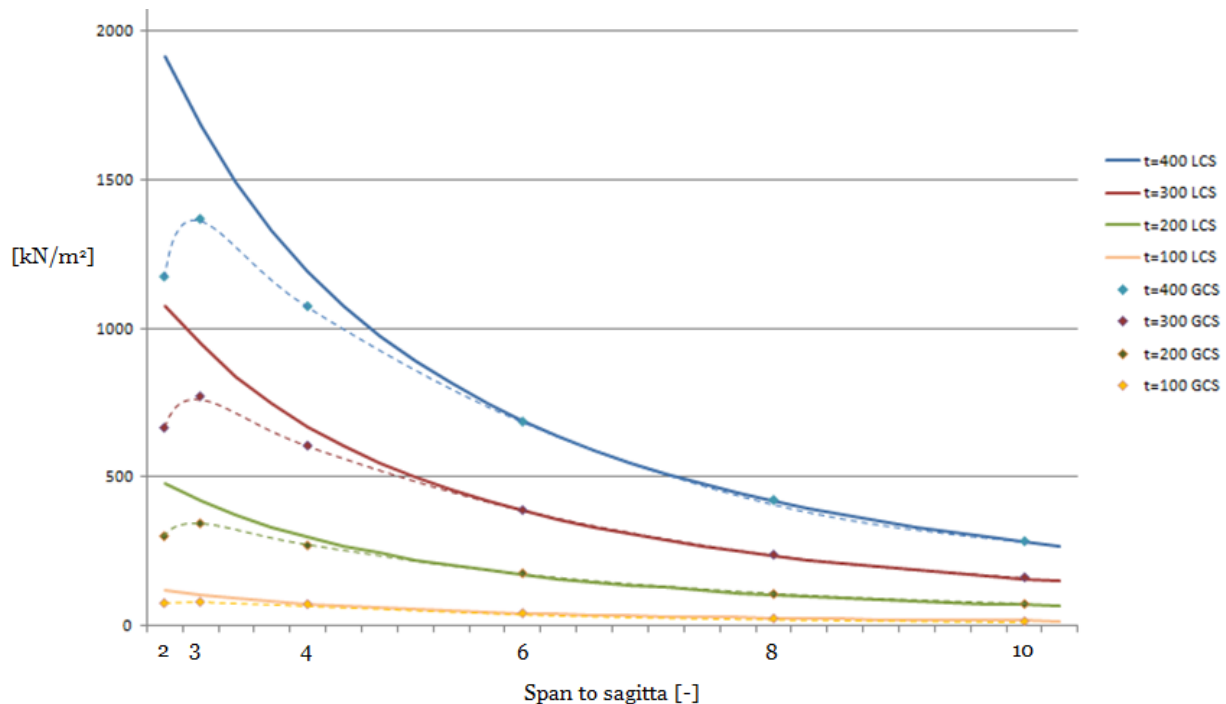
Fig.D32. Linear critical buckling load for thickness and ratio

The increase of curvature shows a relative fall-back as compared to the perpendicular load for span to sagitta ratios smaller than 6. The differences when the ratio is 2, a hemisphere, is remarkable. It appears that the vertical loading for hemispheres is relatively more unfavorable compared than to geometries with less curvature. The effect is explained by looking at the buckling figures for several geometries as presented below.

It is noted that the buckling loads are determined by several critical coefficients for which the smallest is decisive. All geometries show multiple buckling coefficients which are very close to each other. Therefore it is concluded that the sagitta to span ratio for this type of shell of revolution does not affect the sensitivity to compound buckling. This sensitivity will have to be dealt with by other structural and possible geometrical means.

Shells with high sagittae subjected to vertical load show a high sensitivity to local buckling near the supports which explain the lower critical buckling load. This is, in combination with possible high stress and edge disturbances, an additional reason to optimize the edge thickness, as is described in chapter 8.2.

d / s = 2 λ ≈ 1900	d / s = 3 λ ≈ 1630	d / s = 6 λ ≈ 690
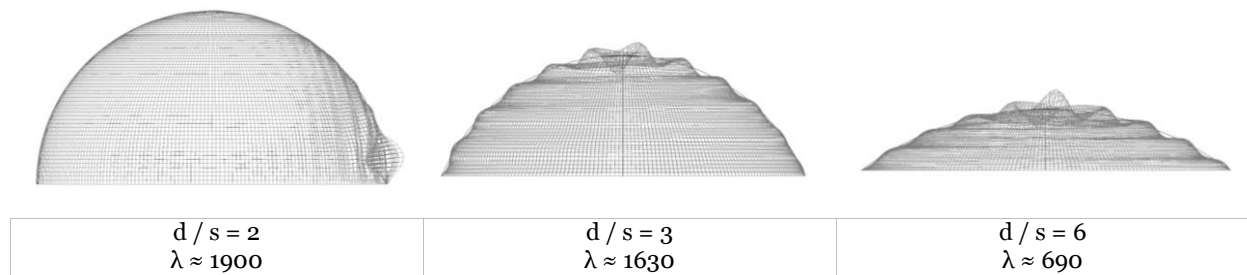
Fig.D33a. Buckling figures for shells subjected to perpendicular load
t = 400mm

d / s = 2 λ ≈ 1180	d / s = 3 λ ≈ 1330	d / s = 6 λ ≈ 690
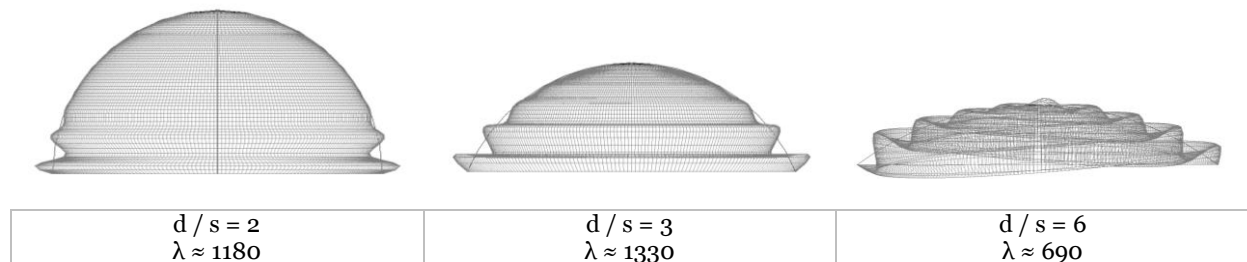
Fig.D33b. Buckling figures for shells subjected to vertical load
t = 400mm

With the results presented in the graph above and the given loads it can be predicted which (equivalent) thickness is needed for several amounts of curvature for the structure. The formula for the linear critical buckling load is added by two factors being the knock down factor C and the factor γ, which defines the proportion in the buckling load by vertical loading compared to the buckling load subjected to perpendicular loading. The γ -factor is determined by the graph above, which can be used to determine proportional changes of buckling resistance with respect to geometry.

It is concluded by the numerical values for the buckling coefficient that the γ –factor is of the same order of magnitude for the various thicknesses. The factor is determined to be equal to 1,0 for span to sagitta ratios larger than 6.

Span to sagitta:	γ –factor
2	0.627
3	0.814
4	0.919
6	1.00
8	1.00
10	1.00

Tab.D10. γ-factor for span to sagitta-ratios

The design formulas, considering the required shell thickness with respect to buckling, now hold:

$$p_{vert.load}[N/m^2] = C \cdot \gamma \cdot \frac{-2}{\sqrt{3(1-v^2)}} \frac{Et^2}{R^2}$$ Formula 7.1.1.

and

$$t^2 = -p_{vert.load} \cdot \frac{R^2}{E \cdot C \cdot \gamma} \cdot \frac{\sqrt{3(1-v^2)}}{2}$$

It is noted that this is formula is only used as an early design formula to determine an indication of the equivalent concrete thickness because in this formula a couple of important aspects are neglected. Influences of dynamic loads, unequally distributed loading, characteristics of edges and supports, occurring moments and practical dimensioning are to be taken into account in structural design. It is however worthy to use this formula to estimate the design thickness at early stage but might be increased significantly.

As an example a solid shell with a span of 150m and a span to sagitta ratio of 4 is chosen. For solid shells, opposite to sandwich shells, the equivalent thickness is equal to the concrete thickness. The vertical load is, only for validation of the formula, chosen to be equal to dead weight and equally distributed snow load. The dead weight is approximated by 0,1 * 25 + 0,25 = 2,75 kN/m². The snow load is known to be 0,45 kN/m². In ultimate limit state it now holds that:

$$t^2 = (1,2 \cdot 2.75 + 1,5 \cdot 0.45) \cdot \frac{93.75^2 \cdot 6}{58 \cdot 10^6 \cdot 0.919} \cdot \frac{\sqrt{3(1 - 0^2)}}{2}$$

$$t \geq 58mm$$

The result is checked by a stability calculation. The critical buckling coefficient for the shell with a thickness of 58mm, loaded by (1,2*2,75 + 1,5*0,45) kN/m² was found to be $\lambda \approx 5.88$. This value corresponds well, for it has a small deviance of only 2%, to the knock-down factor being 6.

It is validated that the formula gives an appropriate approximation of an early design thickness for a solid shell. The value of 58mm gives a Radius over thickness ratio of $93,75 \cdot 10^3 / 58 \approx 1600$, which is large when compared to existing shells, which do typically not exceed a R/t-value of 500. For these existing shells are constructed out of concrete with a minor Young's modulus the difference in the ratio can be explained for a considerable part. Also, merely dead weight and evenly distributed snow load are taken into account. The boundary conditions of the shell is thus far schematized as fully hinged whereas in practice the shell will be supported by a, possibly less ideal, edge ring. Numerous of existing shell are cast in-situ reinforced shells, constructional processes and reinforcement coverage have also played a role in dimensioning their shell thicknesses. Having considered this, it is noted that occurring imperfections are expected to have a relatively larger effect for thinner elements, causing that the effects because of imperfections can be presumably larger.

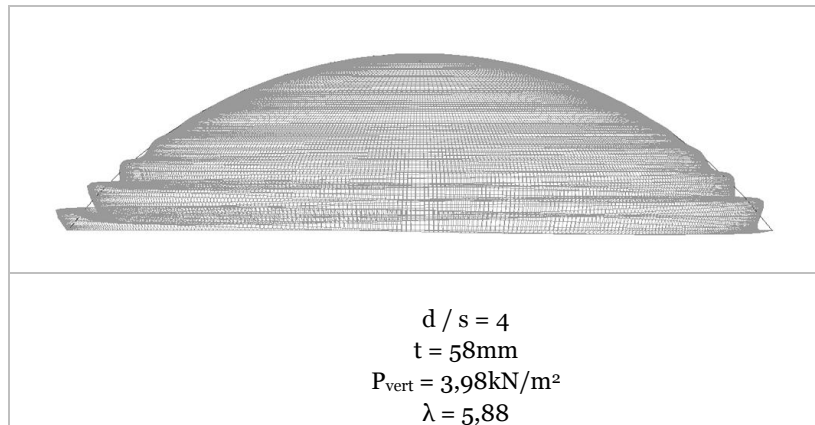d / s = 4
t = 58mm
P_{vert} = 3,98kN/m²
λ = 5,88

Fig.D34. Formula validation

Design check

It is checked whether this solid shell, with given dimensions and a thickness, satisfies for the different load cases including wind and redistributed snow. The thickness of 58mm was determined by an approximation of the permanent load, based on an assumed thickness of 100mm. This thickness was then used for the validation of formula 7.1.1., where the knock-down factor was checked for given loading and thickness.

The determined shell thickness of 60mm will therefore easily satisfy the demands for its permanent load and evenly distributed snow load. The thickness is chosen to be maintained to check whether the shell satisfies the other load cases. The load cases are all in ULS, the shell satisfies when all critical factors are larger than the safety factor 6.

	Buckling load	25,1 kN/m²
LC1	Permanent load	$\lambda = 12,2$
LC2	Permanent load + Wind load	$\lambda = 08,6$
LC3	Permanent load + Snow load (evenly distributed)	$\lambda = 09.2$
LC4	Permanent load + Snow load (redistributed)	$\lambda = 07.7$

LC1 $\lambda = 12,2$	LC2 $\lambda = 08,6$
LC3 $\lambda = 09.2$	LC4 $\lambda = 07.7$
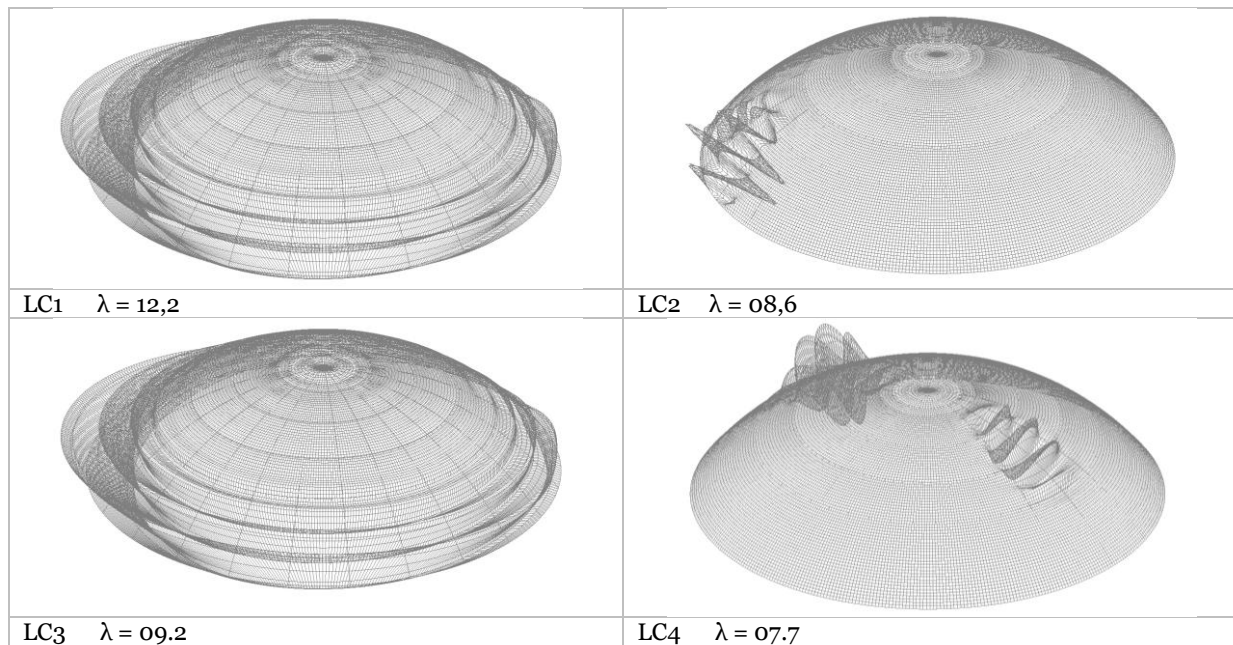
Fig.D35. Buckling patterns and safety factors

It is hereby concluded that the constant shell thickness of 60mm is a valid design value and it will therefore be used in further considerations. Furthermore it is concluded that the local effects of the redistributed snow load have the most unfavorable effect on the safety of the shell.

8.1.2. Concrete strength

Besides vertical loading due to permanent loads the effects of the wind load on the stress in circumferential and meridian direction are of interest. The possibility for occurrence of large tensile - and compressive stresses is examined for the effects of the loads on the stresses are yet unknown. Here, the stress resultants in meridional and circumferential direction are of interest. Edge disturbances and possible moments and shear forces are neglected since they are taken into account in further design calculations. The aim of this calculation is to find a required thickness of a solid shell based on its design strength.

The stress resultants in meridional and circumferential direction were found in part B. The circumferential stress, which may be tensional, for spherical shell with free edges which is vertically loaded is given by:

$$n_{\theta\theta} = pR\left(\frac{1}{1+\cos\phi} - \cos\phi\right)$$

The maximal sagitta to span ratio, for which tensional stress theoretically will not occur for vertical loading, was found to be 1 over 4,12 in part B chapter 3.4.2. Led by this value, which is based on purely vertical load, the first calculation is based on a shell with a slightly less favorable, in preventing tensile stress to occur, sagitta to span ratio of 1 over 4. This choice is made to be able to chart the magnitudes and locations of tensile stresses for a relatively high structure. Also, the preliminary design for Fiere Terp, as a design directive has a height of 35m with a span of approximately 37m with the same span.

The parameters, considering geometry and wind loading, which apply for these calculations, are shown in the table above. The results are filtered and presented in general values in N/mm² and N/mm. The stress as a result of dead load, in N/mm², is independent of the shell thickness since a larger thickness leads to a proportional larger load. The force in the cross section as a result of snow or wind load is independent of the element thickness and given in Newton per unit length.

The required element thickness is determined by adding the stress due to permanent load with the forces found by the envelop results of the various wind and snow loads. The thickness is found by comparison with the design values for compressive and tensile strength.

For a shell of constant thickness it is concluded that for the given geometry the minimum required thickness based on strength considerations is based on occurring tensile stress. The minimum required thickness is found to be 27mm, which is significantly smaller than the 58mm which is calculated before.

By the formulas of the previous chapter it can be calculated what the buckling load of this hypothetical shell would be:

$$p_{max.vert.load}[N/m^2] = C \cdot \gamma \cdot \frac{-2}{\sqrt{3(1-v^2)}} \frac{Et^2}{R^2} = 1/6 \cdot 0.919 \cdot \frac{-2}{\sqrt{3(1-0,2^2)}} \frac{58 \cdot 10^9 \cdot (27 \cdot 10^{-3})^2}{93,75^2} = 868 N/m^2$$

which is of course clearly insufficient.

8.1.3. Conclusions

It can be concluded that the effect of multiple load cases does not influence the final required concrete thickness. It is confirmed that buckling under vertical loading is leading over compressive strength, as was expected in the hypotheses of the research, as well as tensile strength. The fact that tensile strength is, in this phase, not found to be leading provides a confirmation to the idea not to apply passive reinforcement in the shell elements. Also, the concrete thickness is likely to be increased in regions where tensile stresses can occur.

For this calculation a large shell with a span of 150m and a sagitta of ¼ * 150 = 37,5m was chosen. This high span to sagitta ratio gives an clear insight in the effect of wind loads to this rather high structure. It was concluded that the influence on stresses due to the various load cases was not of influence to the required thickness.

A design formula for a first estimation of the concrete thickness was determined. In this formula a couple of important aspects are neglected and therefore this formula cannot be used in practice. Influences of lateral loads, unequally distributed loading, wind vibrations, characteristics of edges and supports, occurring moments and practical dimensioning are to be taken into account in structural design. It is however worthy to use this formula to estimate an early design thickness.

8.2. Edge ring

- Calculation results in appendix Calculations 8.2 -

The principle of the use of an edge ring was described in part B, chapter 3.4.6. Since the boundary conditions of the shell is thus far schematized as fully hinged it is of interest what the influence of the edge ring is, with respect to the idealized boundary conditions, on the buckling load.

It was explicated that a shell will require, among other things, certain boundary conditions to develop its advantageous membrane behavior. The ideal membrane compatible boundary conditions, as seen in figure B27b, in practice is approached by a vertical foundation and a tension ring in horizontal direction, figure B27d.
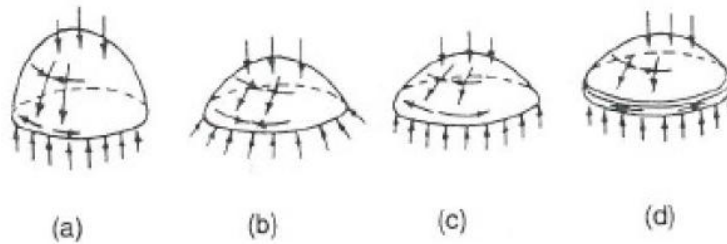
Fig.B27. (rep)   Membrane behavior of axisymmetrically loaded domes   [Farshad]
(a) A 'high rise' dome with vertical support
(b) A low rise dome with hinged support
(c) A low rise dome with vertical support
(d) A low rise dome with vertical support and edge ring

The question now arises which characteristics are required for the edge ring and what are their effects. The shell itself is dimensioned to minimize the occurrence of tensile stress within the circumferential direction. However, without an edge ring the occurrence of tensile stress within the shell is inevitable. So, the edge ring is dimensioned for the resistance of the tension which originates from the load action on the shell.

The tension ring is modeled as a prestressed continuous beam, for design considerations the prestressing force is modeled as an constant force. It is noted that this is an unrealistic assumption since in practice the prestress within the element differs along the element length and depends on the installment of the prestress force, friction losses, relaxation etc. These influences however are within this research left out of consideration since the magnitude of the force on the bearing capacity of the shell in comparison to a fully hinged support is investigated.

For these calculations the next parameters hold:

Parameters:	
Span:	d = 150m
Sagitta:	= ¼ *150 = 37.5m
Overall thickness:	t = 60mm
Supports:	All hinged & All rolled plus edge ring
Loads:	General vertical load

Variables:	
Edge ring	Dimensions Material Prestress
Design limitations:	
Buckling:	Linear elastic calculation

For a shell with the parameters given above the intensity on the supports as a result of the load actions is calculated. By these values an indication for the required prestressing force within the ring is obtained. The relation between the horizontal action of the shell on the foundation and the force within the ring is obtained below.

A thin-walled ring-element of the horizontal ring is considered with a radius r_0 and a normal force N within the axis of the element. Following Bernoulli's theory the rotation of the right-hand side of the element is described by

Δdα compared to the left-hand side. The deformation of the fiber AB to A'B' is caused by the normal force and transverse strain.
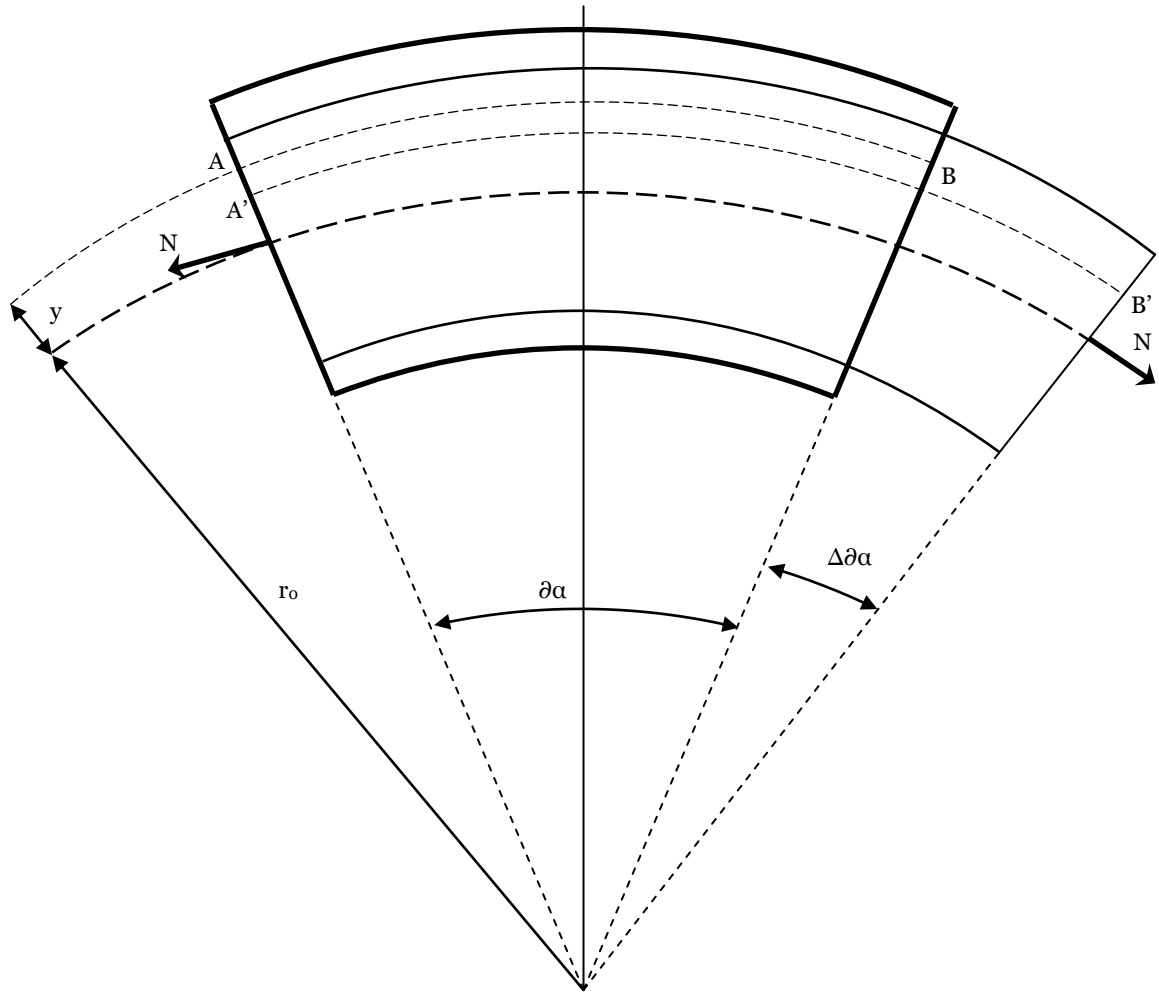

Fig.D36. Section of edge ring

Within this consideration the transverse strain is neglected with respect to the total radius (r_o+y). This is sufficiently accurate for actual materials and a large radius. The strain of fiber AB is now determined by:

$$\varepsilon = \frac{\overline{A'B'} - \overline{AB}}{\overline{AB}} = \frac{(r_o + y)(\partial\alpha + \Delta\partial\alpha) - (r_o + y)\partial\alpha}{(r_o + y)\partial\alpha} = \frac{(r_o + y)\Delta\partial\alpha}{(r_o + y)\partial\alpha} = \frac{\Delta\partial\alpha}{\partial\alpha}$$

It is concluded that for a ring-element with a large radius compared to its thickness the strain is independent of the position of y, which indicates that the strain and stress are constant over the cross-section. Therefore for this ring-element the formulas for elements with a straight axis apply.

Now the ring can be considered as thin-walled ring subjected to internal pressure in kN per unit length. Since the pressure within the ring is, in case of axisymmetric load, universal it now holds that:
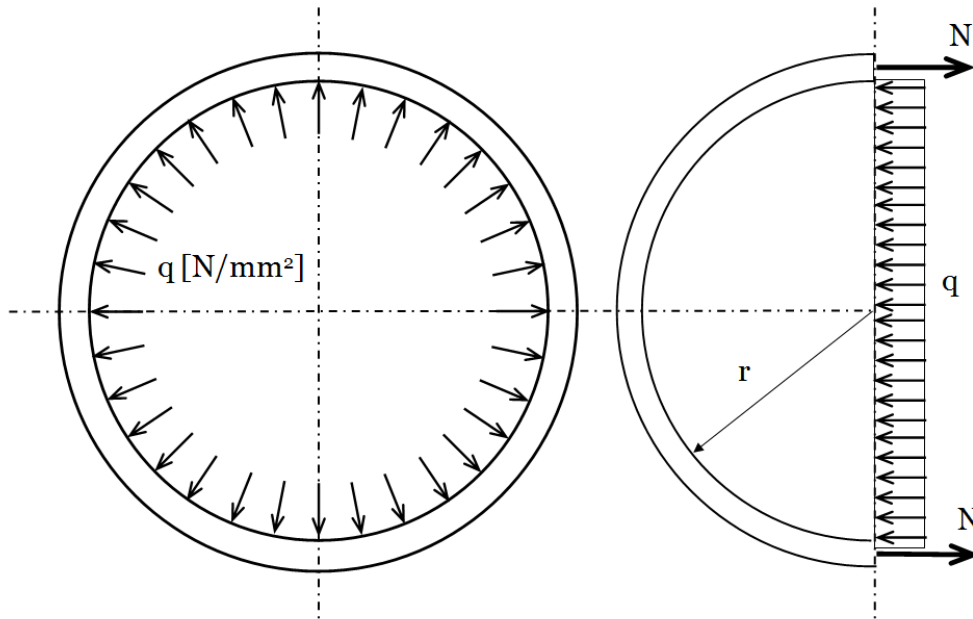
Fig.D37. Forces on edge ring

$$2N = Q \cdot d = Q \cdot 2r_o$$
$$N = \sigma \cdot A$$
$$\sigma = \frac{Q \cdot r_o}{A}$$

This formula, known as Barlow's formula, is applied to determine the required prestress in the edge ring. The results of the calculations for a shell with a fully hinged support are known and result in:

Horizontal reaction (pressure):   Permanent load (SLS)   61.0 kN/m
                                  Normative combination Snow total (SLS)   76.9 kN/m

It is seen that, for a shell with a thickness of 100mm, the contribution to the ring pressure of the dead load is approximately 80%. The required prestress force is determined by $N = Q \cdot r_o = 61.0 \cdot 75 = 4575 kN$

This force is easy to be applied within the ring, a steel type of FeP1860 leads to a required area of 2460 mm², which can be achieved by 18 strands of for instance 7 wires. The actual total number of wires and strands to be applied depends on multiple aspects such as expected long-term behavior and application method.

With this indication of the required prestress force the displacements due to permanent load in SLS are restricted to virtually zero. The choice for this prestress force is based on this restriction. Now the effect on the buckling load of the shell depends on the stiffness of the edge ring. The results are presented below.

8.2.1. Results

Material	Cross-section [h x w]	Buckling load factor (β)	Buckling load
C90/105	500 x 500	0,54	14.8
C90/105	600 x 600	0.67	18.4
C90/105	750 x 750	0.82	22.5
C90/105	850 x 850	0.86	23.6
C90/105	1000 x 1000	0.94	25.7
C90/105	1500 x 1500	1.00	27.4
C90/105	2000 x 2000	1.00	27.4

Tab. D11. Calculation results for edge beam

8.2.2. Conclusions

It is concluded that the prestressed edge ring has a significant effect on the ultimate buckling load. The buckling load as was determined for a shell with a full hinged support is easily approached, as represented in the buckling factor in table above. Not merely the application of the prestress within the edge ring is of influence, also the effect of the dimension of the ring is eminent. This is explained by the occurrence of, ultimately inevitable, deformations of the edge ring when the vertical load exceeds the SLS permanent load, after which the inertia of the ring cross section evidently has its effect.

Furthermore it is concluded that the buckling load of the shell, as was predicted in the chapter above, does not need to be reduced significantly. For a shell with a span of 150m an edge ring with realistic dimensions has an acceptable effect on the reduction of the idealized buckling load, represented in the buckling factor β. Now, the design formula for the thickness of the shell is adapted to:

$$p_{vert.load}[N/m^2] = C \cdot \gamma \cdot \frac{-2}{\sqrt{3(1-v^2)}} \frac{Et^2}{R^2} \cdot \beta$$

$$t^2 = -p_{vert.load} \cdot \frac{R^2}{E \cdot C \cdot \gamma \cdot \beta} \cdot \frac{\sqrt{3(1-v^2)}}{2}$$

In which the buckling factor β accounts for the fall-back of the buckling load from a fully hinged support to the applied edge ring. This implies that the factor should be determined, iteratively, for the specific shell geometry. It is noted that it is well feasible to exclude this fall-back so a buckling factor β =1,0 is obtained. This will be aspired within the final design.

8.3. Rib stiffening

- Calculation results in appendix Calculations 8.3 -

The principle of rib stiffening is described in chapter 3.4.4. The location of the ribs and stiffeners with respect to the shell are influenced by the dimensions of the prefabricated elements and are determined to be at all 4 edges of the elements, as described in chapter 6.

With the location of the ribs and stiffeners and the configuration of the elements as described in paragraph 6.4 an efficient material ratio between the shell thickness and ribs and stiffeners thickness is investigated in this paragraph. The stiffeners will be given the same cross section as the ribs, their width is held constant at 60mm. The ratio between the shell elements itself and the ribs will be used within the overall design when the design conclusions are combined.

The value for the initial overall shell thickness is based on the findings of chapter 8.1. It was concluded that the linear buckling load of 25kN/m², corresponding to a thickness of 60mm, satisfies for all ULS load combinations. The magnitude of this linear buckling load is used to obtain a configuration for the element thickness and the thickness of the ribs and stiffeners. It is foreseen that the shell thickness of 60mm can be decreased because of the positive effect of the ribs and stiffeners.

Parameters:	
Span:	d = 150m
Sagitta:	= ¼ *150 = 37.5m
Overall thickness:	t = 60mm
Supports:	All hinged
Loads:	Buckling load
Width ribs & stiffeners:	60mm

Variables:	
Thickness distribution:	According to table D12
Design limitations:	
Buckling:	Linear elastic calculation

8.3.1. Results

The results of the calculations are presented in the table and graph below.

Shell thickness [mm]	Ribs & Stiffeners [mm]	Buckling load [kN/m²]	Weight [MN]	Ratio [Buck.L / W * 100]
60	0	25	38,0	65,8
	60	27,5	39,8	69,2
	120	31,1	41,5	75,0
	180	35,8	43,3	82,7
	240	42,5	45,1	94,3
	300	46,2	46,9	98,5
	360	48,9	48,6	100,6

Tab. D12. Calculation results for ribs & stiffeners configurations
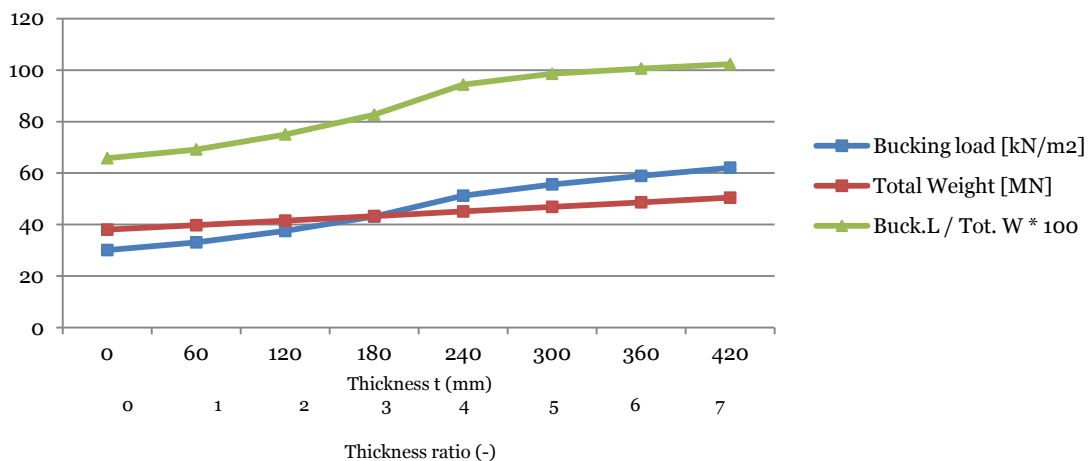
Fig. D38. Calculation results for ribs & stiffeners configurations

It is seen that the efficient material use is largely increased for all configurations of thickness ratios. Also, the marginal profit of increasing the thickness of the ribs and stiffeners decreases for thickness ratios larger than 4. Multiple configurations with thinner shell elements are now tested and compared for all ULS load cases.

Shell thickness [mm]	Ribs & Stiffeners [mm]	Thickness ratio	Buckling load [kN/m²]	Safety factor LC5	Weight [MN]
30	240	8	14.5	5.9	28.8
35	180	5.1	17.5	6.2	29.8
40	100	2.5	17.1	6.1	30.1
50	120	2.4	26.8	8.5	36.1

Tab. D13. Calculation results for further ribs & stiffeners configurations

It is concluded from the results in table D13, which is a extraction of the results in appendix Calculations 8.4, that the shell thickness can be very thin. The safety factor for LC5 represents the value for the buckling load under redistributed snow loads, which therefore additionally represents the safety for local effects. From the results above it is chosen to dimension the structure as light weighted as possible with practical dimension.

A minimum thickness of 30mm for elements was used as a minimum considering production. It is seen that the rib stiffening for this thickness demands a ratio of approximately 1 of 8. When the shell thickness is increased to 35mm, which is expected to be positive for the fiber distribution, the satisfying ratio and dimensions are considered to be more practical.

As a comparison a shell with constant thickness with the same weight is compared to the shell of 35mm with rib stiffening of 180mm. This rib stiffened shell is comparable to a solid shell of 44mm thickness as for total weight.

Shell thickness	Ribs & Stiffeners	Buckling load	Safety factor LC5	Weight (MN)
35	180	17.5	6.2	29.8
44	0	13.8	4.3	29.4
		27% increase	44% increase	

Tab. D14. Comparison rib stiffening to solid shell

8.3.2. Conclusions

It is seen that the distribution of material use from a solid shell to a rib stiffened shell has a major positive effect to the bearing capacity of the structure. Both the buckling load for constant vertical load and especially the safety against buckling for local effect, as illustrated for redistributed snow, are severely increased.

It is interesting to see that the buckling patterns of the stiffened shells, as shown in the results of appendix Calculations 8.4, show that the location of buckling is for all cases, 1 to 7, located at the top of the shell.

8.4. Edge thickness

- Calculation results in appendix Calculations 8.4 -

Within the theory of part B the in-plane shell behavior is explicated. The positive effect of this shell behavior is that it enables membrane action and inherent material savings. A consequence of a thin shell cross section is that the edge disturbances are to be taken into account. Compatibility requirements, such as local compatibility moments, occur at the supports together with the largest meridional stress. Also, the buckling patterns show a opportunity for more effective material use when element thickening applied close to the supports, as is illustrated below for a shell with a constant thickness of 60mm.
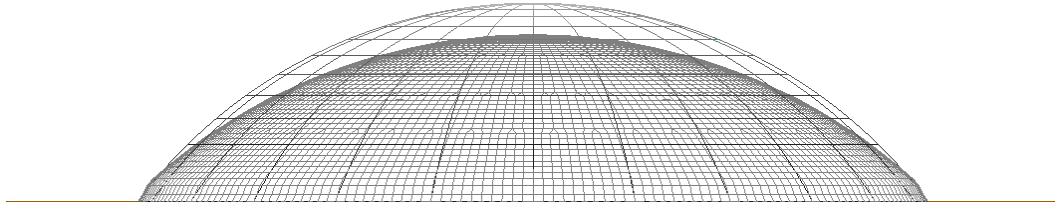
Fig. D39. Deformation (Dead load, illustrative)
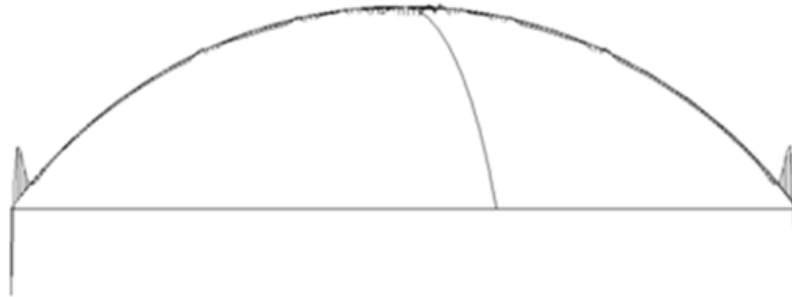
Fig. D40. Edge disturbance; compatibility moment (Dead load, illustrative)
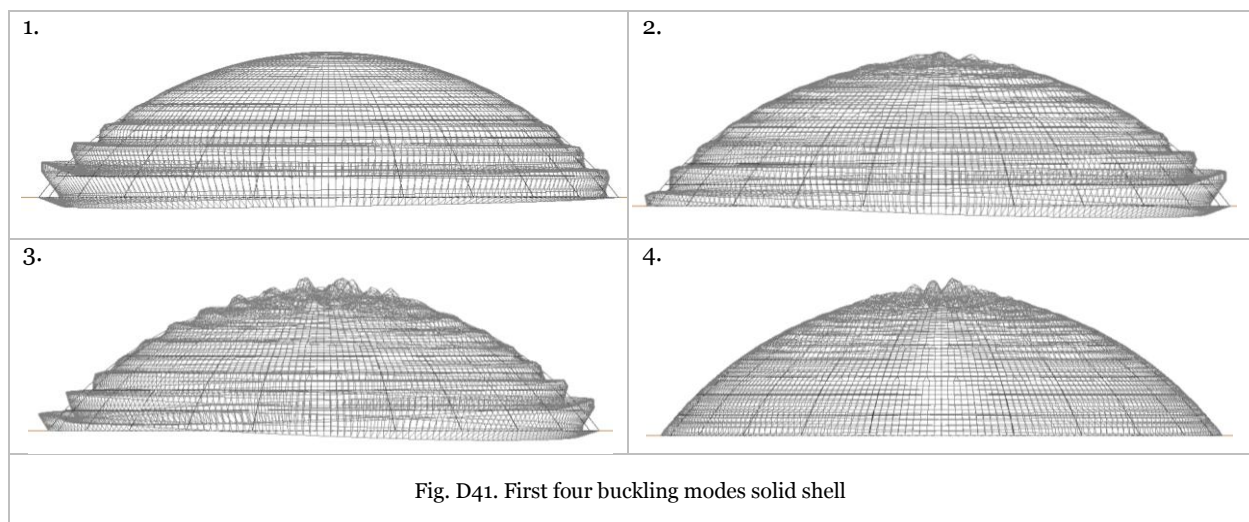
Fig. D41. First four buckling modes solid shell

The aim of this calculation is to find a more optimal material distribution along the meridional axis. This is achieved by comparing multiple configurations from which a more optimal ratio of shell thickness in comparison to solid shells is found. The distribution can then act as guideline for further design. The configurations are multiple cases which are determined for a constant thickness increase, the differences in material increase between the adjacent rings is neglected.

As an early estimate for the influence length, where the effect of edge effects is considerable and therefore the increase of edge thickness is likely to be most significant, the conclusions of part B are taken. The influence length was described as:

$$l_i \approx \pi \cdot \frac{\sqrt{Rt}}{\sqrt[4]{3}} \approx 2,4\sqrt{Rt}$$

From figure B15 and the equations shown in graph B13 it concluded that the length is to be increased by a factor of approximately 1,5. The distribution of element thicknesses is of importance within this calculation. The configurations are compared on their effect on the buckling load.

Parameters:		Variables:	
Span:	d = 150m	Thickness distribution:	According to tables appendix Calculations 8.4
Sagitta:	= ¼ *150 = 37.5m		
Overall thickness:	t = 60mm		
		Design limitations:	
Loads:	According to Chapter 5	Buckling:	Linear elastic calculation

The value for the influence length is seen as a minimum for which t is expected to be advantageous to increase the shell thickness. The influence length is estimated by:

$$l_i \approx 1,5 \cdot 2,4\sqrt{Rt} = 1,5 \cdot 2,4\sqrt{93.75 \cdot 0,06} = 8.5m$$

8.4.1. Results

It is now of interest to observe the effect of local increase of shell thickness on the buckling load. Within this calculation the shell geometries are comparable for the total material use is set constant. The half of the shell length is divided in 11 parts, based on the element configuration of chapter 6, and the material distribution is set into multiple cases.

Within the calculations, of which the results are shown in appendix Calculations 9.4, the increase of material use is first set to an extra of 60mm, which is spread over multiple variants. It can be seen that the buckling load increases with a maximal percentage increase of 15% for the material increase of 8%. It is interesting to see that the buckling load is the same for Case 4 to Case 8. Within the figure below the first buckling mode of these cases shows that the first three buckling modes of a solid shell (figure D41) are neutralized and the shell shows a local buckling pattern at its top. For Case 4 to Case 8 it holds that their first three buckling loads are equal.
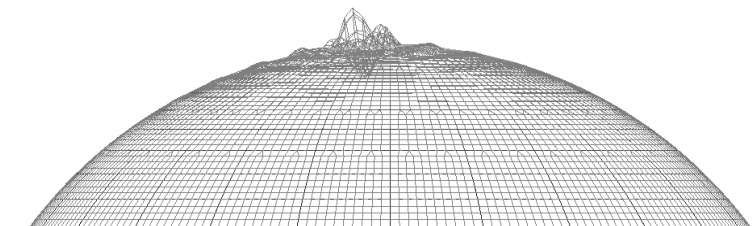
Fig. D42. Indication of the first buckling mode for Case 4 to Case 8

8.4.2. Optimization and conclusions

Within the first calculations the choice was made to make use of an overall increase of 60mm, equally spread along the meridional axis, implying a material increase of approximately 9.1%. Since it is concluded that the increase of shell thickness leads to a shift to the top of the shell where buckling occurs it is the question for which configuration of relative increase of shell thickness the same buckling load can be found.

From the results, which are presented in appendix calculations 9.4, it is concluded that for a total material usage increase of 3,4% the increase of buckling resistance of 15% is achieved. This is a result of the fact that when the edged thickness is increased the buckling pattern of the shell is shifted from the bottom edge to the top of the shell. This is accomplished if the meridional generator line (half of the shell span length) is thickened by 10% over approximately the first one third of its length. This length is larger than the influence length, which suggest that the increase is positive for the buckling load as the edge disturbances. The principle is illustrated below.

It is noted that the increase of the first 4 elements corresponds to the segment configuration as is proposed is chapter 6.6.
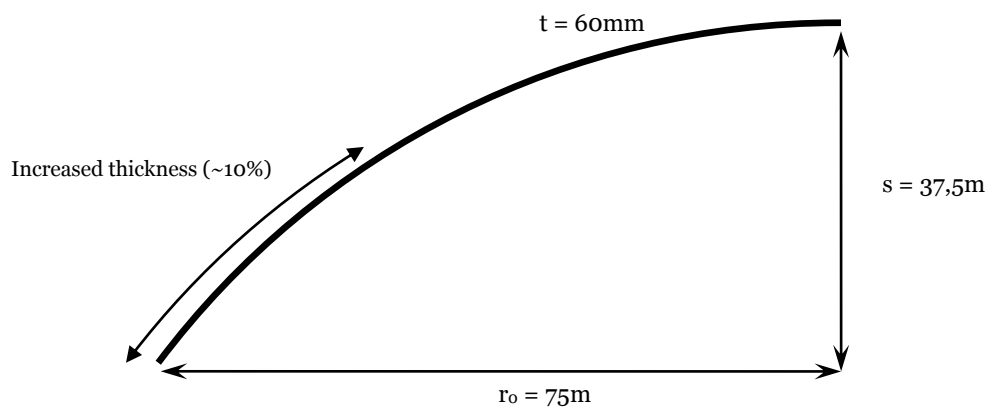
Fig. D43. Schematic presentation of edge thickness

8.5. Connection requirements

- Calculation results in appendix Calculations 8.5 -

As was described in chapter 7, the application of joint methods is of great importance for the potential of prefabricated shell structures in their mechanical behavior and their influence on the construction method. The stresses in circumferential and meridional directions were charted within chapter 8.1 and its corresponding appendix.

Parameters:	
Span:	d = 150m
Sagitta to Span - ratio:	1/4
Loads:	According to Chapter 5

Variables:
-

It was concluded that the results for the force distribution within the shell correspond to what was expected from the theory described in part B. The shell is mainly subjected to normal forces, the shear forces and moments are very small and therefore negligible.

Since the predominant occurrence of compressive stress, mainly within meridional direction but also within circumferential direction, it is of interest to see for what thickness the occurrence of tensile stresses, caused by the normative load case wind load, is excluded by dead weight of the shell. The maximum tensile stresses are found by the calculations of paragraph 8.1.

Meridional direction:
    Max. tensile stress: 99.8 N/mm
    Stress due to dead load: 1.3 N/mm²

$$t_{req}: \quad \frac{1,5 \cdot 99,8}{0,9 \cdot 1,3} = 128mm$$

Circumferential direction:
    Max. tensile stress: 96.9 N/mm
    Stress due to dead load: 1.2 N/mm²

$$t_{req}: \quad \frac{1,5 \cdot 96,9}{0,9 \cdot 1,2} = 135mm$$

Since the thickness is to be significantly increased, from the early estimated design thickness of approximately 60 to 135mm, to prevent tensile stresses to occur, it is concluded that this is not an opportunity for further design. It is therefore concluded that the connections in both meridional and circumferential direction the shell are subjected to tension, which is of importance for the choice of connection principle(s) to be applied. This conclusion is used in the connection considerations of chapter 7.

The determination of the requirements of the application of the connections will be determined for the overall design in which the design considerations are combined.

8.6. Dynamic response

- Calculation results in appendix Calculations 8.6 -

Since within the design of shell structures it is customary to design a slender structure it is of relevance to observe the dynamical behavior of such a slender and lightweight structure. The natural frequencies, eigenfrequencies, of the structure are therefore determined. If this frequency corresponds to the frequency to which the building is subjected undesirable magnification of deformation and stresses can occur.

Eurocode 1990 describes that if the SLS is not to be exceeded while being subjected to vibration, the eigenfrequency of the structural element has to be higher than the terminated values which depend of the functions of the building and external effects. These vibrations might be induced by humans, machines, subsoil vibrance, traffic and wind loads.

Eurocode 1991 mentions that concerning the SLS a complete dynamic analysis is not required for standard floors in dwellings or utility buildings where the eigenfrequency is larger than 3 Hz. The same holds for floors which are subjected to harmonic vertical loads, such as dancing, if the first natural frequency is larger than 5 Hz.

Parameters:		Variables:	-
Span:	d = 150m	Design limitations:	Eigenfrequencies
Thickness:	t = 60 mm		
Sagitta to Span - ratio:	1/4		
Support:	All hinged		

8.6.1. Results

Natural frequency	f [Hz]	T [sec]
1	7,54	0.13
2	7,62	0.13
3	7,63	0.13
4	8,09	0.12

Tab. D15. Results for natural frequencies

The first natural frequency of the structure is determined to be f = 7,5 Hz.
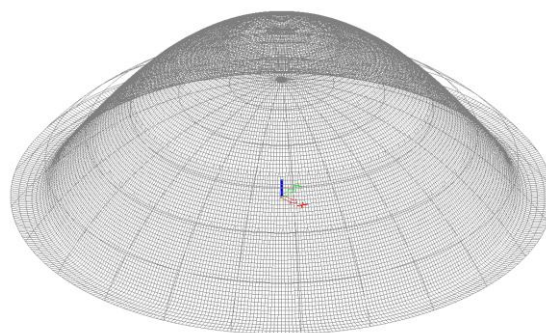
Fig. D44. Vibration shape corresponding to first natural frequency for vertical loads

8.6.2. Conclusions

The value for the first eigenfrequency of the structure of 7,5 Hz (T=0,13 sec) is not expected to cause possible dynamic magnifying effects for it is not expected for dynamic loads to occur with this frequency, let alone for a considerable time span. As mentioned, floors subjected to harmonic vertical loads do not require dynamic analysis is their eigenfrequency is larger than 5 Hz. Because of these deliberations it is concluded that the dynamic response of a shell with these given dimensions satisfies the demands.

8.7. Thermal response

- Calculation results in appendix Calculations 8.7 -

The effect that temperature distributions within the shell may have on stresses, strains and displacements has not yet been discussed. In linear thermo-elasticity, which is applied within this calculation, it holds that thermal stresses, strains and displacements can be linearly superimposed upon those of mechanical loads.

For the extremely advantageous characteristics of UHPC concerning durability it is interesting to research whether it is possible to execute a large span shell within the open air. Therefore, within this research a distinction is made between two possibilities, being a concrete shell with external insulation and internal insulation.

The distinction between the location of the insulation effects the difference between the temperature of the concrete within the summer (e.g. Fig.D45. left line) and winter (e.g. Fig.D45. right line). It is noted that the internal temperature difference within the concrete between the top and bottom fiber for both cases is comparable throughout the cross section of the concrete but the absolute difference between the seasons is differs significantly. This is explicated within the example below where the exterior is heated to 70°C and an internal climate of 25°C.

Concrete roof, insulation on top side

Concrete roof, insulation on bottom side
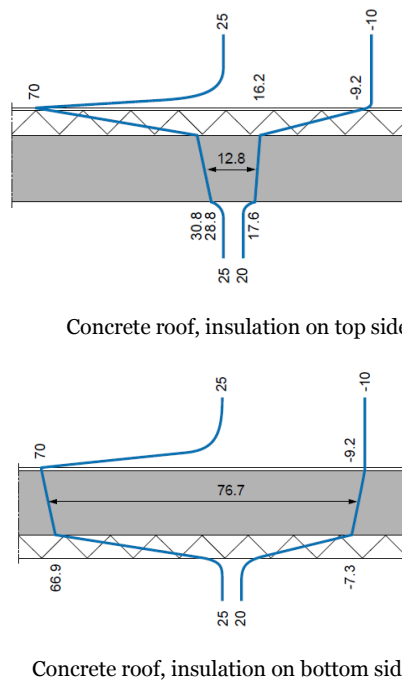
Fig. D45.   Insulated concrete roof temperature progression   [°C]   [79]

It can be easily imagined that for shells the response of the structure is different than for beams. For beams, thermal expansion will, in case expansion is not restricted, result in thermal strains but no stresses, or, in case of rigid end restrains, thermal stresses but no strains. For a three-dimensional shell these characteristics are likely to differ since strains can take place in perpendicular direction of the shell, which results for instance in bulging as demonstrated in figure D46.

The characteristics of the edge supports can be of significant influence on the strains and stresses. Within these calculations the edges are therefore modeled by realistic characteristics, providing a support restrain in between fundamental cases as described above. It is decided to model the edge ring by a 1000x1000mm² beam with a prestressing force of 4600 kN.
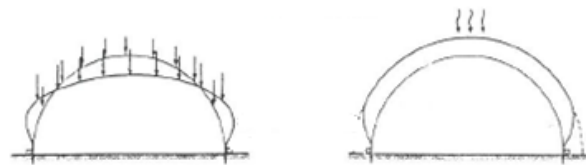
Fig. D46. Applied load and temperature effects on dome with fixed edge constrains [42]

Parameters:		Variables:	Temperature distribution
Span:	d = 150m		
Thickness:	t = 60 mm	Design limitations:	Stresses, deformations
Sagitta to Span - ratio:	1/4		
Thermal expansion:	11,8*10-6 m/m/°C		
Loads:	Temperature loads NEN-EN 1991-1-5 Based on figure D29.		

For an indication of the temperature gradient over the shell thickness figure D45 is used. From this figure it is concluded that for a basic amount of insulation the temperature gradient in the concrete cross-section has a small difference from the top to bottom side. Now, to present the effect of temperature on the shell three load cases are examined in which a maximum temperature gradient over the shell thickness of 5°C is assumed. The first two load cases are extreme circumstances for summer and winter in which the inside and outside temperature are assumed constant. The third case contains an estimated realistic temperature difference over the shell as is illustrated below. In all cases the temperature of the edge ring is held constant.
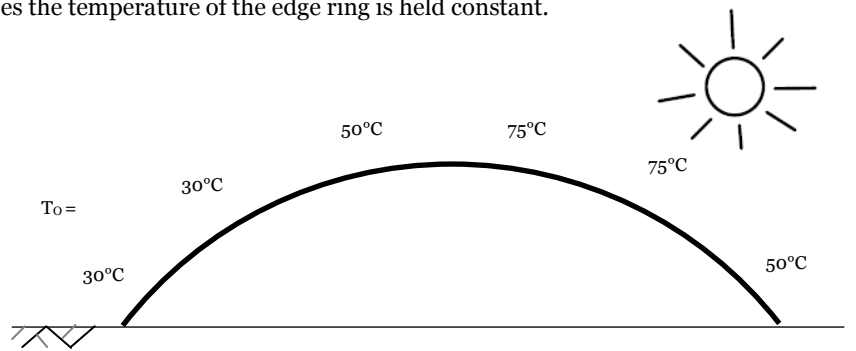
Fig. D47.   Shell surface subjected to estimated external temperature distribution

8.7.1. Conclusions

The results in appendix Calculations 8.7 show that the shell indeed, for a large fraction, shows strains but no stresses while it is practically restricted at its supports. This was predicted and is a result of the thermal strains which in these parts of the shell can take place in perpendicular direction of the shell.

In the case where the concrete is insulated at the inside of the building the deformations show a maximum of +55mm in summer and a minimum of -5mm in winter. Insulation at the outside of course shows a smaller difference of +15mm and -2.5mm.

The deformations of the structure in both the cases do not lead to stresses in most of the structure. As expected, the connection to the edge ring causes a restrain and its accompanying stresses. These stresses are of course larger in case the insulation is applied at the inside of the structure. The magnitude of the stresses however are not very disconcerting. The largest tensile stress of 176kN/m (winter, internal insulation) can easily be absorbed by the UHPC with sufficient thickness and the connections. The same holds for the largest compressive stress of 1950kN/m (summer, internal insulation).

It is concluded that a the concrete large span shell can be executed with internal insulation. With this, the UHPC itself can be exposed to the environment, meaning the durability aspects of UHPC are exploited and that roof covering is not to be replaced in the future.

9. Overall design

9.1. Design considerations conclusions

Within this paragraph the results of the final chapter are discussed. In the next paragraph the conclusions are combined for the final design dimensions.

Sagitta to span ratio

The intended sagitta to span ratio of 1 over 4 was concluded to be a feasible ratio. For a span of 150m and a height of 37,5m (both founded on the Fiere Terp-design) it was concluded that the effect of the various load cases does not have an influence on the final required concrete thickness. It was confirmed that buckling under vertical loading is leading over compressive strength. The tensile strength was not found to be leading which provides the idea not to apply passive reinforcement in the shell elements.

Edge ring

It is concluded that the prestressed edge ring and its dimensions have a significant effect on the ultimate buckling load. The buckling load of the edge ring strengthened shell is easily equal to the buckling load for an ideally restraint structure. The required prestress force is determined by a model with hinged supports to exclude displacements in the SLS permanent load case.

Rib stiffening

The edges of the shell elements are designed thicker to form ribs and stiffeners, as was determined in paragraph 6.7. With the locations of the element edges known from the determined geometry it is concluded that the efficient material use within the structure can be largely increased by the application of ribs and stiffeners. Furthermore it was concluded that the buckling mode is influenced by the stiffening and has its buckling pattern at the top of the shell instead of the bottom, which is the case for unstiffened shells.

Edge thickness

It is concluded that for a solid shell a total material usage increase of 3,4% can lead to a possible increase of buckling resistance of 15%. This is a result of the fact that when the edged thickness is increased the buckling pattern of the shell is shifted from the bottom edge to the top of the shell. This is accomplished if the meridional generator line (half of the shell span length) is thickened by 10% over approximately the first one third of its length. This length is larger than the influence length, which means that the increase is positive for both the buckling load as the edge disturbances.

Since both rib stiffening as well as the increase of the edge thickness have proven to lead to a shift of the buckling pattern from the bottom to the top of the shell it is questioned whether both aspects are required. Rib stiffening will be applied for connections and edges of the elements. The need for the increase of edge thickness is therefore only applied if needed for edge disturbances.

Connections

It is therefore concluded that the connections in both meridional and circumferential direction the shell and its connections are subjected to tension, which is of importance for the choice of connection principle(s) to be applied. the tensile stresses which occur for a solid shell were found to be rather small. The connection forces are determined for the overall design were ribs and stiffeners are applied.

Dynamic response

It is concluded for that the dynamic response of a large span solid shell satisfies the demands. The shell is tested with a solid cross-section. The change to a thinner shell with ribs and stiffeners is examined for the overall design. When the eigenfrequencies of the structure are larger than 5 Hz the structure dynamic response is considered sufficient.

<u>Thermal response</u>

The thermal response for the large span structure mainly demonstrates in relatively small deformations, this is explained by the fact that the structure is allowed to deform. Only at the edge of the shell temperature stresses arise which are not expected to lead to major adjustments to the element dimensions.

It is concluded that a concrete large span shell can be executed with internal insulation. With this, the UHPC itself can be exposed to the outside environment, meaning the durability aspects of UHPC are exploited and that roof covering is not to be replaced in the future.

<u>Compound buckling</u>

In addition it is noted that the buckling results of every design calculation expose the occurrence of the phenomenon of compound buckling, described in section 3.3.1. This refers to the fact that several buckling modes have approximately the same critical load.

It is found that the design adjustments can have a severe effect on the buckling load itself. However, none of the adjustments affects the deviances between multiple adjacent critical loads.

9.2. Final design

In the paragraphs above the possibilities and preferences for the element geometry, element dimensions, connection type are elaborated.

9.2.1. Overall dimensions

Again, as a reference, the dimensions of the design for a large span shell are selected to have a span of 150m with a height of 37,5m. These dimensions are slightly based on the design dimensions for the preliminary design for Fiere Terp [Part E]. Before the discussion on the possible construction methods a clear view on the dimensions is presented. With the span and sagitta known, the other parameters are determined by the relations of the proportions in shells of appendix 4.

Diameter	d	150m
Sagitta	s	37.5m
Radius	R	93.75m
Arch length	L	~174m
Perimeter base	P	~470m
Area Shell	A	~22000m²

Tab. D16. Dimensions of final design
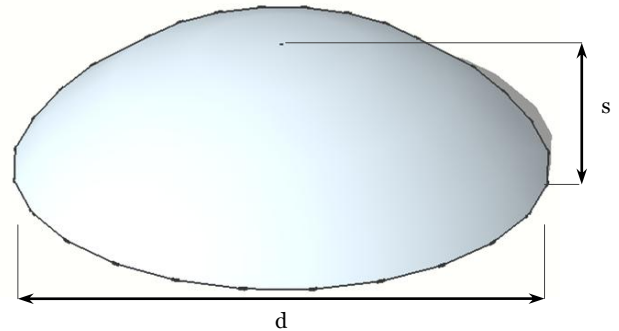
Fig. D48. Overall dimensions final design

9.2.2. Element dimensions

From the design calculations of chapter 8.3 it was concluded that, for the given element configuration, the shell elements can have a thickness of 35mm with ribs and stiffeners with a height of 180mm along the edges of each element. For figure D49 it is noted that the small curvature of the elements is barely visible.
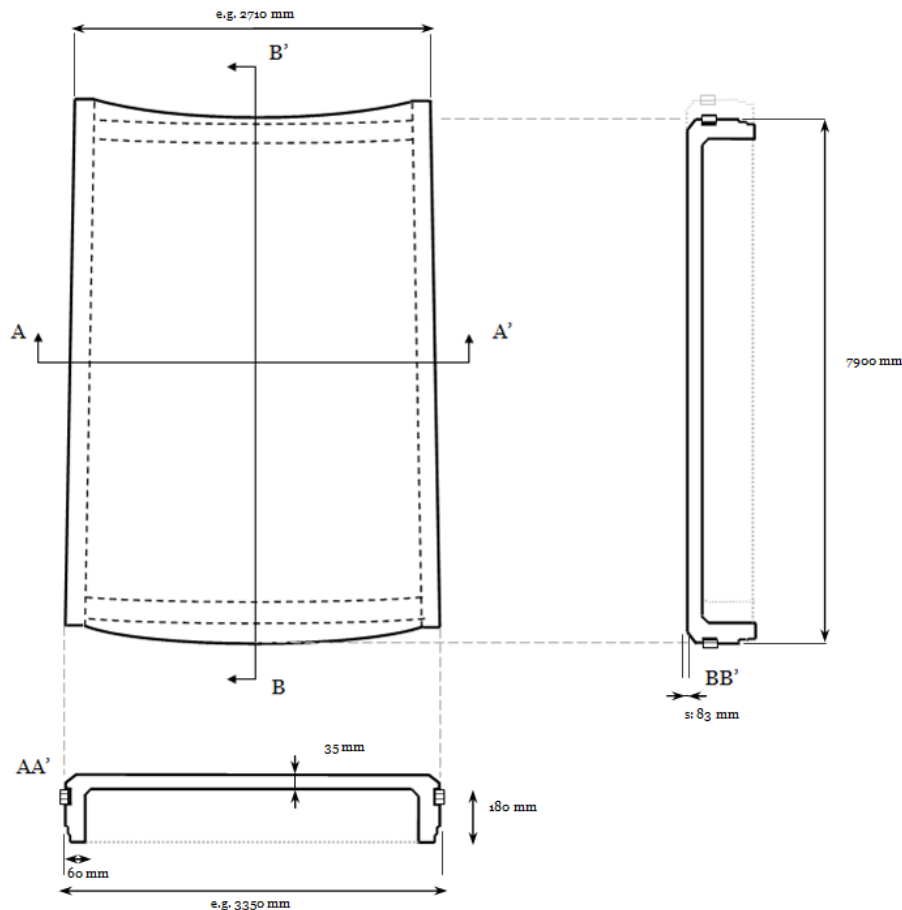
Fig. D49. Element dimensions (not to scale)

Element configuration

Ring	# Elements	Element surface [m²]
1	144	25,0
2	144	23,1
3	144	21,2
4	144	19,1
5	72	33,6
6	72	28,9
7	72	23,9
8	72	18,8
9	36	27,0
10	36	16,3
11	9	21,8
Total	945	~22000

Tab. D9. (rep)   Total build up of elements

Fig. D26.(rep)   Total build up of elements

9.2.3. Edge ring

Again, as in paragraph 8.2, the required prestressing force within the edge ring is determined with Barlow's formula by the SLS Permanent load for a model with hinged supports. This results in:

Horizontal reaction (pressure):

Permanent load (SLS)	52.3 kN/m	at location of stiffeners
	44.5 kN/m	at element edges
Normative combination Snow total (SLS)	69.4 kN/m	at location of stiffeners
	59.5 kN/m	at element edges
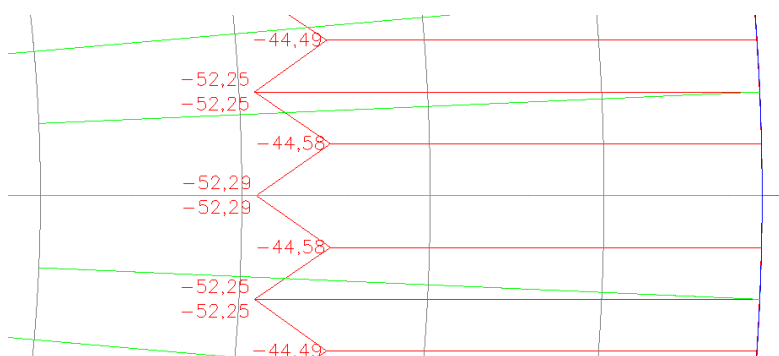
Fig. D50. Support reaction intensity for SLS Permanent

It is seen for this thin ribbed stiffened shell that the contribution to the ring pressure of the permanent load is approximately 75% of the normative combination Snow Total (SLS). The values for the permanent load are used as an indication for the required prestress force and is applied in an edge ring with dimension 1500 x 1500 mm².

The force is determined with $N = Q \cdot r_o = \left(\dfrac{52.3 + 44.6}{2} \right) \cdot 75 = 3634 kN$. This force is easy to be applied within the

ring, a steel type of FeP1860 leads to a required area of 1960 mm², which can be achieved by 14 strands of for instance 7 wires. The actual total number of wires and strands to be applied depends on multiple aspects such as expected long-term behavior and application method.

9.2.4. Stability calculation

With the dimensions, element- configuration, -geometry and edge ring characteristics known a stability calculation is performed for all load cases as defined in chapter 6. The safety factor needs to be larger than 6, as was determined in section 2.4.8.

Load case	Buckling load [kN/m²]
Total	17.5

Load case	Safety factor (>6)
ULS Permanent	10.7
ULS Wind	7.9
ULS Snow distributed	7.2
ULS Snow redistributed	6.2
ULS Maintenance*	9.5

Load case	Safety factor (>6)
SLS Permanent	12.8
SLS Wind	10.5
SLS Snow distributed	9.3
SLS Snow redistributed	8.3
SLS Maintenance*	11.8

*A maintenance load of 1,0 kN/m² is applied on a loaded area of 10m² (3.2 x 3.2m²) close to the top of the shell.

Tab. D17.   Results for buckling safety

It is concluded that the structure, with the results from paragraph 8.2 and 8.3 combined, satisfies the demands concerning stability.

9.2.5. Connection calculation

The connections are applied to withstand tension caused by wind loading as well as to ensure compression within the gaskets for water tight connections. The tension force is determined in the locations as shown in figure D51. The magnitudes for the tensile forces lead to the consideration whether post-tensioning or more regular connections are to be applied.

It was concluded from the theory of part B and confirmed in the findings of paragraph 8.5 that the shell and its connections will be mainly subjected to normal forces and moments and shear forces can be neglected. From the findings of paragraph 8.7 it was concluded that possible temperature loads have no effect to the shell other than edge disturbances. For these reasons the requirements of the connections are determined for normal forces only within this paragraph. Since within the applied model for the calculations of the final design the adjacent ribs and stiffeners are modeled as a single beam, with double width, the results found are halved to find the actual load. The stresses within the elements are multiplied with their corresponding surface.
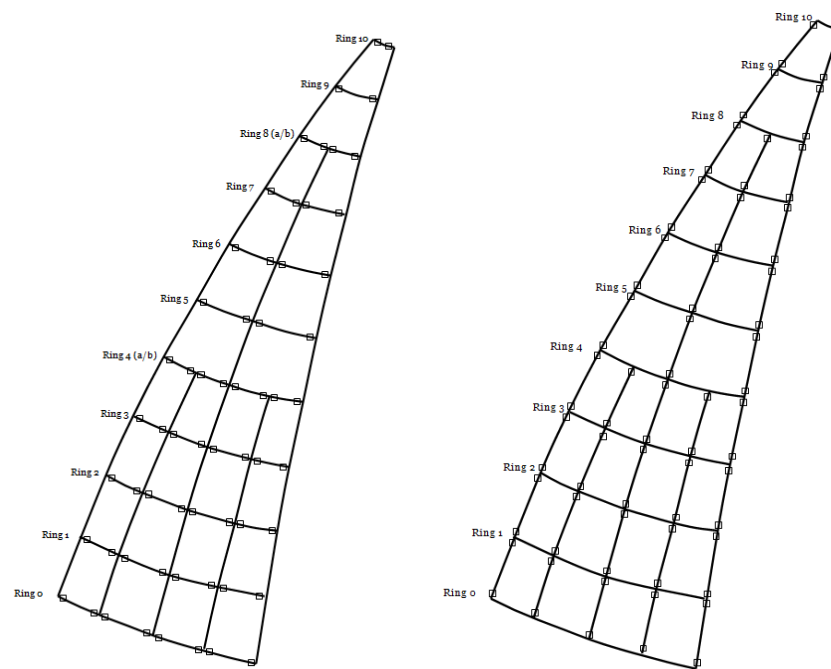
Fig. D51. Locations of meridional connectors (left) and circumferential connectors (right)

Normal forces

Meridional direction; Ny

SLS Permanent Load   Force per unit length [N/mm]
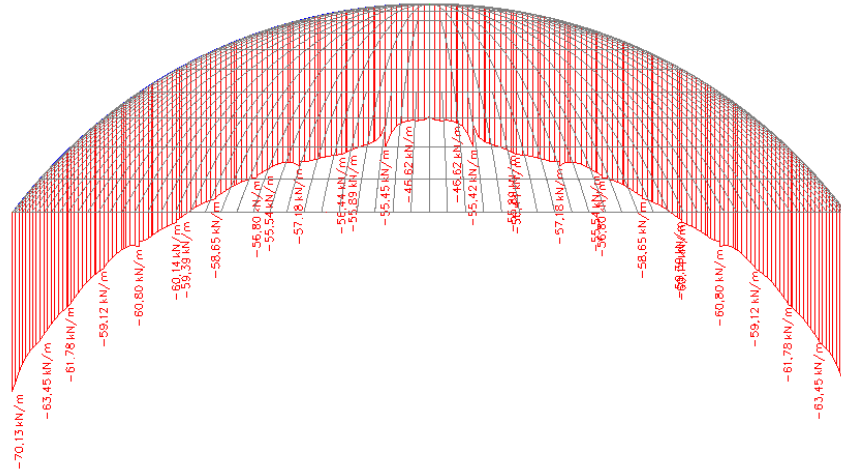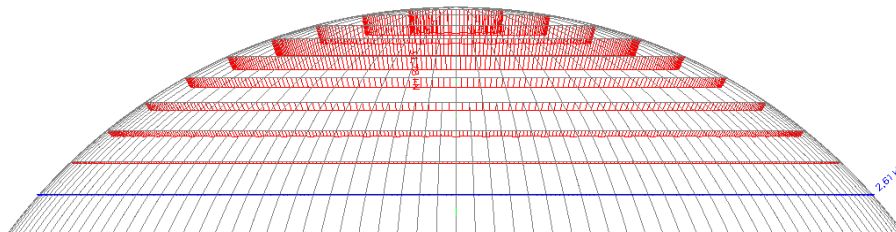
Shell elements

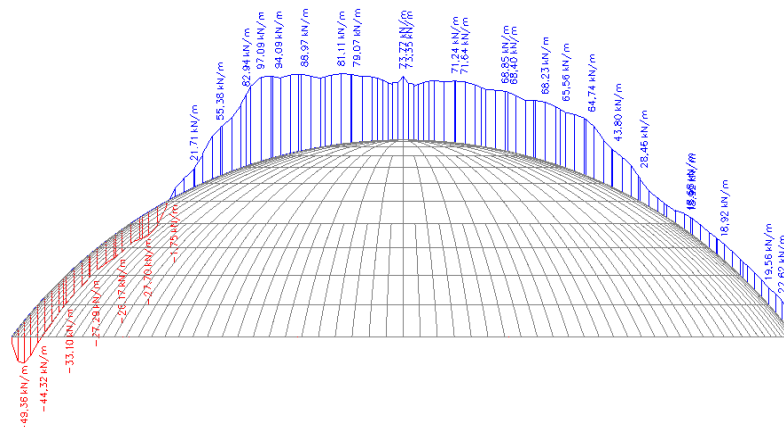Ribs   Force [kN]
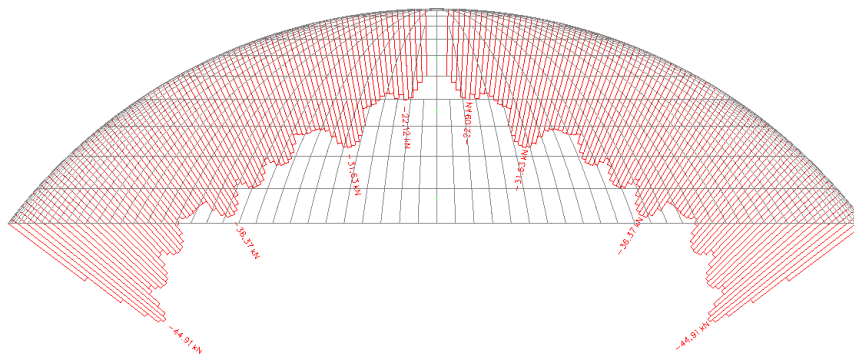

Normative load case:
Load case 3: wind.   Force per unit length [N/mm]

Shell elements
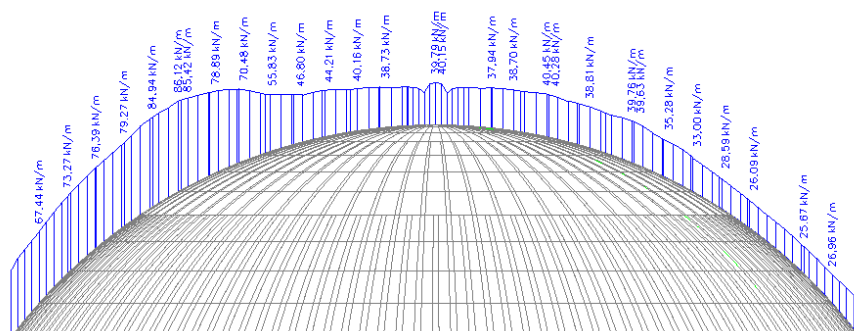
*Not in wind-direction

Ribs   Force [kN]
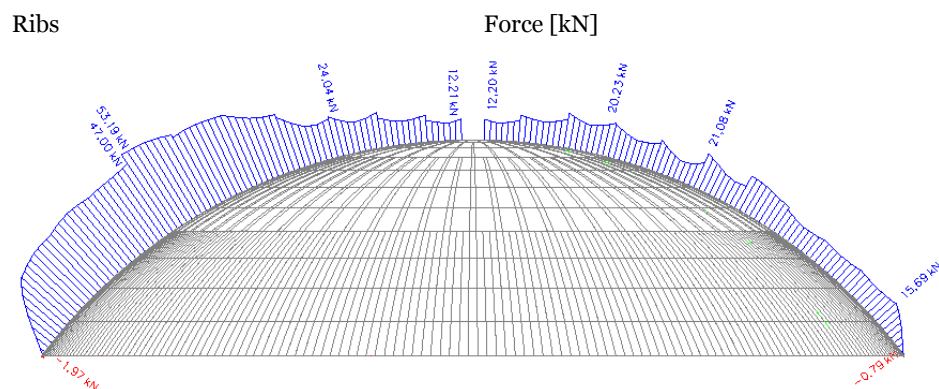
*Not in wind-direction

$F_{meridional}$	Permanent load		Variable load		Tension ULS
Ring	Elements [kN]	Ribs [kN]	Elements [kN]	Ribs [kN]	0,9 * Permanent – 1,5* Variable [kN]
1	-93.0	-19.0	98.7	19.1	75.9
2	-82.8	-16.7	98.2	22.7	91.8
3	-71.5	-15.3	92.4	23.1	95.1
4a	-63.9	-16.4	84.5	23.5	89.7
4b	-63.9	-	84.5	-	69.2
5	-109.8	-15.2	155.4	23.6	**156.0**
6	-88.9	-14.6	130.4	22.7	136.5
7	-66.0	-13.6	85.7	17.4	83.0
8a	-48.3	-14.1	47.7	12.0	33.4
8b	-48.3	-	47.7	-	28.1
9	-57.9	-13.2	45.7	11.9	22.4
10	-33.5	-11.1	26.7	8.4	12.5

Tab. D18.   Forces in meridional connections

It is seen that the normative tension in meridional direction is found at the location of ring 5. This is explained by both the large wind suction and the larger element size at this location.

Circumferential direction; Nx

SLS Permanent Load   Force per unit length [N/mm]
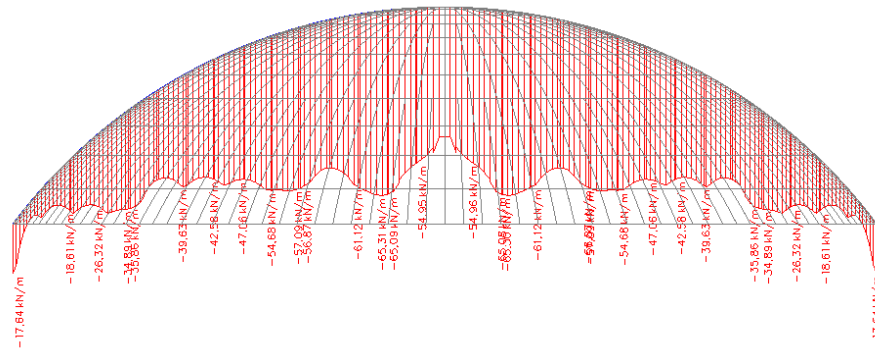
Shell elements

Stiffeners   Force [kN]

Normative Load case:
Load case 3: wind x.   Force per unit length [N/mm]

Shell elements

Stiffeners   Force [kN]
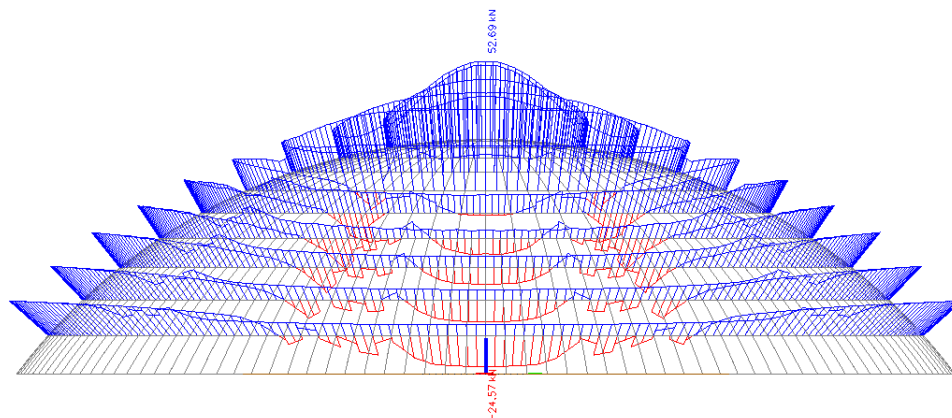
F$_{circumferential}$	Permanent load		Variable load		Tension ULS
Ring	Elements [kN]	Ribs [kN]	Elements [kN]	Ribs [kN]	0,9 * Permanent − 1,5* Variable [kN]
0	-69.5	0	39.5	0	-3.3
1	-59.3	1.3	77.4	13.7	84.5
2	-73.5	-2.4	75.1	12.3	62.8
3	-110.6	-5.8	74.7	12.0	25.3
4	-126.4	-7.2	73.5	10.4	5.6
5	-156.4	-8.4	112.6	10.1	35.7
6	-177.8	-10.5	173.0	13.1	109.7
7	-216.1	-13.0	259.1	21.4	214.6
8	-217.3	-14.1	269.4	26.4	**235.4**
9	-248.9	-14.6	276.5	22.2	210.9
10	-233.1	-17.4	284.4	19.9	231.0

Tab. D19.   Forces in circumferential connections

It is seen that the normative tension in circumferential direction is found at the top of the shell. This is explained by the large wind suction at this location.

Conclusions

It is concluded that the meridional tensile forces have a maximum of 156.0 kN and the circumferential tensile forces have a maximum of 235.4 kN. With this maximum values it is concluded that the local connectors do not require a large cross-section when a standard steel quality is applied.

From the possible connections and their configurations discussed in paragraph 7.3 the alternative with continuous prestress tendons, which could have been required for larger tensile forces, is not demanded and will not be applied. With this choice the disadvantage of the need for continuous ducts and the more labor-intensive installment are avoided. This option was only to be applied when the tensile forces were found not be withstood by standard steel. Connecting by local connections entails merely local installment and cause an easy and fast construction.

Since the steel within the connections can certainly withstand the forces the most important test now is whether the concrete is capable to withstand the tensile forces. The contribution of the fibers within UHPC to the tensile strength as well as to the force spreading throughout the concrete was found to be substantial and therefore likely to act positively. Because of this, the application of merely local connections, as shown in paragraph 7.3, might be sufficient since the tensile force can be distributed over the element. In case the fiber reinforced concrete element does not satisfy the demands the element can be enforced with regular reinforcement or extra steel provisions, which makes the connection feasible.

Irrespective of the method to be applied, it is considered to be a necessity to elaborately test the connections and the force distribution through the element since the precise effect of the fiber reinforcement is of interest and regulations are often limited to conventional concrete. In this way the possibly complex force distribution which is expected for the load case represented in figure D52 is tested and the verification of the connection is done by experimentation.

In the most positive case the force distribution through the element is sufficient and merely local connections satisfy. However, this favorable case cannot be assumed to occur and it is therefore assumed within further design that provisions are required. For this reason it is chosen to apply a single reinforcement bar per rib and stiffener.
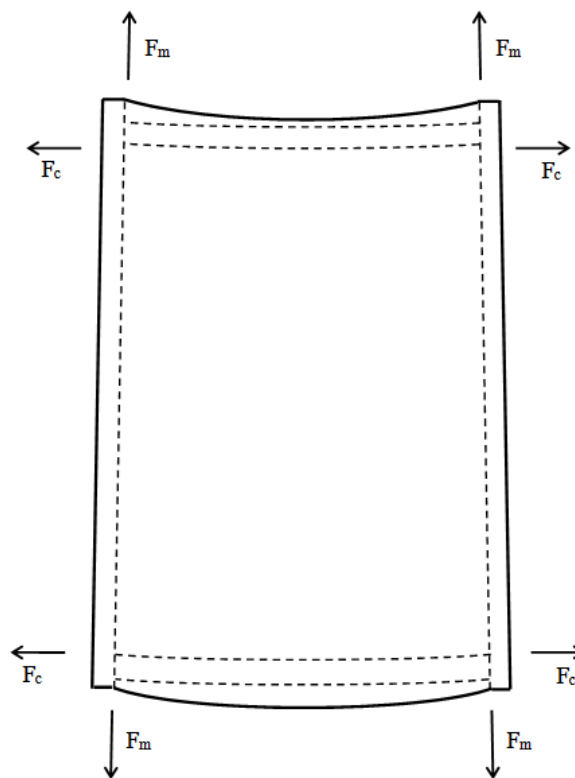
Fig. D52.   Tensile forces on local connections

In the tables below the tensile capacity per bar is given and it is determined which bar diameter is required per element.

Tension force per bar in kN [FeB 500, f_s = 435 N/mm²]								
Bar diameter [mm]	8	10	12	16	20	25	32	40
$F_{t;u}$ [kN]	22	34	49	88	137	214	350	547

<p align="center">Tab. D20.   Tension force per bar diameter</p>

	$F_{meridional}$ Tension ULS					$F_{circumferential}$ Tension ULS		
Ring	0,9 * Permanent – 1,5* Variable [kN]	Required Ø	Applied Ø		Ring	0,9 * Permanent – 1,5* Variable [kN]	Required Ø	Applied Ø
0	-				0	-3.3		16
1	75.9	16	20		1	84.5	16	16
2	91.8	20	20		2	62.8	16	16
3	95.1	20	20		3	25.3	10	16
4a	89.7	20	20		4	5.6	8	16
4b	69.2	16	20					
5	**156.0**	25	25		5	35.7	12	16 / 20
6	136.5	20	25		6	109.7	20	20 / 32
7	83.0	16	20		7	214.6	32	32
8a	33.4	10	16		8	**235.4**	32	32
8b	28.1	10	16					
9	22.4	10	16		9	210.9	25	32
10	12.5	8	16		10	231.0	32	32

<p align="center">Tab. D21.   ULS Tensile forces in connections and required bar diameter</p>

Table D21 shows a large variety for the required bar diameter per ring. It is chosen to apply the normative required bar diameter where the force has its maximum, the other reinforcement bars are applied by an even decline in diameter with a minimum of 16mm. This minimum diameter is chosen for the coherence in the structure and production process.
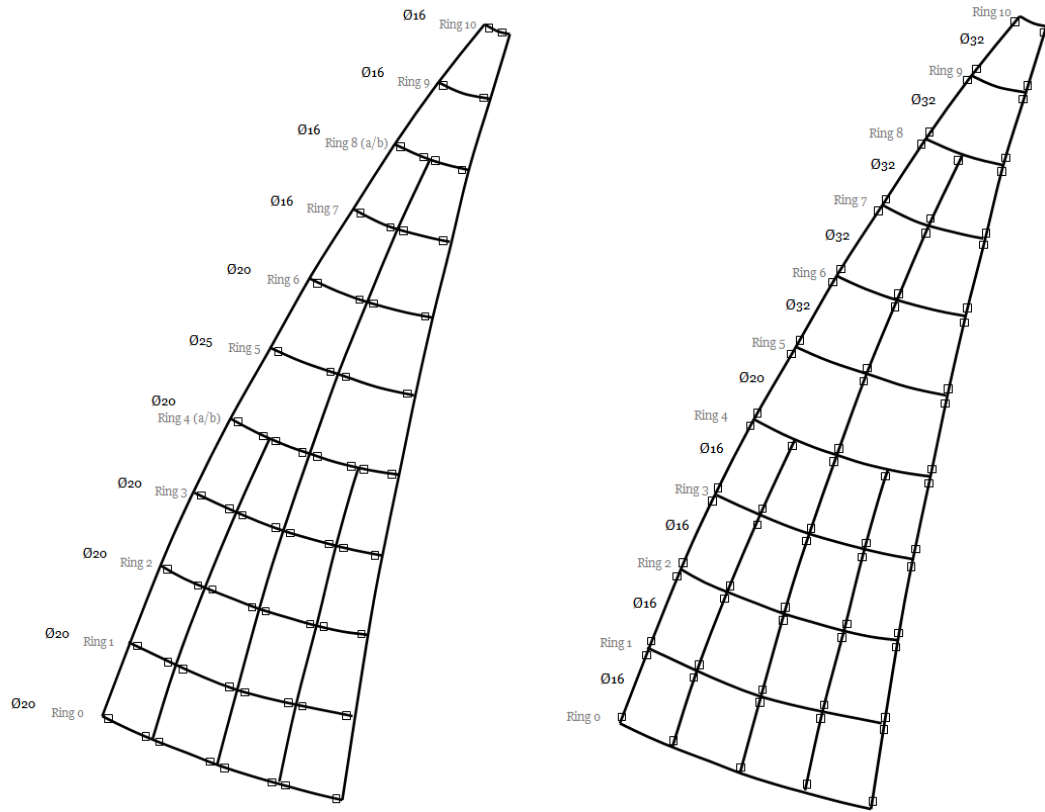
Fig. D53. Applied reinforcement bars per elements
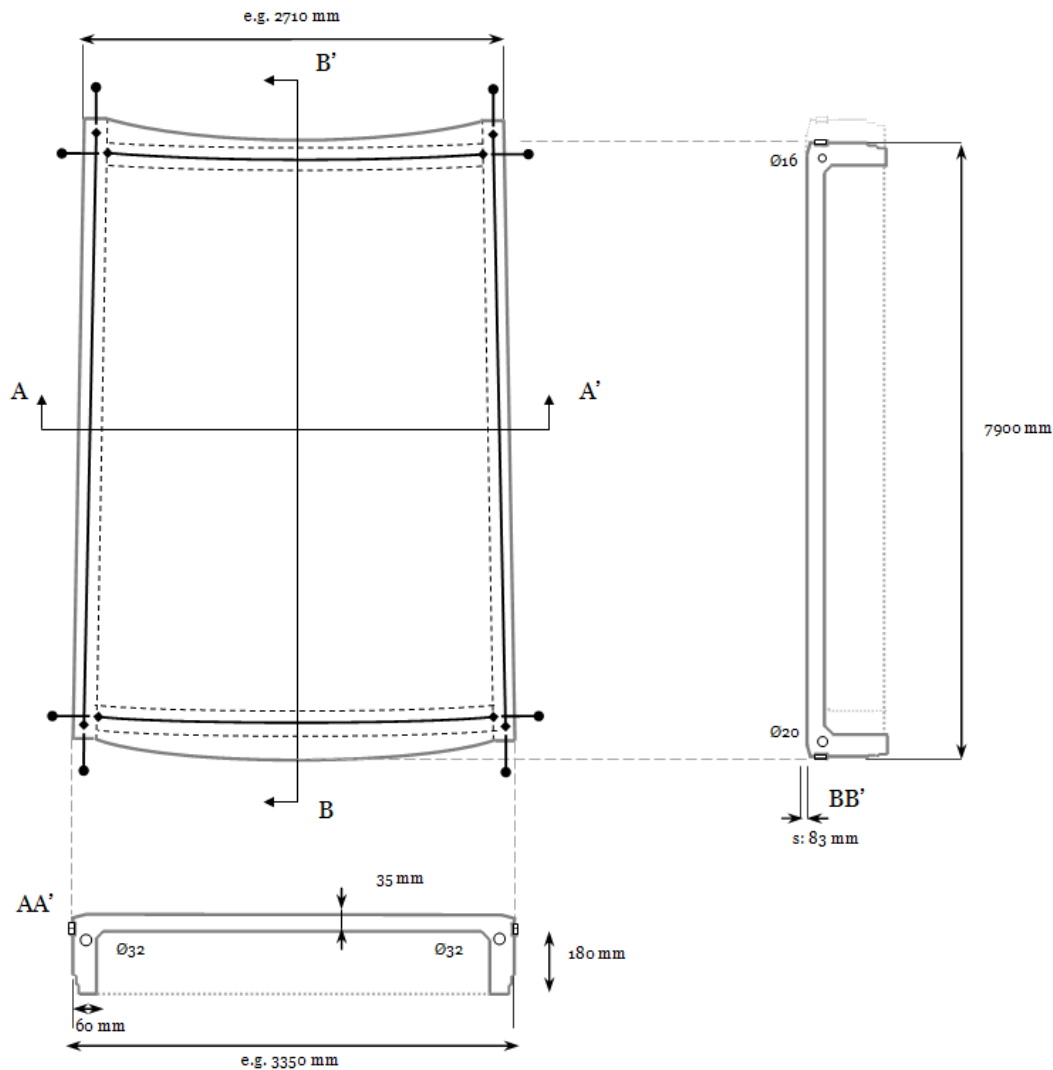
Fig. D54. Applied reinforcement bars; example element ring 7

The connecting of the elements by a fast and non-labor-intensive method is of importance. The bolted connections, described in section 7.2.2., which are applied for connecting tunnel segments serve as a reference. These principles are combined with the principles for the construction systems as bolt- and rebar-anchors, which are used frequently in practice. It is noted that when the proposed geometry may cause difficulties around the connections the elements can be applied with local thickening.

The proposed connection system, as show in figure D55 below, presents the coupling between the reinforcement bars together by connection bolts and rebar-anchors. The tension force capacity of standard bolts is given in table D22. The table shows that, if the most commonly used class 8.8 is applied, a maximum diameter of 27mm is required.
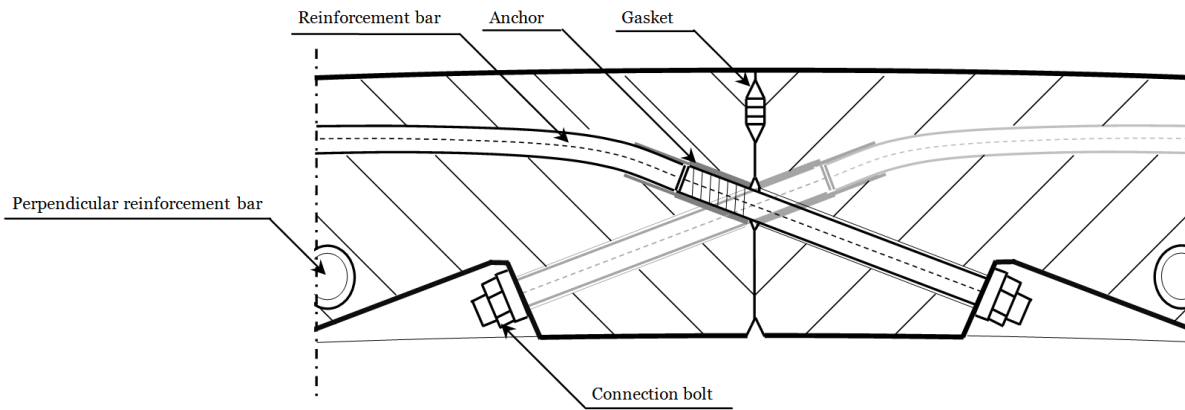
Fig. D55. Vertical & horizontal cross-section of local connection between two elements; not to scale

Tension force per bolt in kN								
Bolt diameter [mm]	Class	12	16	20	24	27	30	36
$F_{t;u}$ [kN]	4.6	24	45	70	102	132	161	235
	8.8	49	90	141	203	265	323	471
	10.9	61	113	176	254	331	404	588

Tab. D22. Tension force capacity for standard bolts

The connection system is highly expected to be capable to fulfill the structural demands. Moreover, the provisions to be taken within prefabrication are not demanding since merely slightly curved reinforcement bars and standard anchor types are to be applied. The bolts can be applied with a tightening torque by which the applied force, which secures compression in the connection, is measured. It is noted that the principle of a spring collar can be applied to secure a required prestress by which the gaskets will be compressed permanently to secure the watertight connection. Also, between the head of the bolt and the UHPC a rectangular steel plate can be applied, opposite to merely a steel ring, to secure a satisfying force introduction.

As was explicated in chapter 6 the recommended production method with steel moulds can be highly precise, causing placing difficulties due to deviances to be diminished. The placement of the elements and the installment of the bolts is further elaborated within the next chapter in which the construction is discussed.

9.2.6. Edge disturbances

The thermal response check in paragraph 8.7 showed that the shell showed mainly deformations and only little effects to stresses around the edge of the shell. This is confirmed for the rib-stiffened shell of figure D26. The maximum displacement of the top of the shell was found to be 60mm in the summer and -8mm in winter. The edge disturbances are leading is the summer but are found not to be largest for the compatibility moments, with a maximum in the ribs of 16kNm it is concluded that the dimensions of the ribs and the applied reinforcement do not have to be adapted.

9.2.7. Dynamic response check

The check in paragraph 8.6 on the dynamic response was performed for a shell with an overall thickness of 60mm. The structure within this paragraph is significantly lighter and is therefore checked for its dynamic response.

Eigenfrequencies dead weight

Natural frequency	f [Hz]	T [sec]
1	6.80	0.15
2	6.80	0.15
3	7,02	0.14
4	7.09	0.14

Tab. D23. Eigenfrequencies for final design

Vibration shapes

1	2
3	4
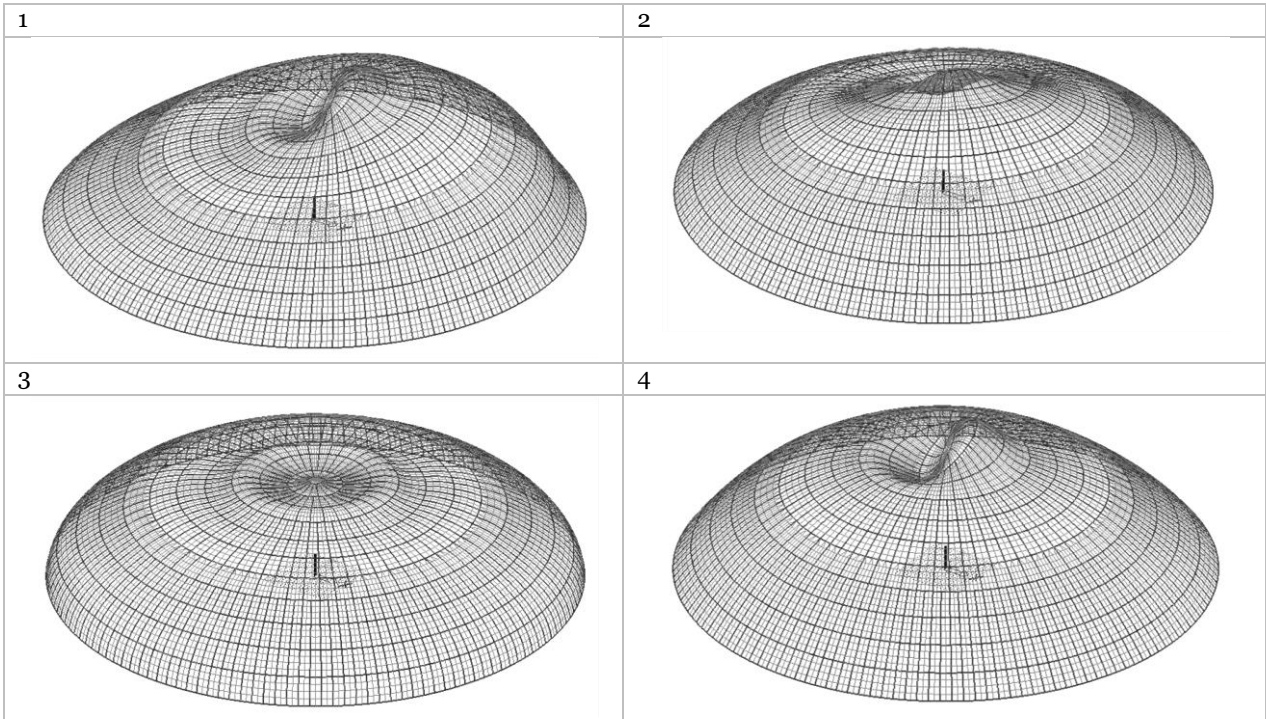
The value for the eigenfrequency of the structure of 6.8 Hz (T=0,15 sec) is not expected to cause possible dynamic magnifying effects for it is not expected for dynamic loads to occur with this frequency. As mentioned before, the dynamic response is considered sufficient when the eigenfrequencies of the structure are larger than 5 Hz.

9.2.8. Structural coherence

To ensure that the structure shows sufficient structural coherence the design is tested for its response to openings in the shell, possibly as a result of accidental loads. Two load cases are tested for their bearing capacity and the effect to the force distribution in SLS. The cases are case 1 in at which at the bottom of the shell 3 elements are absent and case 2 at which close to the top 2 elements are absent. The buckling patterns are shown below.

Case 1 P = 17,4 kN/m²	Case 2 P = 16.7 kN/m²
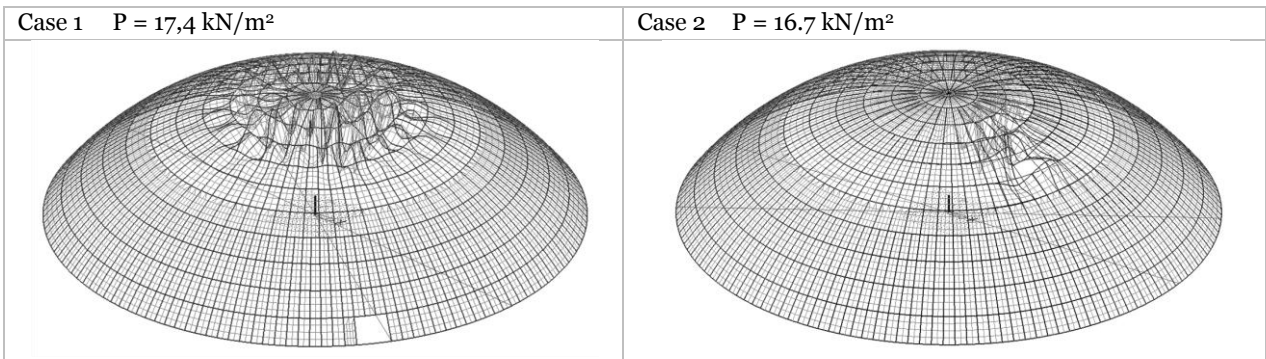
The buckling calculations show that in case 1 the opening has no effect to the buckling pattern and a neglectable effect to the linear critical load. For case 2 it holds that the buckling pattern occurs at the location of the opening, the linear buckling load is reduced by 5%. Both cases show an occurrence of tensile stresses and a disturbance in the membrane behavior in the region of the opening. The value of the tensile stresses, with a maximum of n_x = 15kN/m, and moments, with maximum of m_x = 0,1kNm/m, around these areas are not expected to cause problems because of the connection capacity and the inertia of the ribs and stiffeners. Also, since the effect on the bearing capacity is small it is concluded that the structure has sufficient structural coherence.

10. Shell Construction

According to [46] a designer of shell structures faces four essential challenges. These are enumerated, in more or less in order of importance: construction method, testing, analysis and appearance. The aspect of construction is of this great importance because of the geometrical complexity of shell structures, which differ in various aspects from more conventional 'framed' structures. The structural behavior of shells, described in part B, originate from their geometrical features. A consequence of the geometrical features is that the realization of these structures is challenging. The design aspects resulting from these geometry aspects for shell construction are described in this chapter.

10.1. Introduction

Traditionally, shell construction methods have often been based on the principals of timber formwork and supporting framework. Understandably, the application of formwork, and especially double curved formwork, can be labor intensive and time consuming. Thus, however shell construction may lead to a favorable ratio for material use to column-free span, this can be opposed by labor intensive practice on the building site.

In addition to the intensive labor, over the decades, due to various economical aspects, labor costs in Western Europe have increased relatively more than the material costs. Driven by this increase, other construction methods than the traditional form- and framework were investigated. These methods include for instance the use of prefabricated elements and numerous alternatives of inflatable formwork. The research has also focused on the use of innovative new materials and on addition of fibers within conventional materials, such as concrete or polymers, which has the expected potential of a total replacement of passive reinforcement.

The application of UHPC and its potential within the field of shell structures has its relevance for both important design aspects, effective material use and construction method, described above. The highest potential for the application is ought to be obtained when both aspects are optimized. Optimization of material use involves structural optimization; an effective construction method is, as was concluded by literature and references, highly interlinked with the construction with prefabricated elements.

Regarding the construction of a shell structure not only UHPC itself appears to be most suitable for precasting. Moreover, the challenging construction of shell structures lead to an economical driven choice for an increase of the use of repeatable prefabrication within a project. Since it is concluded that precasting seems the most valid alternative for the construction of the shell it has to be studied what consequences are subsequent and what conditions are required for precasting to be successfully applied.

10.2. Construction methods

The design of a segmental shell requires a study on the construction phase. This study has its relation to the handling, erection, form control and temporary supports during construction. Multiple construction possibilities are deliberated within this paragraph and judged for their feasibility based on pre-construction activities, form control, ease of construction, stability, supports and risks.

10.2.1. Studies on execution

Within the construction phase the question arises whether the large amount of scaffolding, as was applied in classic shell construction, can be limited for a shell with precast elements. A second consideration in to ease the application of the connections. A number of ideas for the construction method are presented below.

The considered methods are:
- Igloo method
- Igloo method II
- Top-down construction
- Segmental construction

Igloo –method I

The main idea of this method, in which the elements are installed in circumferential direction, is to create a stable ring of the structure and continuing this construction to the top. When a ring is finished it may have a certain stability, which can result in a reduction of the use of scaffolding since the support of the first ring may be removed when installing the next rings.
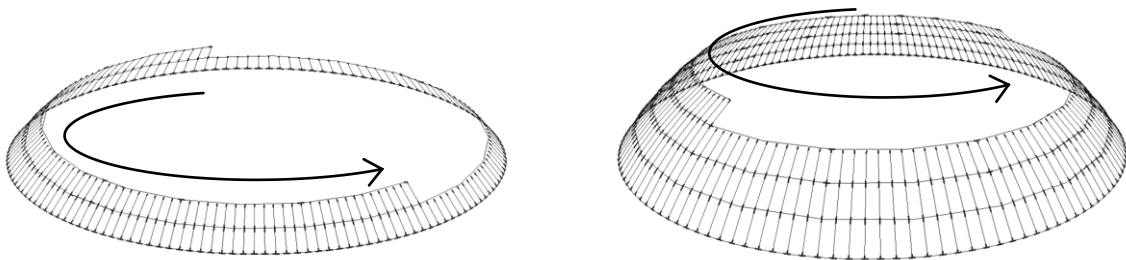
Fig.D56. Principle of igloo-method

Igloo –method II

To improve the igloo-method it might be beneficial to connect multiple elements in meridional direction before installment on the final location. In this case the connections between the elements can be made at ground level before placement, meaning easy assembling and control, and scaffolding may not have to be applied at every ring.

The application of the placement of multiple elements at once is dependent of the crane capacity and the possible positive effect on deformations during construction.
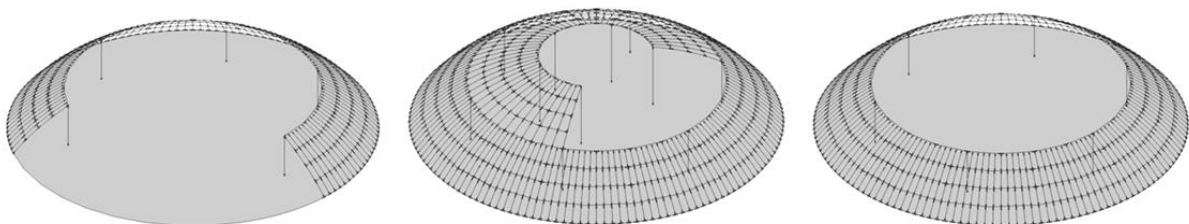
Fig.D57. Principle of igloo-method II

Top-down method

An alternative for the build up from bottom up is to build the shell from the top, making use of the method of a self-erection lifting support in the middle of the shell.
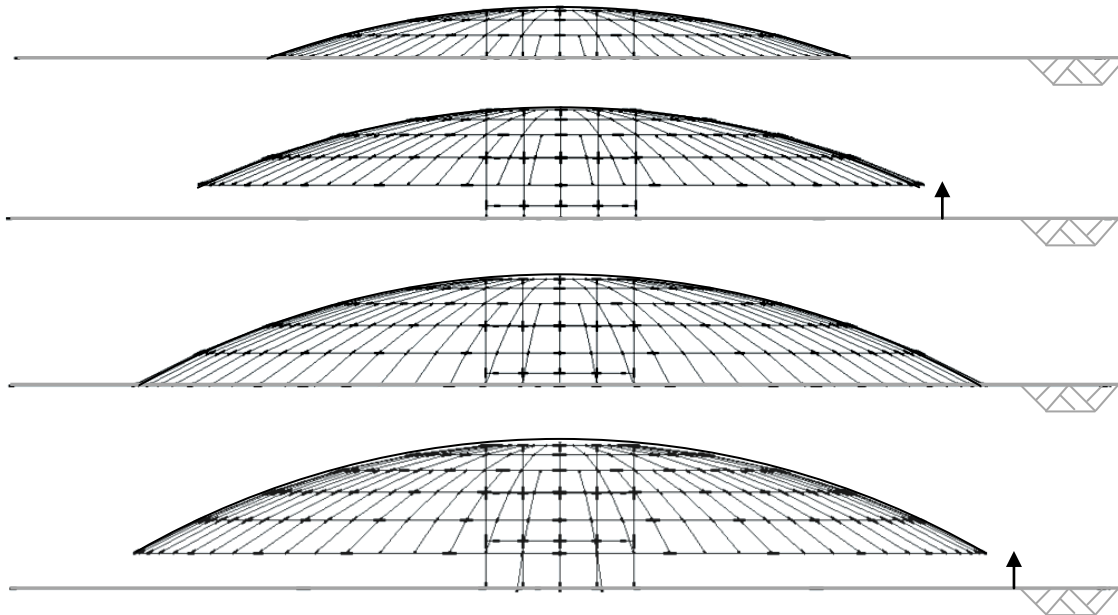
Fig.D58.   Principle of top-down method

This unconventional construction method has the advantage that the installment of elements is merely done at ground level. During construction phase the force distribution within the shell is opposite to that of the final stage, causing large tensile stress within the elements and connections. By this, the structure should be adapted significantly to load cases during construction. Also, the final step of placing the shell at its final location and connecting it to the edge ring is expected to be difficult. All in all the method is considered not to be feasible.

Frame method

This method comprehends the construction of independent frame by ribs and stiffeners to quickly construct a stable framework on which the elements will be connected later. The advantage is that scaffolding can be limited since the stable frame of the final structure assures stability during construction.
The disadvantage is that the elements now, beside their mutual connection, also have to be connected to the frame. Also, this method is in contradiction to the aspiration to coincide the ribs and stiffeners within the elements to provide a stiffened shell by basically one type of element.
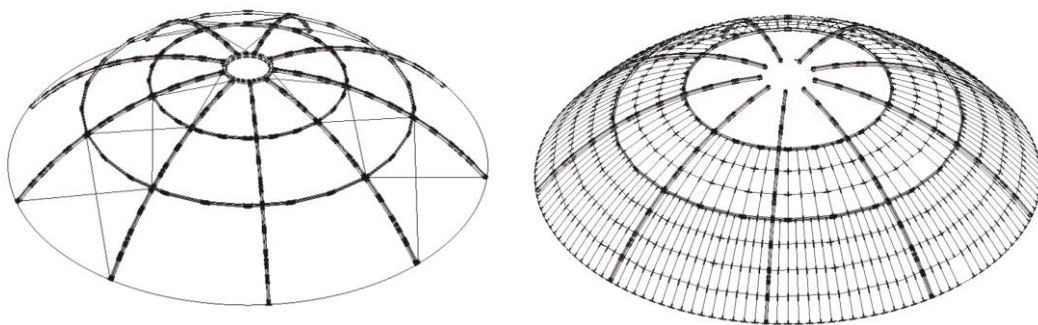
Fig.D59. Principle of frame method

<u>Segmental method</u>

Similar to the igloo-method the idea of the segmental method is to provide a stable part of the structure in an early stage of construction. For the igloo-method this stable part is provided in circumferential direction, for the segmental method the idea is to construct a stable arch in early construction stage which will be completed later. The arch can be constructed either by placement by crane or by the segmental flap method described in appendix 3.3. This method, together with the igloo-method, implies that elements are to be connected before placement, which means that connecting can take place at ground level, meaning easy assembling and form control. The method is dependent on the weight of the segment and crane capacity.
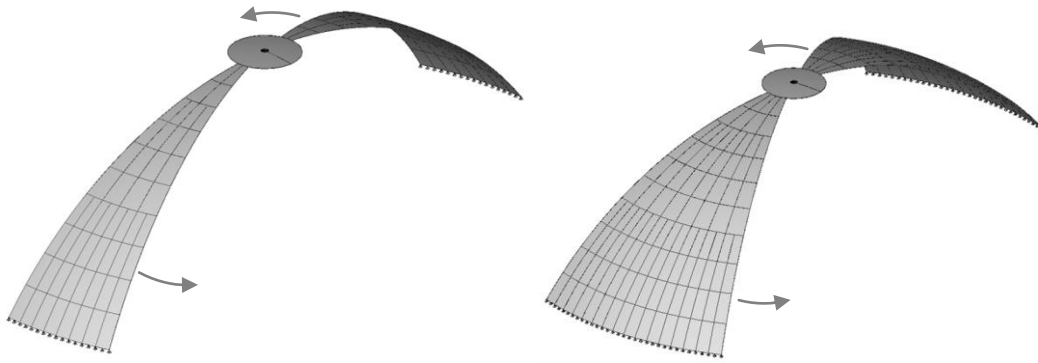
Fig.D60. Principle of segmental method

A short deliberation shows that the proposed arch does not provide sufficient stability to avoid the employment of scaffolding. Also the placement of two segments opposite to each other causes that in the final stage at two locations a closing segment will have to be placed within a fixed structure. Therefore it is deliberated that if the crane capacity gives the opportunity to place a large segment as demonstrated in figure D60 and since the stability of the arch falls short, it is considered to be more easy to apply the segmental method in one rotating direction. Causing that in the final stage at only one location a closing segment is to be placed.

10.3. Execution proposal

10.3.1. Method

It is concluded that the igloo method, meaning construction along the circumferential axis, is most promising as construction method. Both the discussed methods named 'igloo method II' and 'segmental method' support the idea to connect elements at ground level and then place as many elements as possible per lift. This implies that the requirement of scaffolding can be minimized to merely the locations providing stability during construction and connection which are to be made between segments. Hereby there is no requirement for scaffolding at most of the connection locations.

10.3.2. Crane

It is seen that the crane capacity is a decisive factor in the choice for the construction method. A number of ideas for the supply of elements to their location by crane are deliberated.

The most standard location would be to place the crane outside the perimeter of the shell. Since a large span shell causes the crane to span a large distance a question is what amount of elements can be placed at the middle of the final shell, meaning half the diameter needs to be spanned. The total ground area of the shell can be covered by multiple fixed cranes or a single mobile crane, or a crane on temporary rails around the base of the structure.

When it appears that multiple cranes outside the perimeter of the shell are required an alternative is to place a single crane at the middle of the shell which can cover the whole area. A downside of this method is that the dismantlement of the crane can cause difficulties and that the elements at the very top of the shell cannot be placed by this crane.

Another alternative is to supply the element by a temporary structure on top of the already constructed shell towards the centre, making use of the already constructed shell to transport the shell elements towards the middle. The temporary structure and its loading on the shell in construction phase are however less straight-forward than the application of a crane.

From the described alternatives the preference is given to the application of a mobile crane outside the perimeter of the shell. To observe the possible application of a mobile crane the element configuration is observed to determine the concrete weight of multiple adjacent elements.

Ring	# Elements	Element surface [m²]	Weight UHPC [kN]
1	144	25,0	27,8
2	144	23,1	26,1
3	144	21,2	24,3
4	144	19,1	22,3
5	72	33,6	36,0
6	72	28,9	31,5
7	72	23,9	26,8
8	72	18,8	22,0
9	36	27,0	29,7
10	36	16,3	19,6
11	9	21,8	24,8
Total	945	~22000	

Tab. D9. (rep)   Total build up of elements
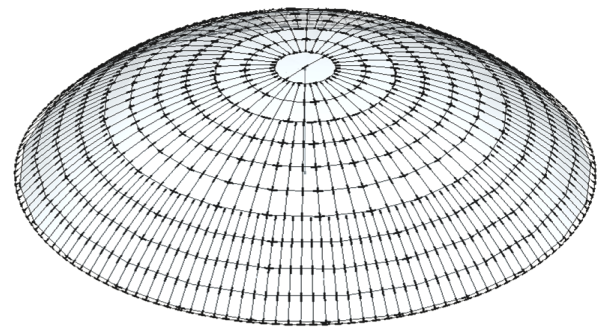
Fig. D26.(rep)   Total build up of elements

Now the question is what amount of elements can be lifted by a mobile crane over a sufficient distance. It is considered to be beneficial if the shell is divided into segments, in this case placing a new segment adjacent to an already placed segment has to deal with merely one boundary. This is not the case when the shell is constructed by the igloo-method. If the shell is divided radially into 36 segments the concrete weight of one segment, shown in figure D61, is:

$$4 \cdot (27.8 + 26.1 + 24.3 + 22.3) + 2 \cdot (36.0 + 31.5 + 26.8 + 22.0) + (29.7 + 19.6) = 684 kN = 68.4t$$

If the segments are equipped with roof finishing this value is increased by:

$$p_{fin.} \cdot \left(\frac{1}{36}\right) \cdot A = p_{fin.} \cdot \frac{2\pi R s}{36} = 0{,}25 \cdot \frac{\pi \cdot 93{,}75 \cdot 37{,}5}{18} = 15{,}3t$$
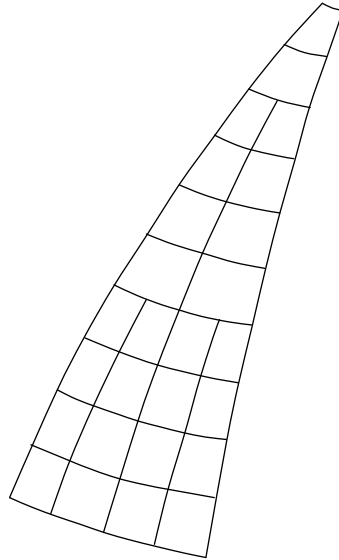
Fig. D61. Segment of the shell

The segment itself is, because of its slenderness, highly sensitive to deformations. As a result it is required to lift the segment while being carried at multiple locations. To distribute the forces and control the placement of the segment an assisting structure is proposed, as shown in figure D62.
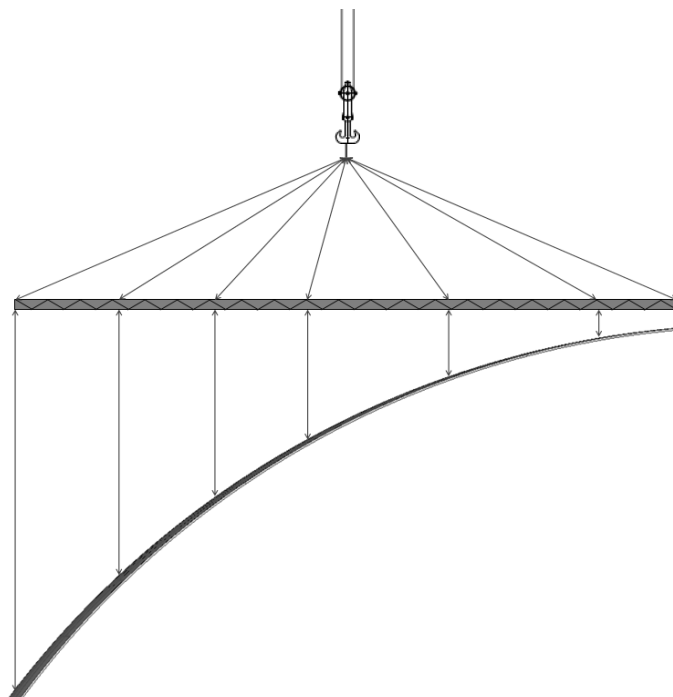
Fig. D62. Principle of assisting structure

The supporting structure of figure D62 is represented as a space frame. This is expected to be required for a stiff application of the segments. The system including a space frame and vertical cables should be applied at precise dimensions so the segment holds its shape during handling.

As a reference for a mobile crane a Liebherr LG-LGD 1550 is chosen. A standard composition of this crane, with a boom length of 35m and a jib length of 42m and a counterweight of 250t has the capacity of 95 tonnes at a radius of 40 meter. The capacity is more than required since it is reckoned that the undimensioned spaceframe also is to be carried. It is noted that other cranes and compositions are applicable as well, this particular crane and composition are used to demonstrate the feasibility of the construction method.
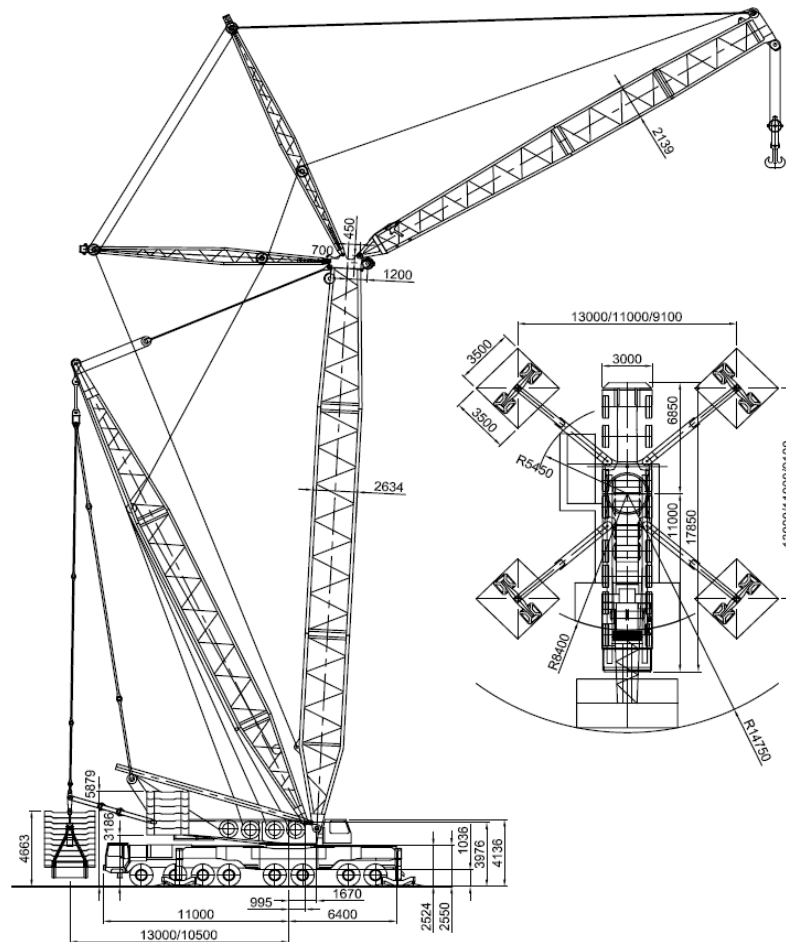
Fig. D63. Liebherr LG-LGD 1550; dimensions in mm [78]

It is concluded that this segmental method where the shell is divided in 36 segments has a high feasibility to be applied successfully and that applying merely one crane has economical value. The majority of the connections can be made easily on ground level, where also form control and possible necessary adjustments can take place. The crane usage is limited to about 36 equal handlings, for which a supporting structure is to be made. An advantage of the geometric simple shape is that for a shell of revolution the supporting structure does not need to be adapted.

10.3.3. Chronological presentation
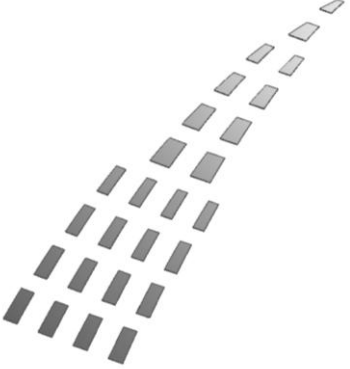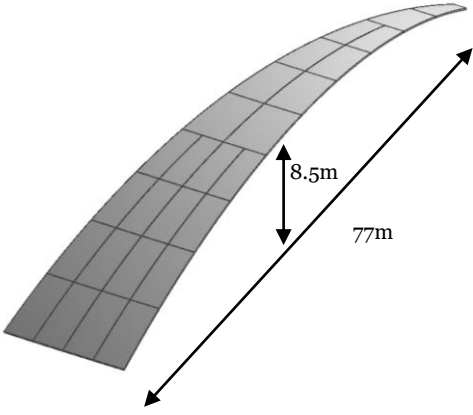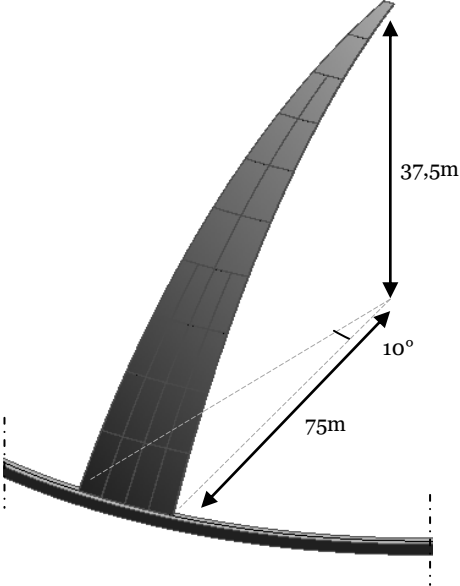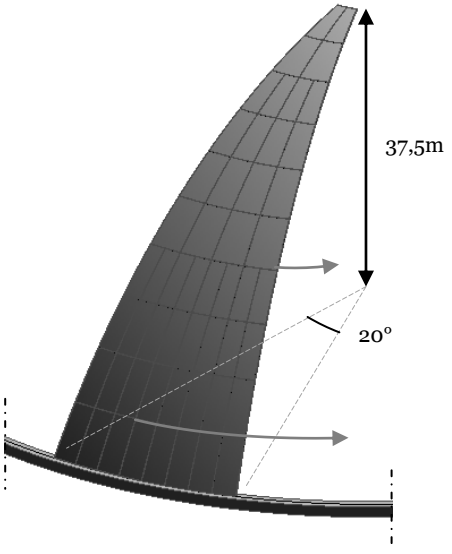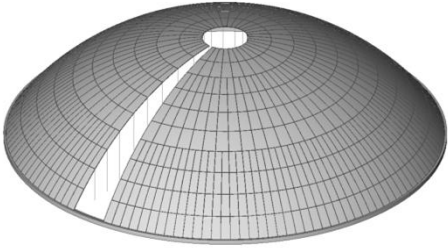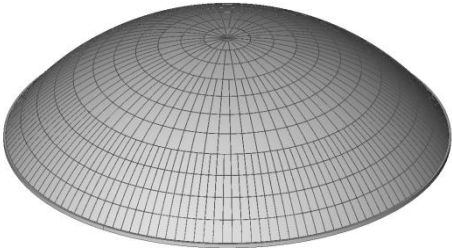
Step 1. Placing elements at ground level	Stage 2. Connecting the segment at ground level
	8.5m 77m
Stage 3. Lifting segment to final location	Stage 4. Repeatedly start from Stage 1
37,5m 10° 75m	37,5m 20°
Stage 5. Key segment	Stage 6. End stage

Fig. D64. Construction stages

The proposed construction method consists of 6 steps which are presented above.

Stage 1.   Placing the elements at ground level

The elements are placed per segment, in this case a segment consists of 26 elements. This Stage is executed at ground level. This means that the elements, with a maximum weight of 31,5 kN, can be handled with a small crane. The elements are ought to be numbered per ring and substitute elements should be provided to prevent construction delay.

Stage 2. Connecting the segment at ground level

The connections between the elements can be made by the principle shown in figure D55, which was explicated in section 9.2.5. This implies that a construction worker has to tighten the bolts. The specifications for the bolts and their application can be matched by making use of a torque wrench, which allows the operator to measure the torque applied to the fastener. The tightening should be applied in a controlled manner. The required force within the connection and corresponding torque are to be determined and are influenced by the demands for the elements to perform water tight by closing the elastic gaskets.

In figure D64 it can be seen that the segment asks for a demand that on ground level a small amount of scaffolding is required for the segment has a sagitta of 8,5m.

After stage 2 the segment is checked on form control. In this way it is assured that the elements of the segment are accurately connected, which diminishes the occurrence of deviances and possible installment difficulties of further segments.
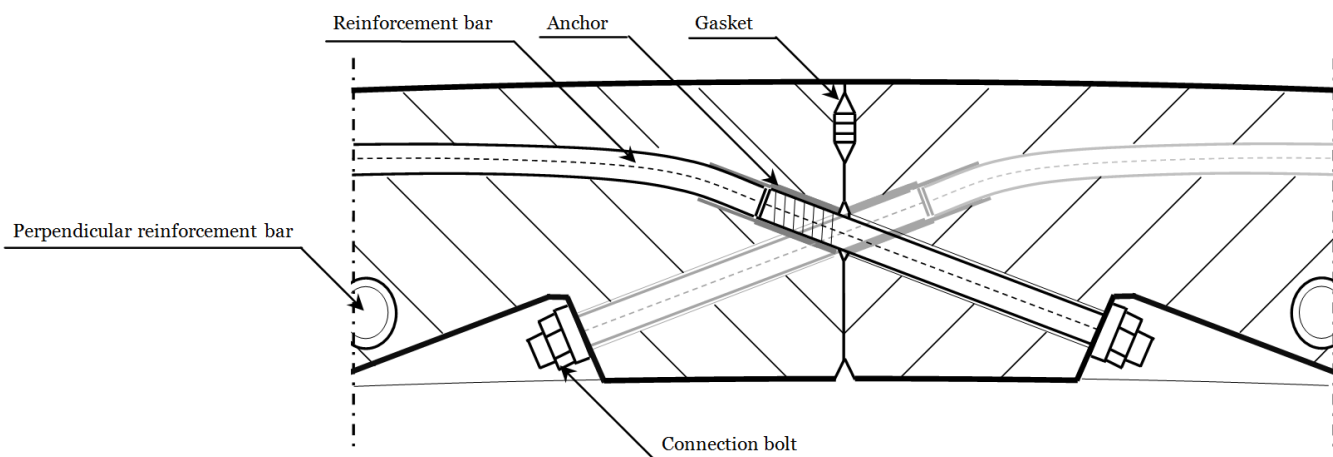
Fig. D55.(rep)   Vertical & horizontal cross-section of local connection between two elements; not to scale

Stage 3. Lifting segment to final location

The segment can be lifted by a crane with the help of a supporting structure. The segment must be accurately placed and connected to an anchor to the initially placed edge ring, which acts beside a structural connection as a placing assistance.

The segment is then supported by scaffolding. The application of scaffolding in this stage is inevitable and for the first segment will be permanently placed for the support of the segment is of importance for later stages, especially the final stage.

Stage 4. Repeat from stage 1

The next step is to repeatedly add segments to the structure. An advantage of the method is that stage 1 can be executed independently from the other stages so this stage can be separated from the critical construction path.

The connection between the individual segments is done with the same method as the other connections. This entails that locally, along the edge of the previous segment, a temporary measure is to be taken for the connection to be applied.

In this stage the stability of the structure is increased after every added and connected segment. The amount of scaffolding under previous segments can be reduced locally, which is financially advantageous.

Stage 5. Key segment

The placement of the final segment is logically the most challenging stage with regard to placing segments at their final location. In theory the placement of segments can be assumed to be perfectly executed, meaning that the segments are perfectly placed at their intended positions. In practice the final segment, often referred to as ' key segment' in tunnel lining construction, is not expected to fit perfectly. The intended available space can be either too narrow or too wide.

In tunnel lining construction, in case of a too narrow space the key segment is enforced to fit. In case of too wide space the ring is not successfully closed. From tunneling references it is concluded that forcing the key segment, which is often an trapezoid segment which can glide into the already applied segments, can result into locally high stresses. Also the gaskets, which are in contact between the new segment and the adjoining segments, can roll up due to frictional stress which can cause leakage to occur.

Dissimilar to tunnel construction the construction of the shell has two advantages. At first the segments can be placed on the initially installed edge ring, which serves as an placement assistance. Secondly, the structure is not yet subjected to deformations due to loading for the reason that it is supported. With these consideration known a number of alternatives for the placement of the final segment were considered of which the two most promising are presented.

Method 1:
This method is formed on the basis that the available space is too narrow and the fact that a forced placement of the key segment should be avoided.   If the available space is too narrow it is a possibility to make use of the fact that the shell is not yet finished and sensitive for deformations. The idea is to lift the edges of the adjacent shell segments which is ought to result in sufficient spacing, represented in figure D65 as distance Δx. The lifting can be applied at one or both edges.
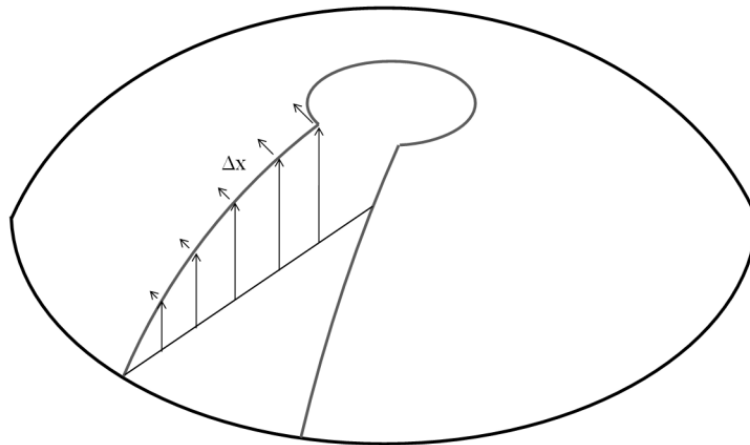
Fig. D65. Method 1; lifting adjacent segments along their edge

Calculations on how the already connected segments respond to the imposed vertical displacement show that the effect of lifting the edges next to the key segment effects numerous adjacent segments. It is concluded that the lifting is to be continued for the supports of those segments.

The effect on the requested horizontal displacements in comparison to the imposed vertical displacement is investigated. In case the shell is opened, as in figure D65, an imposed vertical displacement of 120mm is required to acquire an opening of 20mm, which occurs at a quarter of the span. Due to the low deformation capacity close to the edge ring and at the top of the shell the displacements are practically nil.
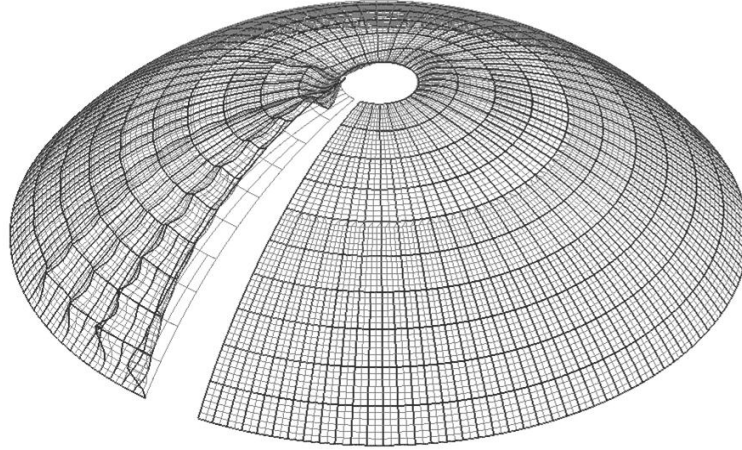

Fig. D66. Method 1; lifting adjacent segments along their edge

Too improve the method the shape of the final segment can be adapted as seen figure D67. With this shape the difficulties at the top and bottom of the shell can be fixed. The spacings at the top and bottom of the shell can be filled later.
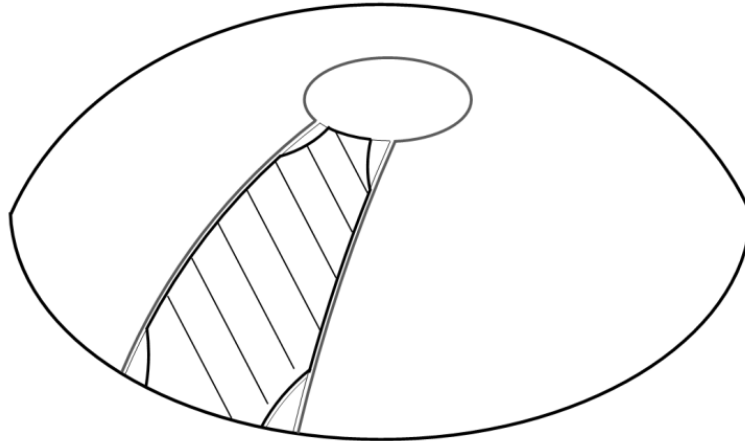
Fig. D67. Method 1: lifting adjacent segments along their edge

This method is considered to be labor intensive due to the required adjustments to a large amount of supports. Also, the implied vertical displacement has to be applied with caution. Not only do the supports have to be lifted, they also have the requirement to be able to displace horizontally. All in all this method is considered to be laborious and not very efficient due to the small obtained horizontal space in proportion to the implied vertical displacement.

Method 2:

In case the available space is too wide the remaining vertical opening, represented in figure D68 as distance Δx, can be filled by a field-cast joint fill solution of UHPC (appendix 6.2). The remaining space can be created deliberately so the final segment fits for certain.
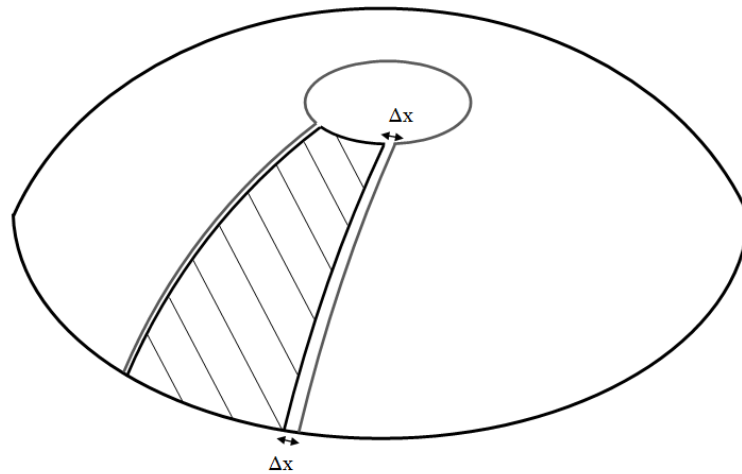
Fig. D68. Method 2: smaller key segment; remaining space to be filled

The disadvantage of this method is that facilities have to be taken, after the segment is placed, to fill the space. It is positive that these facilities, most likely being a double mould, are only to be applied once and that the fact that the method requires more time is not decisive since the efficiency of the quick erection of the rest of the shell. Also, the spacing Δx can be chosen so that possible placing deviances can be easily handled.

Considerations

For both methods, I & II, it is considered to be beneficial to keep the top of the shell open. When this is done the final segment has solely 2 boundaries to reckon with instead of 3, the third being the top of the shell. Also the shell is slightly less constrained in its movement, which is necessary for method 1.
For both cases it holds that the placement of the connections is more difficult for the final segment than for earlier placed segments. The solution can be to firstly connect the bolts at one edges and subsequently adjust the other edge by temporary support to install the last connections. Also, it is proposed to enlarge the margin of the holes for the connecting bolts in the crucial segments so the placement of the bolts can be guaranteed. Another option is to apply a local exception to the connections which is to apply injection bolts within the elements.

It is concluded that key segment method 2 is most promising. The right placement of the key segment is guaranteed by the fact that the available space can be chosen and determined in consolation with the building contractor. It is also considered to be less difficult than method 1 since the supports do not have to be lifted. The fact that an field-cast joint fill solution of Ductal is commercially available supports the choice for this method. The lower performance of this field-cast solution, shown in appendix 6.2, show that this UHPC-variant are somewhat less good than for BS1000. This local reduction of material capacity can be taken care of by thickening the joint.

Stage 6. End stage.

After the top segment, which is to be lifted with the same mobile crane, is placed the installment of the prestress within the edge ring can be applied. The schematization of the prestress in the edge ring is done as an equally distributed load and should be approached in practice.

It is advised to remove the supports gradually per ring, for which it seems to be most logical to start at the top of the structure since construction workers are already at this point to connect the last bolts. By removing the supports per ring the forces in the shell are gradually introduced.

Part E
Design Study

11. Fiere Terp

As was described in the introduction of this report the aspect of thin shells within this research originates from a preliminary design for a project named 'Fiere Terp'. This design is handled in this chapter as a case study for which the design recommendations can apply.

It is repeated that the case study has served as a problem definition and guideline for the applied dimensions for a large span shell within the research. The design recommendations for the use of UHPC within shell large span shell structures which are obtained for a shell of revolution might now be transformed for this design. Beside the recommendations the design for the Fiere Terp can be improved wherein fundamental modifications are permitted.

11.1 Project description

The early-stage project named 'Fiere Terp' is a preliminary design for a shell structure which was the motive for the research on shell structures within this thesis. The choice was made to consider a shell of the required dimensions and type of curvature of this project as a guideline for a design within this thesis. A description of the design is given below:

The design for the Fiere Terp is an ambitious plan for a large sport and culture center which is an initiative of the foundation Multifunctionele Innovatieve Centra Friesland. The design has the shape of a 'pompeblêd', meaning the leaf of a white waterlily in the Frisian language. In the dome created by the leaf among other things a 400m indoor racetrack, a 460m long speed skate track and an ice hockey field are planned. The largest span of the shell, from the center to the outer ring is about 140 meter.
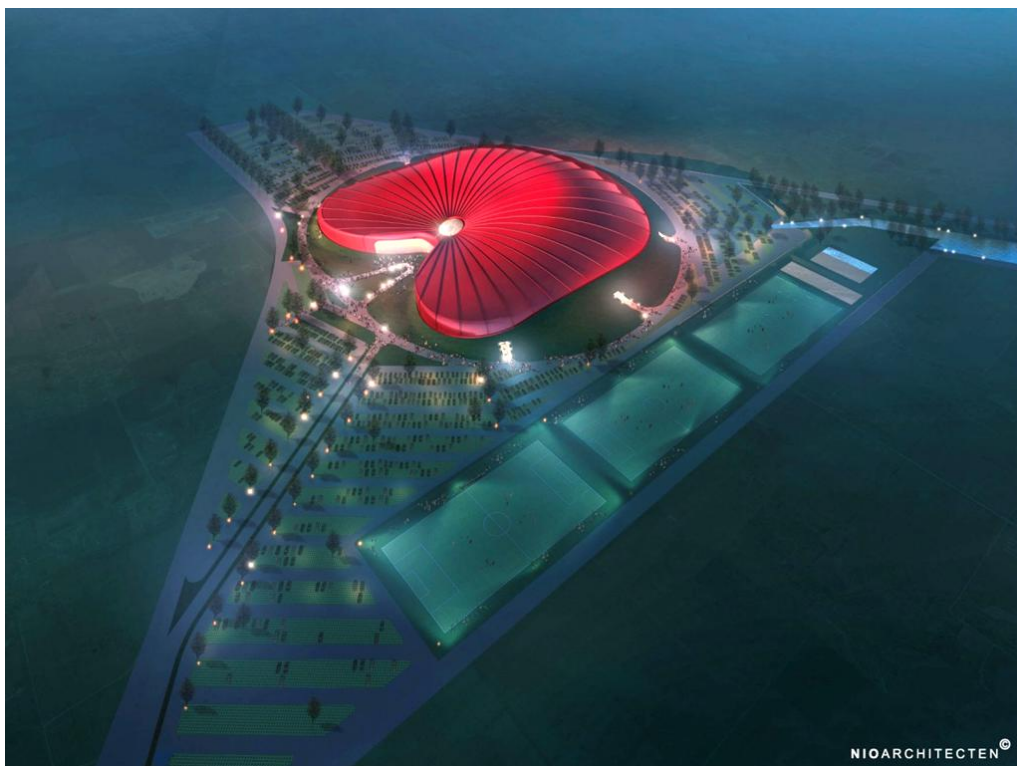
Fig. E1.   Impression Fiere Terp   [*NIO Architects*]

11.2. Starting points

The conclusions from the researches of chapter 8, summoned in paragraph 9.1, can be used as a guideline for a design of other shells with similar dimensions. The strength of the shell of revolution was found lie within its regular shape, leading to a regular force distribution when loaded by vertical loading and the fact that its general curvature leads to an overall buckling resistance.

The geometry of the preliminary design for the Fiere Terp differs considerably from a shell of revolution, as can be seen in the illustrations below. Therefore, its structural behavior will be different since, as it is known from theory, the geometry of a shell determines its structural behavior. It is of interest to research whether the proposed shape approached optimal shell behavior and where it can be improved.

It was concluded in chapter 6 that the repetition of elements is highly beneficial for an economical application of prefabricated elements. Because of this it is worthy to investigate what is the potential of repetition within the design and what adaptations can be made not only to improve the structural behavior but coherently to improve the element production and possibly perhaps even construction. For those reason it is investigated whether the design can be optimized structurally as well as economically.

Within this chapter the proposed design is deliberated after which a number of adjustments are considered. Three variants based on the original design are then discussed. For a comparison of their structural behavior the proposed designs are given an overall UHPC-thickness of 100mm and their supports are modeled as all-hinged. Since their dimensions considering their ground base and height are similar the results can be used for as an indication of their structural behavior and used for a judgment on their potential.

Illustrations preliminary design
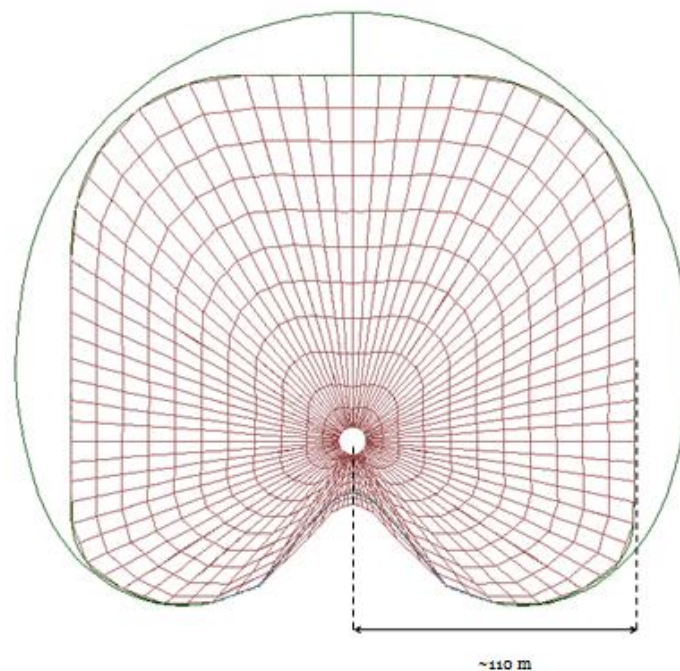
Fig. E2.   Top view Fiere Terp   [*NIO Architects*]
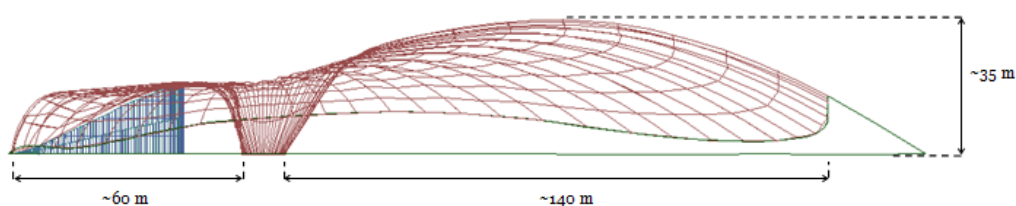
Fig. E3.   Side view Fiere Terp   [*NIO Architects*]
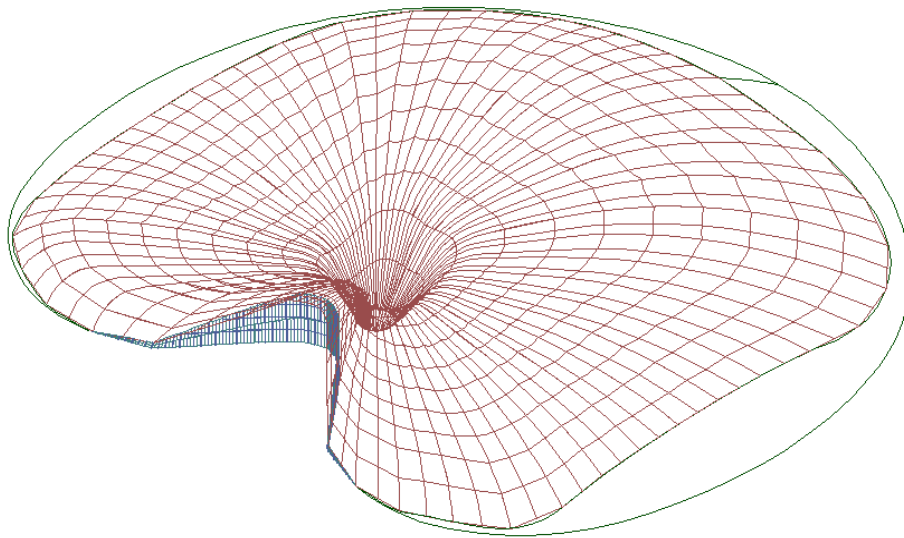
Fig. E4.   Bird's eye view Fiere Terp   [*NIO Architects*]

Fig. E5.   Original shape of a 'pompeblêd'

11.3. Structural design

11.3.1. Preliminary design
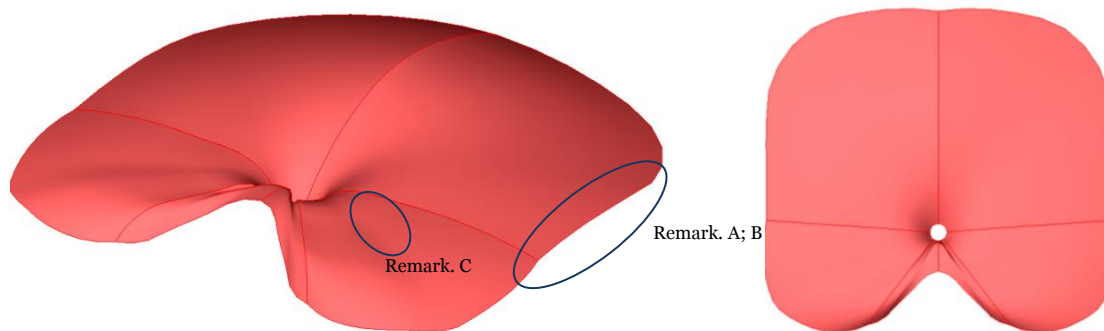
Fig. E6.   FEM-Structural model of preliminary design

The preliminary design is characterized by an overall positive Gaussian curvature and mirror symmetry. It is clearly seen in the side view of figure E3 that within the initial design the shell is not connected to ground level and can therefore not be connected to a edge ring. Since the application of an edge ring is undisputed for a favorable shell behavior the proposed shell is adapted at his edges (remark A).

The edges of the proposed design are, as can be seen in the top view of figure E2, formed by straight lines. This influences the force distribution of the shell resulting in, when subjected to vertical load, an uneven force distribution over the elements. Also the absent of curvature results in the fact that the elements along the edges are unique and are ought to be produced exclusively. Therefore the straight edges are proposed to be regularly curved (remark B).

The construction method as proposed in section 10.3.3. is to be adapted for this geometry. It is not expected that the span between the middle of the structure to its edge can be placed easily since a crane now has to span approximately 75m. The construction can be adapted by for instance first placing segments at the area around the middle of the shell and subsequently the outer shell area. Still, the construction of this design is expected to be much more difficult than for a more regular shell.

In comparison to the regular shape of the shell of revolution. which is characterized by an overall equal amount of curvature, the more complex preliminary design has an alternated amount of curvature over its surface. Since a curved surface is highly beneficial for shell behavior the lack of curvature which is seen at the left of figure E3 is to be adapted (remark C). The effect of the lack of curvature to the deflection is seen in figure E7, still the buckling pattern remarkably shows that its pattern around the equally curved area. When given an overall shell thickness of 100mm the found maximum deflection due to dead load is 2000mm and buckling load is 1 kN/m².
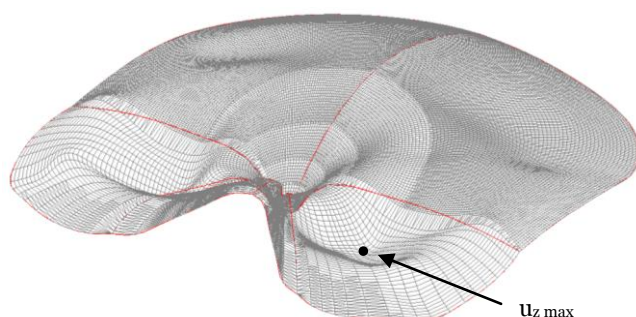
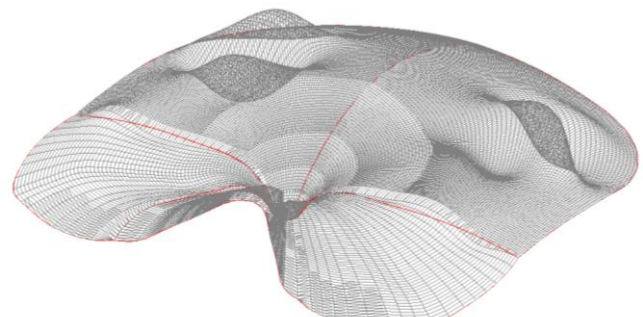Fig.E7. Example of buckling pattern under vertical load

Fig.E8. Example of buckling pattern under vertical load
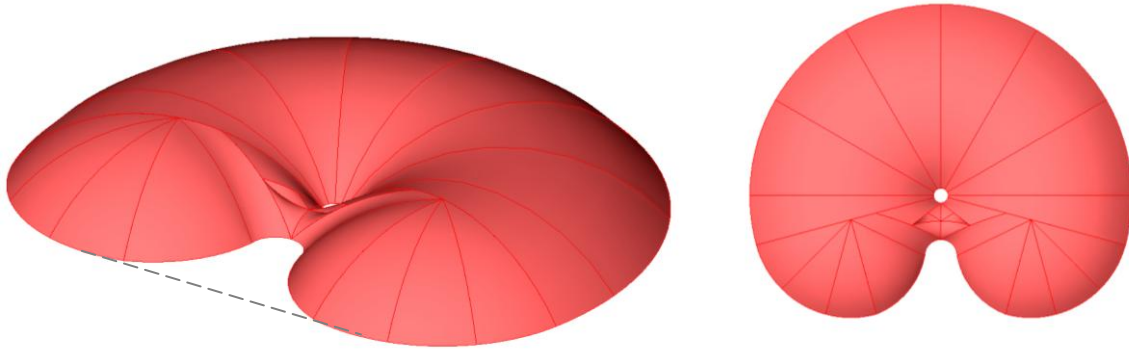
11.3.2. Variant A; Curved preliminary design

Fig. E9.   FEM-Structural model of variant A

Variant A is characterized by having almost the same basic plan as the preliminary design but with more curvature. The perimeter of the design is practically equal to that of figure E5. The fact that the shell is connected to ground level causes that an edge ring can be applied. The shape of the edge ring is thought to be placed curved around the perimeter and linear between the 'opening', as shown by the dashed line.

The result of the adaptation is that much repetition of elements can be acquired because a larger amount of the shell surface shows regular and constant curvature. The geometry however still shows a complex part of the structure around the opening where the surface changes from convex to concave.

Considering the construction method the same principles hold as described for the preliminary design itself, meaning no improvement is made on this aspect.

Both the deflection under dead load and the buckling pattern show that the middle area is crucial within the geometry. With an overall shell thickness of 100mm the found maximum deflection due to dead load is decreased to 43mm and buckling load is increased to 3.5 kN/m². It is hereafter investigated whether the complex geometry around the middle of the shell can be adapted and what is the effect on both the structural behavior.
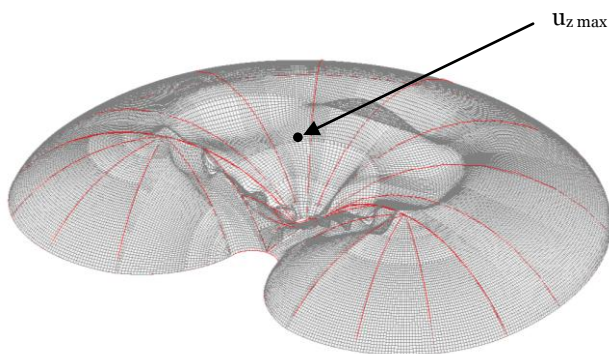
Fig.E10. Illustrative deflection under dead load
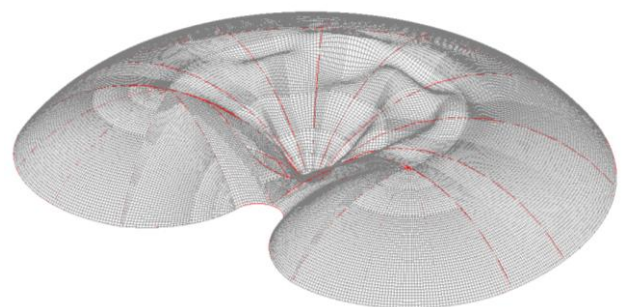
Fig.E11. Example of buckling pattern under vertical load

11.3.3. Variant B; 'Shell of revolution'
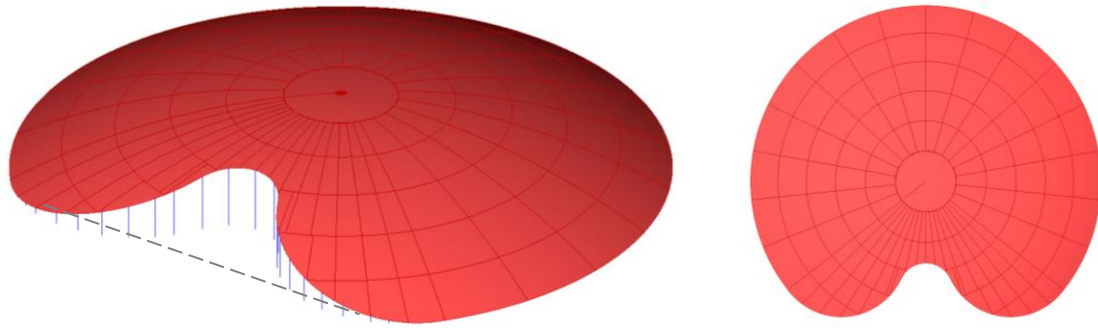
Fig. E12. FEM-Structural model of variant B

Based on the described favorable characteristics of a shell of revolution and on the fact that the design of the Fiere Terp was based on the shape shown in figure E5 the design of this variant is basically a shell of revolution which is adapted by a cutout. The geometrical change of the cutout causes that the forces within the shell as well as the edge ring are disturbed. The maximum span within this variant is enlarged from 140m to approximately 270m, which is a result of the fact that within this design the principle of the middle ground point is taken out of the design.

The strength of this adaptation is the regularity of the shape, causing for an equally transmitted force distribution within a stiff shell. Also, the fact that the shell is a surface of revolution causes the ability to make use of the same elements along a major part of the circumferential direction. Also, the same segmental construction method as proposed in section 10.3.3. can be applied for this shell. It is however expected that this method is to be more difficult since the connection to the edge beam and columns. Also, the fact that the shell diameter is significantly increased results in the assumption that the shell is to be divided in more segments than for the design of chapter 10.

Both the deflection under dead load and the buckling pattern show that the cutout of the shell is crucial for the shell behavior. This is explained by the fact that around this area the optimal shell behavior is interrupted, causing the forces to 'flow' around the area to the foundation as well loading on the free edge. This free edge causes for the requirement to apply columns as well as an edge beam among the free edge to deal with the shell discontinuity.

With an overall shell thickness of 100mm and relatively stiff concrete columns and beams (1000 x 1000mm) the found maximum deflection due to dead load is 80mm and buckling load is increased to 5.0 kN/m², with a pattern close to the free edge. It is concluded that the application of a free edge is rather complex since it has to handle the disturbances caused by the cutout.

It is hereafter investigated whether the geometry based on a shell of revolution can be combined with a perimeter based on figure E5.
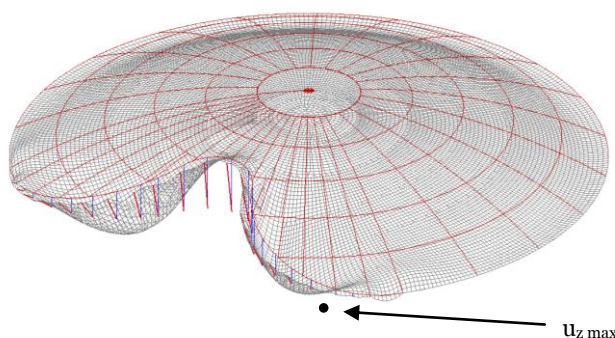

$u_{z\,max}$

Fig.E13. Illustrative deflection under dead load
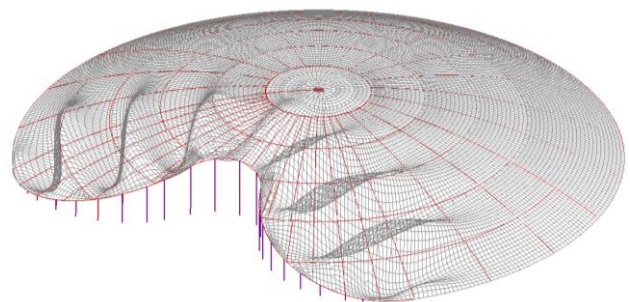

Fig.E14. Example of buckling pattern under vertical load

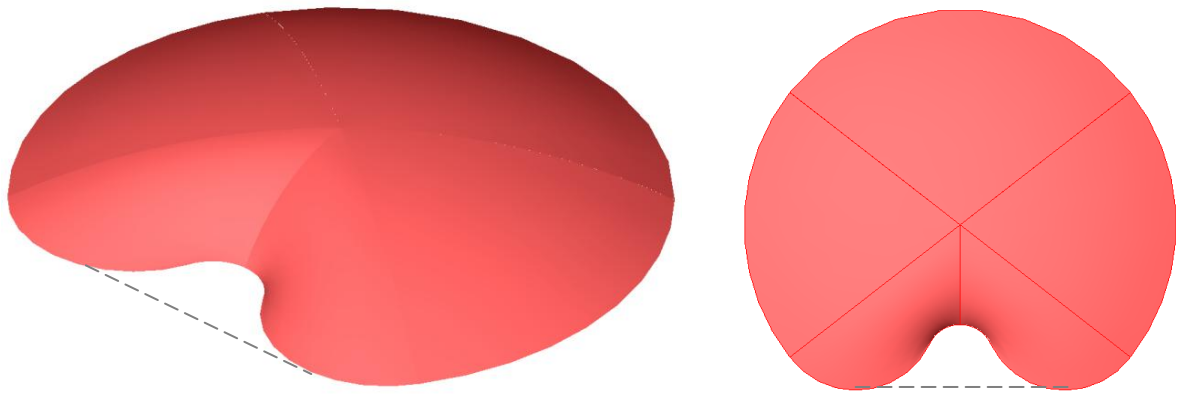### 11.3.4. Variant C; 'Pompeblêd'

Fig. E15.   FEM-Structural model of variant C

The shape for this variant is based on the positive characteristics of a shell of revolution and has the same perimeter of variant B, with the difference that the shell is connected to the ground. Similar to variant B the maximum span within this variant is enlarged from 140m to 270m, which is a result of the fact that within this design the principle of the middle ground point is taken out of the design.

The strength of this design is that the shell membrane behavior is not entirely disturbed by the deviance of a regular shell of revolution. This is correlated to the fact that more than three quarter of the surface consist of a shell of revolution, resulting in a stiff shell with a large potential for repetition.

The same segmental construction method as proposed in section 10.3.3. can be applied for this shell. The fact that the shell diameter is significantly increased results in the expectation that the shell is to be divided in more segments than for the design of chapter 10.

With an overall shell thickness of 100mm and the found maximum deflection due to dead load is 26mm and buckling load is increased to 6.5 kN/m². In it concluded that the 'dent' of the shell surface act as a stiffening part to the rest of the structure which results in a stiffer shell behavior than previous variants. The transition from the shell part which is a surface of revolution to this 'dent' is characterized by differences in deflection and a buckling pattern close to this edge, which may lead to a high demands for this area.
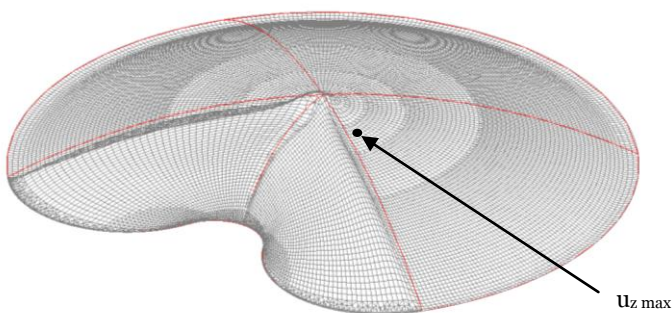

$u_{z\,max}$

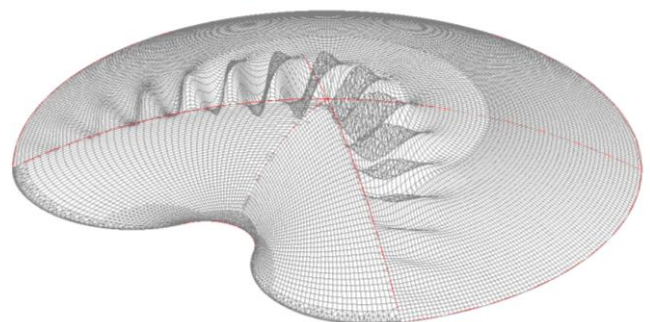Fig.E16. Illustrative deflection under dead load

Fig.E17. Example of buckling pattern under vertical load

11.4. Final design recommendations

From the reflections of the previous paragraph it is concluded that the design of variant C is most promising. This judgment is based on both the positive structural behavior as well as the resemblance to the initial shape. As can be seen in figure E18.
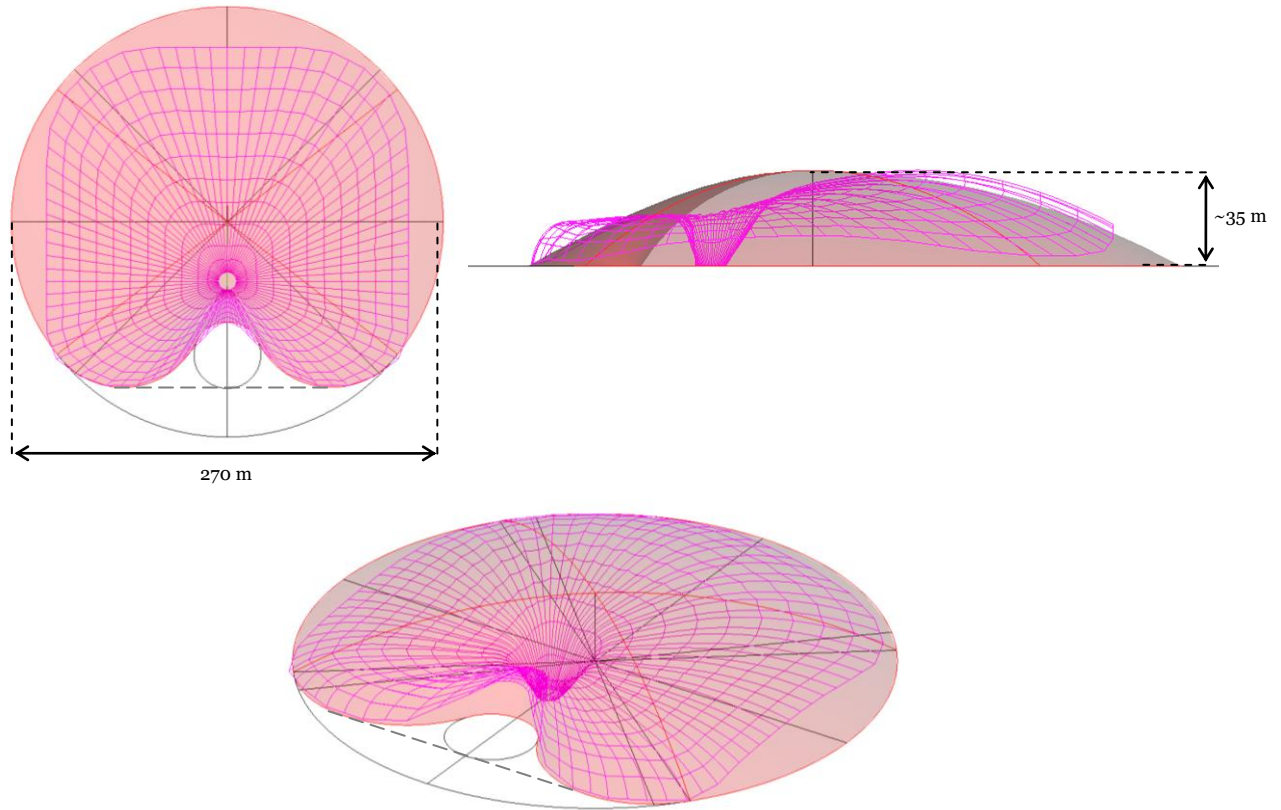

Fig. E18. Impressions of variant for Fiere Terp

Diameter	d	270m
Sagitta	s	35m
Radius	R	~277m
Arch length	L	~280m
Perimeter base	P	~860m
Area Shell	A	~58630m²

Tab. E1. Dimensions of final design

The fact that this geometry spans approximately 270m is not considered to be unfeasible. This is based on the results for a large span shell structure which was elaborated in part D. It was concluded that for a shell with a span of 150m, a height of 37,5m and an equivalent UHPC-thickness of only 44mm (table D14.) satisfies the demands. Therefore, it is concluded that a shell with the dimensions of variant C can be executed with suitable dimensions as well.

The weakness of the proposed design is that the ratio between span to sagitta (270 / 35 = 7.7) is much higher than the ratio of the elaborated design of chapter 8. The higher ratio leads to a smaller amount of curvature, which is unbeneficial for the buckling capacity of the structure. An option to increase the buckling capacity would be to increase the sagitta of the shell so the sagitta to span ratio will be in the domain of 1/4.82 to 1/7.46, as was described in section 3.4.2.

The fact that the shape of the shell has a lower potential buckling capacity, together with the increased span to 270m, leads to the expectation that the shell thickness is to be increased significantly.
Both the increased thickness as well as the larger shell area leads to much higher demands for the edge ring. It holds that both the edge ring dimensions as well as the prestress force are ought to be increased. This aspects are however not expected to make the design unfeasible since, in theory, these aspects can be increased to required characteristics.

The fact that the geometry is severely different causes that the optimal proportion of shell thickness to rib stiffening is expected to be highly different for this design. This is also caused by the fact that the division of the shell into elements, which is interlinked with the location of the ribs and stiffeners, is severely changed by this geometry modification.

All in all it is expected, based on the results of chapter 8 and 9, that the design for a large shell with a span of 270m and the same height as the of 35m can be dimensioned into a highly feasible design.

12. Conclusions

This chapter reports on the most important conclusions of the individual parts of the reports.

Part A. Ultra High Performance Concrete

The study on UHPC confirms the high expectations which apply for this material. UHPC shows a high compressive strength together with high durability properties and ductility with only a slight increase of cubic weight compared to conventional concrete. Not solely the compressive strength but also the tensile strength and the Young's modulus distinguish UHPC from conventional concrete. The outstanding qualities in terms of durability of UHPC makes it possible to envisage thin structural components with very long lifetimes without maintenance or repair.

The employment of fiber reinforcement is not solely important for the ductile behavior under compression and tension. The advantages for contribution to brittle behavior, crack width control and the resistance to concentrated forces are valuable aspects.

UHPC has the possibility to design without passive reinforcement and to get to economic buildings with an extraordinary slim design The combination between fiber reinforcement and passive or active reinforcement can be highly advantageous since the structural and deformation behavior in serviceability as well as in ultimate limit state are affected significantly.

For the production of UHPC is highly demanding a requirement for successful production is a controlled precast environment which is most suitable for precast instead of in situ casting.

There are no internationally accepted design regulations for the application of UHPC. Partially this is due to insufficient information with regard to the properties of the material. In comparison with existing codes for structural concrete new design aspects are required. Light, large span, elegant and material saving structures in UHPC are only possible if reliable rules are available.

It is complicated to determine a cost price for UHPC since many factors are of influence. Independent production would imply separate parties which deliver the various material components. For this, an overall indication of a cubic price of 700 euro/m³ can be applied. Overall the expectancy for economical savings of a UHPC-project is not purely based on material costs and savings. It also involves less demands for the shell foundation, less necessary transport, possibilities for construction as less hoist handlings and an improved lifespan.

Part B. Thin concrete shells

Shell structures present immense structural and architectural potential in the field of civil and architectural engineering. The spatially curved surface structures can be referred to as 'form resistant structures', which implies that the structure obtains its strength from its shape. The advantageous shell behavior is caused by the fact that thin shells have a small thickness-to-radius ratio which results in the shell to have a much smaller flexural rigidity than extensional rigidity. As a result, when subjected to an applied load, it mainly produces in-plane actions, also named membrane forces.

A consequence of the positive effect by the relatively small thickness is that the strength of the shell design is mostly governed by its buckling capacity. For shell structures, which are mostly subjected to compressive forces, the failure mode is therefore mostly influenced by insufficient stability rather than high compressive strength exceeding the material strength, especially for shells in UHPC.

The buckling resistance can be highly influenced by material nonlinearity, such as cracking and crushing, or by a combination of both geometry- and material non-linearity. This causes the bifurcation point, for which the loading condition corresponds to the critical load, never to be reached. So, besides being a 'from resistant structure' shell structures are also 'imperfection-sensitive structures'. To indicate the difference between the linear critical buckling load and the actual critical buckling load the knock-down factor is applied. The factor takes into account imperfections and geometrical and physical nonlinearities with influence to the failure mode. It is, because of multiple phenomena, coherent that the factor is experimentally determined. If little about these phenomena for a project is known the factor C = $\frac{1}{6}$ can be used.

For shells it may apply that several buckling modes are associated with the same linear critical load which is referred to as compound buckling behavior or multi-mode buckling. In general, thinner shells experience this compound buckling up to a higher degree than thicker shells.

The research has mainly focused on spherical shells of revolution and its mechanical behavior. The buckling capacity, an important design aspect, for these shells is positively influenced by the amount of curvature. The curvature of the shell depends on the ratio between the span and sagitta, or height, of the shell. However, a large amount of curvature leads to higher opening angles at the edges of the shell. This causes that the positive effect on buckling capacity can be counteracted by the possible existence of tension forces in circumferential direction in the base of the shell.

A shell will have a pure membrane behavior provided certain boundary requirements, loading conditions and geometrical configurations are satisfied. In order for membrane theory to be totally applicable, the forces and the displacements at the shell boundaries must be force-compatible and deformation-compatible with the true membrane behavior of the shell.

In practice, shell structures are regularly provided with an edge ring. The actual support displacement conditions impose constrains to such free boundary displacements and hence disturb the pure membrane field. In regions where the membrane theory does not hold bending field components are produced to compensate the inadequacies of the membrane field. The corresponding analysis to these phenomena describes the bending theory of thin elastic shells. the edge disturbance can be predicted for a length which is referred to as the influence length.

In multiple aspects of shell behavior it is concluded that a relative increase of the shell thickness at its supports can severely enhance the structural behavior. Compatibility requirements, such as local increase of moments, occur at the supports together with the largest meridional stress. Also, buckling is likely to occur at the shell edges.

To improve the inertia of the cross-section the principles of sandwich panels of rib-stiffened shells can be applied. Both principles can be referred to as composite shells. It was concluded that the disadvantage of sandwich panels, being more complex production and temperature differences in top and bottom layer, lead to the preference not to apply this principle. Rib-stiffening can severely increase the critical load of the whole shell structure in an economical, material efficient, manner. It holds that the distance between the ribs needs to be smaller than the buckling length of the unstiffened shell itself. Also, ribs and stiffeners are introduced to resist external concentrated loads since they distribute the load over a larger part of the shell surface. Furthermore the edges are an ideal location for connectors and neoprene gaskets to be placed.

For shell- as well as arch analysis and design, the dead load was to be an important component. It is therefore that the pressure line caused by the dead load is analyzed. The research which is done for finding an optimal geometry based on the dead load led to the consideration whether to design by a geometry based on a catenary line or to design a fully stressed dome. It was concluded that both principles will not be applied since for a span to sagitta ratio of 4 or higher the deviance between a catenary line and a circular line is small and an equal amount of curvature caused by a circular line is advantageous for reusability of formwork. Furthermore it was found that the principle for a fully stressed dome for UHPC would lead to a geometry with a negligible overall curvature, and will therefore not be applied since the negative effect on the bearing capacity and the aesthetical demands of a shell structure.

Part C. Computational modeling

The finite element method is a numerical analysis technique for obtaining approximate solutions to boundary value problems for engineering problems by solving partial differential equations. The analysis is particularly suited for solving partial differential equations on complex geometries and can be largely automated. This is particularly advantageous for structural design phases in which it is likely that the design is frequently adapted, as for this research.

The method is well suited to efficient computer implementation within the engineering industry. During the development of the finite element method the input of elements and mesh generation are severely simplified. Still, sufficient knowledge on the background of the applied software is often useful in practice.

For this research the software package Scia Engineer, an example of a wide-scale used commercial software package, is applied. The program combines a convenient interface and straight-forward utilization and is suitable for a design research where multiple models and parameters are compared. The software, which is primarily designed to serve civil engineers, is applied for many types of structural analysis as for stability, prestressing and dynamics calculation.

Part D. Analysis & design

Design aspects

The application of precast elements is chosen based on the production demands for UHPC and the possibility for a significant overall increased economic value of construction. Successful production is highly dependent on the applied method and the ability to repeatedly use the moulds. When the rate of repetition of the elements can be significant, so can the economical positive effect.

The production of thin elements requires the moulds to be manufactured with precise tolerances. From the experience of reference projects it is concluded that moulds of plate steel can be applied with high accurate precision of ±0.3mm. To improve the financial feasibility it is proposed to make use of a master mould which can be adapted for the production of various elements.

To oppose the disadvantages of prefabrication, being possible damage of elements during transport and construction, it is chosen to combine the principle of a rib-stiffened shell with the prefabrication of elements by the application of thick element edges which will ultimately form the ribs and stiffeners of the shell. This corresponds with the idea that for the production of elements it is beneficial if one type of element can be applied.

The geometry of the elements is influenced by the geometry of the shell. It is shown that the dimensions of the total structure have a significant influence on the curvature and sagitta of prefabricated elements.

As a consequence, the demands for the production of the curved elements will not be very demanding for the majority of elements. This has led to the consideration whether to apply flat elements. It is concluded that even small curvature has a significant effect on the mechanical behavior, and especially buckling load, of the shell. This effect can be explained by the fact that thin flat elements initially deflect considerably more, with respect to their thickness when subjected to vertical load. Given the little sagitta of the elements it is not expected that the choice for curved elements is disadvantageous for production as well as for efficient transport.

The principles which are further applied to the elements are based on the principles found in concrete linings of shield tunnels, where curved prefabricated elements are applied. The principles which are taken from tunnel engineering are the shape of element edges which make use of a dowel and socket system, which is advantageous for both the placing of the elements as well as minimizing possible negative effects of production deviances to unfavorable force introduction, and the incorporation of neoprene gaskets in the lining which will provide water-tightness. During the placement of the elements the gaskets can slide over each other, protecting the elements from colliding.

The utilization of precast elements requires a division of the total surface in multiple elements. The optimal configuration is proposed to be done by a geometrical straightforward composition called the 'ribbed dome', which makes use of more or less rectangular elements which mutually differ only slightly. This configuration is considered to be advantageous in consideration of element size, production, storage, transport and handling. With this configuration, which is not compatible for flat elements, the edges of the curved elements will form ribs and stiffeners in a logical pattern.

For the elements to become an integral structure the joint construction is vital and is therefore subjected to structural, physical and assembly demands. The connections should among other things provide fast and durable connections with sufficient strength to meet erection sequence and to maintain compression of the sealing gaskets. Multiple connection methods discussed are proven to be suitable connection methods for precast elements and are applicable for UHPC. The methods are compared with regard by these demands.

Two factors were decisive for the choice for local connections to be applied. Those are the fact that local force introduction is well feasible for UHPC and the fact that immediate connecting is favorable for a quick construction phase. The local force introduction in UHPC is well possible because of the fact that peak stresses can be distributed through the material because of the three-dimensional orientation of fiber reinforcement. Local

connectors demand local connection facilities, which ask for provisions to be installed during the production of the elements. These design for these provisions are based on common provision principles as bolt anchors.

Calculations on design aspects

For a span of 150m and a height of 37,5m it was concluded that the effect of the various load cases does not have an influence on the final required concrete thickness for both occurring maximum compression as tension stresses. The intended sagitta to span ratio, being 1 over 4, was concluded to be a feasible ratio, which is not disadvantageous for the meridional stress at the edges of the shell. It was confirmed that buckling under vertical loading is leading over compressive strength. The tensile strength was not found to be leading which provided the idea only to apply passive reinforcement where needed.

It is concluded that the characteristics of a prestressed edge ring have a significant effect on the ultimate buckling load of the shell. The required prestress force is determined by a model with hinged supports to ultimately exclude displacements in the SLS permanent load case. It was concluded that the buckling load for a shell with a full hinged support can be easily approached and is aspired for the design. It was found that not merely the application of the prestress within the edge ring is of influence; also the effect of the dimension of the ring is eminent. This is explained by the occurrence of inevitable deformations of the edge ring when the vertical load exceeds the SLS permanent load.

It is concluded that the distribution of material use from a solid shell to a rib stiffened shell has a major positive effect to the bearing capacity of the structure. Both the buckling load for constant vertical load and especially the safety against buckling for local effect, as was illustrated for redistributed snow, are significantly increased.
The results show that, for a shell span of 150m and a height of 37,5m and a proposed element geometry based on a maximum element size of 8x4m², a shell thickness of 35mm with ribs and stiffeners of 180mm x 60mm satisfies the structural demands.
Furthermore it is concluded that the buckling mode is influenced by the stiffening and has its buckling pattern at the top of the shell instead of the bottom, which is the case for unstiffened shells.

For an unstiffened shell it was found that an increase of the edge thickness by a total material usage increase of 3,4% an increase of buckling resistance of 15% can be achieved. This is accomplished if the meridional generator line (half of the shell span length) is thickened by 10% over approximately the first one third of its length. This is larger than the influence length, which means that the increase is positive for both the edge disturbances as well as for the buckling load. As for the rib stiffened shell it is concluded that the buckling capacity increase is accompanied by a shift of the buckling pattern from the bottom edge to the top of the shell. Since rib stiffened elements are applied the need for edge thickening has a low necessity.

The calculations for connection requirements result in the conclusion that the connections in both meridional and circumferential direction of the shell are subjected to tension which is the result of wind load. The tensile forces are determined for all connection locations at the ribs and stiffeners. It was determined that the connectors do not require a large cross-section when a standard steel quality is applied and the connections can be made by standard bolts. The ribs and stiffeners are enforced with single regular reinforcement bars to be certain that the tensile force are distributed among the elements and to improve the advantageous structural behavior of the combination of fiber reinforcement and passive reinforcement.

To connect the elements by a fast and non-labor-intensive method and to make sure the provisions to be taken in production phase are common the principle of bolt- and rebar-anchors is applied. By this connection the coupling is made between the continuous reinforcement bars together with connecting bolts. The largest reinforcement diameter is 32mm and the maximum diameter for the 8.8 bolt is 27mm. The connection will be compressed permanently and consequently provide water tight connection.

It is concluded that the large span shell can be executed with internal insulation. With this, the UHPC can be exposed to the environment, meaning the durability aspects of UHPC are exploited and that roof covering is not to be replaced in the future. The thermal response for the large span structure mainly demonstrates in deformations, which are relatively small. This is explained by the fact that the structure is allowed to deform. Only at the edge of the shell temperature stresses arise which do not to lead to major adjustments to the element dimensions.

The dynamic behavior of the shell is tested by finding the eigenfrequencies of the structure. The value for the eigenfrequency of the structure of 6.8 Hz is not expected to cause possible dynamic magnifying effects for it is not

expected for dynamic loads to occur with this frequency. The dynamic response is considered sufficient when the eigenfrequencies of the structure are larger than 5 Hz.

To ensure that the structure shows sufficient structural coherence the design is tested for bearing capacity and the effect to the force distribution in SLS for two load cases which involve openings in the shell surface. It is determined that the bearing capacity of the structures is hardly affected and the disturbed membrane behavior does not lead to difficulties. It is therefore concluded that the structure has sufficient structural coherence.

It is noted that the buckling results of every design aspect calculation expose the occurrence of the phenomenon of compound buckling. Although it is found that the design adjustments have a severe effect on the buckling load itself, none of the adjustments affect the deviances between multiple adjacent critical loads.

Shell construction

The realization of shell structures can, because of its geometry and mechanical behavior, be challenging. The application of formwork can be labor intensive and time consuming. However, since the application of formwork is found to be inevitable it is aspired to ease the construction phase and save on construction time.

Multiple construction possibilities are reflected by the relations to handling, erection and form control during construction. It was concluded that the idea to connect elements at ground level and subsequently place segments consisting of as many elements as possible per lift is positive for installment of the connections, form control and saving of number of hoist handlings. This implies that the requirement of scaffolding can be minimized to merely the locations providing stability during construction and connections which are to be made between segments.

Because of the slender design it was concluded that the crane capacity is sufficient to lift and place numerous elements per handling. Within the design study the shell is divided in 36 segments and can be constructed by just one mobile crane. The segment itself is, because of its slenderness, highly sensitive to deformations and is therefore proposed to be lifted, and later supported, by an assisting structure. An advantage of the geometric simple shape is that for a shell of revolution the supporting structure does not need to be adapted for different segments.

For the placement of the final segment it is reckoned that correct placement is hard to be guaranteed. It is proposed to work with an applied available space which is larger than the width of the segment, meaning that the final segment is to be smaller than other segments. The right placement of the key segment is guaranteed by the fact that the available space can be chosen and determined in consolation with the building contractor. The connection between the final segment and the first segment is a cast in/situ connection by a field-cast joint fill solution of Ductal.

After the top segment is placed the installment of the prestress within the edge ring is to be applied. After which the supports can be gradually removed per ring.

Overall conclusion

In the design study it is demonstrated that the combination of UHPC and large span shell structures has a high potential. The most advantageous points for the design are the overall savings on material use which leads to a lower total weight of the shell and decreases the demands for the foundation and edge ring as well as for transport and construction. It is proven that the shell can be built with making use of the durability aspects of UHPC which causes the expected lifespan to be higher than 50 years, even 100 years.

Together with these aspects it is believed that the main profit of the application of UHPC within large span shell structures can be made within the construction phase. The described construction method makes use of the advantages of UHPC by making use of the ease of bolted connections which are fast to connect and make use of the force distribution ability of fiber reinforcement. Also, the light-weight structure can be handled and placed easily by relatively few handlings.

Based on the results and conclusions of the research it can be concluded that the combination of UHPC and large span shell structures is a very promising concept for the future.

Part E. Case study

The project named 'Fiere Terp', a preliminary design for a shell structure, was the motive for the research within this thesis and served as a problem definition as well as guideline for the applied dimensions of a large span shell structure. The design is handled as a case study for which the design recommendations are applied.

The design for Fiere Terp is discussed and improvements are proposed by deliberation of multiple variants and preferences based on the earlier research. It was concluded that the design can be mostly improved when the greater part of the geometry is based on a regular shape in combination with sufficient curvature. The design proposal is too large extend a spherical shell of revolution which is completed by an anticlastic part. This geometry shows a high resemblance to the initial design and well functioning shell behavior. Based on the results for a large span shell structure in earlier research it is declared that the design for this large span shell, with different geometry, is highly feasible as well.

13. Recommendations

In this paragraph a number of recommendations for further analysis are proposed. The recommendations reported in the following are ordered corresponding to their subject.

<u>UHPC</u>
During the research the choice was made to apply the characteristics of the commercial product Ductal BS1000. The fact that the applied UHPC is used in a large volume means that optimization of UHPC specific for the project depended purposes is expected to be useful in practice. The goal of the optimization can be to determine what mechanical characteristics are most demanded and for what mixture of components these characteristics can be achieved combined with a possible reduction of costs.

For the increase of the application of UHPC it is advised that a design code is developed and more specific tests are executed for these types of concretes.

<u>Thin concrete shells</u>
The knock-down factor which is used within the research is based on experimental research. This experimental research is executed on different shell geometries, mainly on cylinders. Especially since the dimensions of the final design are very slender it is recommended that the factor is determined for shells with a comparable geometry.

Up to thus far no non-linear terms are taken into account in the calculation. The results of these calculations are of interest when the structural design is finalized. However, the results of the linear calculation show that the structure performs properly and displacements and deformations will be small, therefore nonlinear effects are expected to be negligible.

More research to the structural behavior and the stability of prefabricated concrete shell structures and the influence of the connections has to be performed.

<u>Joint design</u>
Irrespective of the method to be applied, it is considered to be a necessity to elaborately test the connections and the force distribution through the element . To guaranty satisfactory behavior of the joints the connections should be manufactured and experimentally tested in a full-scale model. It should be carefully investigated what the influence of the increased local stresses around the joint will be.

<u>Overall design</u>
A good method to check the real mechanical behavior of the shell in UHPC compared to the FEM model is to create and test a physical scale model. This model can give an insight in the realistic behavior of the dome for both bearing capacity as well as forces due to wind-loads.

Accidental loads, caused by for instance explosions or collisions are neglected within the research but must be taken into account for definitive design.

<u>Construction</u>
For both the production of the elements as well as the linking of elements regulations should be composed describing the maximum deviances.

The use of scaffolding during construction can be optimized. Of course the structure needs to be stable during construction, but the amount of scaffolding might be locally decreased since the stability of the structure gains after a number of segments are installed.

In practice the application of a site factory might be more beneficial for the construction stage. This consideration will be mostly based on financial profit. When a site factory is applied the location of ribs and stiffeners can be independent chosen of the edges of elements, meaning that another configuration is more optimal.

<u>Support conditions</u>
The amount of required prestress force has been investigated in the thesis. The force is been assumed equally distributed equally throughout the ring. In practice this application is to be investigated if this schematization can be approached.

Also, the shell foundation might be subjected to settlement differences. A settlement difference can induce supplementary stresses in the dome and decrease the load bearing capacity.

<u>Financial feasibility</u>
For a project to be actually built the financial feasibility is of high interest. An extensive research is compulsory on this aspect. The feasibility of the project should take all aspects for UHPC into consideration, including the impressive durability aspects, savings on foundation, transport and construction stage.

Appendices

Appendix 1.
Personal and graduation committee information

Personal Information

Name: Richard Niels ter Maten
Student Number: 1211641
Date of Birth: August 11, 1986
Home Address: Hoveniersstraat 34, 3031 PD Rotterdam
Telephone: +31 6 41101868
E-mail: R.N.terMaten@student.tudelft.nl

Work location: Zonneveld Ingenieurs B.V.
                             Delftseplein 27
                             3013 AA Rotterdam

Master thesis committee

Prof.dr.ir. J.C. Walraven
Concrete Structures   TU Delft
J.C.Walraven@tudelft.nl

Ing. J. van der Windt
Managing Director   Zonneveld Ingenieurs B.V.
Windt@zonneveld.com

Ir. S. Pasterkamp
Structural and Building Engineering   TU Delft
S.Pasterkamp@tudelft.nl

Dr.ir. P.C.J. Hoogenboom
Structural Mechanics   TU Delft
P.C.J.Hoogenboom@tudelft.nl

Dr.ir. S. Grünewald
Concrete Structures   TU Delft / Hurks Beton
S.Grunewald@tudelft.nl

Graduation coordinator
Master Track Building Engineering:
Ir. K.C. Terwel
K.C.Terwel@tudelft.nl

Appendix 2. References

Building codes:

[1]   French UHPC Interim Recommendations (SETRA-AFGC, 2002)

[2]   German UHPC Recommendations (DAfStb Deutscher Ausschuss für Stahlbeton)

[3]   European Committee for Standardization (2002)
           EN 1990: Basis of structural design
           EN 1991: (Eurocode 1) Actions on structures
           EN 1992: (Eurocode 2) Design of concrete structures

Literature on (Ultra High Performance) Concrete:

From:
Ultra High Performance Concrete (UHPC) Heft 3 (2004)
Universität Kassel

[4]   A. Korpa; R. Trettin
        The use of synthetic colloidal silica dispersions for making HPC and UHPC systems, preliminary comparison results between colloidal silica dispersions and silica fumes (SF)

[5]   K. Jayakumar *Role of Silica fume Concrete in Concrete Technology*

[6]   J. Ma; M. Orgass; F. Dehn; D. Schmidt; N. V. Tue
        Comparative Investigations on Ultra-High Performance Concrete with and without Coarse Aggregates

[7]   K. van Breugel; Y. Guang
        Analyses of hydration processes and microstructural development of UHPC through numerical simulation

[8]   K. Droll *Influence of additions on ultra high performance concretes – grain size optimisation*

[9]   T. Teichmann; M. Schmidt
        Influence of the packing density of fine particles on structure, strength and durability of UHPC

[10]   E. Fehling; K. Bunje; T. Leutbecher *Design relevant properties of hardened UHPC*

[11]   J. Hegger; D. Tuchlinkski; B. Kommer *Bond Anchorage Behavior and Shear Capacity of UHPC Beams*

[12]   E. S. Lappa; C. R. Braam; J. C. Walraven *Static and fatigue bending tests of UHPC*

[13]   M. Teutsch; J. Grunert *Bending design of steel-fibre-strengthened UHPC*

[14]   J. Jungwirth; A. Muttoni *Structural Behavior of Tension Members in UHPC*

[15]   M. Orgass; Y. Klug *Fibre Reinforced Ultra-High Strength Concretes*

[16]   A. Lichtenfels *Ultra High Performance Concrete for shells*

[17]   G. Zimmermann; T. Teichmann *Membrane Concrete Grid Shells – UHPC Grid Shells*

[18]   J.C. Walraven *Designing with Ultra High Performance Concrete: Basics. Potential and perspectives*

From:
Ultra High Performance Concrete (UHPC) Heft 10 (2008)
Universität Kassel

[19]   J.C. Walraven *On the way to design recommendations for UHPFRC*

[20]   I. Burkart; H.S. Muller *Creep and shrinkage characteristics of UHPC*

[21]   M. Curbach; K. Speck *Ultra High Performance Concrete under Biaxial Compression*

[22]   T. Leutbecher; E. Fehling *Crack Formation and Tensile behaviour of UHPC Reinforced with a combination of Rebars and Fibres* (2004)

[23]   J. Hegger; S. Rauscher *UHPC in Composite Construction*

[24]   E. Fehling; T. Leutbecher; F.K. Roder; S. Sturwald *Structural behavior of UHPC under biaxial loading*

[25]   B. Aarup *Compact Reinforced Composite (CRC) - Structural Applications of UHPFRC*

From:
High Strength / High Performance Concrete (Leipzig, 2002)
Edited by: G. Konig. F. Dehn, T. Faust

[27]   J.C. Walraven *From High Strength, through High Performance, to Defined Performance*

[28]   U. Montag; M. Andres; R. Harte; W. Kratzig *Cooling Tower Shell made of High Performance Concrete*

[29]   I. Jovanovic; A. Paatsch; A. Durukal *Ductal: a New Generation of Ultra High Performance Fibre Reinforced Concrete*

[30]   M. Schmidt; E. Fehling; T. Teichmann; K. Bunje *Durability of Ultra High Performance Concrete*

Other sources:

[31]   N. Kaptijn *Toekomstige ontwikkelingen van zeer-hogesterktebeton (Cement, 2002)*

[32]   Reinhardt, H.W. *Beton als constructiemateriaal; eigenschappen en duurzaamheid (1985, herzien: 2000)*

[33]   Walraven, J.C. *Gewapend beton. Delft: Delft University of Technology (2002)*

[34]   Walraven, J.C. *Prestressed Concrete (2006)*

[35]   Walraven, J.C. *Ultra-hogesterktebeton: een materiaal in ontwikkeling. (Cement, 2006)*

[36]   Walraven, J.C. *Van exotisch naar volwassen product. (Cement, 2011)*

Literature on shell structures:

[37]   Borgart, A. *The relationship between form and force of curved surfaces: A graphical solution* (2007)

[38]   Borgart, A. *The relationship between form and force of curved surfaces: The Rain Flow analysis* (2007)

[39]   Elferink, B. *De optimale koepel* (2010)

[40]   Hoefakker, J.H. and J. Blaauwendraad, J. *Theory of Shells* (2003)

[41]   Hoogenboom, P. *Lectures on Shell Analysis, Theory and Application, TU Delft*

[42]   Farshad, M. *Design and Analysis of Shell Structures* (1992)

[43]   Kollar, L. and Dulacska, E. *Buckling of Shells for Engineers* (1984)

[44]   Koten, H van, *Structural Analysis of Shells* (1993)

[45]   Medwadowski, S.J. and Popov, E.P. *Concrete Shell Buckling* (1981)

[46]   Medwadowski, S.J. *Concrete Thin Shells* (1971)

[47]   Samuelson, L; Eggwertz, S. *Shell Stability Handbook* (1992)

[48]   Timoshenko, S. and Woinowsky-Krieger, S. *Theory of Plates and Shells* (1959)

[49]   Timoshenko, S. and Young, D.H. *Theory of Structures* (1945)

[50]   Reader Structural *Design: Special Structures*. Delft: Delft University of Technology.

Finite Element Method & Software:

[51]   Manual Scia Engineer
                 Stability Calculations
                 Workshop Concrete
                 Workshop Prestressing
                 Workshop Dynamics

[52]   Thompson, E. *Introduction to the finite element method: theory, programming & applications* (2005)

[53]   Huebner, K. H. *Meet the finite element method*

[54]   Vree, J.H.P. de. *Eindige Elementen Methode* (2002). Eindhoven University of Technology.

Reference projects:

[55]   PCI Journal *First Use of UHPFRC in Thin Precast Concrete Roof Shell for Canadian LRT Station* (2005)

[56]   Riciotti, R. *Ductal® Pont du Diable footbridge, France*(2008)

[57]   Reichel, Freytag, Sparowitz *Road Bridge WILD - UHPFRC for a segmental arch structure* (2009)

[58]   H. Wapperom *Boogbrug in UHSB* (Cement, 2010)

[59]   Riciotti, R. *Le Stade Jean Bouin* (2009)

[60]   F. Toutlemonde *HPC Applications in France* (2007)

[61]   E. Fehling; K. Bunje *Ultra High Performance Composite Bridge across the River Fulda in Kassel* (2004)

[62]   De Ingenieur Creatief met beton, *Folly in Hilversum laat vorderingen constructietechniek zien* (2005)

[63]   V. Perry *The world's first long-span roof constructed in Ductal (2003)*

[63]   J. Resplendino *First recommendations for UHPC and examples of application* (2004)

[64]   M. Rebentrost, G. Wight *Experience and Applications of UHPC in Asia* (2008)

[65]   Perry, Scalzo, Weiss *Innovative Field Cast UHPC Joints for Precast Deck Panel Bridge Superstructures*

[66]   Hikari, Koichi *The first highway bridge applying UHSFRC in Japan*

[66]   Tekeste Teshome Gebregziabhier *Durability problems of 20th century reinforced concrete heritage structures and their restorations* (2008)

[67]   Thierry Thibaux *UHPFRC prestressed beams as an alternative to composite steel-concrete decks: The example of Pinel Bridge* (France)

[68]   Domingo A., Lázaro C., Serna P. Construction of *JChypar*, a steel fiber reinforced concrete thin shell structure. Proceedings of the IASS Symposium 2001

Further sources:

[69]   The British Tunnelling Society and The Institution of Civil Engineers *Tunnel lining design guide* (2004)

[70]   C.B.M. Blom *Design philosophy of concrete linings for tunnels in soft soils* (2002)

[71]   A.C. vd Linden   *Building physics lectures*

[72]   TBM Method   www.p3planningengineer.com

[73]   Fiere Terp   www.defiereterp.nl

[74]   Lafarge   www.lafarge.com

[75]   BINI Shells   www.binishells.com

[76]   Structurae   en.structurae.de

[77]   Monolithic   www.monolithic.com

[78]   Mammoet   www.mammoet.com

[79]   Norm-teq   www.norm-teq.nl

Appendix 3.
Reference projects UHPC

This appendix represents a number of reference projects in which the construction material Ultra High Performance Concrete (UHPC) is applied in practice. A significant amount of realized projects in UHPC are in the field of bridge structures; being new bridges as well as renovation of bridge decks. Other projects examples are the roofing and façade of a stadium and clinker silo.

Ap3.1.   LRT Station, shells in UHPFRC, Canada

Ap3.2.   The Angels bridge, France

Ap3.3.   Road Bridge WILD - UHPFRC for a segmental arch structure, France

Ap3.4.   Stadium Le Stade Jean Bouin; France

Ap3.5.   Millau Tollgate; France

Ap3.6.   Bridge across River Fulda (Gärtnerplatzbrücke) Kassel, Germany

Ap3.7.   Folly in UHPC; double curved, the Netherlands

Ap3.8.   Clinker Silo; Illinois; USA

Ap3.9.   Sherbrooke Pedestrian bridge, Canada

Ap3.10. Sunyudo Footbridge: Seoul, Korea

Ap3.11. Innovative Field Cast UHPC Joints for Precast Bridge Systems

Ap3.1. LRT Station, shells in UHPFRC, Canada

A very thin architectural shell was selected for the roof structure of the new Shawnessy Light Rail Transit (LRT) Station in Calgary, Alberta, Canada. Twenty-four unique, thin-shelled precast concrete canopies measuring 5 x 6 m and just 20 mm thick, supported on single columns, provide an attractive light-filled shelter for commuters. This unprecedented structure was made possible with the design flexibility of a new generation of ultra-high performance fiber reinforced concrete (UHPFRC) materials that offer a combination of superior technical characteristics including ductility, strength, and durability without using mild reinforcing steel, while providing highly moldable products with an excellent surface quality. The UHPFRC compressive strength was 150 MPa and flexural strength was 18 MPa (2600 psi). This article reveals the many, advantages of this innovative technology and presents the material's mechanical properties as well as the challenges faced in structural design, manufacturing and erection.

Fig.Ap3.1 .   The LRT station   [Courtesy of Tucker Photo]

Precast concrete solutions can provide superior finishes, tight construction tolerances, speed of construction, lower maintenance requirements, and increased economic value to these transit projects. However, this new UHPFRC technology can challenge existing paradigms surrounding precast concrete systems, as evidenced in the LRT station project that is the subject of this article.

The Shawnessy LRT Station, constructed in 2004 in Calgary, Alberta, Canada, is an excellent example of the successful melding of emerging technology, inventive design, and manufacturing savvy. Originally conceived in a steel design, the canopies were changed early in the design process to a precast concrete solution for economic, durability and aesthetic reasons.

The canopies are bolted together to create a roof that is about 76 m wide x 5 m wide, which covers most of each platform. For this project, the material's compressive strength was 150 MPa with a flexural strength of 18 MPa.

With a carbonation depth penetration of < 0.5 mm there is almost no carbonation or penetration of chlorides or sulphides and the material possesses a high resistance to acid attack. The superior durability characteristics of the product are due to a combination of fine powders, selected for their chemical reactivity and relative grain size, with a maximum size of 0.5 mm. The net effect of this mix design is maximum component compactness and a small, disconnected pore structure.

Following thermal treatment at 60" C for 72 hours, the material becomes dimensionally stable, with a creep coefficient of 0.2 and no long-term shrinkage, thus making it very suitable for precast/prestressed concrete applications. The use of this material for construction is simplified through the elimination of mild reinforcing steel and the ability of the material to be virtually self- placing or dry-cast. The following list of properties is an example of the range of material characteristics for a formulation with organic fibers.

Strength
Compressive strength:	120 to 150 MPa
Flexural strength:	15 to 25 MPa
Modulus of elasticity. E:	45 to 50 GPa

Durability
Freeze/thaw (after 300 cycles):	2 percent
Salt-scaling (loss of residue):	< 60 g/m²
Abrasion (relative volume loss index):	1.7
Oxygen permeability:	< to^{-20} m²
Cl permeability (total load):	< to
Carbonation depth:	< 0.5 mm

Materials were supplied to the precaster, Lafarge Canada Inc., of Calgary, Alberta, in a three-component premix. Powders were pre-blended in bulk-bags at a facility in Kansas. Chryso, of France, manufactured the superplasticizer, and Kuraray America Inc., of Japan, manufactured the organic fibers.
Currently, this malarial is only used in precast/prestressed concrete applications. Due to the mixing requirements, casting techniques, and shrinkage characteristics during setting and curing, further development work is required prior to its use in cast-in-place applications.

After looking at the architectural conceptual renderings of the Shawnessy LRT Station, Lafarge proposed the construction of partial-dome-like canopies out of a new UHPFRC material. Reinforced with polyvinyl alcohol fibers and no mild steel reinforcement, this novel material would be shaped into a thin shell only 20 mm (3/4 in.) thick. Since this would be the first use of this malarial for shell structures, the owner, the City of Calgary, requested that a full-sized prototype canopy be sent to the University of Calgary's Centre for Innovative Technology (CCIT) for extensive testing under the design dead and live loads for snow and wind uplift, as well as a determination of The prototype's response to dynamic loading. Slantec Architecture Lld's (formerly CPV Group LId.) Structural Engineering Department carried out a finite element model (FEM) analysis of the structure under load combinations of dead load, wind, snow, and earthquake to determine whether the structure could be physically built.

In addition to the normal elastic analysis with FEM, a post-cracking elastoplastic analysis was performed, a necessary design check for materials that exhibit a pseudo-ductile behavior. The elastoplastic analysis provides member stress values after a stress redistribution due to plastic deformations When compared with sophisticated computer modeled calculations, the data confirmed that the canopy not only surpassed the less criterion of maximum allowable crack width opening of 0.3 mm, but it carried full -factored live and dead loads without cracking.

Innovative Product ion Techniques UHPFRC is a new material with unique properties that are different from any other existing product. Manufacturing precast products using this material presented the industry with new challenges and opportunities for the precaster, Lafarge Canada Inc. of Calgary, Alberta. Recognizing that old methods were not adequate for the new requisites of UHPFRC production, a fundamental change in the conventional manufacturing process was required. A precaster team of individuals with expertise in sales, engineering, production and erection was established to identify the challenges posed by this new materials technology and to create the novel solutions necessary for successful production of UHPFRC. The Lafarge precast team identified six major questions, or manufacturing challenges:

1. Conventional concrete belching and mixing methods would not work because of the extreme accuracy required for measurement of ingredients, the requirement for high shear energy mixing, and the need to dissipate entrapped air in the plastic mix. What modifications to traditional batching and mixing methods are required to successfully produce UHPFRC?

2. Because of the material's high viscosity, conventional concrete finishing techniques could not be used. Therefore, casting the material into a horizontal form and finishing the top surface was not possible. What manufacturing methods are required to produce precast concrete components with a consistent smooth surface?

3. The material properties, particularly with a flexural strength of 21 to 48 MPa (3000 to 7000 psi), are influenced by the fiber orientation within the material's matrix. What precast production methods will maximize the efficiencies of fiber orientation during placement?

4. UHPFRC will shrink Twice as much as normal concrete, in part because of the particle size distribution within the malarial's matrix, which by design eliminates the formation of an aggregate skeleton structure that restrains shrinkage in conventional concrete. What processes will allow unrestrained shrinkage to occur during the initial set of the material - while maintaining the structural integrity of the UHPFRC - when the fresh concrete is still in a form that is essentially closed on all sides?

5. Because the 24 canopy elements were only 20 mm (V4 in.) thick and constructed with intersecting curves, it would be necessary to achieve precise tolerances to form the complex geometric shape. In addition, final product finish quality as well as material placement must be taken into account. What quality control methods would have to the implemented to ensure success with such complex shapes?

6. Since the UHPFRC needed to be placed in the form within 20 minutes from the time the product was mixed, placement by pumping appeared to have potential. What pumping methods would efficiently propel a viscous material with very high fiber content?

To address these challenges, the precasting beam held a series of brainstorming sessions to general viable solutions. Concepts were closely evaluated and tested against the existing global knowledge database on UHPFRC. A research and development (R& D) program was undertaken to provide answers to unprecedented manufacturing challenges that were not answered by any prior experience or research. At first, some of the production problems appeared to be minor, for example. Finding the best combination of mold surface and release agents. However, when the final solution turned out to be an epoxy coating on steel combined with bees wax as the dispersing agent. It became apparent that striking upon workable solutions were not always as simple as first imagined.

Batching and Mixing

The key to producing UHPFRC is very accurate proportion control of ingredients and temperature. A high shear mixer is required to disperse water only the cement panicles without healing the mix through kinetic energy generated by the mixing process. It is necessary, moreover, to control the temperature of
The raw ingredients because with such precise mixture proportioning required to produce UHPFRC, the amount of water or ice that can be added is insufficient to affect a significant temperature change.
All ingredients including the water had to be accurately weighed. There is a distinctive power consumption curve that a mixer demonstrates when mixing UHPFRC: the power consumption is initially low as the dry ingredients are blended and increases substantially when the water is added and dispersed.
The power demand then drops as the superplasticizer makes effect. This power consumption curve was first identified during laboratory testing and was measured in production for control purposes to determine the mixing time and when to introduce fibers.

The temperature of the mix was measured using a laser targeted portable infrared thermometer, which gave instantaneous readings from a safe distance. Because the process of high speed mixing generates entrapped air into the mix that can lead to a weaker matrix and poor surface finish, it is necessary to slow the mixer at the end of the mix cycle to allow the entrapped air to escape.

Forming

Successful execution of the project depends upon design of the molds and procedures developed to use them. Traditional hand screeding and finishing of UHPFRC is not possible because of the high viscosity and high fiber content of the plastic mix. The material also has no internal shear in the plastic stale and behaves similar to self-consolidating concrete. This means that in order to manufacture the components with the desired surface finish, all exposed surfaces have to he formed. The unusually slender 20 mm (3/4in.) thick, canopies required the forms to be designed to limit live load deflections and to be manufactured to precise tolerances. This daunting

specification can be exemplified by realizing that only y a 3 mm (1/8 in.) form deflection (common in typical precast production) can increase the product thickness by almost 20 percent. Clearly, mold construction and deflections are of utmost importance. The canopy forms were made of plate steel. A THREE-dimensional model of the casting and form was generated by a computer model.
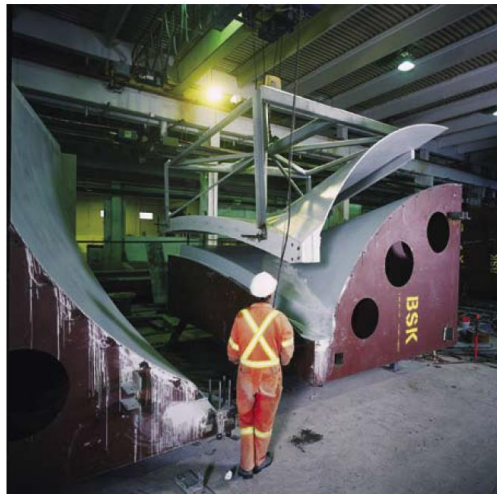

Fig.Ap3.2.   Demolding of precast canopy element   [Courtesy of Tucker Photo]

Product Handling and Jigging

A compile canopy on The Shawnessy project consists of right and left castings joined together with a bolted seam at the apex of the curve and a beam tension tie across the opening at the base. Once assembled, the unit is structurally stable. However, prior to assembly, the individual elements are very sensitive to the forces that occur during handling and storage. Lift hooks and lifting inserts were eliminated from the precast concrete components. Instead, handling frames were fabricated with pins that would engage bolt holes in the product. These holes served two purposes: initial handling and openings for boll locations needed in final assembly. The frames were designed to accommodate vertical lifting forces without introducing any unnecessary stresses into the pieces. An assembly jig was used to accurately locate the individual casting halves and allow them to be rolled together. The interfacing sections were "buttered" with epoxy and the stainless steel connection bolts were lightened al the apex of the curve and on the beam tension lie at the base to complete the assembly.

Fig.Ap3.3.   Crane set of canopy   [Courtesy of Tucker Photo]

Since the architect originally conceived the canopies to be made of steel, the actual UHPFRC canopies have demonstrated that thin-shelled systems can be produced with similar thicknesses to steel, but with much greater advantages.

Ap3.2.   The Angel's bridge; La passerelle des Anges

Based on original article: 'La passerelle des Anges 'from BFUP 2009 / UHPFRC 2009 publications
Year: 2009
Location: Hérault, France
Concrete: Ductal FM
Connections: Post-tensioning; Epoxy binding

With 67.5 m span and a 1.80 m height this footbridge makes a new structural performance. This design also considered significant innovations in terms of environmental impact, process constructive and project economics. Located at the exit of the gorges of the Herault, great classified site UNESCO World Heritage site, it is an essential part of the footpath constructed. The bridge consists of 15 precast segments Ductal, placed on hangers and assembled by preload. After recalling the context and studies, the proposed presentation illustrates each phase of construction: mold making, casting segments factory installation hanger, establishment and adjustment of segments, implementation of the preload and damping.

1. Overview

The environment of the project suggests a span at once without intermediate support, that is to say a crossing 70 m at one time, and minimizing its visual impact in elevation, So without bow or shrouds. The gateway is thus formed of two parallel beams forming railing. The material of the bridge, Ductal FM family of fiber reinforced, ultra-high Performance (UHPFRC), is especially chosen with the aim to solve elegantly all these technical and environmental constraints. In general, the construction of this bridge is an opportunity to develop technologies optimized to fit quietly in this wild site:

- At the structural level: the UHPFRC allows its highest compressive strength to implement prestressing is very important. The two beams are optimized using a bone-shaped to limit the impact on the landscape of the bridge with a twinge ultrahigh (total height 1.80 m, 67.5 m range). A width of 1.88 m for pedestrians and cyclists, is then released between the two beams
- In processes of construction: the entire structure is prefabricated. The bridge is performed following 15 segments of 4.60 m monolithic prefabricated from a single mold. The segments are then transported and assembled by post-tensioning on a hanger. The yard is shorter, simpler, with an impact on site limited to the minimum security conditions improved in shipyard
- In terms of sustainability: the mechanical characteristics of UHPFRC, including their exceptional resistance to chemical attack, allow to consider reduced maintenance and maximum durability of the structure, unlike the works conventional structural steel or wood
- In terms of overall environmental impact: UHPFRC sections are both very thin and have a high mechanical efficiency (100% of the material is structural). This use of concrete material is characterized by small amounts of material which are also associated with industrial production cycles short and simple (compared to steel). The frame consumes very little primary energy, is responsible for low emissions polluting air and water, and do not participate in the depletion of natural resources
- At the cost and time: studies, prefabrication, construction methods, and implementation of prestressing is very important, allow control of the deadlines: 3 months of prefabrication, 1 month of site preparation, one week of installation and adjustment, 1 dismantling week, less than two months on site. Similarly, costs (980 000 €) become competitive with wood and metal solutions, with an additional cost almost zero maintenance (no repair systems to protect against corrosion etc...)

Fig.Ap3.4.   Overview of Angel's bridge

The technological challenges presented are detailed in the following paragraphs. They relate including:

- the geometric definition of parts, molds and prestressing systems
- the nature of the materials used and their experimental validation
- study the oscillation behavior, including aero-elastic
- site preparation, methods of installation, adjustment and prestressing
- operation tests

Ductal FM Gray, formulation 3GM2.0
Supplier: Lafarge Cements

Mechanical:
Compressive strength: 180 MPa

Tensile strength: 7.5 MPa
Young's modulus 50 000 MPa

Durability: Density: 2.5
Capillary porosity: 0.5 to 0.7%
Porosity: 1.9 to 2.8%

2. Studies of execution

Studies and implementation of methods have been conducted internally by the technical department Freyssinet France. The calculation of a prestressed bridge is no longer a novelty, but the slenderness made possible by the outstanding qualities of Ductal generates several problems:

-        The implementation of prestressing ducts and anchorages in sections as small.
-        The small thickness of beam web, generating the risk of spills top chord compression.
-        The flexibility of the structure, with risks to resonate by pedestrians and wind.
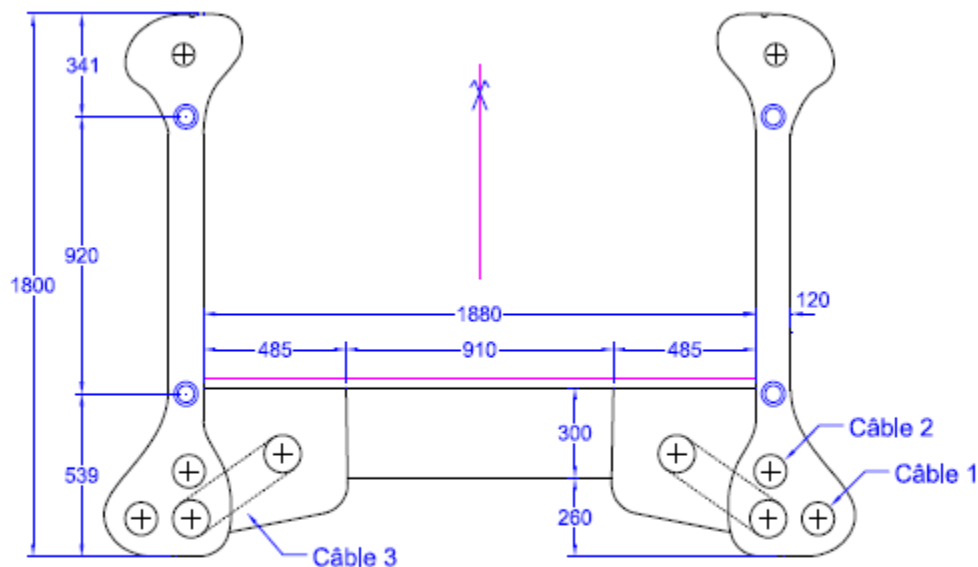
Fig.Ap3.5.   Section with main dimensions

The first point, the small size of the sections, is at the three tensioning ducts at the lower chord of only 0.10 m² of section. With these requirements, the coating has been reduced to a radius of sheath only. This reduction is justified by the following arguments:

- Using protected strands, so protective demands of the coating is reduced.
- Use of Ductal, thus reduced risk of cracking due to the presence of fibers metal.

The second point considers the upper chord, which is conventional in the walkways structural steel beams that form railings. The third point, flexible structure, can suppress any problem comfort of pedestrians with a fundamental mode of vertical bending only at 0.85 Hertz, and first harmonic 4 x 0, 85 = 3.4 Hz, any risk of resonance with the passage of pedestrians (an excitation frequency of about 2Hz) was excluded. For cons, the phenomena of vortex shedding and galloping thus became problematic. The following paragraph returns on these phenomena.

Finally, the bracing of the structure has proved more problematic than what had been expected in the first analysis. Indeed, the deck can be poured at the same time as the segments. Transmission effort crosswind can therefore be secured without mechanical connection decking, connecting difficult to achieve in the thickness of 4cm of the decking. The problem was eventually solved by integrating the underside of decking ribs forming crosses.

Fig.Ap3.6.   Detail of a cross on the underside of deck
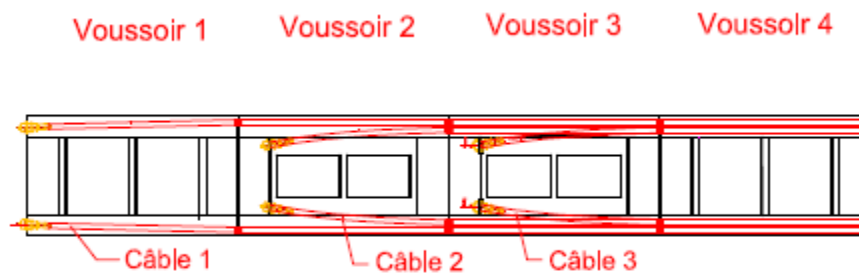
Fig.Ap3.7.   Wiring, top view

3. Aero-elastic behavior.

The vibration behavior of the structure was subjected to two tests:
- Analysis of the vibration response of the bridge under the action of pedestrians, according to Methodological guide SETRA
- Analysis of aero-elastic behavior, vortex shedding and instability gallop, from Eurocode 1

The very high slenderness of structure has the corollary that it is a dynamic behavior necessary to analyze in detail. The eigenmodes, from modal analysis (analytical calculations and finite element calculations) are:

- First mode, vertical longitudinal bending, 0.85 Hz
- Second mode, horizontal longitudinal bending, 1.85 Hz
- Third mode, longitudinal torsion, 2 Hz
- Fourth mode, vertical longitudinal bending, 3.4 Hz

This modal behavior has to be placed in levels of comfort for pedestrians tried satisfactory, with risks of setting low or negligible following resonance modes and low accelerations. In contrast, the transverse wind showed, according to the Eurocode approach, risk of instability for moderate wind speeds, and thus with probability stresses sustained significant. The Eurocode approach is strongly dependent coefficients, with values available that represent too distant the actual behavior of the bridge.

A wind tunnel study (CSTB Nantes - M. Grillaut team) was performed. Experimental results and theoretical calculations have shown similar results when the behavior of the bridge, and in particular on the efficiency of a system of tuned mass dampers. These elements were then studied, performed and paid by the Company with

Michael GERB Maillard. At the end of construction, dynamic loading tests have confirmed the theoretical calculations and wind tunnel simulations.

4. Precast segments and decking

4.1. Vaults
4.1.1. Mould

A steel mold for casting upside down is applied. This solution allowed to obtain a perfect surface which was very important for aesthetics of the bridge. The mold is modular and thus allows produce the 15 elements of the bridge. The mold was made with utmost precision. The precision was less than 0.2mm at the bottom and 0.3mm in dimension.

Fig.Ap3.8.   View of the steel mould

The choice to use machined mold rather than pouring more classic was for the ability to run the first 11 segments, then the 4 segments with anchor cables, with one modification operation of the mold, instead of 4 with segments cast of "in order".

4.1.2. Preparation of Ductal

The segments were made at the factory Bonna Sabla Vendargues of the mixer which has been validated collaboration with Lafarge concretes conveniences and prototyping of similar items. As with all cases of Ductal FM, a test of convenience and control plan very strict has been established to validate each stage of manufacture, including, to ensure non-segregation of the fibers.
All the material characterization tests were also done in collaboration with the Central Laboratory of Lafarge, which operates in fact an external control.

4.1.3. Casting

The preparation of the concrete segments was completed in five successive batches. The method of casting has been developed in collaboration with technicians including Lafarge for the proper combination of different materials and the fiber orientation according to material flow.

4.1.4.Finishing / curing

At the end of casting a cure has been applied. Parallel samples were taken during manufacture and were placed in identical conditions of treatment of the product in order to perform compression tests before release and confirm it.

4.1.5. Demoulding

The demoulding was carried out by "peeling" of the mold, the product remains in place. After stripping, the product was transported to the heat treatment station. The product has received heat treatment while maintaining temperature at 90 ° for 48 hours in saturated atmosphere. The energy used was live steam-driven regulation. The handling of the products was carried out using inserts placed at points calculated to operate handling at young age. The product after this heat treatment is stored. Note that all inserts are stainless to avoid subjection to further protection.

5. Implementation

5.1. Arch

The site commanded respect from the vast vegetation adjacent to the bridge, rocky deposits present on the bottom of the trough and endemic species of frogs that had been observed in the creek. Shoring have been laid on transverse bars in prefabricated reinforced concrete to reduce stress on the ground. In the central part, height of the bridge is 10m.

Fig.Ap3.9.   View of the arch during erection

5.2. Installation and adjustment of the segments

Two girders were arranged being HEB160 forks in shoring heads. The segments were placed on sectors with a 300t crane. Necessary adjustments to the alignment of transverse and vertical elements were made using screws included with hooves. This adjustment was carried out under continuous geometric control to 1/10th of a millimeter. The bonding was provided by an epoxy adhesive on manually setting up the concrete beams.

Fig.Ap3.10.   View of the installation of a cowling

5.3. Adjustment, interim clamping.

The elements were brought together and tightened using annular cylinders and bars. A first clamp is made to ensure a good fit of the segments together. The parts are then separated, then glued tightened and put into pressure.

Fig.Ap3.11.   View of the interim clamping system

5.4. Threading injection tensioning.

The tendons were wrapped protected and injected in a conventional manner. Indeed, the work period (early July) combined with the black color of the segments generated strong thermal variations during the day, so that the seals were opened in lower in the afternoon under the effect of the gradient. The injection is not possible in these conditions, the two cables, high and low, ranging from one end to the other gateway has been blood before injection, to close seams.

5.5. Rests on support

After tensioning of 37 strands per beam (out of 49 total), the gateway is capable of resume its own weight and the extra yard. After adjustment level using jacks, we proceeded to matting between supports and neoprene underside of a beam, then bridge has been placed on its final support. The remaining strands were then tensioned.

5.6. Implementation of the tuned mass dampers

Both absorbers are located on both sides. They are of course implemented before laying decking. The frequency and rate damping of the structure are measured in situ by the resonance of the structure and control accelerometer. The resonance is obtained by simple genuflection, controlled metronome 4 persons. The system is thus set according to the actual frequency of the structure, and effectiveness of the damping is controlled.

Fig.Ap3.12.   Implementation of dampers

5.7. Finishing, testing

After installation of decking located at the joints, the bridge is completed. The tests under three quarters of the load were performed by loading the strips with HEB160 foundations and pathways.

6. Conclusion

Beyond the technical challenge of achieving an extraordinary bridge by its material, its shape and slenderness, is remembered as a team in which each actor, the Project management companies, has put his best to solve the problems each phase of the design and realization. The bridge, moreover, presents the ambition, across lifecycles, with a very small footprint and a need low maintenance.

Ap3.3.   Road Bridge WILD

Based on original article:	'Road Bridge WILD - UHPFRC for a segmental arch structure' from BFUP 2009 / UHPFRC 2009 publications
Year:	2010
Location:	Carinthia, Austria
Concrete:	Compressive strength 165 MPa; flexural strength 18 MPa
Connections:	Post-tensioning; unbonded monostrands

Summary

With the pilot project "Road Bridge - Wild" the UHPFRC segmental construction method combined with the swivel in method for arch erection comes to application. So the eminent properties and possibilities of UHPFRC are utilized in two regards: quick erecting and durable structures. The 157m long bridge consists of two foreland bridges and an UHPFRC segmental arch which spans 70m. The halves of the arches are built up vertically, tied together by external tendons and easily swivelled in. Afterwards the columns and deck slab are conventionally completed. Because current codes and guidelines do not cover the application of UHPFRC, full scale tests, many other tests for local response and various numerical investigations have been necessary for a save realization. This contribution describes design, construction, scientific investigations and the learning effect which gives us conclusions for both, further applications and continuative research.

Introduction

UHPFRC with its inherent benefits of high compression strength and extraordinary durability opens new possibilities in structural engineering. Studies have shown that very light and thin-walled cross sections with sufficient stiffness are required. If such light cross sections in conjunction with prefabricated segmental construction, external prestressing and dry joints come to application, new or adapted and very fast erection methods in bridge construction are imaginable. These should compensate the higher material costs. By the high durability compared to conventional concrete bridges, the life-span shall be increased to 200% while the costs of maintenance shall be halved. Since these aims can be met, the life cycle costs will decrease to 50%, which causes low afford for maintenance and a long lifetime. Last but not least these advantages unburden our political economy.

Fig.Ap3.13.   Visualization of pilot project Road Bridge WILD

Due to its geometrical stiffness arch structures provide excellent possibilities for maximum utilization of the high compression strength of UHPFRC due to transfer of the loads mainly by compression. Such utilization can never be reached in beam structures for traffic bridges because of the strict limits regarding the deformation and vibration for road and in particular rail bridges to achieve sufficient traffic safety. Some studies and other pilot projects have been shown that compression strengths of more than 150 MPa are not necessary for beam structures. If the thrust line of the arch is optimal adapted to the acting loads, tensile stresses and shear forces in the structure are very low. So an arch bridge is very predestined for a first UHPFRC pilot project in such dimensions.

2. The pilot project Road Bridge – WILD

The pilot project road bridge - WILD in Carinthia, Austria for an UHPFRC-segmental-arch-bridge, is an example of the swivel-in-method that is used in realization. The polygonal-arranged UHPFRC segmental arches consist of individual 6 cm thin-walled (and for this reason very light) precast UHPFRC-segmental-box-girders made of C 165/185. They are assembled by the use of external tendons running inside the arches. Since the actual shear force

in the arches is very low, the thin-walled webs made of UHPFRC do not need any shear reinforcement for carrying the loads.

Assuming that the dead load of the arches is low compared to the further loadings from columns, deck construction and traffic, the thrust line of the arch is polygonal. The additional prestress, applied by the use of external tendons, reduces the eccentricity of the loads and causes an important increase of the bending stiffness of the arch. These tendons are unbonded monostrands which are easy to assemble and exchange.

characteristic compressive strength cylinder f_{ck} (ø/h = 150/300 mm)	≥ 165 MPa
modulus of elasticity E_{cm}	≥ 50.000 MPa
characteristic flexural tensile strength $f_{ctk,flex,0,5\,mm}$ (four point bending test 150 x 150 x 600 cm; DBV)	≥ 18 MPa
characteristic direct tensile strength at loss of linearity behaviour f_{ctk}	≥ 7 MPa
characteristic direct tensile strength (fibre bridging) f_{ctk}	≥ 7 MPa
characteristic friction coefficient at joint surface μ_k	≥ 0.20
evenness at surface of segmental joint	± 0,1 mm

Tab.Ap3.1.   Required material strengths and properties of UHPFRC

3. Assembling and erection of the arch

After completion of the foreland bridges, the several arch-segments are assembled in a vertical position using external tendons. The effort for equipment is minimal: a mobile crane for the manipulation and temporary ties for fixing the arch's position. The very light arch halves can easily be swiveled in and are jointed at the crown (figure 3.14). The hinge for swiveling is a simple steel bolt with a diameter of merely 80 mm. The maximum force in the swiveling cable is about 2x450 kN, which can be borne by 2x4 monostrands. After joining the arch halves further tendons overlapping at the arch's crown, are installed. Due to pouring the hinge between the arch and the springing foundation, the arch gets a rigid restraint.

Too large production tolerances of the precast arch segments will have far-reaching consequences on the erection work and on the final arch shape. For this reason project-oriented considerations have already been made during the bidding procedure. The permitted deviations of the single segments as well as for the final arch shape have been specified. At present these demands can only be met, when the joint surfaces are milled by a CNC-machine.

The construction supervisor claims extensive industrial safety rules during vertical assembling and swiveling. Amongst others, it was not permitted for working staff to stay in the inside of the arches during the vertical assembly. Therefore the problem arise how to perform the successive installation of the external tendons in the arch. The combination of afore installed ropes, the use of complex coupling systems and guiding devices leads to a threading procedure, which allows pulling the tendons from the top of the arch to the springing without any working staff in the inside of the hollow box girders.

The concentrated loads due to lifting devices or other anchorage elements during assembling can hardly be introduced and distributed in the thin walled elements. Even the space necessary for conventional lifting devices is not available in most cases. Only at the more massive knee-elements it is possible to fix temporary lifting devices. Also special considerations regarding storage, transportation and handling during assembly must be made during design in order to avoid damage or harmful cracking of the filigree thin walled elements. Specially developed lifting devices and a mobile crane with two independent winches provide simple and fast adjustment in all directions. Doing it that way, the required assembling accuracy can be ensured. Further the fixing of the rotation axis of the swiveling hinge at the springing will be carried out not before the real geometry of all segments will have been measured and therefore the correct position of the arch's crown is known. Little deviations at the arch's crown will be corrected with a special centering device. The restrains resulting from this correction are taken into account in the further design calculations.

4. Design and test

Present design codes and guidelines do not completely cover the use of UHPFRC in relation to the structure presented. Experimental tests will answer open questions in designing and construction. In addition to many other experiments, full-scale laboratory tests within the scope of the pilot project are carried out.
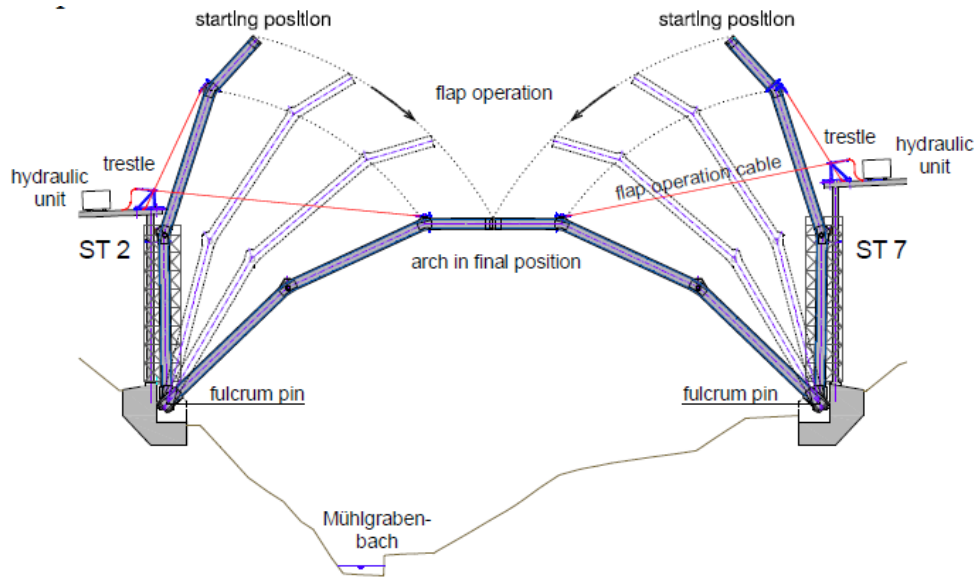
Fig.Ap3.14.   Segmental Flap Method; closing both arch-halves   [fib Symposium Prague 2011]

The full scale test shows the same load carrying behavior and failure as found in the preliminary nonlinear FEM-analysis for the preparation and also the recalculation of the full scale test. At the loading levels which represent the serviceability limit state with characteristic loads and the ultimate limit state there was absolutely no indication of a failure. Even with 1.5 times magnified ultimate loads and at the maximum force of the servo-hydraulic testing jack the point of failure could not be reached.

The test elements for the first full scale test have been fabricated by the laboratory of structural engineering of the TU Graz without the possibility for a mechanical treatment of the joint's surface by CNC grinding and milling. The accuracy of the joint's evenness is in the range of 2 mm so that there is no uniformly distributed contact in the joint. This punctual compression in the joint leads to single stress peaks which cause tensile stress in transverse direction with longitudinal crack formation in the thin-walled box girder. These longitudinal cracks have no influence on the global failure load but substantiate the necessity of a maximum deviation of 0,1 mm of the joint's evenness to transfer the high compressive stresses. At further tests with accurate joint surfaces no longitudinal cracks in the box girder are observed.

5. Final comments

The tensile behavior of UHPFRC depends significantly on the fiber orientation and distribution in the real structure. Therefore it is not sufficient to define in the bidding procedures the required mechanical properties which should be determined on the basis of test specimens. Additional information about one or more required suitability tests should be given. The specimens for these suitability tests should be produced with a representative geometry and the way of placing the concrete as in the real structure in an early state before the production process of the segments will have started. The results from the bending test give information about the real tensile strength at the real structure in different directions.

6. Conclusions

New construction principles that lead to segmental construction methods can be deduced thanks to a detailed and continuous involvement of the material properties of UHPFRC, the possibilities provided by the precasting industries and the inclusion of erection methods in bridge construction. With proper and wise use of UHPFRC the typical design rules and construction principles of structural concrete and structural steel will be merged. As far as the lightness is concerned, UHPFRC segmental bridges bring economical advantages in comparison to common concrete bridges, because they will be built faster, will be easier to maintain and will have a longer service lifetime. The presented pilot project points clearly out the high performance of UHPFRC.

Ap3.4.   Stadium Le Stade Jean Bouin

Based on original article: 'Le Stade Jean Bouin' (French) from BFUP 2009 / UHPFRC 2009 publications
Year: 2012
Location: Paris, France
Concrete: Ductal
Connections: Interlocking gutters; no further information

The rebuilding of the Stage Jean Bouin presents more than 20000 m ² of lattice UHPC. The lattice forms the envelope in facade and tight cover by describing a stiff surface. The whole of the design is based on the effective use of all the characteristics of the UHPC. Vis-a-vis the geometrical complexity of the project, the performances of the UHPC make it possible to consider a simplification of all the constructive processes. Skin UHPC presents in only one layer, the primary and secondary structure, the tight skin and the architectonic envelope.

The whole is prefabricated in factory then posed in only once. In particular, a new process of inclusion of glass during the casting of elements UHPC in cover was developed and validate by the CSTB.

Lastly, the use of very small quantities of matters leads to a project with a ultra-reduced environmental print.

General presentation

The rebuilding of the Stage Jean Bouin will start 2009 at the end of the year, with a delivery planned for the season of Rugby 2012-2013. The stage will contain 20000 seats, as well as cabins, trade and a carpark. The actors of the project are the following:

- the building owner, the town hall of Paris, direction of youth and the sports
- the driver of the operation, direction of the inheritance and architecture, town hall of Paris
- the architect, Rudy Ricciotti
- the research department UHPC, Lamoureux & Ricciotti Engineering
- the research department metal frame, Group Viola Marc Malinowsky
- the CSTB of Champs-sur-Marne
- the office of control, Qualiconsult, experimental validation by ATEx
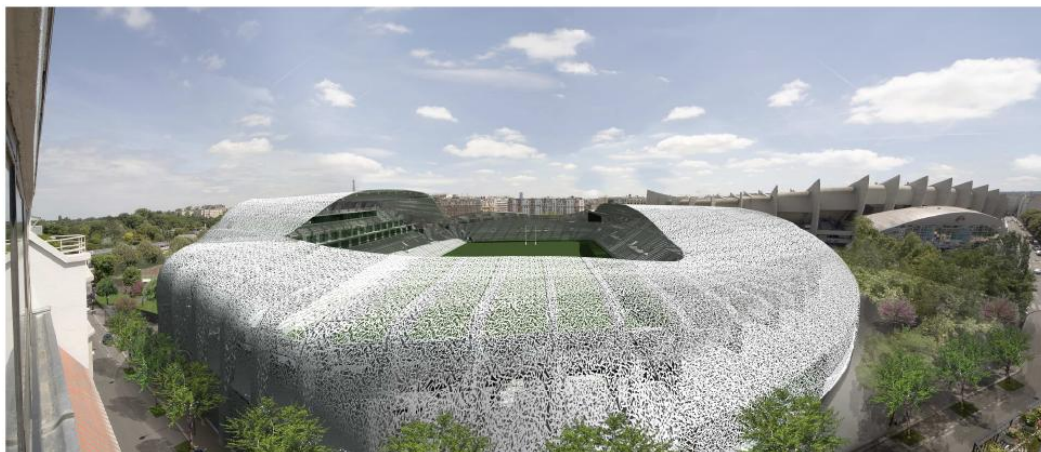
Fig.Ap3.15.   An impression of the future stadium

The envelope of the stage is described by a lattice of UHPC developed in cover on 11500 m ² and facade on 9500 m². The role of this lattice is multiple:

- the lattice is an architectonic envelope:
  ◦ the geometry of the lattice is a stiff surface with S curve which exploits with maximum gauges authorized by the local plan of town planning.
  ◦ it presents borings seen in a random way
  ◦ it is carried out in UHPC
  ◦ these essential points make it possible to reduce the visual impact of the work in the city
- the lattice, only in cover, is a protection of the spectators against the rain
- the lattice forms a structural and carrying support:

◦ of the climatic loads
◦ of the loads related on the monitoring and the maintenance of the elements
◦ as much in cover that in facade
- the lattice presents an intelligent environmental entity:
◦ it is optimized in quantities of matter, minimizing the impacts:
◦ in cost and planning
◦ in energy
◦ in transport, handling and poses
◦ in maintenance in financial costs
- it is carried out starting from materials:
◦ with low consumption of primary energy (of the concrete rather than of steel and aluminium)
◦ not taking part in the exhaustion of the natural resources
◦ and minimizing the air pollution and of water
- the lattice is designed in a quasi-monolithic way, on only one thickness in order to optimize the whole of the constructive process and methodologies:
◦ prefabrication
◦ standardization of the gestures and the constructive processes
◦ design of the elements in only one thickness, without brought back elements:
structural (primary education and secondary)
impermeable (in cover)
and architectonic
◦ simplification and reduction of the cycles of installation
◦ improvement of the work conditions
◦ procedure of maintenance facilitated

The constructive resolution of this program consists in proposing a grid of the envelope starting from mono-piece plane triangular panels of approximately 10 m ^{2}, posed on the plagues out of metal frame, according to an average distance between centers of 8m.
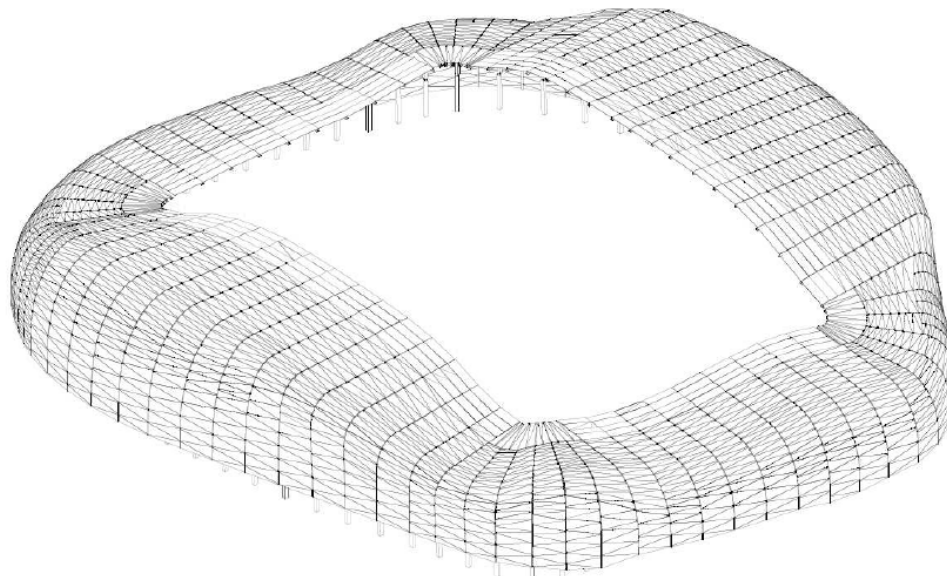
Fig.Ap3.16.   The composition of the structure

The triangle is indeed the form most adapted to build this stiff surface. The meshes are thus some 2,4 m broad triangular panels ribbed and 8,2 m length on height. The size of the elementary mesh must be optimized so as to minimize the number of constructive gestures, while making it possible to rebuild surface with sufficient definition.

It is a question of carrying out approximately 1900 triangles of cover and 1600 triangles of facade. The meshes all are different but resulting from an identical and repetitive manufacturing process.

The exterior wall panels are panels of bits fixed in three points on metal curved profiles. The rate of vacuum is approximately 60%.

The panels of cover are of design more complex, in particular because they must form a protection seal for spectators against the rain. The vacuum of the panels (approximately 30%) is filled by glass included with the casting. The system of inclusion of glass is described here. It was the subject of an Experimental Technical Appreciation favorable to close to the CSTB.

The technological challenges met during the design engineering are presented and detailed in the following paragraphs. They relate to only the panels of cover, in particular:
- dimensioning structural of the panels
- design of the interface glass UHPC
- tests of ATEx of design to the CSTB

Design of cover UHPC

The cover extends on 11500 m². Beyond the party taken architectonic, the cover has two crucial roles:
  - it forms a protection of the spectators against the rain
  - the ribbed panels are carrying the whole of the loads on an average distance between centres of 8 m.

The use of the UHPC is justified here of course by its mechanical performances, but also by its cementing matrix with null connected porosity, which makes a tight skin of it. The very first drafts of the project defined a double skin with a lace in UHPC and a skin out of glass. The design engineering pushed a little further the interest from material: random borings are directly conceived out of glass.

The interest is multiple:
  - glass of course is saved: only the negative one of the concrete is out of glass, that is to say 70% of economy
  - one frees oneself from structure carrying glass
  - one facilitates the calepinage cover
  - the maintenance and the maintenance of the cover are facilitated

Under these conditions, one integrates in a structural thickness:
  - the primary structure (longitudinal veins)
  - the secondary structure (plate openwork)
  - architectonic skin: lace in UHPC and glass

Structural description

The standard panel has following dimensions:
- maximum width 2,4 m
- length (height of the triangle) 8,2 m
- veins: inertia equivalent to a R6x20 rectangle
- plate: 0,035 m

The panel was dimensioned while following Recommendations UHPC of the AFGC of 2002. Calculation is carried out starting from models with the finite elements and modules of special post-processing UHPC.

Treatment of the joints of fractionation
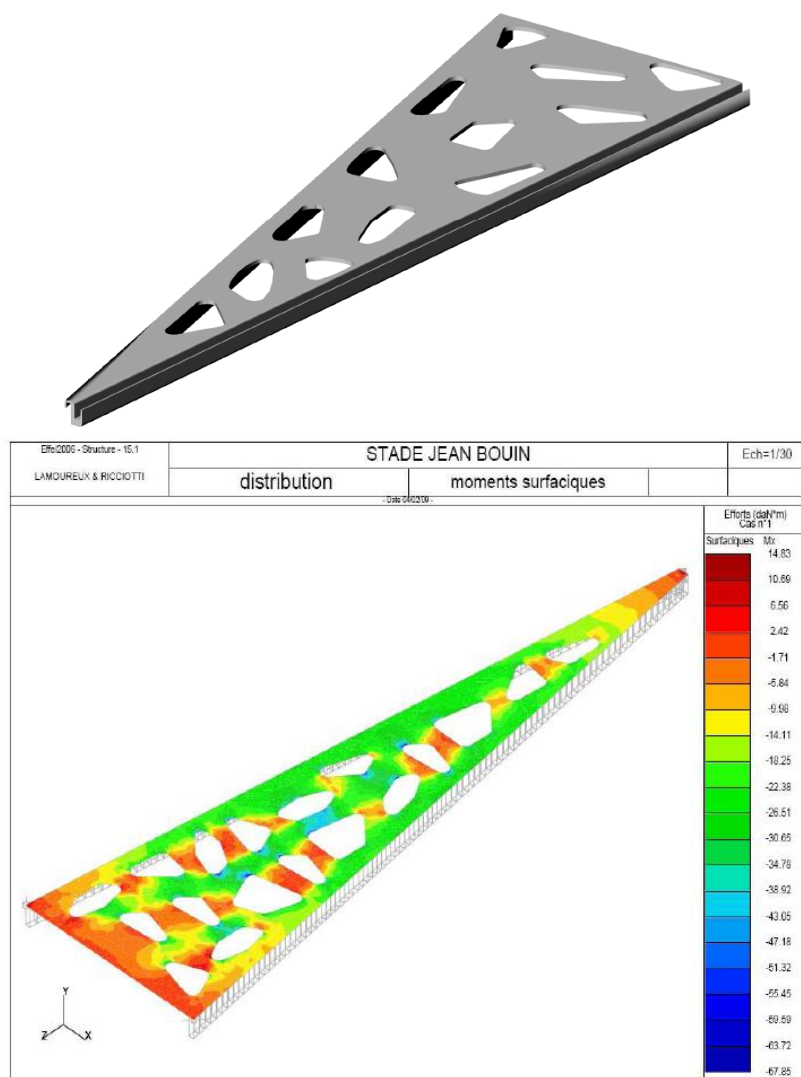
Fig.Ap3.17.   Elements and analysis

The joints between prefabricated panels are sealed thanks to the shape of the side veins of the panels, cased in the shape of interlocking gutters.

The male and female veins are calculated so as to present an equivalent inertia, to balance operation in longitudinal inflection of the panel. The sections of drainage are dimensioned in accordance with the DTU and are advantageously used to decrease bottom fiber tensile stresses.
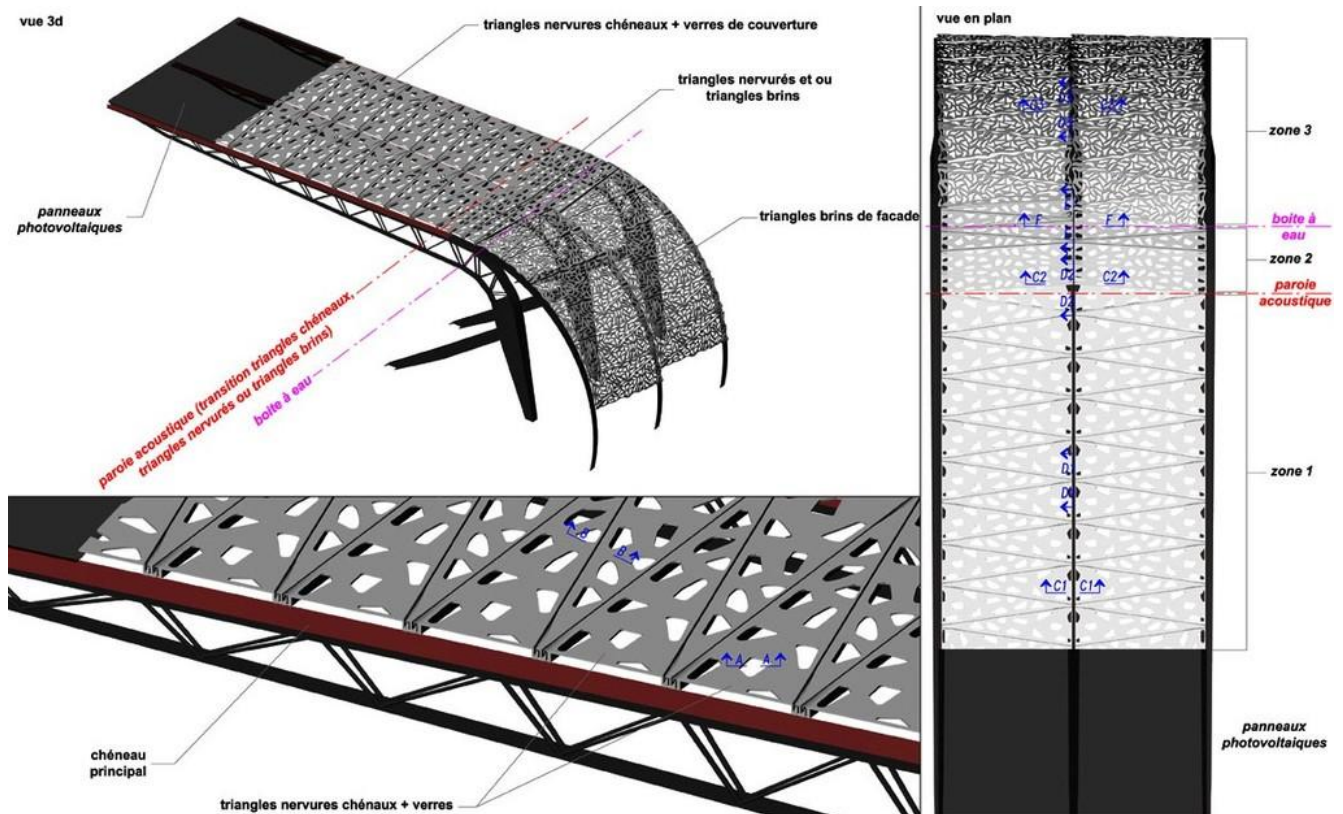
Fig.Ap3.18.   Illustration of architect's proposal for joints

Inclusion of glass

The current lawful context does not make it possible to consider glass included in concrete. Several reasons with that, in particular the chemical incompatibility of two materials, as well as different mechanical behaviors in particular under thermal dilation.

Nevertheless, the will to rationalize to the maximum the process of prefabrication of cover UHPC and to allow a decisive standardization of the techniques, pushed the design to use to the maximum porosity off-line of the UHPC.

A process of inclusion of the reasons for glass to the casting was developed by the control of work at the time of the design engineering.

Glass is included during the casting of panels UHPC, it is to the same naked superior as the concrete. The geometry and the nature of glasses, their provisions within plate UHPC were studied so as to avoid the secondary stresses on the level of the interfaces.

The complex must form a tight whole: after tiredness of the structure, under thermal shocks, after cycles of accelerated ageing.

The objective is one lifespan higher than 50 years, even 100 years. Being given the new character of the process, a trial run, associated with a procedure of ATEx, were carried out during the design engineering. ATEx delivered an favorable opinion.

Figures

Surface cover	11500 m ^{2}
Surface facade	09500 m ^{2}
Distances between centers of the frame	6 m - 8,6 m
Weight of cover	110 - 130 daN/m ^{2}
Average thickness UHPC	4 cm - 4,8 cm

<u>Conclusion</u>

The rebuilding of the Stage Jean Bouin was the occasion, at the time of the design engineering, to exploit to the maximum and in an exhaustive way the multiple performances of UHPC: performances structural, durability, sealing.

Sight geometrical complexity of the project, the consequences are immediate on the simplification of the processes of construction, the costs and times of work, but also on the maintenance and the durability of the work.

Moreover, the optimal use of this material makes it possible to propose a project responsible with respect to the current environmental stakes for construction. Contrary to other techniques of cover (metal), design UHPC minimizes in a decisive way the quantities of matter and thus the ecological print of this work (primary energy, air pollution, of water, exhaustion of the natural resources).

Ap3.5. Millau Tollgate

Year: 2004
Location: Millau, France
Concrete: Ceracem
Connections: Longitudinal prestressing

A spectacular example of architecture taking advantage of the special benefits of UHPC is the toll-gate of the Millau Viaduct in France. The figure below shows the elegant roof 'looking like an enormous twisted sheet of paper', 98 m long and 28 m wide with a maximum thickness of 85 cm at the center with a hollow core, the skins are only 100mm thick. It is made of 53 match-cast prefabricated 2 m wide segments connected by an internal longitudinal prestressing.

The elegant roof is a thin Ceracem® (ex-BSI) shell and is seen as a next step in the development of this material. The precast elements are connected by an internal longitudinal prestressing. In all, 1,000 m3 of Ceracem® is used, weighing a total of about 2,800 tons.

Fig.Ap3.19.   Arial view of Millau Tollgate

The 53 elements were poured on a special site located near the north side of the viaduct. In 6 months, from ctober 2003 to April 2004, the 53 elements were produced. A self-propelled truck of 500 horsepower and with no fewer than 120 wheels was used to transport the elements to the tollgate worksite. These were then taken over by a crane and positioned in their final location.

The elements are put side-by-side on temporary framework and, subsequently, the elements are pressed together by longitudinal prestressing ties. The positioning of the elements is executed using temporary scaffolding. The special part is the fact that the elements are prefabricated on site, avoiding maximum transportation sizes (except for the crane capacity).
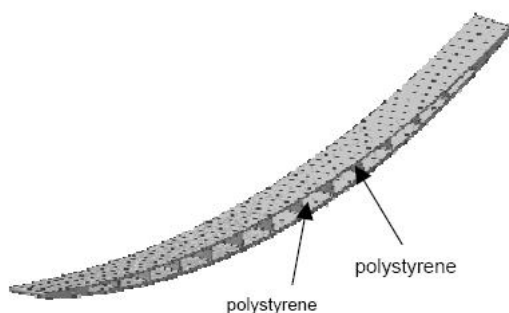
Fig.Ap3.20.   The applied elements   [Eiffage]

Ap3.6 Bridge across River Fulda (Gärtnerplatzbrücke)

Based on original article:	'UHPC composite bridge across the river Fulda in Kassel; conceptual design, design calculations and invitation to tender'
Year:	2007
Location:	Kassel, Germany
Concrete:	Presumably; Compressive strength 165 MPa; flexural strength 15 MPa
Connections:	Prestressing; glued connections at decks

The bridge structure has 6 spans with a total length of 133.2 m and a maximum free span of 36 m. The bridge deck consists of precast prestressed UHPC slab elements. The longitudinal structure consists of a continuous truss girder system with triangular cross section. The truss girder consists of two upper chords of precast prestressed UHPC and a lower chord and diagonals made of tubular steel sections. Glued connections are used between the upper chords and the deck as well as between the deck plates.

It is intended as the first project of a UHPC-bridge in Germany to set up a pedestrian and cycle track bridge across the Fulda by the City of Kassel as client. The planed bridge is a hybrid construction made of steel and Ultra High Performance Concrete. This bridge shall replace an existing wood bridge which shows severe damage.
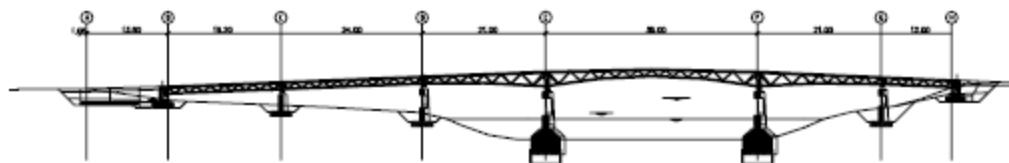
Fig.Ap3.21.   Longitudinal section

After extensive variant examinations, the following load-bearing structure was selected. The bridge girder is formed by a truss with three booms with variable building height; the top booms consist of UHPC while the sub boom is formed by tubular steel. The diagonals also consist of tubular steel. The bridge deck consists of 5.00 m wide prestressed precast UHPC plates with 8 - 10 cm of thickness. The UHPC plates will be interlinked and connected to the top belts of the truss girder using epoxide resin glue. Figure 6 shows the new cross section.
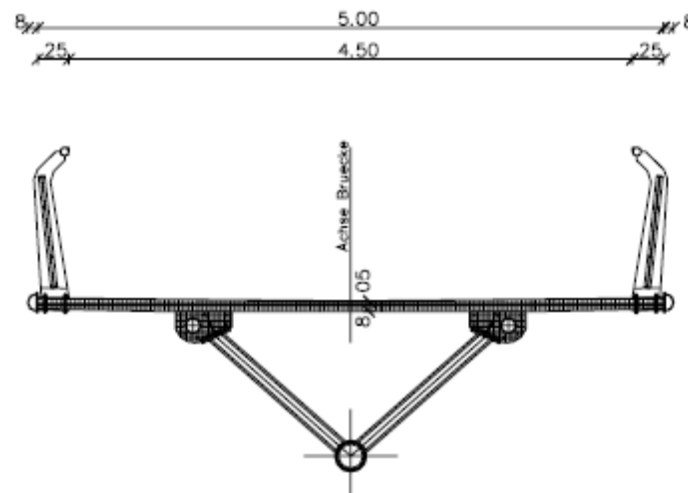
Fig.Ap3.21.   Cross section

The single span girders consist of the UHPC top booms which are precast in a stressing bed and the steel parts of the truss girder (bottom boom and diagonals). In the end the prestressed precast UHPC deck plates will be mounted. A shear resistant connection in the composite joint between the plates and the top booms will be established by an epoxide resin glue. Simultaneously, the precast UHPC plates are also interconnected by glued connections. To ensure that there are no tensile stresses under permanent action in the bridge deck in longitudinal direction, the top booms will be equipped with tendons along the full length of the construction. The tendons which prestress both, the precast plates and the top booms will be anchored in the end cross beams.

Fig.Ap3.22.   A 3-dimensional presentation of the bridge

Using a Finite Element program, a three dimensional model of the bridge structure for the design calculations was set up. The calculations considered the process of construction on site and the effects due to creep and shrinkage. Tests on heat treated construction elements made of UHPC have shown, that the creep behavior is very low and that there is almost no shrinkage left. Therefore a heat treatment of the precast elements is intended.

Fig.Ap3.23.   A 3-dimensional model of bridge structure

A failure of the glued connections is considered in design calculations for the ultimate limit state. To this it is proved that the load bearing safety of the complete system is ensured also at failure of single slabs and that they can be exchanged if necessary.

Ap3.7. Folly in UHPC; double curved, the Netherlands

Based on original article:	Luifel Zonnestraal, Hilversum, The Netherlands by H.-J. Henket
Year:	2005
Location:	Hilversum, The Netherlands
Concrete:	Precise data unknown
Connections:	Stainless steel bolts

A pavilion on the terrain of the previous sanatorium 'De Zonnestraal' presents the latest developments on the domain of concrete technology and construction techniques; prefab, demountable and high strength concrete elements.

Shape of the shed

The basic surface of the shed is 9 by 9m and 3.5m high. The plate is segmented in 4 elements of identical properties and size, to make the fabrication, transport and montage easier. The plate is just, thanks to the use of high strength concrete, 2.5cm thick and stiffened by transversal and radial ribs with a thickness of 4cm. The 4 quadrants are connected to each other with bolts, trough stainless steel elements inserted in the concrete during molding.

Composition of the Concrete

The shed roof is constructed with UHPC, 'Ultra High Performance Concrete', which is, due to the higher amount of cement and specific additives, 5 times stronger than ordinary concrete. And, also 5 to 10 times more expensive than standard concrete. The four arms of the shed roof are composed of fibre-reinforced UHPC. The fibres have a diameter of 1mm.

Fig.Ap3. 24.   The roof of the shed is 25mm thick and the stiffening ribs are 40mm thick

Formwork

The double curved components of the roof are composed with the file-to-factory method; on the basis of 2D drawings, 3D drawings are composed. The formwork is made out of 2 thick multiplex laminated plates; where with the aid of the 3D-CAD-file, a grinder turning around 3 axes, drill out the shape of the arms. The components are not treated with a finishing material; this is not necessary due to the low porosity of the UHPC and the exact fitting of the components.
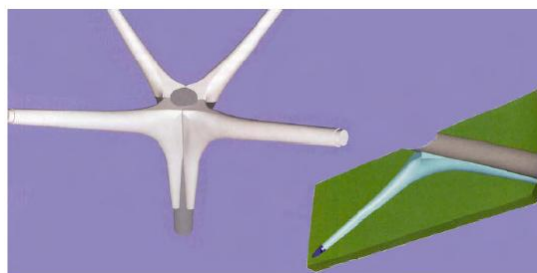
Fig.Ap3.25.   The roof of the shed rests on a steel column onto which the fiber reinforced
UHPC arms are attached.

Ap3.8. Clinker Silo; Illinois; USA

Based on original article:	The world's first long-span roof constructed in Ductal
Year:	2001
Location:	Joppa, Illinois, USA
Concrete:	Ductal
Connections:	Unknown

In 2001, a clinker silo in Joppa, Illinois became the first building in the world to have a long-span roof constructed with Ductal ®. Ductal is a revolutionary, ultra-high performance concrete (UHPC) material that provides a unique combination of ductility, strength, durability, and aesthetic flexibility - with compressive strengths up to 32,000 psi (220 MPa) and flexural strengths of up to 7,200 psi (50 MPa). The project, estimated at $34M (US), was an upgrade to a cement manufacturing facility. Ductal was used to construct one of three clinker silo roofs while at the same time a conventional steel solution was used on the other two. The steel and Ductal options were each designed by the engineers and tendered competitively. The Ductal roof consists of 24 precast, pie-shaped panels with a 12.7 mm skin thickness for the 18 m diameter silo. The panels were designed to act as a thin ribbed plate, supporting a two story mechanical penthouse, centered at the top of the cone shaped roof.

Fig.Ap3.26. The silo during construction

Ductal's unique combination of superior properties enabled the designer to create thinner sections and longer spans for a tall structure that is lighter, more graceful and innovative in geometry and form.

This is the first known use of UHPC used in a long-span roof system.

The ultra light, thin, precast panels did not use any reinforcing bars.

It took just 11 days to install the Ductal roof, vs. 35 days for the steel roof.

The Ductal roof panels were more accommodating to the construction tolerances for out-of-roundness and flatness of the top of the slip-formed silo walls.

Improved site safety: there were fewer personnel climbing over the structure during installation, thereby reducing potential for fall accidents and fewer protruding obstacles such as rebar or steel elements which could cause tripping.

Reduction in non-renewable resources: due to a reduction in the total quantity of materials consumed and the use of recycled materials in Ductal (such as Silica Fume).

The Ductal roof is air and water-tight, thereby resulting in reduced environmental impact and reduced maintenance: due to Ductal's low permeability and improved durability, and the elimination of a waterproofing membrane.

Due to the lightweight design, the precast roof panels were easily transported.

The ductile behavior of this material is a first for concrete. It has the capacity to deform and support flexural and tensile loads, even after initial cracking.
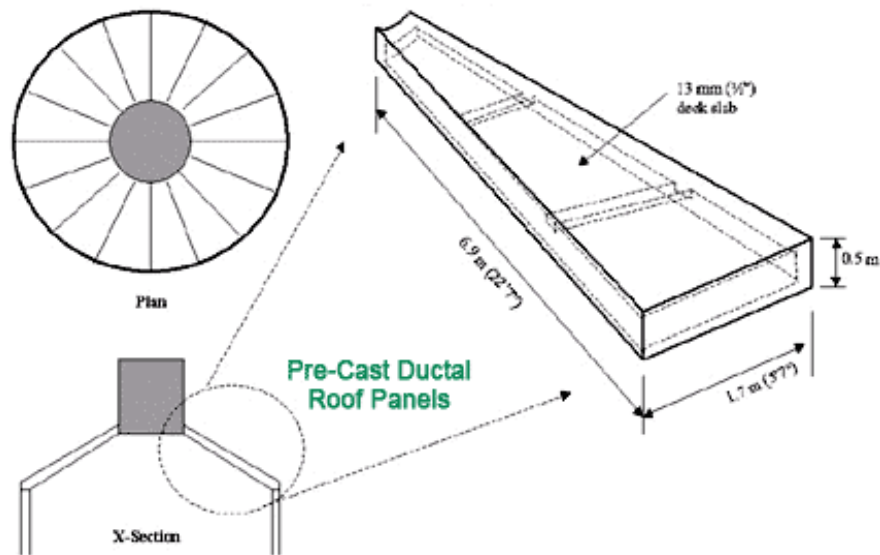
Fig.Ap3.27.   An overview on the element dimension

Ap3.9. Sherbrooke Pedestrian bridge

Based on original article:	'First recommendations for Ultra-High-Performance Concretes and examples of application'
Year:	1997
Location:	Sherbrooke, Canada
Concrete:	Precise data unknown
Connections:	Prestressing

The world's first engineering structure designed with Ductal was the Sherbrooke footbridge in Sherbrooke, Quebec, built in 1997. Spanning 60 m, this precast, prestressed pedestrian bridge is a post-tensioned open-web space RPC truss, with 4 access spans. The main span is an assembly of six prefabricated match-cast segments of 10m each.

Fig.Ap3.28. General view of Sherbrooke footbridge

The cross section is made of a ribbed slab 30 mm thick, with a transverse prestressing made of greased-sheathed monostrands. The truss webs are made of RPC confined in stainless steel tubes.
The structure is longitudinally prestressed by an internal prestressing placed in each longitudinal flange and an external prestressing anchored at the upper part of the end diaphragms and deviated in blocks placed at the level of the lower flange.

Ap3.10. Seonyu Footbridge

Based on original article:	'Experience and Applications of Ultra-high Performance Concrete in Asia'
Year:	2002
Location:	Seoul, Korea
Concrete:	Ductal
Connections:	Post-tensioning

To date, the Seonyu Footbridge in Seoul is the largest UHPC bridge in the world with a single span of 120m. The type of UHPC which is applied is Ductal and is designed by Rudy Ricciotti. It is comprised of six precast and post-tensioned segments of PI-shaped section. The section developed for the Sunyundo Footbridge, consists of a transversally ribbed upper slab and two girders. The width of the arch is 4.3m, has a section depth of 1.3m and a thin (30mm) slab supported by transversal ribs at 1.225m, and two longitudinal ribs at the extremities of the transversal section. This ribbed slab is supported by two 160m thick webs. The transversal ribs are prestressed by ⌀12.7mm sheathed and greased monostrands. Small specially adapted anchors similar to those used in the construction of the Sherbrooke footbridge were used to transfer the prestressing forces. In the longitudinal direction, the structure is prestressed by three tendons in each leg. The arch is supported at each end by two reinforced concrete foundations 9m deep resisting the horizontal thrust of the arch. Further design and construction details have been described in other publications.

Fig.Ap3.29. View on Seonyu Footbridge: Seoul, Korea

Ap3.11. Innovative Field Cast UHPC Joints for Precast Bridge Systems

Based on original article:	by Vic H. Perry & Mathew Royce, 2010
Year:	2008
Location:	New York, USA
Concrete:	UHPC Joint fill
Connections:	UHPC Joint fill

Bridge owners are frequently faced with the need to replace critical bridge components during strictly limited or overnight road closure periods. This paper presents the development, testing and installation of precast, high performance concrete bridge elements with field cast ultra-high performance concrete (UHPC) Joint Fill.
The fundamentals of the technology, material properties, design details, manufacturing, prototyping, load testing, erection and a completed project overview are included.

Benefits include: reduced joint size and complexity, improved durability, improved continuity, speed of construction, elimination of post-tensioning and extended usage life. This new innovative joint design eliminates the historical problems associated with the joints in precast bridge decks. This new joint is now the "strongest link" in the precast bridge deck system.

One of the largest and specific challenges facing bridge authorities is the long-term durability of bridge decks which receive continuous impact loading from trucks and changing environmental conditions. The years of continuous flexural and thermal stresses and exposure to corrosive elements create long-term deterioration and maintenance issues for bridge decks. The use of HPC precast deck panels is a common method to speed construction and reduce the user inconvenience; however the jointing of the precast system has been a source of potential maintenance.

While post-tensioning can resolve most of the performance issues, it is not without potential problems. It is expensive, requires specific expertise and equipment for installation; it has potential for corrosion and is not practical for slabs with a cross fall. Furthermore, the analysis is complex in terms of the correct post-tensioning forces (number of strands and forces longitudinal versus transverse), creep losses, grout properties, potential long-term corrosion of the strands and sequencing of P/T versus anchoring of the panels to the superstructure girders (and introduction of P/T forces into the girders), ensuring proper location of decks during fabrication.

In 2008, the New York State Department of Transportation (NYSDOT) decided to investigate the use of UHPC joint fill with full-depth precast deck panels a new solution for replacement of deteriorating highway bridge decks. The solution was to use a precast concrete deck panels with field-cast UHPC joints to develop the continuity in the deck panels.

Utilizing the superior characteristics of the material technology enables the simplification of the precast panel fabrication and installation processes. This simplified design provides the owner with improved tolerances, reduced risk, increased speed of construction, an overall cost savings in construction and a more durable, longer lasting bridge deck solution.
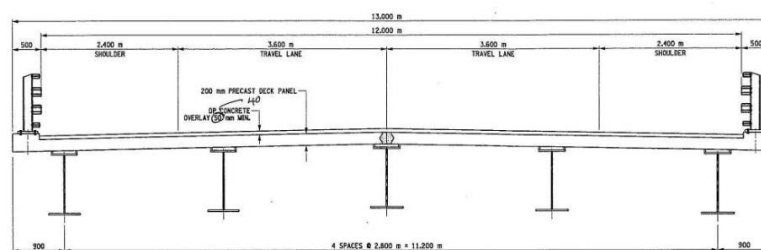
Fig.Ap3.30. Transverse bridge section of precast panels and centerline UHPPC joint fill

Concept

The concept to be implemented by NYSDOT was full-depth precast panels with UHPC joint fill in order to provide continuity.

The UHPC joint material was assumed to provide sufficient bond development to allow full continuity of the rebar, as if it were continuous through the joint. Previous testing has shown that the bond development length of a 13 mm bar in UHPC is less than 75 mm.

The UHPC joint fill material has excellent bond development length, superior freeze/thaw resistance, extremely low porosity, higher than normal flexural strength and superior toughness, which provides improved resistance to climatic conditions and continuous flexing from truck loadings across the joints. With previous projects, field-casting of monolithic.

Even though autogenous shrinkage of UHPC is significant by keeping the joint width small (152 mm), the total shrinkage across the joint is 0.09 mm. Experience on the New York projects show that the total shrinkage is distributed throughout the system and the UHPC/ HPC deck interface is bonded with no potential for leaking.

the joint size is minimized to provide the least possible total shrinkage across the joint. Minimizing the joint size also reduced the quantity of jointing material to be cast on-site and simplified the precast panel manufacturing. Additionally, to enhance the bond between the precast panel and the joint fill, the surface of each HPC precast panel was soaked to saturated surface-dry (SSD), prior to casting the joint fill.
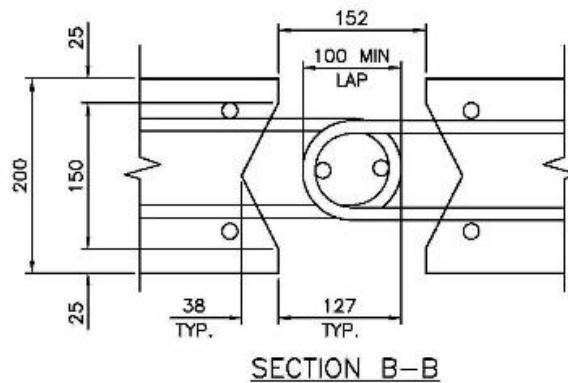
Fig.Ap3.31. End view of the UHPC joint fill between precast deck panels ate the abutment

The precast deck panel area was 504 m² with panels of 200mm thick and 6.4 m x 3.39m. The panels were reinforced with 16 mm galvanized rebar each-way top and bottom, with hairpin bars in the joints. Typical UHPC joints were 152 mm wide and 200 mm deep, utilizing a total volume of 11.5 m³ UHPC joint-fill. The project used the UHPC Joint Fill only in the joints between the panels.

Fig.Ap3.32. Intersection of center line joint and transverse joint prior to filling the joint

The UHPC joint fill materials and portable mixers were delivered to the site by the material supplier and set up for batching. The mixers are set up in pairs to provide a continuous supply of material for the joint filling operation. Mixers are normally set up at the end of the bridge to provide direct access to the bridge deck.

The IMER Mortarman 750 mixers are capable of batching 0.15m3 (5.30 ft3) per 20 minute batch cycle time for a volume of 0.90 m³ /hour per pair of mixers. The number of mixers delivered to the site is determined based on the contractor's schedule. The material supplier provided onsite supervision to ensure continuous and consistent batching performance. Every batch is checked for plastic properties. The hardened compressive strength is also validated.

The UHPC joint material is transported to the joints by power buggy or wheel barrow then dumped directly into the joints. The UHPC material was batched with a minislump of 200 mm to 225 mm (self-consolidating and self-leveling). The rheology of material permitted the UHPC to be poured directly into the joints without any vibration.
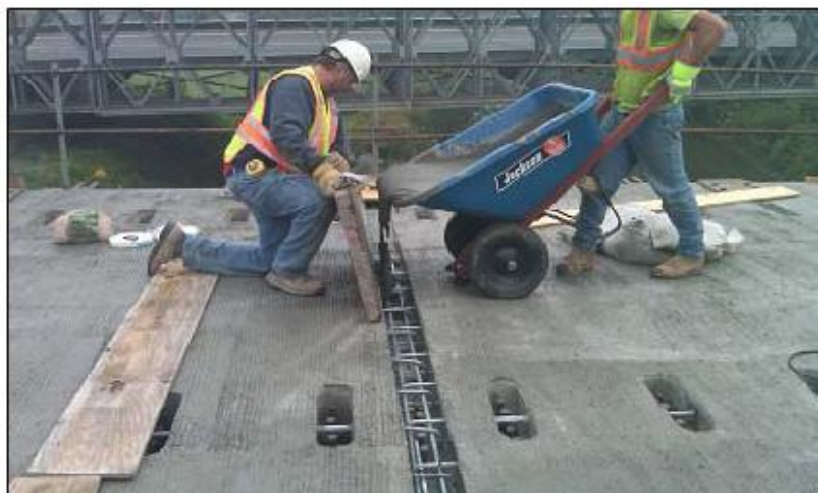
Fig.Ap3.33. Filling the joints with UHPC

The joints are covered with form grade plywood strips (to avoid surface dehydration of the joint fill) and then allowed to cure until reaching 100 MPa, before opening to traffic. The time to reach 100 MPa will vary. At ambient

temperatures (20°C) without any accelerators, this would be approximately 3 days. This can be reduced with accelerator and heat.

While there are still challenges when implementing this solution on a wide scale basis, the real challenge ahead is to identify the optimized shapes for precast deck panels and joints for various deck arrangements. When optimized configurations are determined, precasters, manufacturers and contractors can invest in the formwork and equipment to economically produce these solutions. The true economics of these systems will eventually bring value to highway users through standard mass production of optimized shapes and systems and ultimately, years of low maintenance usage.
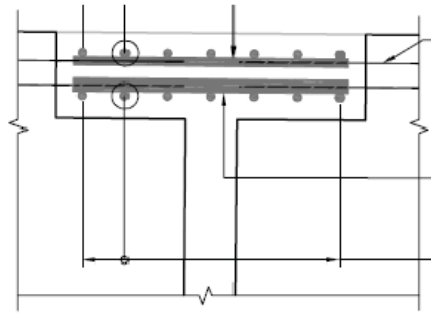
Fig.Ap3.34. Section detail showing reinforcing

Fig.Ap3.35. End of box girders showing reinforcing and exposed aggregate roughening to enhance

Appendix 4.
Proportions in shell design

For the analysis of spherical shell structures the geometrical parameters and their proportions are presented in this appendix.
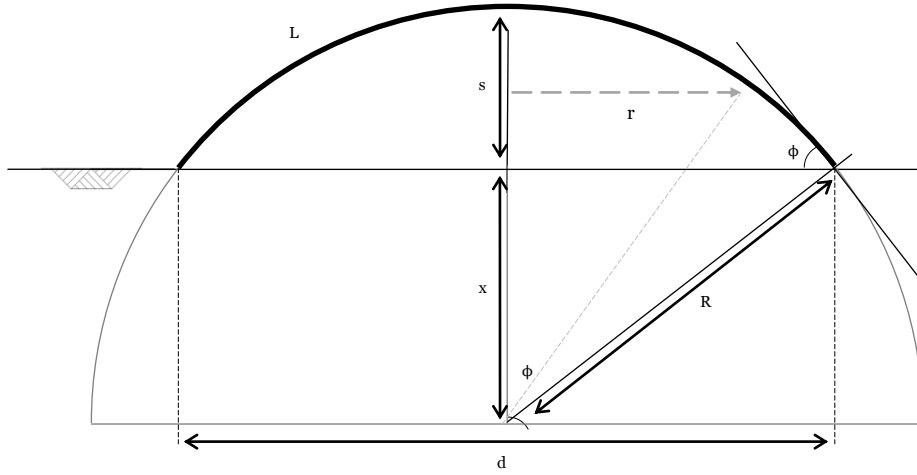
Fig.Ap4.1. Proportions in shell design

The geometric term sagitta (s) refers to the depth, often called height of rise, of an arch. The sagitta, meaning "arrow" in Latin, can also be used for the geometry of shells. Defined by the following, where 's' equals sagitta, 'R' (or sometimes called 'a') equals the radius of the circle, 't' is the shell thickness, 'd' is the span across the base of the arc, 'ϕ' the angle of aperture and 'L' the arch length, it is found that:

$$x^2 + \left(\frac{1}{2}d\right)^2 = (R-s)^2 + \left(\frac{1}{2}d\right)^2 = R^2$$

$$-2Rs + s^2 + \frac{1}{4}d^2 = 0$$

$$R = \frac{-s^2 - \frac{1}{4}d^2}{-2s} = \frac{1}{2}s + \frac{1}{8}\frac{d^2}{s}$$

$$r = d\sin\phi_n$$

Subsequently, it is found that:

$$s = R - \sqrt{R^2 - \frac{1}{4}d^2}$$

$$d = \sqrt{8Rs - 4s^2}$$

$$\phi = \sin^{-1}\left(\frac{d}{2R}\right)$$

In addition:

$$L = \left(\frac{2\phi}{360}\right) \cdot 2\pi R = \frac{\phi\pi R}{90} \qquad \text{and:} \qquad d = 2R\sin\left(\frac{90L}{\pi R}\right)$$

Given: Surface of sphere segment: $A = 2\pi Rs$

Numerical values

From the defined proportions it is interesting to see what these formulas entail for the geometry of spherical shells. The tables give the results for the sagitta (s), radius (R) and opening angle (φ), as a result of a given span (d) and the ratio span to sagitta (d/s). The values for d, s and R are in meter, φ in degrees.

The theoretical turnover point, found in [part B 2.1.4.], is highlighted in bold. The most common span to sagitta ratios are between 6 and 10. Larger values for (d/s) lead to flat shells with low curvature, which is negative for the shell stability.

	d/s	d 50			100			150			200		
		s	R	φ	s	R	φ	s	R	φ	s	R	φ
Hemisphere	2	25,00	25,00	90,00	50,00	50,00	90,00	75,00	75,00	90,00	100,00	100,00	90,00
	3	16,67	27,08	67,38	33,33	54,17	67,38	50,00	81,25	67,38	66,67	108,33	67,38
	4	12,50	31,25	53,13	25,00	62,50	53,13	37,50	93,75	53,13	50,00	125,00	53,13
Theoretical Turnover	**4,1163**	12,15	31,80	51,83	24,29	63,60	51,83	36,44	95,40	51,83	48,59	127,20	51,83
	5	10,00	36,25	43,60	20,00	72,50	43,60	30,00	108,75	43,60	40,00	145,00	43,60
	6	8,33	41,67	36,87	16,67	83,33	36,87	25,00	125,00	36,87	33,33	166,67	36,87
	7	7,14	47,32	31,89	14,29	94,64	31,89	21,43	141,96	31,89	28,57	189,29	31,89
	8	6,25	53,13	28,07	12,50	106,25	28,07	18,75	159,38	28,07	25,00	212,50	28,07
	9	5,56	59,03	25,06	11,11	118,06	25,06	16,67	177,08	25,06	22,22	236,11	25,06
Flat shells	10	5,00	65,00	22,62	10,00	130,00	22,62	15,00	195,00	22,62	20,00	260,00	22,62
	11	4,55	71,02	20,61	9,09	142,05	20,61	13,64	213,07	20,61	18,18	284,09	20,61
	12	4,17	77,08	18,92	8,33	154,17	18,92	12,50	231,25	18,92	16,67	308,33	18,92

Appendix 5.
Comparison theory & FEM

The Finite Element Method and the Scia Engineer software are described in part C. Before the utilization of the software in the design phases, some results from the theory of shells, treated in part B of this report, are cross-checked with results from Scia Engineer.

The results for a hemispherical shell are discussed. The hypothesis considering the opening angle and circumferential stress can hereby be checked. Also the results for linear buckling are checked.

App 5.1. Model

For this test model the next parameters are chosen:

Diameter d:	100m
Material :	UHPC with E_{mod} = 60GPa
Supports:	Rolled supports; horizontally fixed at top
Loading:	Dead weight
Net:	2.0m
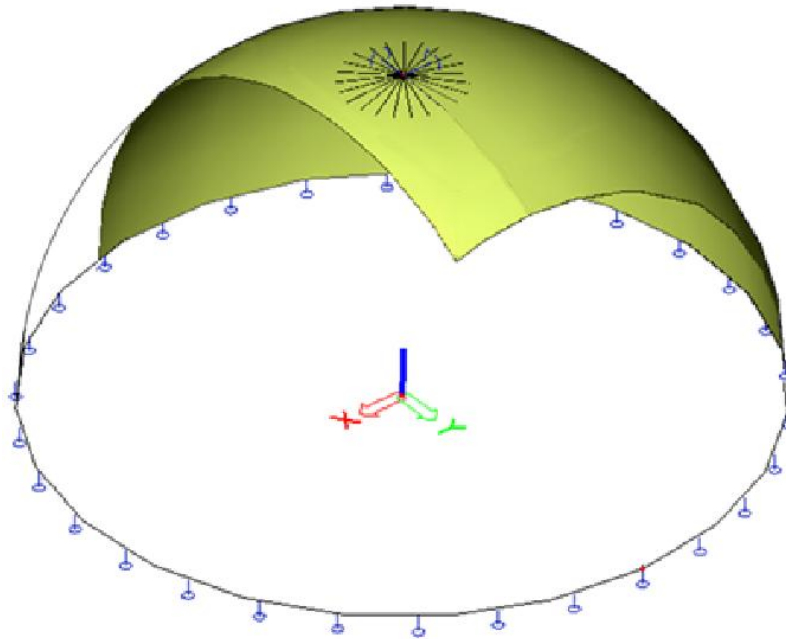
Fig.App5.1.   Analysis model

App 5.2. Results Linear Analysis

<u>Membrane Stress Resultants</u>

The results, following from a Mindlin calculation, show:
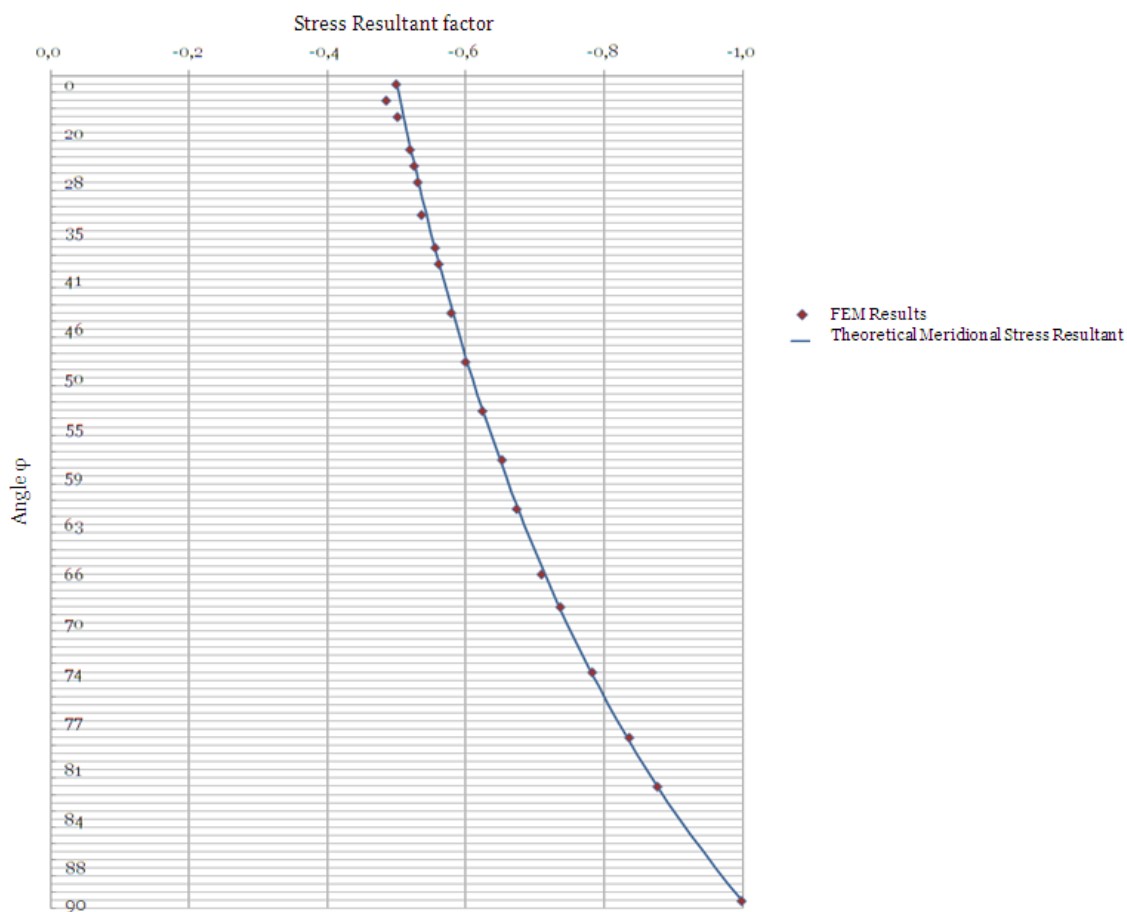
Fig.App5.2.   Results of meridional stress (normalized)
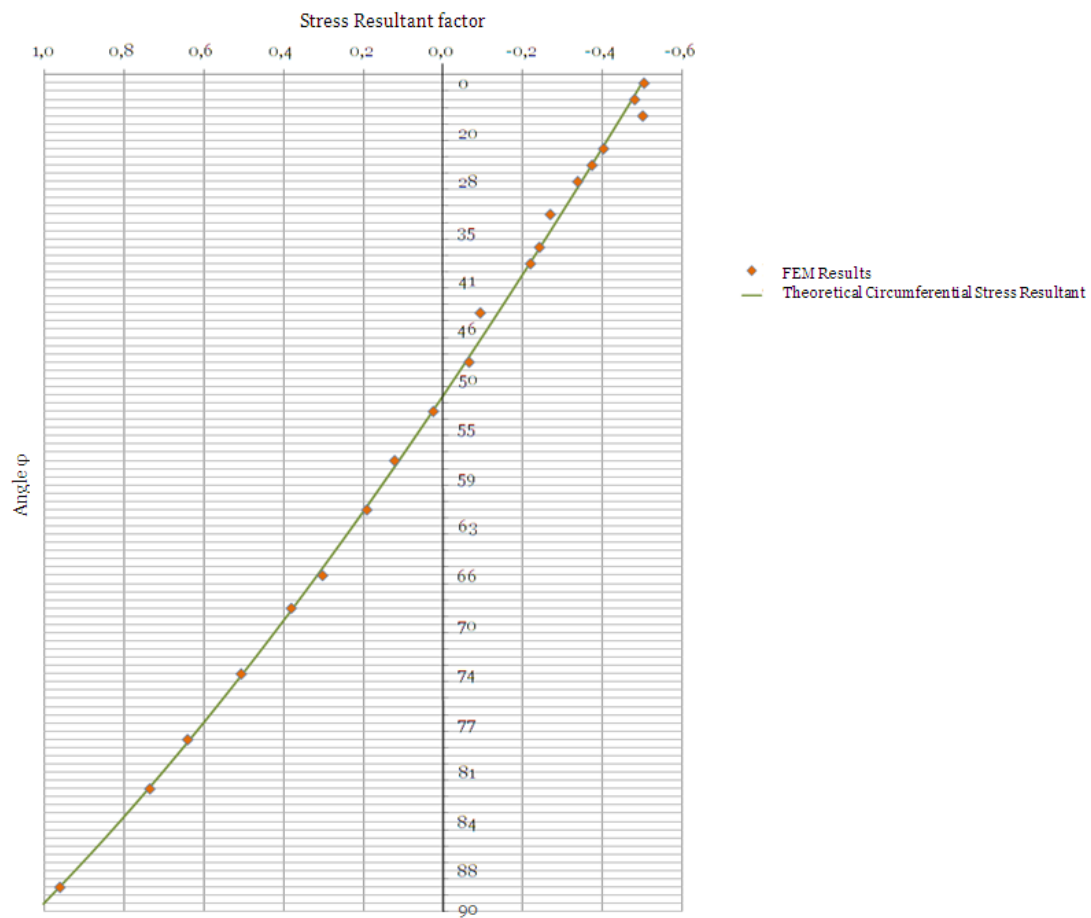
Fig.App5.3.   Results of Circumferential stress (normalized)

From figure App5.2 and figure App5.3 it is concluded that both the FEM-results for the meridional and the circumferential stress show little discrepancy with the theoretical approach. Therefore the FEM results, with the given settings, are considered to be validated for the research.

App 5.3. Linear Buckling Analysis

The linear buckling load for spherical shells of revolution, loaded perpendicular to their surface, was found to be described a simple formula (Formula 2.3.1.1.) as described in part B.

$$p_{cr}^{lin}[N/m^2] = \frac{-2}{\sqrt{3(1-v^2)}}\frac{Et^2}{R^2} \approx -1,16\frac{Et^2}{R^2}$$

(Formula 2.3.1.1.)

The noticeable fact is that the order of magnitude of the buckling load is merely dependent of the radius of the shell. In this appendix it is chosen to compare the FEM results for a hemispherical shell with the theoretical prediction of the linear critical buckling load.

The shell is loaded with two stability combinations which consider loading perpendicular to the surface and loading in vertical direction. Both loads have a magnitude of -1 kN/m².

Load case 1
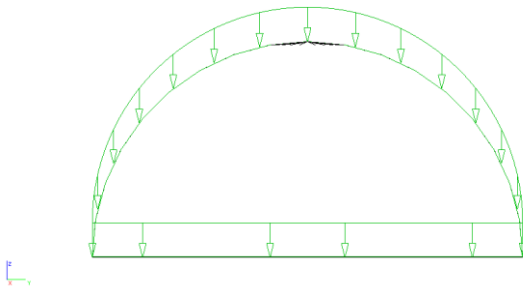
Load case 2
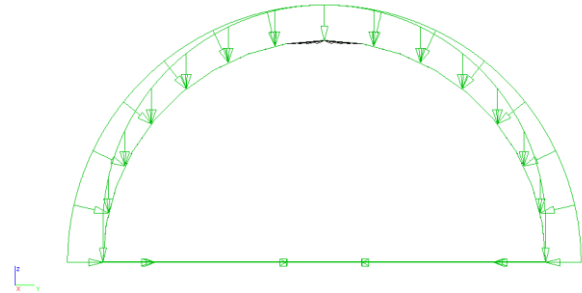
The critical load for load case 2 is predicted by:

$$p_{cr}^{lin} = -1,16\frac{Et^2}{R^2} = -1,16\frac{60.10^9.0,2^2}{25^2} = -4454,4kN/m^2$$

The results, following from a Mindlin calculation, show:

Kritische belastingcoëfficiënten		
Studentenversie *Studentenversie* *Studentenversie* *Si		
N		f
-		[]
Studentenversie *Studentenversie* *Studentenversie*		
Stabiliteit combinatie : S1		
1		2670,54
2		2680,17
3		2680,17
4		2749,46
Stabiliteit combinatie : S2		
1		4546,42
2		4558,55
3		4562,37
4		4575,13

Fig.App5.2.   First buckling pattern for load case 2

The results for this particular model have an overestimation of 2.1% compared to the theoretical buckling load. It is concluded that the linear stability calculation from Scia Engineering gives satisfying results.

Appendix 6.
Ductal properties

6.1. Product data sheet Ductal BS1000

Applied UHPC for research

BS1000

PRODUCT DATA SHEET

Ductal®

LAFARGE
bringing materials to *life* ™

BS1000

structural solutions for columns, long
span roofs/floors, seismic elements,
wall panels and modular precast systems

An exceptional material choice for innovative structural elements that are extremely durable, cost effective and require very little maintenance.

Ductal® is an ultra-high performance, composite material that provides strength, ductility, durability and aesthetics. This unique combination of superior properties facilitates the ability to create innovative designs with new shapes that are thinner, lighter and more graceful.

Reinforced with steel fibers, Ductal® BS1000 is significantly stronger than conventional concrete (with strengths similar to some metals) and performs better in terms of abrasion and chemical resistance, freeze-thaw, carbonation and chloride ion penetration.

Because of its optimized gradation of the raw material components, Ductal® is denser than conventional concrete. This "denseness", along with nanometer sized non-connected pores throughout its cementitious matrix, also attributes to its remarkable imperviousness and durability against adverse conditions or aggressive agents.

PHYSICAL PROPERTIES

Characteristic Values for Design						
	Test Data				Design Values	
	Mean		Standard Deviation			
	MPa	psi	MPa	psi	MPa	psi
Compression	180	26,000	12	1,800	150	22,000
Flexural	35	5,000	5	700	--	--
Direct Tension f_t	10	1,450	1	145	8	1,160
σ_{tk}	12	1,800	2	300	8	1,160
	GPa	ksi	GPa	ksi	GPa	ksi
Youngs Modulus	60	8,700	2	300	55	8,000

BS1000

DURABILITY

- Chloride Ion diffusion — $0.02 \times 10^{-12} m^2/s$
- Carbonation penetration depth — <0.5 mm
- Freeze/thaw (after 300 cycles) — 100%
- Salt-scaling — <0.10 g/m^2
- Abrasion (relative volume loss index) — 1.2

OTHER PROPERTIES

- Density — 2.4 – 2.6 S.G.
- Capillary porosity (>10mm) — <1%
- Total porosity — 2 – 6%
- Post cure shrinkage — $<10^{-5}$
- Creep coefficient — 0.2-0.5

COMPONENTS

A) Premix — silica fume, ground quartz, sand, cement
B) High tensile steel fibers — 0.2 mm (0.008 in) diameter x 14 mm (0.5 in) long (>2000 MPa/ 290 psi)
C) Admixture — high range water reducer/ 3rd generation
+ Water and/or ice

BATCHING

High shear mixers and temperature controlled environments are recommended to successfully produce Ductal® BS1000.

THERMAL TREATMENT

Thermal treatment of 90ºC (195ºF), at 90% relative humidity for 48 hours, is applied after final set produces the required design strength and durability characteristics. For fire rated structures, the Ductal® AF formula is available and provides fire performance similar to normal concrete.

MOLDING

The fineness of Ductal® raw materials and fluidity of the mix facilitates the ability to replicate the micro-texture of the form surface or special mold textures.

PLACING

Ductal® should be placed in a controlled precast environment. Placing techniques include: gravitational flow, injection or auguring.

PRE-STRESSING

The strength of Ductal® allows for solutions to be designed with smaller elements, without the use of passive reinforcement (reinforcing steel), prestressing will further enhance and optimize the designed solution.

Add value with Ductal® BS1000

- superior strength
- ductility
- freeze/thaw resistance
- design flexibility
- longer spans
- shallow, thin, lightweight structures
- reductions in foundations
- faster construction
- reduce or eliminate passive reinforcing
- increased usage life
- improved seismic performance
- impact resistance
- abrasion resistance
- dimensional stability
- lower permeability
- low chloride ion diffusion
- reduced maintenance

Lafarge Canada Inc.
1200, 10655 Southport Road S.W.
Calgary, Alberta, Canada T2W 4Y1
Email: ductal@lafarge-na.com • Tel: 403-271-9110
Toll free: 1-866-238-2825 • www.imagineductal.com

Post Consumer

LAFARGE

6.2. Product data sheet Ductal JS1000

UHPC Field-cast joint fill solution

PRODUCT DATA SHEET

JS1000

Ductal®

LAFARGE
bringing materials to *life* ™
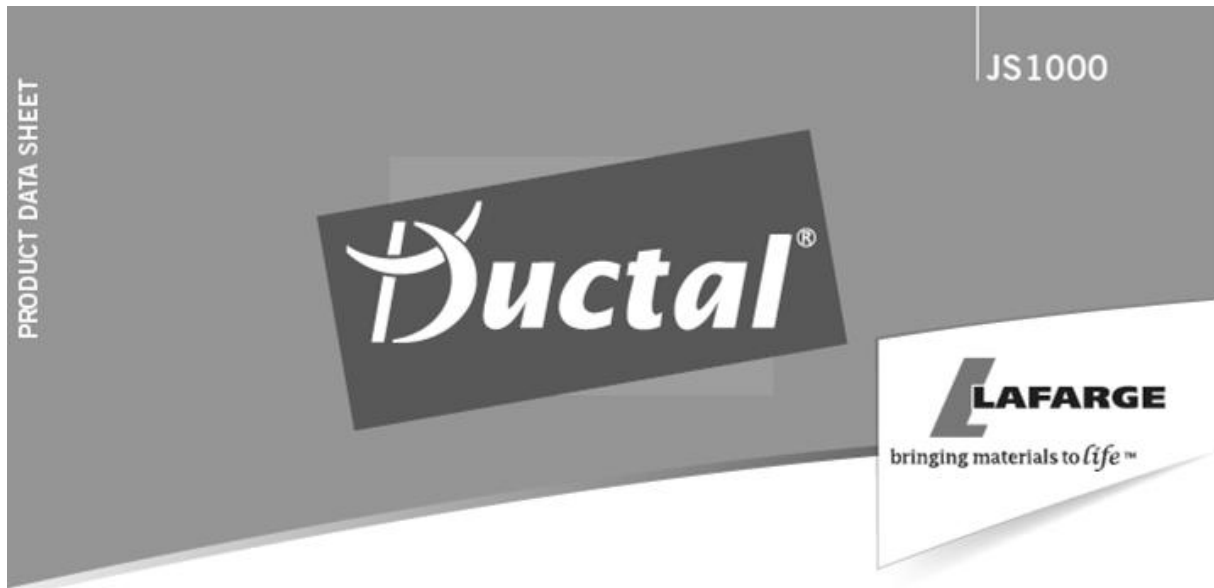
JS1000

field-cast joint fill solutions
for precast deck panel bridges

Ductal® JS1000 offers a combination of superior properties including strength, durability, fluidity and increased bond capacity. By utilizing these superior properties in conjunction with precast deck panels, engineers can create optimized solutions for advanced precast bridge deck systems – with simplified fabrication and installation processes.

Reinforced with steel fibers, Ductal® JS1000 is significantly stronger than conventional concrete and performs better in terms of abrasion and chemical resistance, freeze-thaw, carbonation and chloride ion penetration.

Because of its optimized gradation of the raw material components, Ductal® is also denser than conventional concrete. This "denseness", along with nanometer sized non-connected pores throughout its cementitious matrix, attributes to its remarkable imperviousness and durability against adverse conditions or aggressive agents.

PHYSICAL PROPERTIES

	Test Data				Design Values	
Characteristic Values for Design						
	Mean		Standard Deviation			
	MPa	psi	MPa	psi	MPa	psi
Compression	140	20,000	10	1,400	100	14,500
Flexural	30	4,300	5	700	-	-
Direct Tension f_t	8	1,160	1	145	5	725
	GPa	ksi	GPa	ksi	GPa	ksi
Youngs Modulus	50	7,200	2	300	45	6,500

JS1000

DURABILITY

- Carbonation penetration depth: <0.5 mm
- Freeze/thaw (after 300 cycles): 100%
- Salt-scaling: <0.10 g/m²

OTHER PROPERTIES

- Density: 2.4 – 2.6 S.G.
- Capillary porosity (>10mm): <1%
- Total porosity: 2 – 6%
- Creep coefficient: 0.2-0.5

COMPONENTS

A) Premix — silica fume, ground quartz, sand, cement
B) High tensile steel fibers — 0.2 mm (0.008 in) diameter x 14 mm (0.5 in) long (>2000 MPa/ 290 psi)
C) Admixture — high range water reducer/ 3rd generation
+ Water and/or ice

BATCHING

High shear mixers and an ambient temperature above 16ºC (60ºF) are recommended to successfully produce Ductal® JS1000. Onsite technical assistance by a Lafarge representative is recommended.

PLACING

Ductal® JS1000 can be placed by pouring with the use of a bucket, wheelbarrow or buggy. Any exposed Ductal® surfaces should be covered with poly or vapor barriers to prevent surface dehydration.

JOINT REINFORCING

To minimize any corrosion potential of the reinforcing between the precast panel and joints, non-corrosive rebar (such as GFRP or stainless steel) may be used. Black rebar reinforcement may also be utilized for bottom mat connection.

DESIGN

The high strength of Ductal® JS1000 allows for reduced joint widths. When designing a joint using Ductal® JS1000, the characteristic design values can be reached within 96 hours of casting -- as long as ambient temperatures above 16ºC (60ºF) are ensured. Please contact a Lafarge representative when designing joints with Ductal® JS1000.

Add value with Ductal® JS1000

- improved durability
- increased usage life
- superior freeze/thaw resistance
- impact & abrasion resistance
- reduced joint width and complexity
- dimensional stability
- flexural strength
- lower permeability
- superior toughness
- low chloride ion diffusion
- ductility
- faster construction
- improved resistance to continuous flexing across the joints (from truck loads)
- reduced maintenance
- extremely low porosity
- reduced traffic disruption & risk
- cost effective

Lafarge Canada Inc.
1200, 10655 Southport Road S.W.
Calgary, Alberta, Canada T2W 4Y1
Email: ductal@lafarge-na.com • Tel: 403-271-9110
Toll free: 1-866-238-2825 • www.imagineductal.com

Post Consumer

LAFARGE

Ultra High Performance Concrete in Large Span Shell Structures

Calculations Appendix

R.N. ter Maten

Calculations

Calc. 8.1

Sagitta to span ratio

8.1.1. Model

The model is set up as a monolith dome. For these calculations the next parameters hold:

Parameters:	
Span:	d = 150m
Thickness:	t = 100, 200, 300, 400
Supports:	All hinged
Loads:	According to Chapter 5 Load combinations and general vertical load

Variables:	
Sagitta to Span - ratio:	1/2 to 1/10
Design limitations:	
Buckling:	Linear elastic calculation
Stress:	Design capacities UHPC

A figure of a model, with d/s = 4, is presented below:
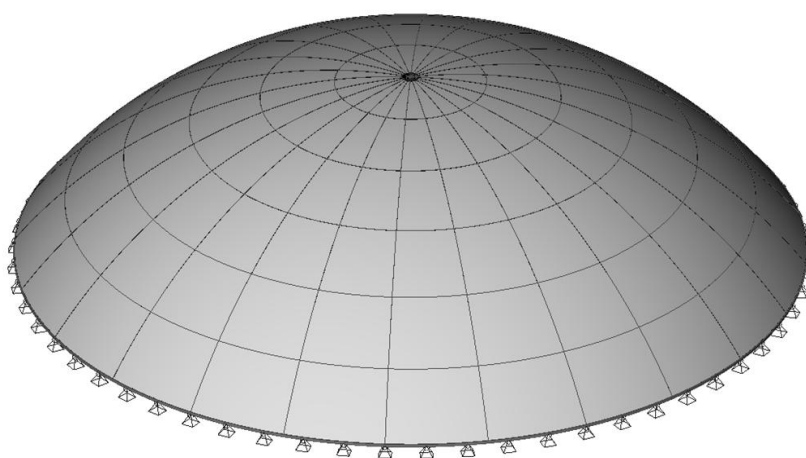
Fig.Calc.7.1.1   FEM-model

8.1.2. Buckling

	Critical perpendicular load [kN/m²]				FEM-result vertical load [kN/m²]				γ –factor
Thickness:	100	200	300	400	100	200	300	400	
Span to sagitta:									
2	120	478	1076	1914	78	300	664	1176	0.627
3	102	408	917	1631	82	336	745	1334	0.814
4	77	306	689	1225	75	276	611	1125	0.919
6	43	172	388	689	45	175	388	688	1.00
8	26	106	238	424	26	106	238	424	1.00
10	18	71	159	283	19	72	162	286	1.00
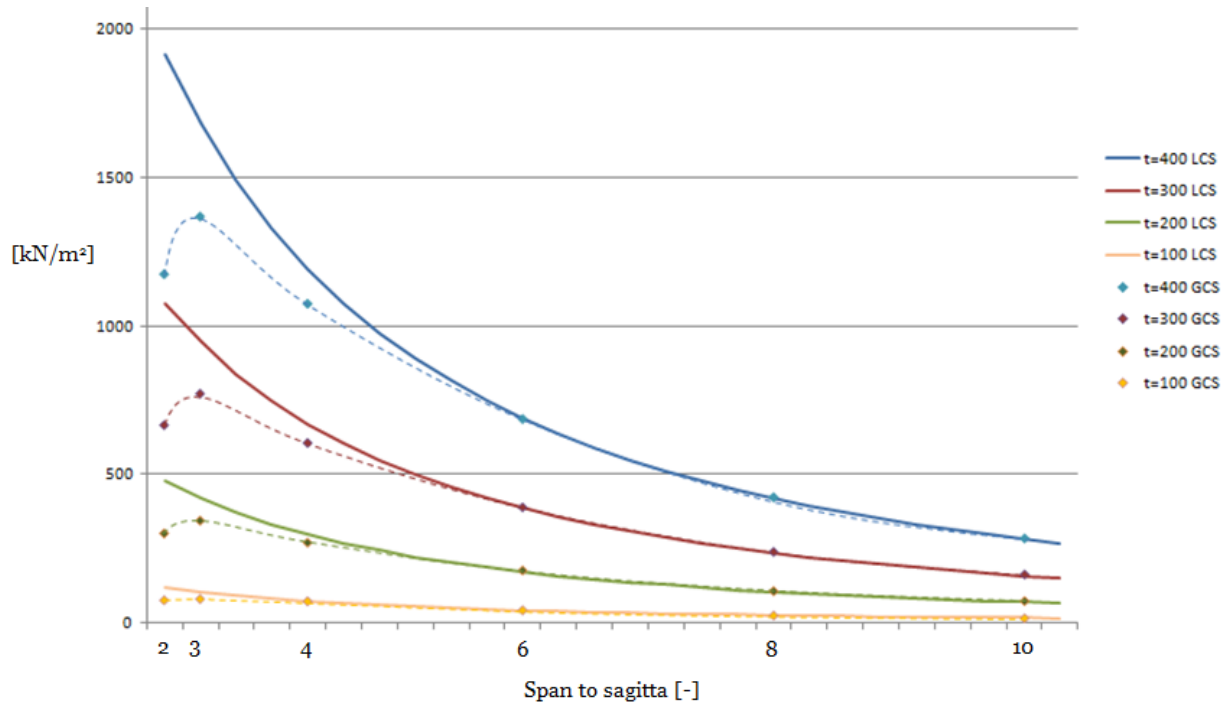
<u>Formula test:</u>

For this calculation the next parameters are chosen:
d/s = 4
d = 150m
R = 93,75m
t =

$$t^2 = (1,2 \cdot 2.75 + 1,5 \cdot 0.45) \cdot \frac{93.75^2 \cdot 6}{58 \cdot 10^6 \cdot 0.919} \cdot \frac{\sqrt{3(1-0^2)}}{2}$$

$$t \geq 58mm$$

t = 58mm
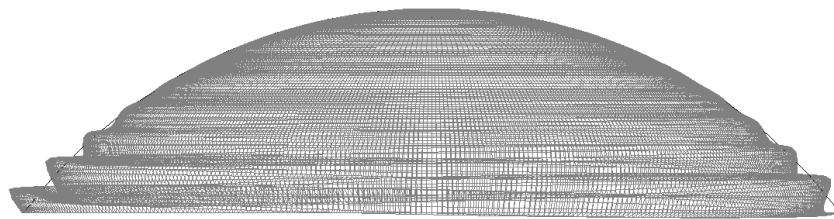
d / s = 4
t = 58mm
P_{vert} = 3,98kN/m²
$\lambda \approx 5,88$

8.1.3. Calculation of shell thickness

Span to sagitta: 04

For this calculation the next parameters hold:

Diameter d: 150m
Sagitta: 150 / 4 = 37,5m
Material: Ductal
Supports: All hinged

The stresses (in N/mm²) due to dead load of the shell are independent of the shell thickness. Other effect are given independent of the thickness when charted in (N/mm).

All maximum and minimum values are found on the x-axis as a result of wind loading in x-direction. This does not hold for meridional stress in case of wind loading. The maximum tension is found at an angle of 50° of the x-axis.

Internal Force distribution
Circumferential stress Nx

	LC Dead load (N/mm2)	LC Wind x (N/mm)	LC Snow. Evenly (N/mm)	LC Snow. Redistr. (N/mm)
Top	-1.3	84.6	-21.0	-16.5
Bottom	-0.3	-90.3 / 20.9	-5.3	-3.1
Max	-	**96.9**	-	6.1
Min	-	-90.3	-	-20.4

SLS Permanent Load. Stress [N/mm²]
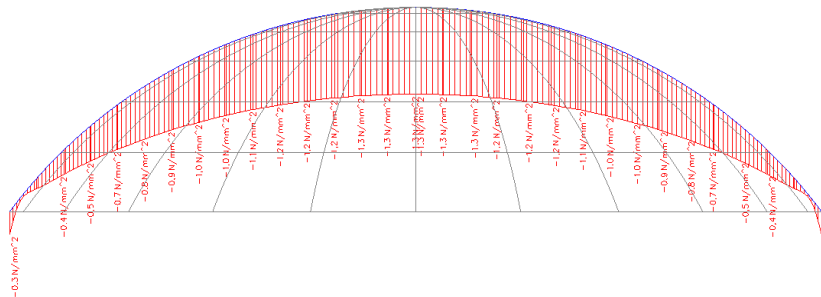
Load cases:
Load case 3: wind x.   Force per unit length [N/mm]
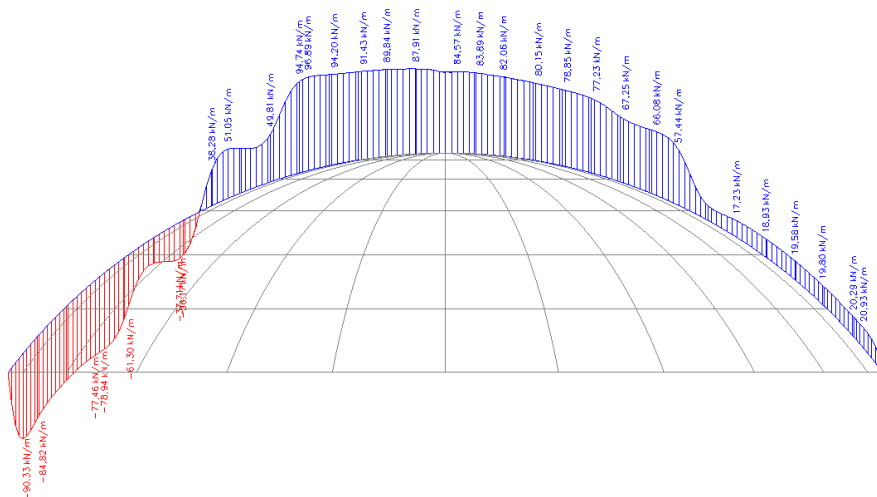
Load case 4: evenly distributed snow.   Force per unit length [N/mm]
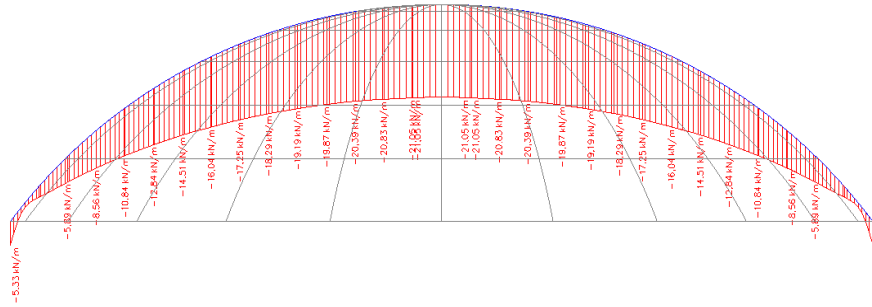
Load case 5: redistributed snow.   Force per unit length [N/mm]
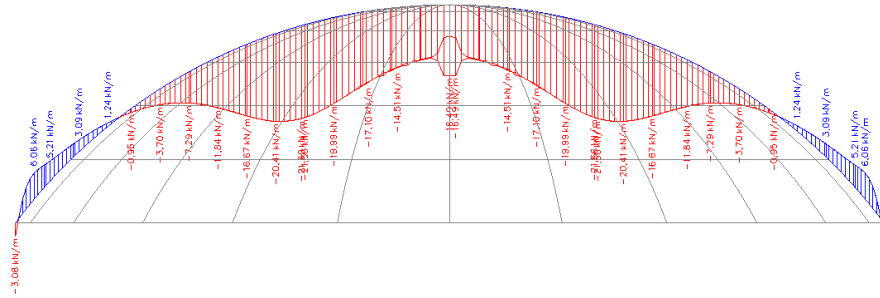
Envelop Circumferential stress Nx for load cases
Minimum:
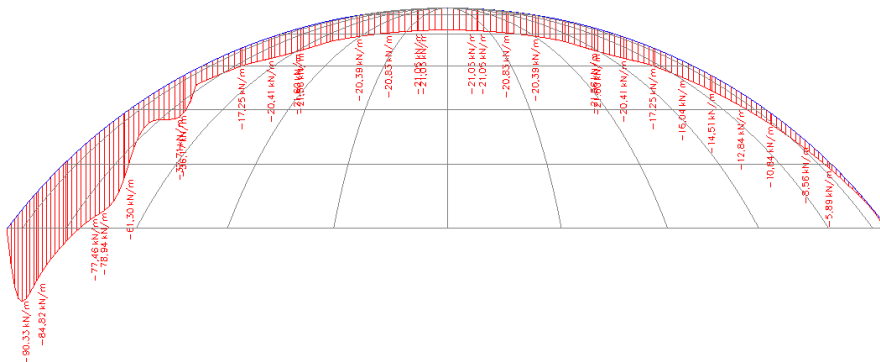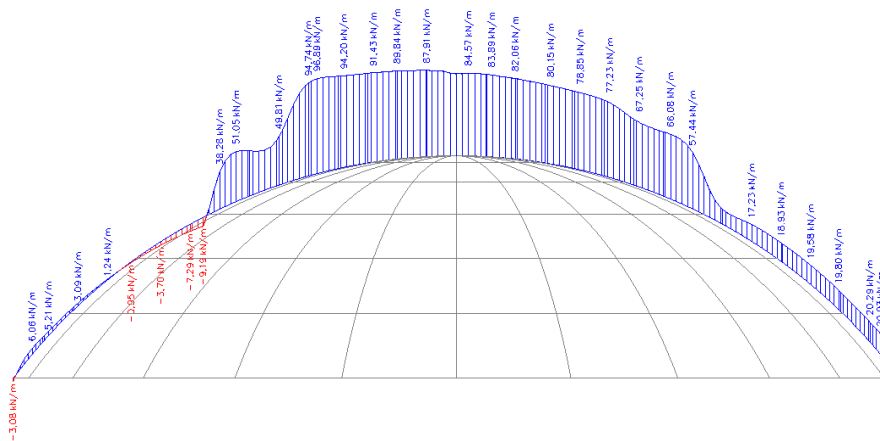
Maximum:

Required thickness

The required thickness is calculated with the maximum occurring tensile and compression due to the independent load cases. The capacity is lowered by the estimated value of the stress due to permanent load at the location of the peak value.

Compression:

$$\frac{f_{d,loadcases}\left[N/mm\right]}{f'_{b}\left[N/mm^2\right]-f_{d,permanent}\left[N/mm^2\right]}=t\left[mm\right]$$

Min. required concrete thickness: $\dfrac{1,5(-90.3)}{-117,7-1.2(-0.10)}=1.2mm$

Tension:

$$\frac{f_{d,loadcases}\left[N/mm\right]}{f_{b}\left[N/mm^2\right]-f_{d,permanent}\left[N/mm^2\right]}=t\left[mm\right]$$

Min. required concrete thickness: $\dfrac{1,5(96.89)}{8-0,9(-1.20)}=27mm$

Internal Force distribution
Meridional stress Ny

	LC Dead load (N/mm2)	LC Wind x (N/mm)	LC Snow. Evenly (N/mm)	LC Snow. Redistr. (N/mm)
Top	-1.3	64.13*	-21.1	-17.2
Bottom	-1.7	-23.3 / 48.9*	-26.5	-15.4
Max	-	99.8	-	-
Min	-	-29.2	-	-1.2

*Not found in wind-direction

SLS Permanent Load. Stress in N/mm²
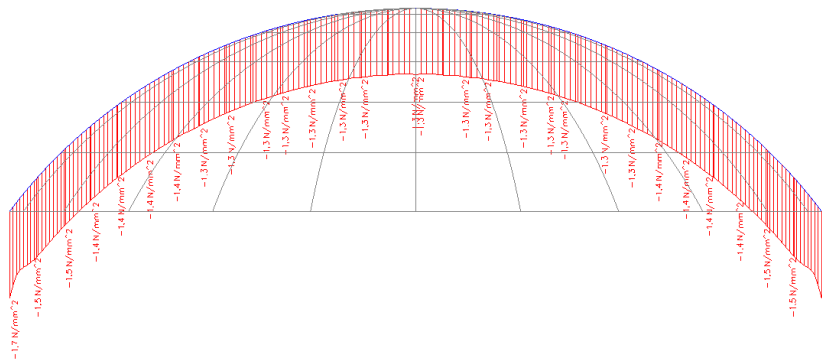
Load case 3: wind x.   Force per unit length [N/mm]
The maximum compression is found by:
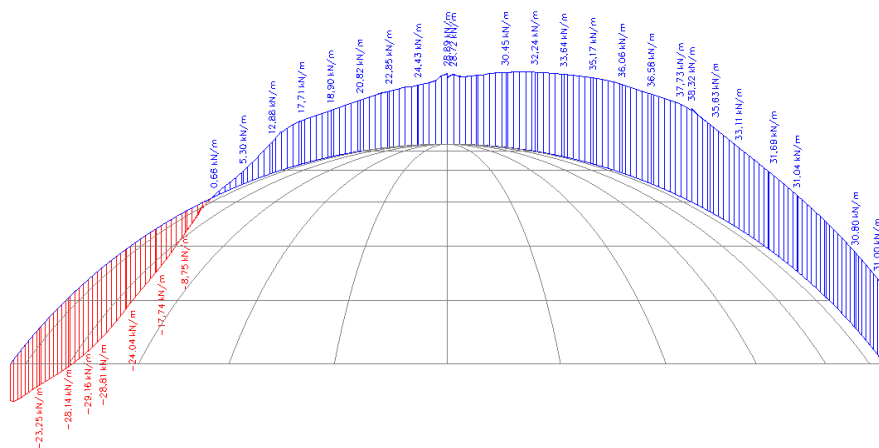
The maximum tension is found by:
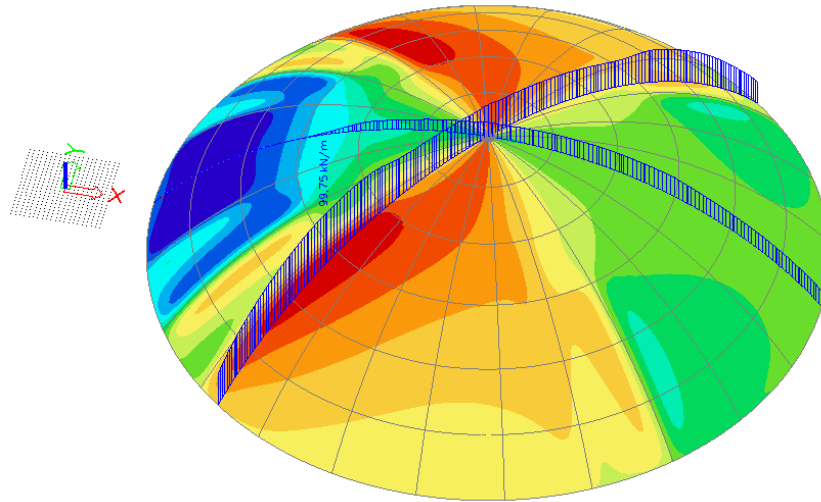
Load case 4: evenly distributed snow.   Force per unit length [N/mm]
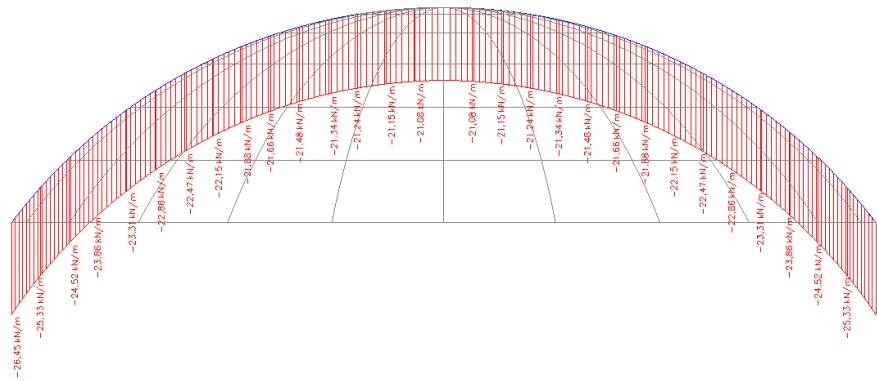
Load case 5: redistributed snow.   Force per unit length [N/mm]
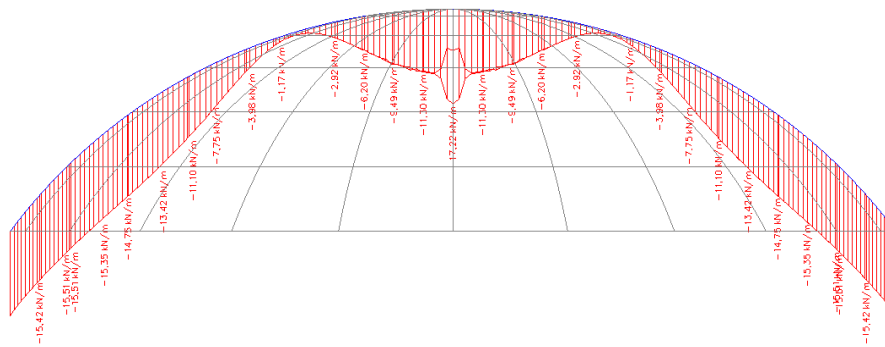
Envelop Circumferential stress Ny for load cases
Minimum:
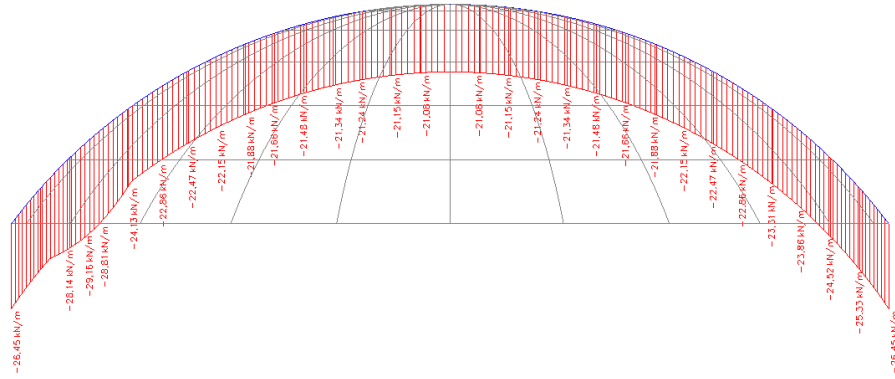
Maximum:
*Not in wind-direction
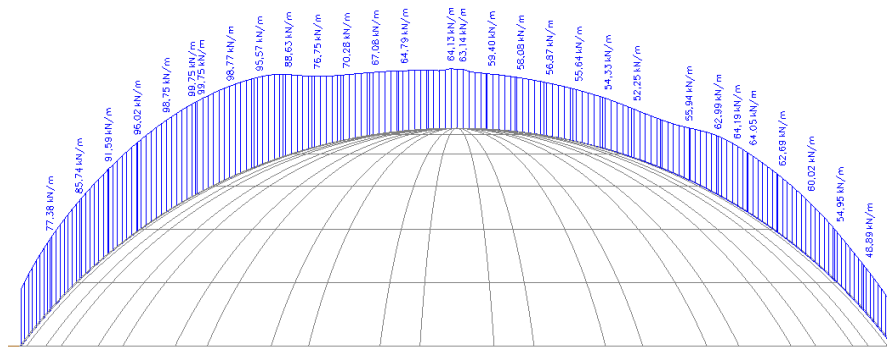
Required thickness

The required thickness is calculated with the maximum occurring tensile and compression due to the independent load cases. The capacity is lowered by the estimated value of the stress due to permanent load at the location of the peak value.

Compression:

$$\frac{f_{d,loadcases}\left[N/mm\right]}{f_b\left[N/mm^2\right]-f_{d,permanent}\left[N/mm^2\right]}=t\left[mm\right]$$

Min. required concrete thickness: $\dfrac{1,5(-29.16)}{-117.7-0.9(-1.40)}=0.4mm$

Tension:

$$\frac{f_{d,loadcases}\left[N/mm\right]}{f_b\left[N/mm^2\right]-f_{d,permanent}\left[N/mm^2\right]}=t\left[mm\right]$$

Min. required concrete thickness: $\dfrac{1,5(99.75)}{4.3-0,9(-1.40)}=27mm$

Calc. 8.2.

Edge ring

8.2.1. Model
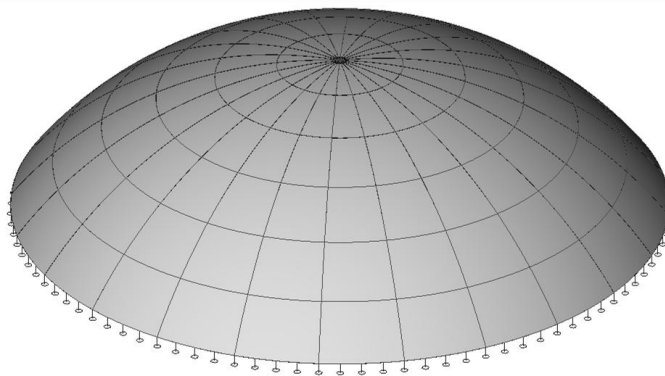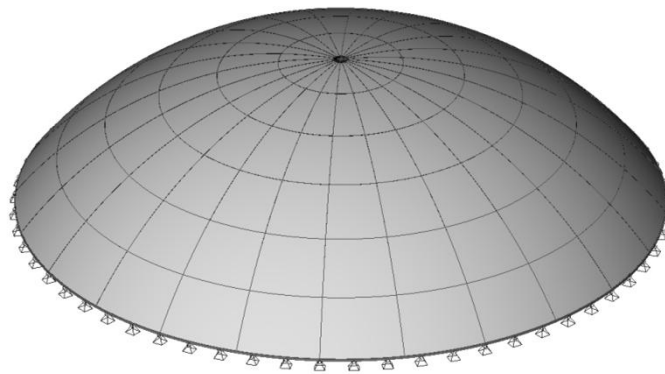
Fig.Calc.7.1.1   FEM-model

Parameters:

Span:	d = 150m
Sagitta:	= ¼ *150 = 37.5m
Overall thickness:	t = 60mm
Supports:	All hinged & All rolled plus edge ring
Loads:	General vertical load

Variables:

Edge ring	Dimensions Material Prestress

Design limitations:

Buckling:	Linear elastic calculation

8.2.1. Model

8.2.2. Results

With the model with hinged supports the horizontal reaction forces for the SLS permanent load are determined.

Horizontal reaction (pressure):   Permanent load (SLS)   61.0 kN/m
                                   Normative combination Snow total (SLS)   76.9 kN/m

It is seen that, for a shell with a thickness of 60mm, the contribution to the ring pressure of the dead load is approximately 80%.

The required prestress force is determined by $N = Q \cdot r_o = 61.0 \cdot 75 = 4575 kN$

It is reasoned that this indication is the required prestress force which causes the displacements due to permanent load in SLS to be restricted to virtually zero. The choice for this prestress force is based on this restriction.

Now the effect on the effect on the buckling load of the shell depends on the stiffness of the edge ring. The results are presented below.

Material	Cross-section [h x w]	Buckling load factor (β)	Buckling load
C90/105	500 x 500	0,54	14.8
C90/105	600 x 600	0.67	18.4
C90/105	750 x 750	0.82	22.5
C90/105	850 x 850	0.86	23.6
C90/105	1000 x 1000	0.94	25.7
C90/105	1500 x 1500	1.00	27.4
C90/105	2000 x 2000	1.00	27.4

Calc. 8.3.

Ribs & Stiffeners

8.3.1. Model

The model is set up as a ribbed dome, as described in chapter 7.5. For these calculations the next parameters hold:

Parameters:	
Span:	d = 150m
Sagitta:	= ¼ *150 = 37.5m
Overall thickness:	t = 60mm
Supports:	All hinged
Loads:	Buckling load
Width ribs & stiffeners:	60mm

Variables:	
Thickness distribution:	According to table Dx.
Design limitations:	
Buckling:	Linear elastic calculation

Figure of the model is presented below:
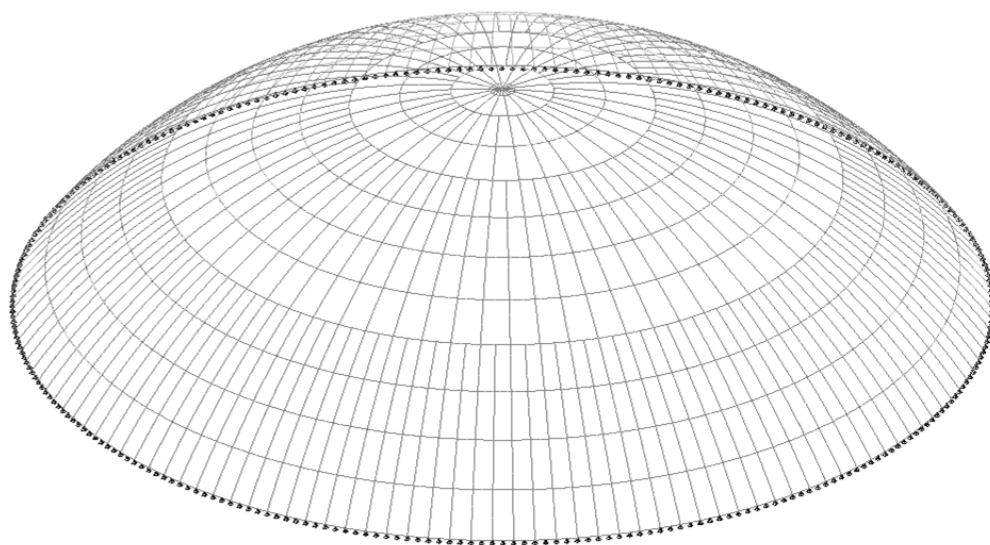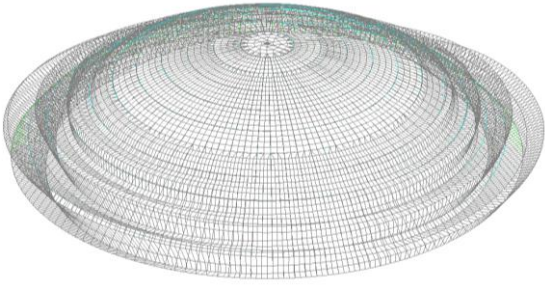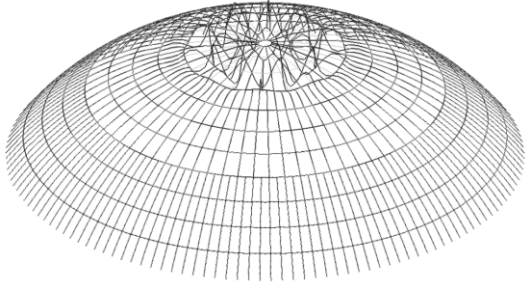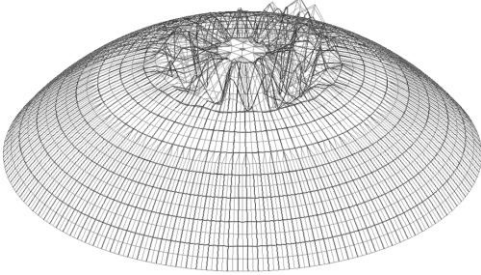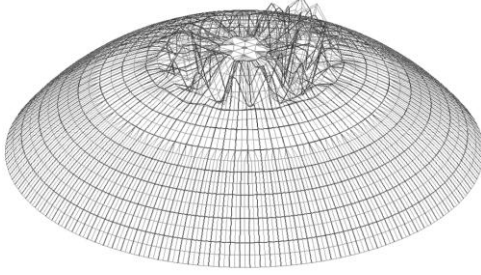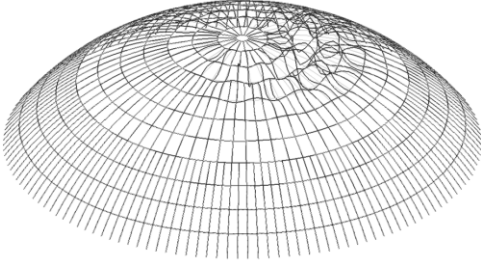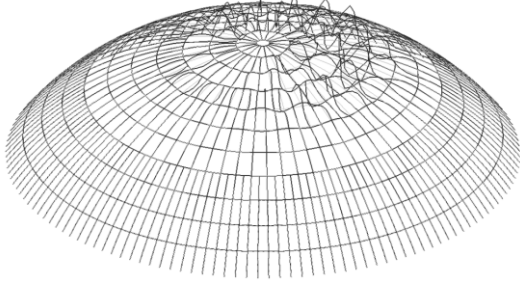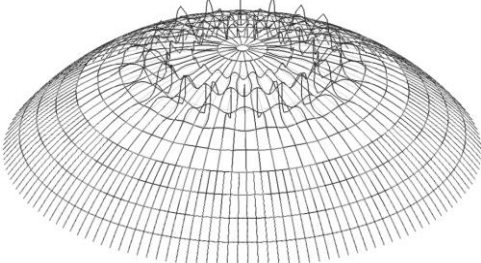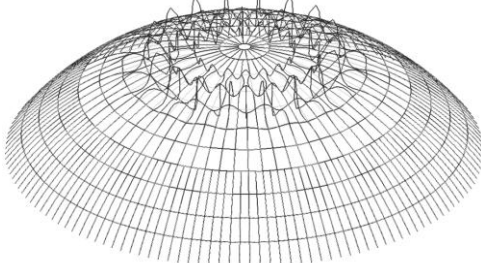
Fig.Calc.7.3.1   FEM-model for calculations [Elements & Ribs]

8.3.2. Results

Case 0. t = 60mm. h = 0mm P = 25 kN/m²	Case 1. t = 60mm. h = 60mm P = 27.5 kN/m²
Case 2. t = 60mm. h = 120mm P = 31.1 kN/m²	Case 3. t = 60mm. h = 180mm P = 35.8 kN/m²
Case 4. t = 60mm. h = 240mm P = 42.5 kN/m²	Case 5. t = 60mm. h = 300mm P = 46.2 kN/m²
Case 6. t = 60mm. h = 360mm P = 48.9 kN/m²	Case 7. t = 60mm. h = 420mm P = 51.6 kN/m²

Results; Comparison to material use

Shell thickness [mm]	Ribs & Stiffeners [mm]	Buckling load [kN/m²]	Weight [MN]	Ratio [Buck.L / W * 100]
60	0	25	38,0	65,8
	60	27,5	39,8	69,2
	120	31,1	41,5	75,0
	180	35,8	43,3	82,7
	240	42,5	45,1	94,3
	300	46,2	46,9	98,5
	360	48,9	48,6	100,6

To see the effect of the ratio for other shell thickness multiple configurations are iteratively tested:

Shell thickness [mm]	Ribs & Stiffeners [mm]	Buckling load [kN/m²]	Safety factor LC5	Weight [MN]
30	240	14.5	5.9	28.8
30	360	16.6	6.8	32.4
35	150	16.1	5.7	28.9
35	180	17.5	6.2	29.8
40	100	17.1	6.1	30.1
40	120	18.1	6.3	30.7
50	120	26.8	8.5	36.1
50	150	29.2	8.9	37.0

The chosen configuration is compared to a shell with constant thickness to illustrate the positive effect of rib stiffening

Shell thickness [mm]	Ribs & Stiffeners [mm]	Buckling load [kN/m²]	Safety factor LC5	Weight [MN]
35	180	17.5	6.2	29.8
44	0	13.8	4.3	29.4
		27% increase	44% increase	

Calc. 8.4

Edge thickness

8.4.1. Model

The model is set up as a monolith dome. For these calculations the next parameters hold:

Parameters:	
Span:	d = 150m
Sagitta:	= ¼ *150 = 37.5m
Overall thickness:	t = 60mm
Loads:	According to Chapter 5

Variables:	
Thickness distribution:	According to tables appendix Calculations 8.4
Design limitations:	
Buckling:	Linear elastic calculation

A figure of the model is presented below:
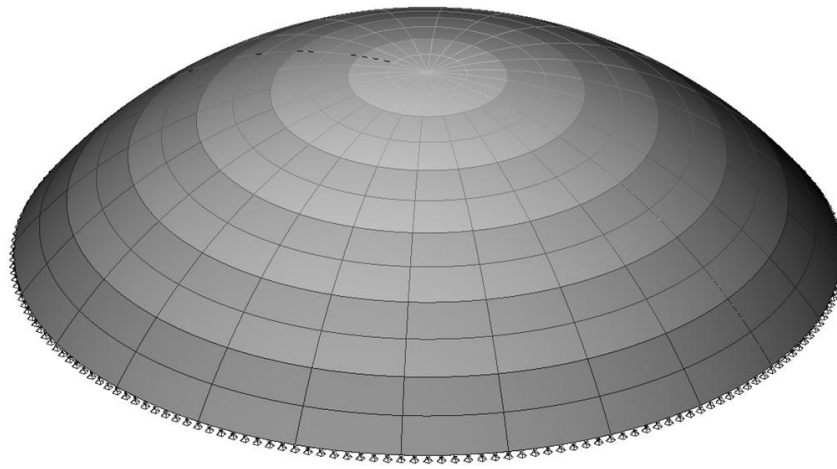
Fig. Calc4.1   FEM-model

8.4.2. Results

The increase of material use is first set to an extra of 60mm, which is equally spread over multiple variants. This implies an overall material increase of approximately 9,1%.

	Case 0	Case 1	Case 2	Case 3	Case 4	Case 5	Case 6	Case 7	Case 8
t1	60	120	90	80	75	72	70	68,6	67,5
t2	60	60	90	80	75	72	70	68,6	67,5
t3	60	60	60	80	75	72	70	68,6	67,5
t4	60	60	60	60	75	72	70	68,6	67,5
t5	60	60	60	60	60	72	70	68,6	67,5
t6	60	60	60	60	60	60	70	68,6	67,5
t7	60	60	60	60	60	60	60	68,6	67,5
t8	60	60	60	60	60	60	60	60	67,5
t9	60	60	60	60	60	60	60	60	60
t10	60	60	60	60	60	60	60	60	60
t11	60	60	60	60	60	60	60	60	60

	Case0	Case1	Case2	Case3	Case4	Case5	Case6	Case7	Case8
Buck.load [kN/m²]	28.6	31.3	32.0	32.6	32.9	32.9	32.9	32.9	32.9
Relative increase [%]		9,4	11,9	14,0	15,0	15,0	15,0	15,0	15,0

Tab.Calc4.1   Results for material increase of 60mm

Case 1	Case 2
Case 3	Case 4 to Case 8
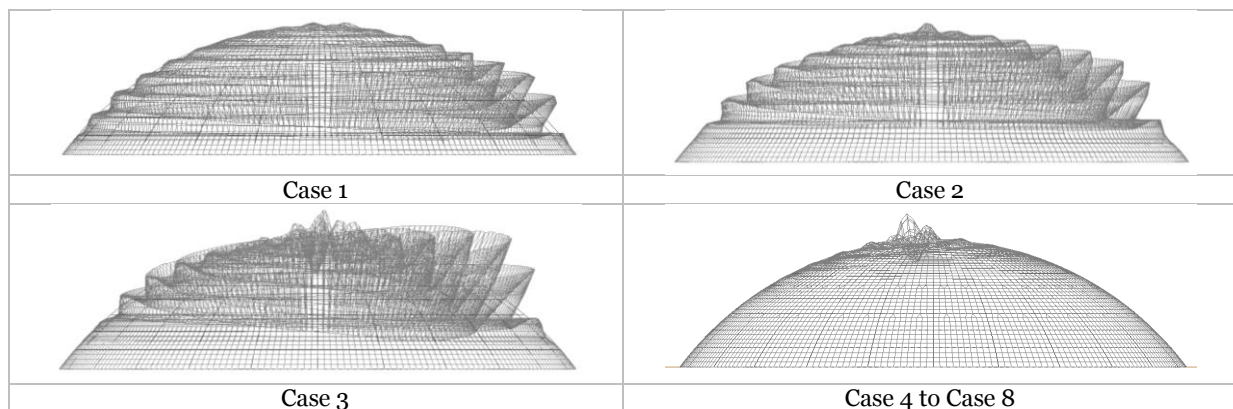
Fig. Calc4.2   Buckling mode for Case 1 to Case 8

Optimization

The conclusion, stating that which was a result of the calculation above is tested for other configurations. Again the principle of a material increase is applied and its held constant, meaning the extra material is spread out over a number of elements.

	Case 0	Case 3x1	Case 4x1	Case 5x1		Case 3x2	Case 4x2	Case 5x2		Case 3x3	Case 4x3	Case 5x3
t1	60	70	67,5	66		67,5	65,6	64,5		65	63,8	63
t2	60	70	67,5	66		67,5	65,6	64,5		65	63,8	63
t3	60	70	67,5	66		67,5	65,6	64,5		65	63,8	63
t4	60	60	67,5	66		60	65,6	64,5		60	63,8	63
t5	60	60	60	66		60	60	64,5		60	60	63
t6	60	60	60	60		60	60	60		60	60	60
t7	60	60	60	60		60	60	60		60	60	60
t8	60	60	60	60		60	60	60		60	60	60
t9	60	60	60	60		60	60	60		60	60	60
t10	60	60	60	60		60	60	60		60	60	60
t11	60	60	60	60		60	60	60		60	60	60

	Case 0	Case 3x1	Case 4x1	Case 5x1		Case 3x2	**Case 4x2**	Case 5x2		Case 3x3	Case 4x3	Case 5x3
Buck.load [kN/m²]	28.6	32,4	32,9	32,9		32,3	**32,9**	32,9		32,2	32,0	31,3
Relative increase [%]		13,3	15,0	15,0		12,9	**15,0**	15,0		12,6	11, 9	09,4

Tab.Calc4.2   Results for material optimization

Calc. 8.5.

Connection requirements

8.5.1. Model

The model is set up as a ribbed dome, as described in chapter 7.5. For these calculations the next parameters hold:

Parameters:

Span: d = 150m
Sagitta to Span - ratio: 1/4

Loads: According to Chapter 5

Variables:
-

Figures of the model are presented below:
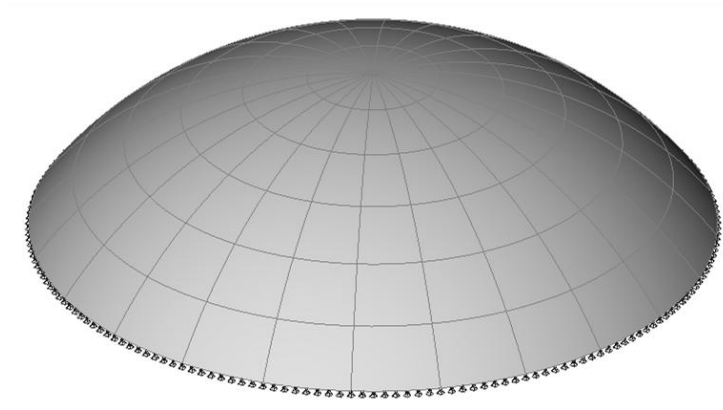
Fig. Calc.5.1.   FEM-model for joint calculations

8.5.2. Results

The maximum tensile stresses are found by the calculations of paragraph 7.1.

Circumferential direction:
SLS Permanent Load. Stress [N/mm²]
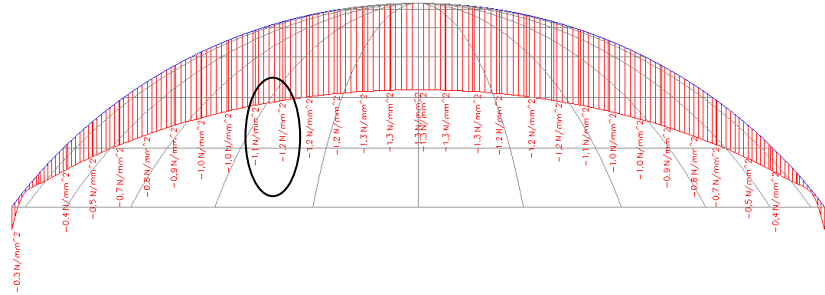
Maximum:
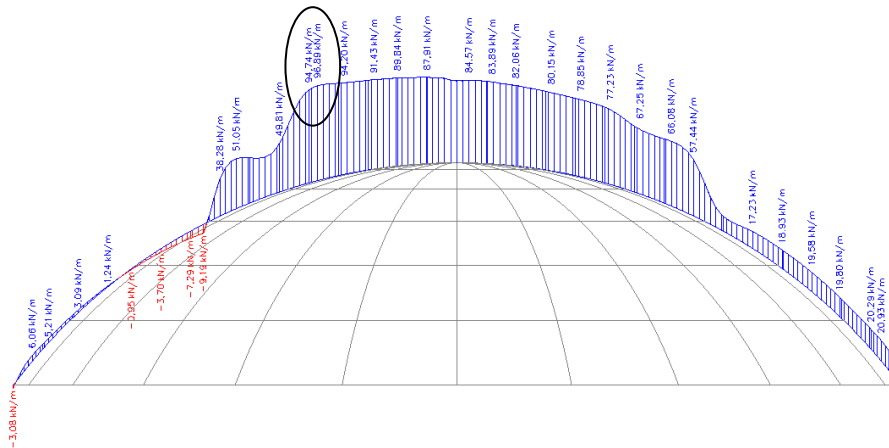
Max. tensile stress:	96.9 N/mm
Stress due to dead load:	1.2 N/mm²

$$t_{req}: \qquad \frac{1,5 \cdot 96,9}{0,9 \cdot 1,2} = 135mm$$

Meridional direction:
SLS Permanent Load. Stress in N/mm²
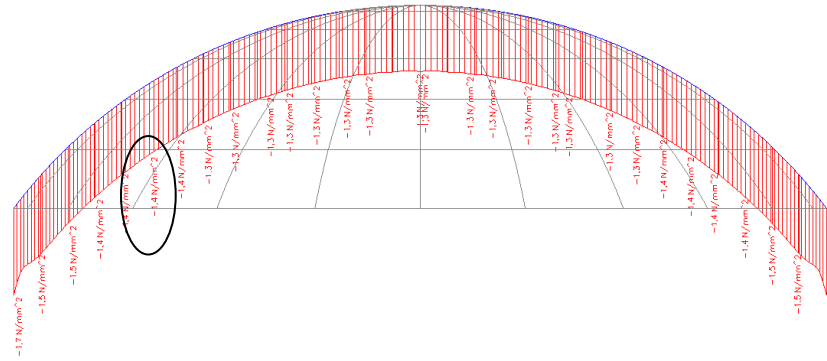
Maximum:
*Not in x-direction
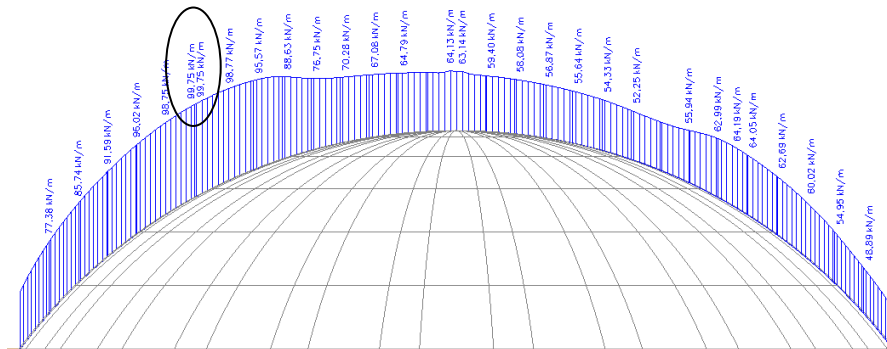
Max. tensile stress: 99.8 N/mm

Stress due to dead load: 1.3 N/mm²

$$t_{req}: \qquad \frac{1,5 \cdot 99,8}{0,9 \cdot 1,3} = 128 \text{mm}$$

If the shell thickness is not increased, for a solid shell of 60mm it holds that the tensile stress are within the order of magnitude:

$$\sigma_{t,meridional} = \frac{1,5 \cdot 99,8}{60} - 0,9 \cdot 1,3 = 1,33 \text{ N/mm}^2$$

$$\sigma_{t,circumferential} = \frac{1,5 \cdot 96,9}{60} - 0,9 \cdot 1,2 = 1,34 \text{ N/mm}^2$$

Moments ; mx
SLS Permanent Load. [kNm/m]
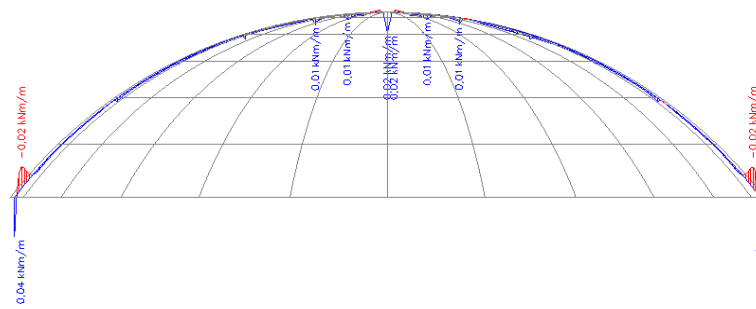
Moments; my
SLS Permanent Load. [kNm/m]
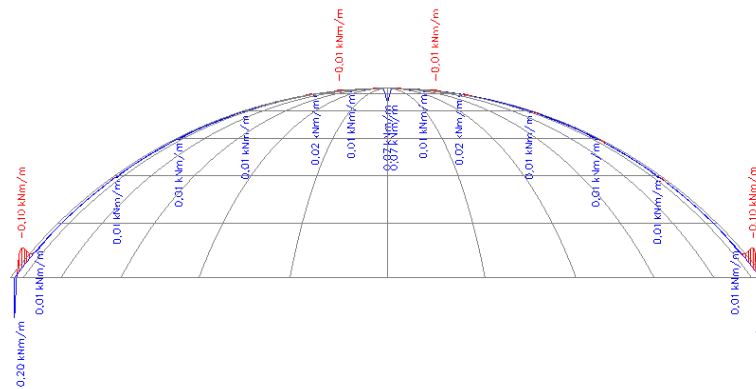
Shear; vx
SLS Permanent Load. [kNm/m]
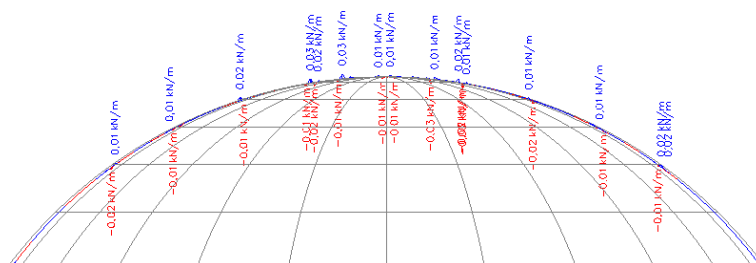
Shear; vx
SLS Permanent Load. [kNm/m]
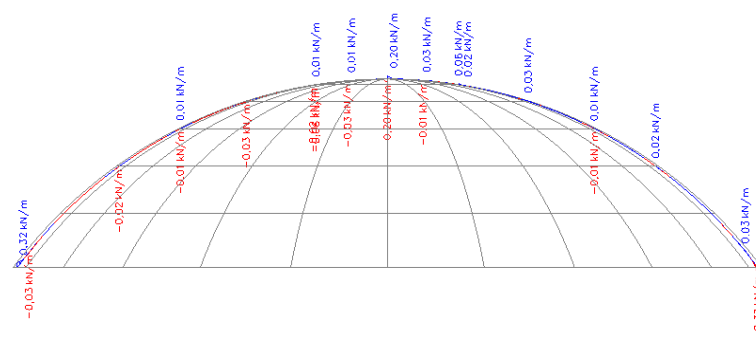
Moments ; mx

Normative Load case: Load case 3: wind x.   Force per unit length [N/mm]
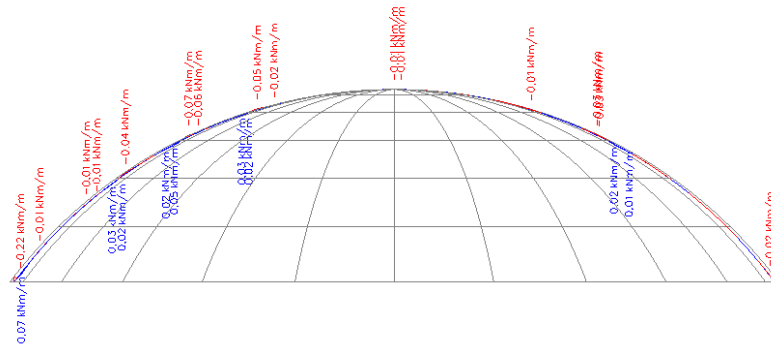
*Not in wind-direction

Moments; my

Normative Load case: Load case 3: wind x.   Force per unit length [N/mm]
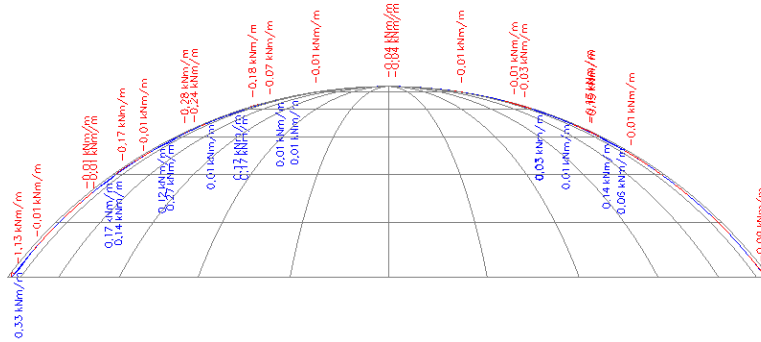
Shear; vx

Normative Load case: Load case 3: wind x.   Force per unit length [N/mm]
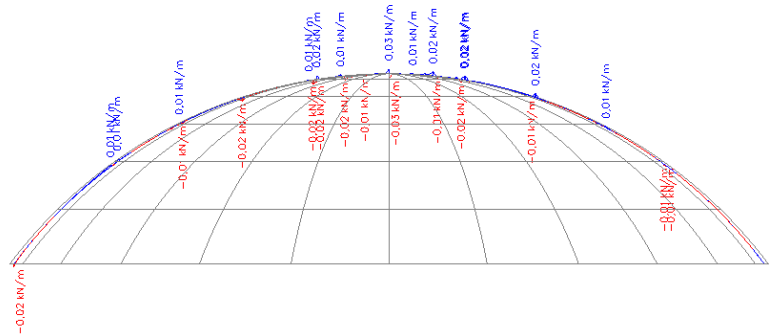
Shear; vx

Normative Load case: Load case 3: wind x.   Force per unit length [N/mm]
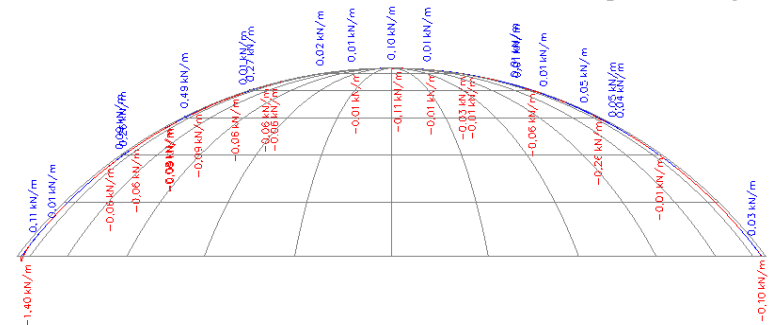
Calc. 8.6.

Dynamic response

8.6.1. Model

The model is set up as a monolith dome. For these calculations the next parameters hold:

Parameters:	
Span:	d = 150m
Thickness:	t = 60 mm
Sagitta to Span - ratio:	1/4
Support:	All hinged

Variables:	-
Design limitations:	Eigenfrequencies

A figure of the model is presented below:
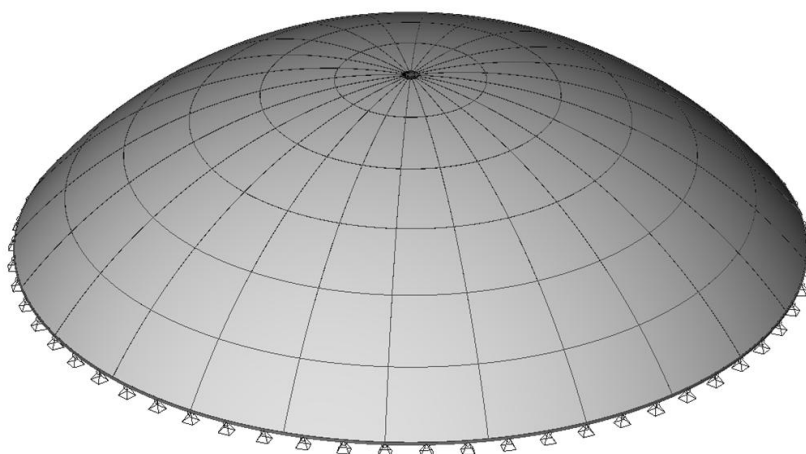
Fig.Calc.6.1   FEM-model for dynamic calculations

8.6.2. Results

Eigenfrequencies Dead weight

Natural frequency	f [Hz]	T [sec]
1	7,54	0.13
2	7,62	0.13
3	7,63	0.13
4	8,09	0.12

Vibration shapes
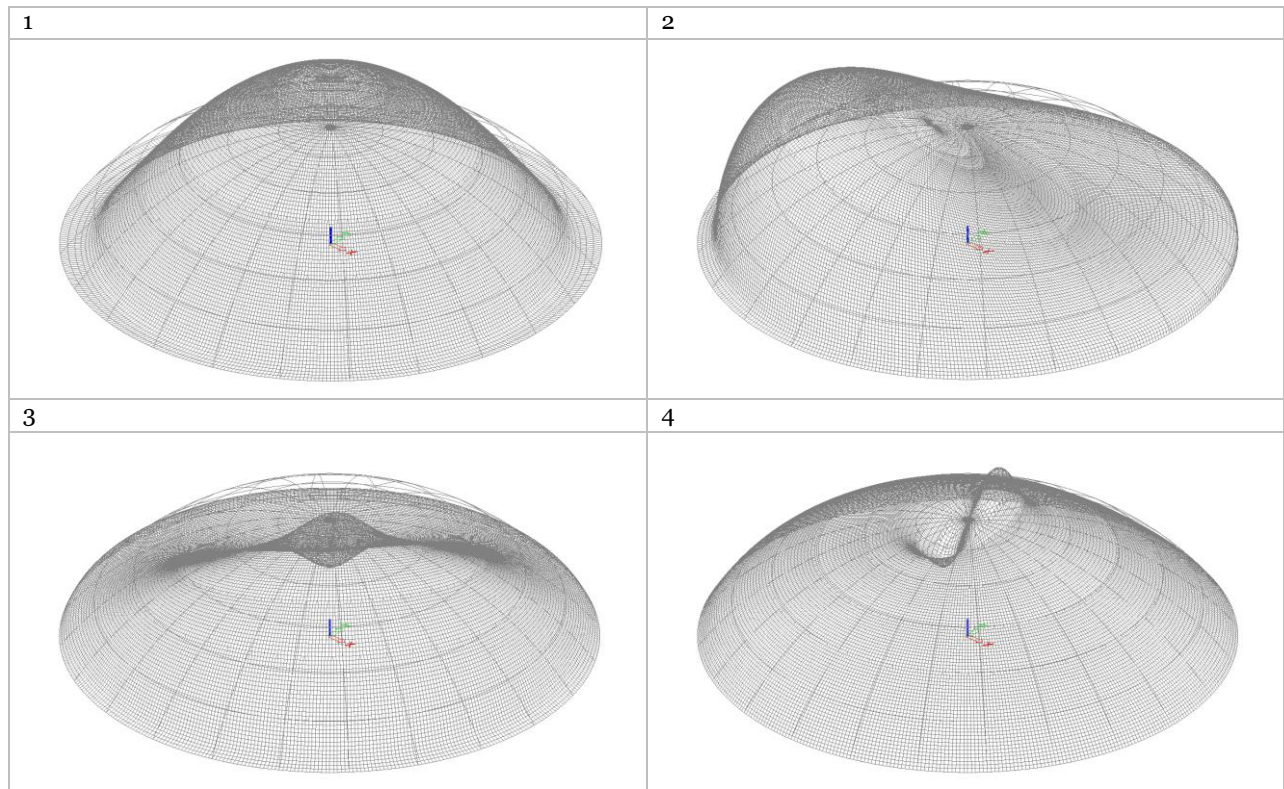
Calc. 8.7

Thermal response

8.7.1. Model

The model is set up as a monolith dome. For these calculations the next parameters hold:

Parameters:	
Span:	d = 150m
Thickness:	t = 60 mm
Sagitta to Span - ratio:	1/4
Thermal expansion:	11,8*10-6 m/m/°C
Loads:	Temperature loads
	NEN-EN 1991-1-5
	Based on figure D29.

Variables:	Temperature distribution
Design limitations:	Stresses, deformations

A figure of the model is presented below:

Fig. Calc7.1   FEM-model for calculations on thermal effects

Season	Temperature	
	Indicative value [°C]	Extreme value [°C]
Summer – outside Indirect radiation	17	30
Direct radiation Bright color[a]	17	50
Light color[b]	17	60
Dark color[c]	17	75
Summer – inside	17	25
Winter – outside	4	-25
Winter – inside	17	20

a	White, yellow
b	Green, light-blue
c	Black, blue, red

Tab. Calc7.1.   Temperatures for calculations on thermal effects   [based on Eurocode 1991-1-5]

Concrete roof, insulation on top side

Concrete roof, insulation on bottom side
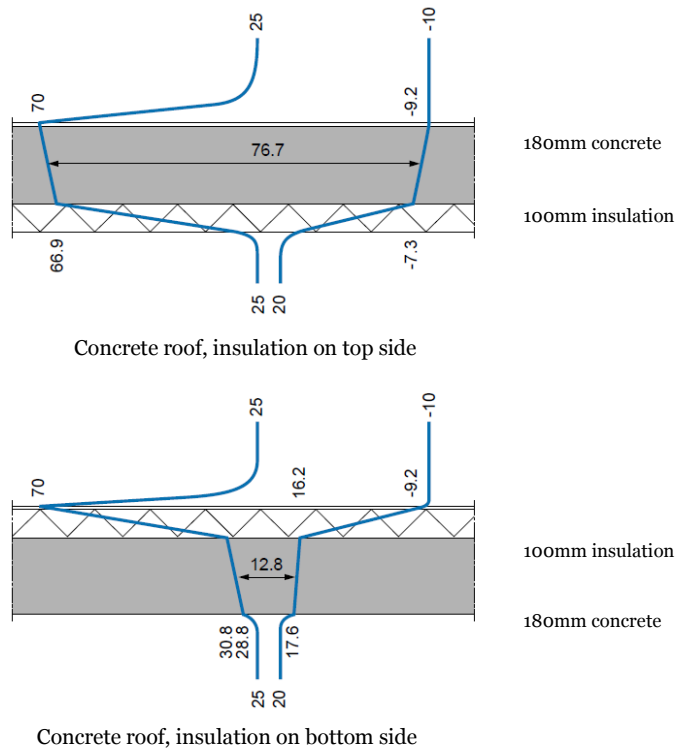
Fig. Calc7.2.   Insulated concrete roof temperature progression
[Building physics, A.C. van der Linden]

Now, to present the effect of temperature on the shell five extreme load cases are examined, for both internal as external insulation. The temperature gradient over the shell cross section is modeled as 5 °C, temperature values are based on figure Calc7.2.

Interior insulation:

Case 1:   Summer; extreme. Temperature distribution constant over shell surface
(T_o = 75 °C, T_i = 70 °C)

Case 2:   Winter; extreme. Temperature distribution constant over shell surface
(T_o = -25 °C, T_i = -20 °C)

Case 3:   Summer; extreme. Estimated realistic temperature distribution over shell surface by figure Calc7.2
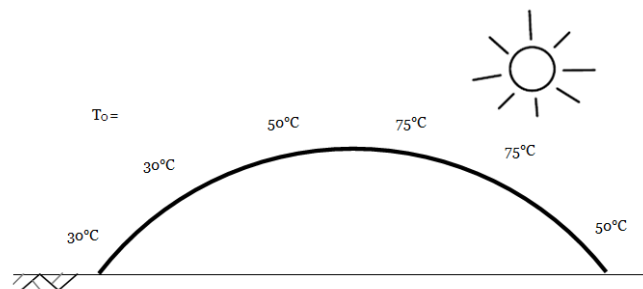
Fig. Calc7.3.   Shell surface subjected to estimated temperature distribution

Exterior insulation:

Case 4:   Summer; extreme. Temperature distribution constant over shell surface
(T_o = 35°C, T_i = 30 °C)

Case 5:   Winter; extreme. Temperature distribution constant over shell surface
(T_o = 15°C, T_i = 20 °C)

8.7.2. Results

<u>Case 1.</u>   Interior insulation: Summer; extreme.   Temperature distribution constant over shell surface

Meridional force (ny):
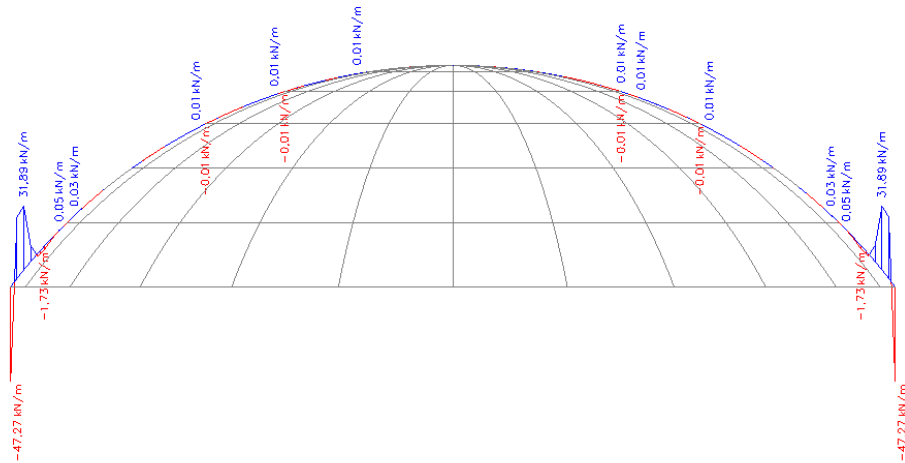
Circumferential force (nx):
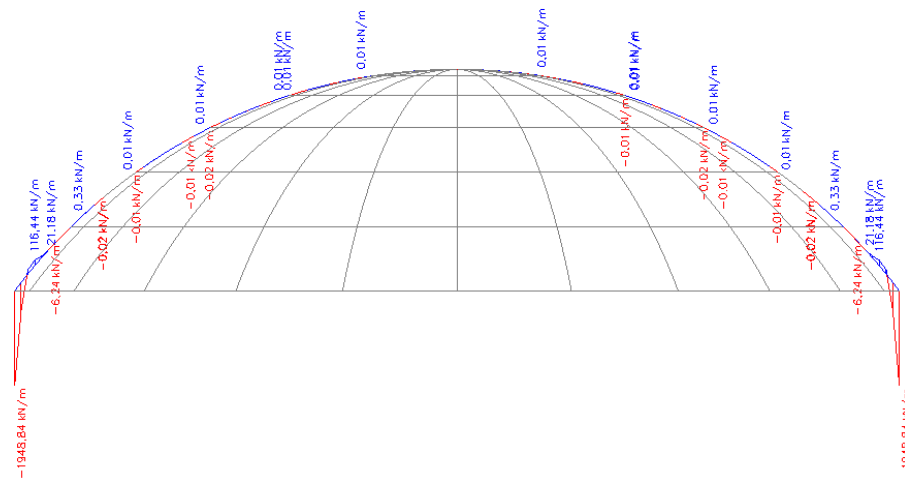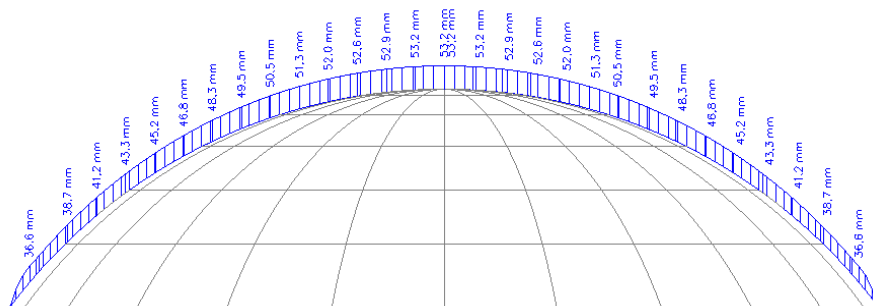
Deformations (uz):

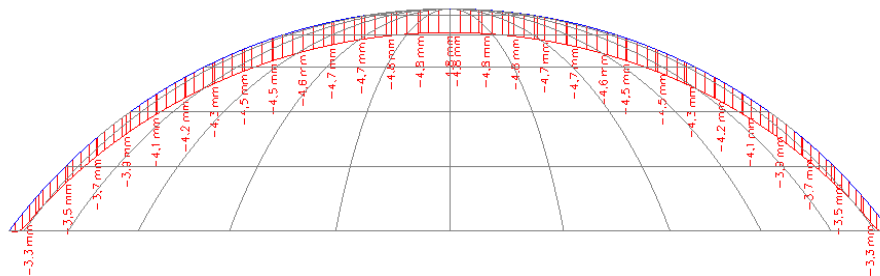Case 2.   Interior insulation: Winter; extreme.   Temperature distribution constant over shell surface
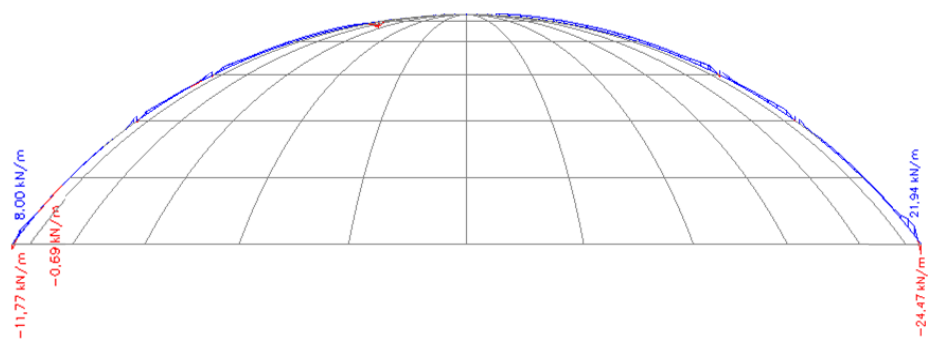
Meridional force (ny):
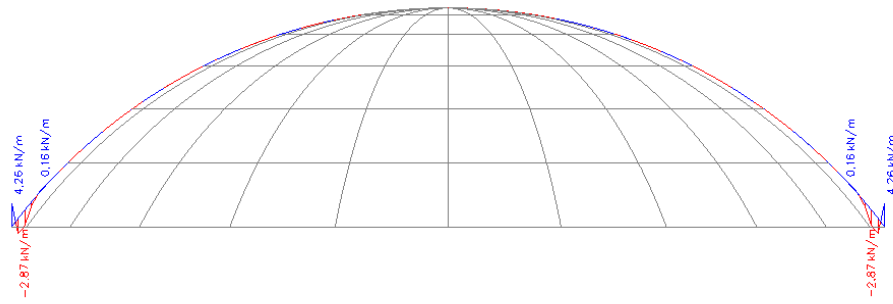
Circumferential force (nx):
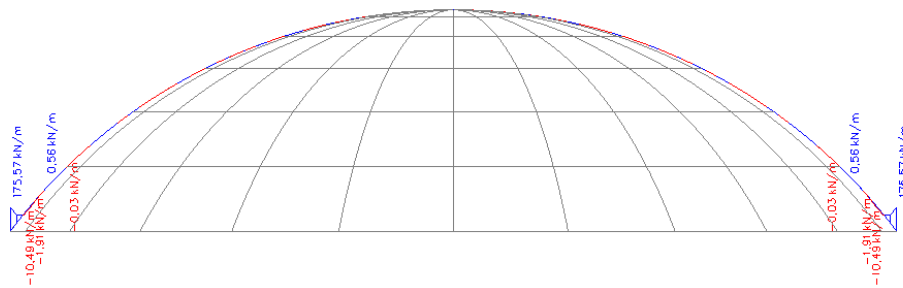
Deformations (uz):
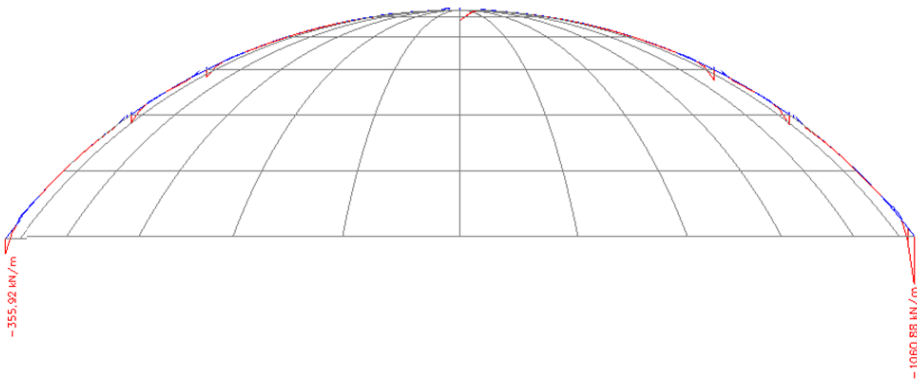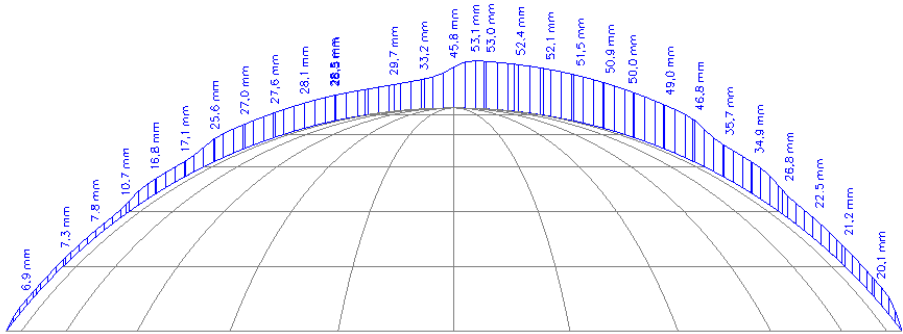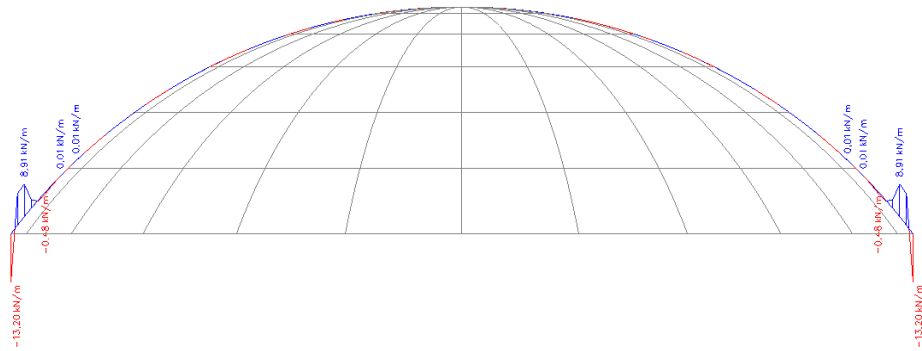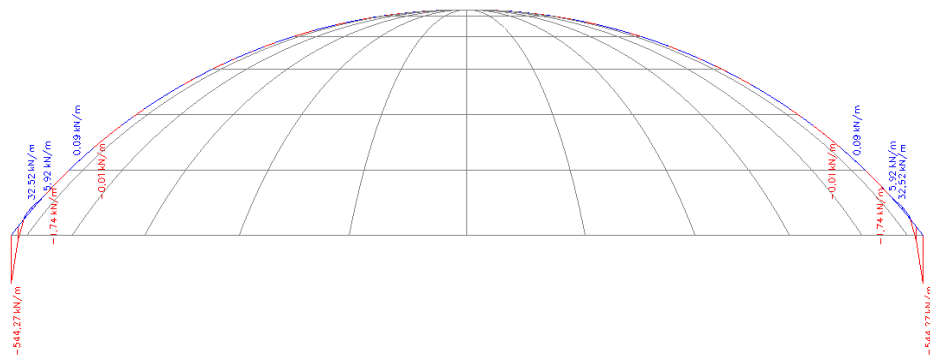
Case 3.   Interior insulation: Summer; extreme.   Estimated realistic temperature distribution

Meridional force (ny):

Circumferential force (nx):

Deformations (uz):

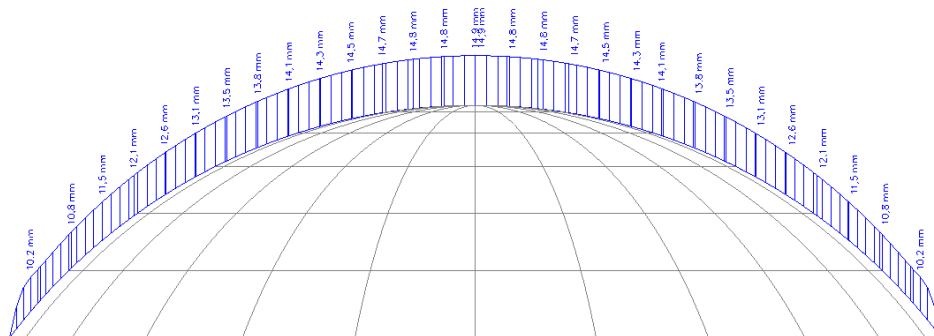Case 4.   Exterior insulation: Summer; extreme.   Temperature distribution constant over shell surface

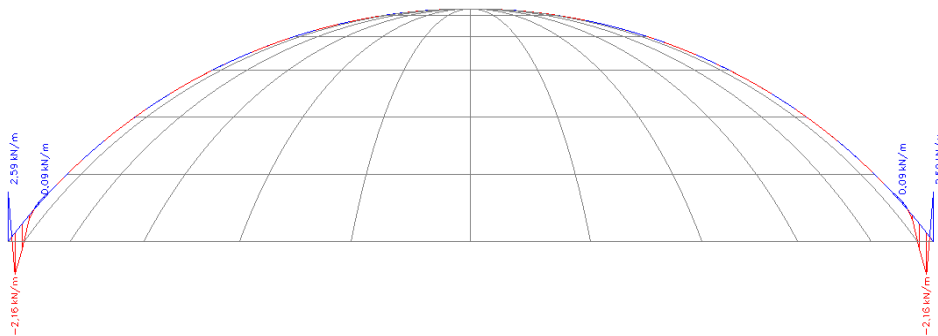Meridional force (ny):

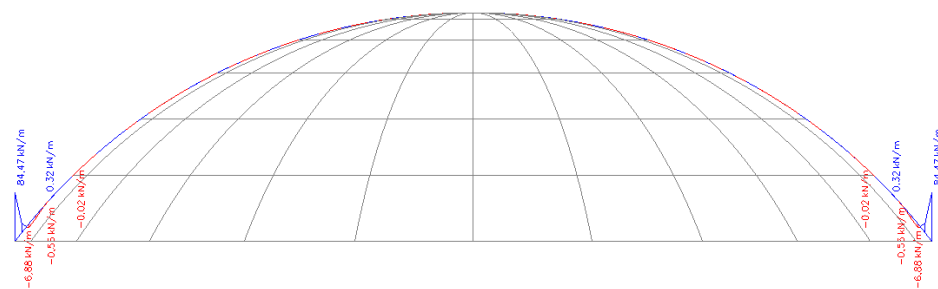Circumferential force (nx):

Deformations (uz):

Case 5. Exterior insulation: Winter; extreme.   Temperature distribution constant over shell surface

Meridional force (ny):

Circumferential force (nx):

Deformations (uz):